IMPLEMENTATION OF CRACK-REDUCING TECHNOLOGIES FOR CONCRETE IN BRIDGE DECKS: SYNTHETIC FIBERS, INTERNAL CURING, AND SHRINKAGE-REDUCING ADMIXTURES

By
Muzai Feng
David Darwin

A Report on Research Sponsored by

THE ACI FOUNDATION

Structural Engineering and Engineering Materials
SM Report No. 136
January 2020

THE UNIVERSITY OF KANSAS CENTER FOR RESEARCH, INC.
2385 Irving Hill Road, Lawrence, Kansas 66045-7563

IMPLEMENTATION OF CRACK-REDUCING TECHNOLOGIES FOR CONCRETE IN BRIDGE DECKS: SYNTHETIC FIBERS, INTERNAL CURING, AND SHRINKAGE-REDUCING ADMIXTURES

By

Muzai Feng

David Darwin

A Report on Research Sponsored by

THE ACI FOUNDATION

Structural Engineering and Engineering Materials

SM Report No. 136

THE UNIVERSITY OF KANSAS CENTER FOR RESEARCH, INC.

LAWRENCE, KANSAS

January 2020

ABSTRACT

Technologies to reduce cracking in bridge decks, including shrinkage-reducing admixtures (SRAs), shrinkage-compensating admixtures (SCAs), fiber reinforcement, and internal curing (IC), are evaluated based on laboratory tests of concrete mixtures with and without slag cement and silica fume and the cracking performance of in-service bridge decks. Additionally, the influence of construction practices used by contractors is evaluated by field evaluation of bridge decks constructed with and without construction issues.

The laboratory portion of this study involves eleven concrete mixtures evaluated based on free shrinkage, scaling resistance, and freeze-thaw durability. The mixtures were cast with or without slag cement and silica fume and contained various quantities of internal curing water; four additional mixtures containing a shrinkage-reducing admixture or one of two shrinkage-compensating admixtures (one of which also contains an SRA) were also evaluated. Results show that the mixtures with slag cement, silica fume, and internal curing exhibited less shrinkage after 20 and 365 days of drying and that shrinkage decreased as the quantity of internal curing water increased from 5.3% to 9.7% by weight of cementitious material. Mixtures with slag cement, silica fume, and 5.3% or 6.5% internal curing water performed well in the freeze-thaw durability test while the mixture with slag cement, silica fume and 9.7% internal curing failed the test. Mixtures with slag cement, silica fume, and internal curing had high mass losses in the scaling resistance test, which was likely due to the harsher test method used in this study or an inadequate air content in the concrete mixture. When a shrinkage-reducing admixture, either by itself or as a part a shrinkage-compensating admixture, is added to the mixture with slag cement, silica fume, and 6.5% internal curing, the freeze-thaw durability and scaling resistance of the mixture was drastically compromised; the mixture with slag cement, silica fume, 6.5% internal curing, and a

CaO-based shrinkage-compensating admixture, on the other hand, performed satisfactorily in the freeze-thaw durability and scaling resistance tests.

The second portion of this study evaluates the cracking performance of 74 bridge deck placements: 10 cast with fiber-reinforced concrete (FRC), four bridge deck placements containing SRAs, six containing IC, and 54 without crack-reducing technologies. The influence of crack-reducing technologies and poor construction practices are evaluated. Results indicate that using a low paste content in the concrete mixture is the most effective way to reduce bridge deck cracking. Bridge decks with paste contents exceeding 27.3% had higher crack densities than decks with lower paste contents. When used in conjunction with a low paste content, SRAs and IC can further reduce cracking in bridge decks. On the other hand, if the contractors fail to follow proper procedures to consolidate, finish, or cure concrete, bridge decks will exhibit substantially greater cracking, even when low paste contents are used. The use of fiber-reinforced concrete can slightly alleviate, but not overcome, the negative effects of poor construction.

Key Words: bridge deck, consolidation, construction practices, cracking, crack-reducing technologies, curing, fiber-reinforced concrete, finishing, freeze-thaw durability, internal curing, lightweight aggregate, scaling resistance, shrinkage-compensating admixtures, shrinkage-reducing admixtures, silica fume, slag cement

ACKNOWLEDGEMENTS

This report is based on a thesis presented by Muzai Feng in partial fulfillment of the requirements for the Ph.D. degree from the University of Kansas. Support was provided by the ACI Foundation and sponsoring organizations: ABC Polymers, the ACI Foundation's Strategic Development Council (SDC), Active Minerals International, the American Society of Concrete Contractors, Baker Concrete Construction, BASF Corporation, FORTA Corporation, the Expanded Shale, Clay and Slate Institute, the Euclid Chemical Company, GCP Applied Technologies, the University of Kansas Transportation Research Institute, PNA Construction Technologies, Inc., Premier Construction Products, Sika Corporation, and Structural Group, Inc.

TABLE OF CONTENTS

LIST OF TABLES

LIST OF FIGURES

CHAPTER 1: INTRODUCTION

1.1 GENERAL

Over the past fifty years, numerous researchers and transportation agencies have reported that cracking in concrete bridge decks leads to accelerated corrosion of reinforcing steel, which increases the maintenance cost and shortens the service life of bridges. According to the American Society of Civil Engineers (ASCE 2018a), in 2017, 9.1% of the bridges in the U.S. were structurally deficient with $123 billion needed for bridge rehabilitation nationwide. A bridge is categorized as structurally deficient if "significant maintenance, rehabilitation, or replacement" is required (ASCE 2018a). In Kansas, which ranks fifth in the U.S. for the total number of bridges, 8.4% of the bridges are considered structurally deficient (ASCE 2018b). According to a national survey by the Federal Highway Administration's (FHWA) High-Performance Concrete Technology Delivery Team (HPC TDT), the top four types of distress noted by state transportation agencies were premature cracking of decks (less than 5 years old), corrosion of reinforcing steel, cracking of girders and substructures, and freezing-and-thawing damage of concrete. As will be discussed later, besides being the top distress, cracking also promotes the other three types of distress.

Since first used in 2003, low-cracking high-performance concrete (LC-HPC) specifications developed by the University of Kansas (KU) and the Kansas Derpartment of Transportaion (KDOT) have been used for the construction of sixteen bridge decks in Kansas. Follow-up evaluations of cracking on those decks have shown improved cracking performance compared to control decks constructed in accordance to the then standard KDOT specifications. The improved crack resistance stems from modified material properties and construction procedures. The LC-HPC specifications have been updated as new findings from laboratory tests and field observations

became available. The LC-HPC specifications, however, have not yet incorporated emerging crack-reducing technologies, such as fiber-reinforced concrete (FRC), shrinkage-reducing admixtures (SRA), and internal curing (IC).

This chapter reviews the significance of concrete cracking, factors affecting the degree of cracking, and results from studies addressing the three cracking-reduction technologies just listed, FRC, SRA, and IC.

1.2 SIGNIFICANCE OF BRIDGE DECK CRACKING

1.2.1 Cracking and Corrosion of Steel

Cracking of concrete in bridge decks is recognized as a major factor promoting the corrosion of reinforcement, which significantly increases the maintenance cost and reduces the service life of bridge decks.

When in contact with oxygen and moisture, steel will react and transform into hydrated ferric oxide (rust), whose volume can be six times the volume of the original steel (Mehta and Monteiro 2006). This expansion will result in spalling of concrete and loss of load-carrying capacity. In reinforced concrete, the highly alkaline environment provided by the concrete pore solution (due to KOH and NaOH) promotes the formation of a tightly adhering passive oxide film on the surface of reinforcing steel that limits the access of oxygen and moisture to the metal. When chloride ions (Cl^-) are present, however, the layer of protective oxide film can be destroyed regardless of the high alkalinity. Furthermore, since Cl^- serves as a catalyst in the chemical reaction, its concentration will increase over time as deicing salts (generally mixtures of NaCl and $CaCl_2$) continue to be used, further accelerating steel corrosion.

In uncracked sections, the low permeability of the material helps limit the diffusion of Cl^-, oxygen, and moisture within the concrete, and thus their ability to reach reinforcing steel. When

cracks are present, however, the protection provided by concrete is drastically compromised because cracks provide a direct path for deleterious substances to the surface of reinforcing steel. In some cases, cracks can even extend through the thickness of the deck and cause corrosion of supporting girders. Lindquist et al. (2005, 2006) found that at crack locations, the chloride concentration at the depth of the reinforcing steel [3.0 in. (76.2 mm) from top surface] exceeded the lower level of the critical chloride corrosion threshold of conventional steel [1.0 lb/yd^3 (0.6 kg/m^3)] within two years of construction for most bridge decks. Away from cracks, however, the chloride concentration remained below the corrosion threshold for at least 12 years, and much longer for most bridge decks. Rodriguez and Hooton (2003) and Weiss et al. (2017) showed that chloride ions not only penetrate vertically into and underneath cracks but can also penetrate horizontally into uncracked regions adjacent to cracks. Weiss et al. (2017) mechanically induced cracks with different widths, decribed in terms of the crack mouth opening displacement (CMOD), on the horizontal surface of concrete specimens that were then ponded with a NaCl solution for 21 days to allow Cl^- to diffuse into the concrete. The values of CMOD ranged from 0.02 to 0.40 mm (0.00079 to 0.016 in.). Figure 1.1 shows how the test results were obtained. After NaCl exposure, the specimens were cut in half, and an $AgNO_3$ solution was applied to the saw-cut surface. The reaction between Cl^- and Ag^+ provides a visible trace of the chloride front. By measuring the width of the chloride profile at various depths below the concrete surface, they were able to study the relationship between crack width, mix design, and how far chloride had penetrated horizontally into the concrete adjacent to the crack. As shown in Figure 1.2, horizontal chloride penetration in specimens with 0.2 mm (0.0079 in.) or wider cracks, although varying moderately with the *w/c* and maximum size of aggregate (MSA), was noticeably increased compared to uncracked

specimens. For a crack width of 0.4 mm (0.016 in.), chloride penetration was similar to that of a free surface indicated by the vertical dashed lines in each figure.

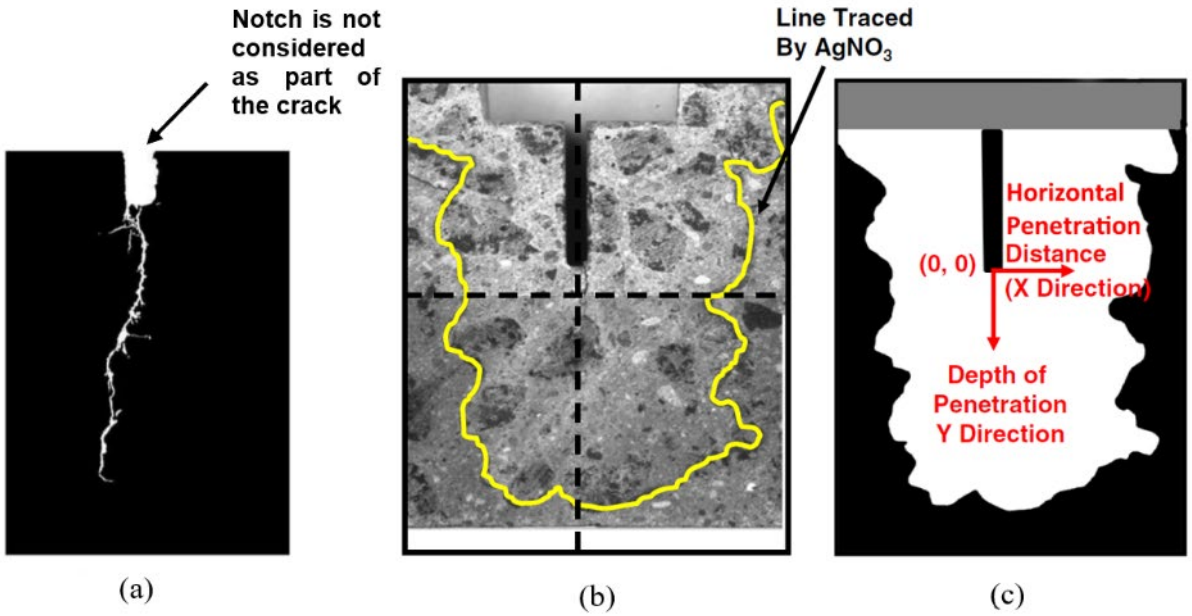

Figure 1.1 – Images used by Weiss et al. (2017) to measure horizontal chloride penetration: (a) a binary image of the saw-cut surface showing the induced crack; (b) an actual image indicating the perimeter of Cl^- penetration; (c) an illustration of the measurements

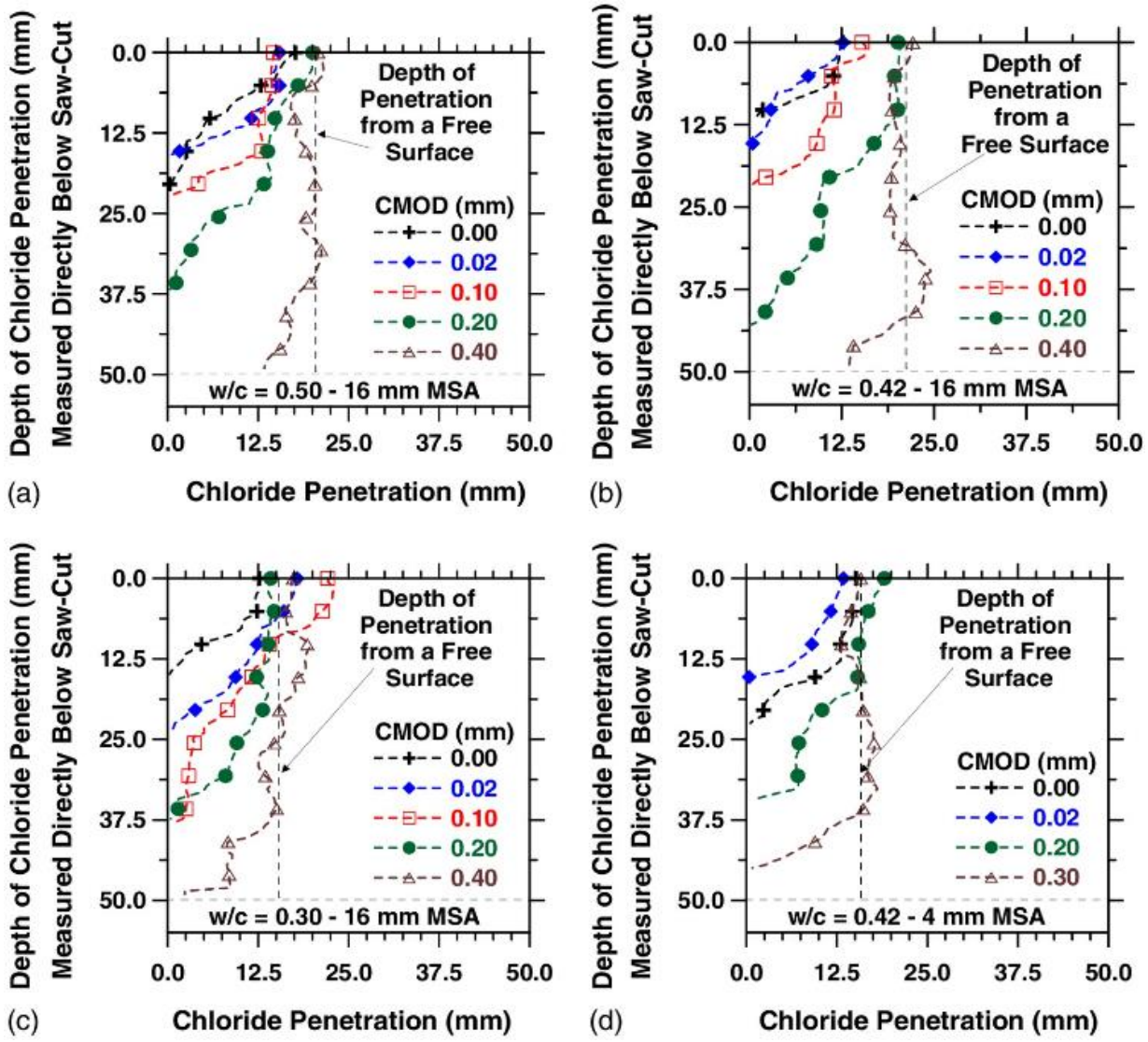

Figure 1.2 – Distance of chloride penetration perpendicular to cracks (X-axis) vs. depth below the surface (Y-axis) for concrete mixtures with: (a) a *w/c* of 0.50 and a MSA of 16 mm (0.63 in.); (b) *w/c* of 0.42 and MSA of 16 mm (0.63 in.); (c) *w/c* of 0.30 and MSA of 16 mm (0.63 in.); (d) *w/c* of 0.42 and MSA of 4 mm (0.16 in.). CMOD = crack mouth opening displacement (Weiss et al. 2017)

1.2.2 Cracking and Freeze-Thaw Durability of Concrete

In addition to promoting corrosion of reinforcement, cracking can also accelerate freeze-thaw damage of concrete by providing a path for liquid to penetrate the concrete.

In regions with cold climates, hardened concrete is prone to damage caused by freezing and thawing cycles (freeze-thaw damage or frost damage). The primary causes of such damage are

the generation of osmotic pressure and the desorption of C-S-H (capillary effect) (Mindess et al. 2003, Mehta and Monteiro 2014). Powers and Helmuth (1953) showed that frost damage in cement paste is primarily caused by the generation of osmotic pressure. Water in the capillaries contains soluble substances such as alkalies, chlorides, and calcium hydroxide. As ice forms in the capillary solution, the concentrations of solutes increase in the liquid adjacent to the freezing site (due to a reducing volume of liquid), which draws water from more dilute pores. Thus, the formation of ice causes water to travel toward the freezing pores due to osmosis and eventually causes destructive local expansion in the paste. Another primary cause of freeze-thaw damage, the desorption of C-S-H, was proposed by Litvan (1970). Water adsorbed on the surface of C-S-H is rigidly held by the gel, which prevents the rearrangement of water molecules to form ice. It is estimated that the adsorbed water will not freeze above -108° F (-78° C) (Mehta and Monteiro 2014). Therefore, when the water in capillary pores freezes, the water adsorbed on C-S-H remains in the liquid state. This creates a thermodynamic disequilibrium between ice (with a lower chemical potential) and the supercooled water in unfrozen pores (with a higher chemical potential). The result is a low effective relative humidity at freezing sites, and water will migrate from C-S-H to the freezing sites to maintain equilibrium. This relocation of water results in an increase of the volume of ice in capillary pores until the entire cavities are occupied. Any subsequent movement of water to ice-bearing regions will result in expansion and tensile stresses in the paste.

Based on the mechanisms described above, it can be deduced that the resistance of concrete to freeze-thaw damage depends on its permeability, the degree of saturation (the ratio of the volume of water to the volume of voids), and the amount of freezable water. Partially dry concrete that has enough empty pores throughout the paste for water to freeze will not suffer freeze-thaw damage (Mindess et al. 2003). Cracks increase the permeability of concrete by providing flow

paths for water, exposing sections of concrete that are otherwise inaccessible to liquid. Under the same weathering conditions, concrete with cracks, therefore, will have a higher degree of saturation and is more vulnerable to freeze-thaw damage than uncracked concrete (Wang et al. 1997, Mindess et al. 2003, Mehta and Monteiro 2006, Pease 2010, Rodrigues and Hooton 2003). Wang et al. (1997) studied the permeability of concrete specimens to water as a function of crack width by measuring the rate of water flow through 1-in. (25-mm) thick disks. They found that the presence of cracks wider than 0.002 in. (0.05 mm) drastically increased permeability. For example, the permeability factor of the specimen with a 0.008-in. (0.2-mm) crack was approximately 10^5 times that of the specimen with no crack. Rodriguez and Hooton (2003) measured the chloride permeability of specimens with a saw-cut crack (smooth crack wall surface) or a fractured crack (rough crack wall surface) with crack widths ranging from 0.003 to 0.027 in. (0.08 to 0.68 mm). Rodriguez and Hooton (2003) concluded that, regardless of crack wall roughness (smooth or rough surface) and for all of the crack widths tested, cracks behaved like free surfaces and allowed chloride to penetrate into uncracked concrete sections from both the exposed top surface and the crack wall. Similarly, Pease (2010) evaluated the ingress of water from a ponding reservoir on the top surface into concrete specimens with crack widths ranging from 0.004 to 0.016 in. (0.10 to 0.40 mm), as well as a specimen without cracks, after exposure times ranging from approximately 3 minutes to 6 hours. Pease (2010) found that even the narrowest crack evaluated in this study [crack width = 0.004 in. (0.10 mm)] allowed moisture to horizontally ingress into specimen like a free surface.

1.3 FACTORS AFFECTING CRACKING IN BRIDGE DECKS

1.3.1 Plastic Shrinkage

Plastic shrinkage takes place when concrete loses water shortly after placement (30 minutes to 6 hours) through evaporation at the surface and suction by formwork or substructures (Neville 1995; Mindess et al. 2003). As water is removed from the cement paste (the mixture of cementitious materials and water), negative capillary stress will be induced and cause a local contraction in the concrete.

In bridge construction, the loss of water to formwork or sub-structures can be largely prevented by wetting them before placement of concrete; however, the loss of moisture due to evaporation cannot be eliminated. Furthermore, since evaporation only happens at the surface, the top layer will shrink at a higher rate than the underlying concrete. The differential shrinkage will induce tensile stresses and lead to surface cracking.

The most fundamental way to reduce plastic shrinkage cracking is to avoid placing concrete under hot, windy, arid weather conditions that cause rapid evaporation of water at the concrete surface. To be specific, the rate of water evaporation should be lower than that at which bleed water reaches the surface until curing is applied (Mindess et al. 2003). The evaporation rate of water at the concrete surface can be calculated based on the air and concrete temperatures, wind speed, and relative humidity. The rate of bleeding, however, is not easily measurable. It is instead common for transportation agencies to specify a maximum allowable evaporation rate during construction, which is most commonly 0.1 or 0.2 $lb/ft^2/h$ (0.5 or 1.0 $kg/m^2/h$) (Mindess et al. 2003, ACI Committee 305 2010; Kansas Department of Transportation 2015; Ohio Department of Transportation 2016; Virginia Department of Transportation 2016; Minnesota Department of Transportation 2018). The rate of evaporation is usually determined using a widely available

nomograph (Menzel 1954, NRMCA 1960, ACI Committee 308 2016). Yuan et al. (2011) analyzed the crack densities of 61 monolithic bridge deck placements at 36 months of age and found that an increase of 10° F (5.6° C) in the maximum air temperature on the day of construction resulted in a 0.06 m/m^2 increase in the crack density, which they attributed to the increased evaporation rate accompanying the higher temperature.

Other measures to reduce plastic shrinkage cracking include promptly applying curing using wet burlap, polyethylene sheets, or both, reducing the evaporation rate by installing wind breaks, replacing mixing water with ice and shading aggregates in hot weather to lower the concrete temperture, using surface films such as curing compounds and evaporation retarders, and avoiding modifications to concrete that lower bleeding rate (avoiding fly ash or silica fume as a cement replacement). Delays in the setting time of concrete lead to an increased probability of plastic shrinkage cracking, which may occur with slow setting cement, a high dosage of set retarder, or excessively cooled concrete (ACI Committee 305 2010).

1.3.2 Plastic Settlement

In plastic concrete, solid particles tend to travel downward due to their higher density compared to water. This phenomenon is called plastic settlement. When plastic settlement is obstructed by reinforcement, tensile stresses will develop directly above the obstacles, which may cause cracking at the concrete surface. In bridge decks, settlement cracks usually appear directly above and parallel to reinforcing bars, providing direct access for deleterious substances to the reinforcement.

Dakhil et al. (1975) used photoelastic evaluation to verify the existence of stresses in concrete due to restrained settlement. Dakhil et al. also found experimentally that settlement cracking can be reduced with increased concrete cover (most important factor), lowered concrete

slump, or reduced bar size. It should be noted that although settlement of concrete alone is not likely to cause cracking in bridge decks due to the relatively thick concrete cover, the subsidence of plastic concrete can still result in a vertical plane of weakness directly above the top reinforcing bars. Later, tensile stresses caused by drying shrinkage, thermal effects, or loading may result in cracking at the weakened plane (Babaei and Fouladgar 1997). Al-Qassag et al. (2015) found that adding synthetic fibers to concrete mixtures significantly reduces settlement cracking.

1.3.3 Drying Shrinkage

After concrete hardens, the loss of water to the environment causes concrete to shrink. If concrete is restrained, tensile stresses will occur. In most cases, aggregate is dimensionally stable. Therefore, drying shrinkage is dominated by the volume change of the paste, while aggregates have a restraining effect on volume change (Mindess et al. 2003).

Much like plastic shrinkage, drying and shrinkage are faster at the concrete surface due to exposure to the environment while interior sections have a relatively more stable moisture content and volume (Bisschop et al. 2001). The drying gradient between exterior and interior sections also induces tensile stresses. Grasley et al. (2006) measured the relative humidity (RH) gradient in 3×3×13 in. (76×76×330 mm) concrete prisms and found that after four days of drying, the RH 0.24 in. (6 mm) from the surface had dropped to 92% while the RH 1.50 in. (38 mm) from the surface was 98%. Subsequent modeling indicated that for a fully restrained specimen, the tensile stresses 0.24 in. (6 mm) and 1.50 in. (38 mm) from surface would be 377 psi (2.6 MPa) and 73 psi (0.5 MPa), respectively. The former exceeds the tensile strength of most concrete and can lead to surface cracking.

A large part of drying shrinkage is caused by capillary stress. As cement hydrates, a network of capillary pores forms. When water (pore solution) is lost in capillary pores, due to

either hydration or evaporation, a meniscus is formed. Due to the interaction between pore walls and pore solution, the meniscus will adopt a concave shape and water is in hydrostatic tension. A corresponding hydrostatic compression is applied to the solid skeleton of concrete that pushes the pore walls closer, which is called capillary stress. The magnitude of the capillary stress (σ_{cap}) can be expressed as:

$$\sigma_{cap} = \frac{2\gamma}{r} \tag{1.1}$$

where σ_{cap} is the hydrostatic stress, γ is the surface tension of the pore solution, and r is the radius of the capillary pore.

As previously stated, drying shrinkage is a paste-controlled phenomenon (Mindess et al. 2003). Therefore, drying shrinkage can be reduced by reducing the volume fraction of paste or reducing or compensating for the drying shrinkage of paste. To be specific, methods used to limit drying shrinkage cracking include reducing the paste content of concrete, replacing a portion of cement with supplementary cementitious materials, internally curing the concrete with saturated lightweight aggregate, and adding specialty admixtures to the concrete.

Reducing paste content (increasing aggregate volume) is the most efficient way to reduce drying shrinkage (ACI Committee 209 2005). Pickett (1956) experimentally measured the shrinkage of neat cement pastes and that of concretes exposed to the same drying environment for at least 224 days. Drying shrinkage decreased monotonically with increasing volumes of aggregate within the tested range [0% (neat paste) to about 70%]. For example, the mixture with a *w/c* ratio of 0.50 containing 30% aggregate by volume exhibited only 46% of the shrinkage experienced by neat cement paste with the same *w/c* ratio. Based on his observations, Pickett (1956) proposed the following equation to approximate the shrinkage of concrete, S_C :

$$S_C = S_P \cdot (1 - V_a)^n \tag{1.2}$$

where S_P is the shrinkage of paste, V_a is the volume fraction of aggregate, and n is a constant ranging between 1.2 and 1.7. As indicated by Eq. (1.2), changes in paste content $(1 - V_a)$ has a greater influence than changes in the shrinkage of the paste (S_P) on the drying shrinkage of concrete (S_C). The reduction in drying shrinkage caused by reduced paste content in concrete mixtures has been demonstrated by a number of other laboratory studies (Alexander and Wardlaw 1959, West et al. 2010). The effectiveness of reducing shrinkage cracking by reducing paste content has been observed in the field as well. Darwin et al. (2004) reported the results from crack surveys performed over a 10-year period and showed that as the paste volume of concrete increases from 26% to 30%, the crack density of bridge decks increases from 0.36 to 0.78 m/m^2. Khajehdehi and Darwin (2018) analyzed the crack densities of 40 bridge decks and found that paste content was the most dominant factor affecting bridge deck cracking among concrete strength, slump, temperature, and air content. These observations are attributed to the increased magnitude of shrinkage accompanying the higher paste content.

Partial replacements of cement with supplementary cementitious materials (SCMs), such as slag cement, fly ash, and metakaolin, can also be used to reduce drying shrinkage. Precautions, however, should be taken in mixture proportioning and curing when SCMs are used to reduce drying shrinkage. Since slag cement usually has a lower specific gravity (approximately 2.90) compared to portland cement (3.15), the replacement of cement with slag cement should be made on a volume basis rather than a weight basis to avoid increasing the paste volume in the concrete (Hooton et al. 2009). It has also been reported that when slag cement is added, longer curing may be required. Yuan et al. (2015) reported that mixtures with *w/cm* ratios of 0.42 or 0.44 and a 30%

volume replacement of cement with slag cement exhibited considerably lower drying shrinkage when cured for 14 days compared to mixtures containing 100% portland cement and the same paste content. When cured for 7 days, however, mixtures containing 30% slag exhibited similar shrinkage to mixtures with 100% portland cement and the same paste content. Fly ash has also been shown to reduce drying shrinkage when used as a partial replacement for cement (Chindaprasirtet al. 2004, Yuan et al. 2011). The curing regime and the class of fly ash, however, need to be carefully selected. Yuan et al. (2011) showed that when a Class F fly ash was added as a 40% volume replacement of cement, the drying shrinkage of the concretes could be reduced only if the concrete was cured for at least 14 days. When cured for 7 days, the mixture containing the Class F fly ash exhibited more drying shrinkage than the mixture containing 100% cement. When a Class C fly ash was used at the same replacement level, in contrast, drying shrinkage at 30 days increased compared to the mixtures without fly ash, regardless of the curing period (up to 56 days). Metakaolin has also been observed to reduce drying shrinkage (Brooks and Johari 2001, Güneyisi et al. 2012, Medjigbodo et al. 2018, and numerous others). Güneyisi et al. (2012) observed an approximately 40% reduction in free shrinkage after 42 days of drying for a mixture containing a 15% weight replacement of cement with metakaolin. In a restrained shrinkage test, although metakaolin did not delay the onset of cracking, the average crack width of the specimens containing 15% metakaolin was significantly lower than that of the control specimens containing 100% portland cement concrete.

Internal curing with pre-wetted fine lightweight aggregate (LWA) is another increasingly popular technique used to combat drying shrinkage cracking. LWA has larger pores than cement paste. When concrete dries and as cement hydration occurs, water is drawn from the pores in the LWA. Browning et al. (2011) observed a 14% reduction in the 30-day drying shrinkage for a

mixture with a *w/c* ratio of 0.44 containing 199 lb/yd^3 (118 kg/m^3) of vacuum-saturated LWA. The reduction in shrinkage accompanying internal curing can be even greater when SCMs are used in conjunction with pre-wetted LWA. Browning et al. (2011) found that 30-day drying shrinkage was reduced by 42% when 195 lb/yd^3 (116 kg/m^3) of vacuum-saturated LWA was used in conjunction with a 30% volume replacement of cement with slag. In addition to reducing drying shrinkage, internal curing can also benefit concrete in other aspects, such as increasing strength (Espinoza-Hijazin and Lopez 2011, Hwang et al. 2013) and reducing chloride permeability (Bentz 2009, Espinoza-Hijazin and Lopez 2011, Bella et al. 2012). It is noteworthy, however, that these additional benefits depend on specific mixture proportions, material properties, and handling of concrete and are not applicable to all concrete mixtures. For example, internal curing can increase concrete strength because internal curing water increases the degree of hydration of cementitious materials. On the other hand, concretes with internal curing have been observed to have lower or similar strength compared to concretes without internal curing, mainly because LWAs are weaker than normalweight aggregates. The overall effects of internal curing on concrete depend on these competing factors and should be evaluated specifically for each project. (Bentz and Weiss 2011). Raoufi et al. (2011) observed that the tensile strength of mortar mixtures decreases progressively (by 5% to 23%) as the volume replacement of pre-wetted fine LWA increased for LWA replacement levels of 8%, 12%, 16%, and 24%.

Shrinkage-reducing admixtures (SRAs) have also been used to help reduce drying shrinkage in concrete. SRAs are organic surfactants that, when mixed in water, reduce the surface tension of the solution [γ in Eq. (1.1)]. As illustrated in Eq. (1.1), this will lead to a reduced driving force for drying shrinkage. SRAs will be discussed in detail in Section 1.5. The effectiveness of SRAs in reducing drying shrinkage in concrete is well-established (Yuan et al. 2011, Silfwerbrand

and Farhang 2014, Ardeshirilajimi et al. 2016, Pendergrass et al. 2017). Increased dosages of some SRAs, however, can destabilize the air void system in concrete (Schemmel et al. 2000, Cope and Ramey 2001, Lindquist et al. 2008, Pendergrass et al. 2017). This is because the addition of SRAs may cause excessive reduction in the surface tension of mixing water and, as a result, the air void system in hardened concrete will have larger voids that are more widely spaced, which harms the freeze-thaw performance of concrete. Pendergrass et al. (2017) tested the freeze-thaw durability of concrete mixtures containing one of two SRAs and one of two air entraining admixtures (AEAs, one surfactant-based and the other foaming polymer-based). They found that when SRAs were used with the surfactant-based AEA, the mixtures exhibited satisfactory freeze-thaw performance. When SRAs were used with the foaming polymer-based AEA, however, the freeze-thaw durability was adversely affected. Subsequent air-void analysis showed a large air-void spacing when foaming polymer-based AEA was combined with an SRA, which was responsible for the decreased freeze-thaw performance.

Shrinkage-compensating admixtures (SCAs) can also be used to combat drying shrinkage (Khayat and Mehdipour 2017, Khajehdehi et al. 2018). SCAs, usually consisting primarily of MgO or CaO, react with mixing water and form hydroxides, causing an expansion in concrete. If the concrete is restrained, such as the case of bridge decks, compressive stresses will be induced in the concrete, which will counteract the tensile stresses caused by restrained shrinkage. Shrinkage-compensating admixtures are used much like expansive cements (Types K, M, S, or O), which depend on the formation of ettringite from calcium aluminates (such as $C_4A_3\overline{S}$ in Type K cement) to induce expansion (Mindess et al. 2003, Mehta and Monteiro 2006). SCAs have also been experimentally demonstrated to be a useful tool against drying shrinkage. Khajehdehi et al. (2018) reported that the addition of an SCA made of CaO caused an expansion of approximately 230

microstrain within 24 hours of casting. When the SCA, SCMs (slag and silica fume), and internal curing were added, the expansion was further increased to approximately 400 microstrain.

1.3.4 Thermally-Induced Stresses

Newly placed concrete experiences a temperature rise in the first few hours after casting due to the exothermic nature of cement hydration. This is especially true in recent years as cement particles get finer (Bentz et al. 2008), increasing the rate of reaction and resulting, not only in a more rapid generation of heat, but an increase in the total heat generated. The expansion of concrete accompanying the initial temperature rise does not induce any measurable compressive stress because the concrete has a low modulus of elasticity and is easily deformed. Concrete subsequently solidifies and shrinks due to cooling (thermal shrinkage). If the concrete is restrained, this shrinkage will cause tensile stresses. Because thermal shrinkage takes place in a short time (usually days), the tensile stresses will not be fully relieved by concrete creep, increasing the probability of cracking.

The magnitudes of tensile stresses and the extent of cracking caused by restrained thermal shrinkage depend on the difference between the peak temperature of concrete and the temperature of girders when concrete temperature is at its peak (usually equal to the ambient temperature) (Purvis et al. 1995). Babaei and Fouladgar (1997) recommended that the thermally-induced contraction should be limited to 150 microstrain, which can be achieved by keeping the temperature difference between the concrete deck and girders within 22°F (12°C) for at least 24 hours after concrete placement.

The relation between plastic concrete temperature and high air temperature on the day of placement also influences the extent of bridge deck cracking. Khajehdehi and Darwin (2018) found that when concrete temperature is controlled (between 58° and 72°F), placing concrete in hot days

(high air temperature between 78° and 88°F) correlates with lower cracking in bridge decks. When the ambient temperature drops, the girders contract while the volume of the concrete remains relatively stable, placing the concrete in compression. This helps counteract the tension caused by drying shrinkage. This advantage is not available on cool days, and Khajehdehi and Darwin (2018) observed no effect of high air temperature on cracking in bridge decks cast when concrete temperature was not controlled.

1.3.5 External Loading

While external loads, including construction load, dead load, and live load, can induce tensile stresses in bridge decks and cause flexural cracking, Krauss and Rogalla (1996) found that, for properly designed and constructed bridges under normal traffic patterns, cracking caused by loading is minimal compared to that caused by shrinkage and thermal stresses.

1.3.6 Construction Practices

Yuan et al. (2011) analyzed the factors affecting the cracking in 40 bridge deck placements at 36 months of age and found that the contractor constructing the deck has a significant influence on cracking behavior. Specifically, the methods by which the contractor consolidates, finishes, and cures the deck appear to have the greatest impact on cracking.

Consolidation removes voids and entrapped air, helps concrete flow into recesses within the forms and around reinforcement, and compacts the concrete. In Kansas, bridge decks are usually consolidated using vertically mounted internal gang vibrators, which consist of a series of spud vibrators mounted 1 ft (0.3 m) apart on a mechanical system that is lowered and raised to preset elevations to ensure uniform consolidation. This procedure works well and has been in use since at least the early 1980s (Donahey and Darwin 1985). Equipment, duration, and operation procedures, however, can affect the quality of consolidation. Vibrators should be left in the

concrete for 2 to 3 seconds, until the coarse aggregate sinks below the surface, and then lifted slowly to remove so that holes left by the vibrators close. Figure 1.3a shows an example where the vibrators were lifted too fast, leaving a series of holes in the concrete that were not closed during finishing. In addition to proper use of the consolidation equipment, consolidated concrete should be free of any further disturbance after vibration is complete. The KDOT specifications for bridge decks construction (Kansas Department of Transportation 2015) require that any voids left by construction personnel should be removed by reconsolidation. Figure 1.3b shows an example where construction workers walked through consolidated concrete; the holes were, again, not closed during finishing.

Finishing is essential to give a bridge deck a properly graded surface. Excessive finishing by the screeding equipment or by bullfloating brings more cement paste to the surface, which leads to increased plastic shrinkage, increased local drying shrinkage, and potentially decreased scaling resistance. The use of a finishing aid increases the water-to cementitious materials (*w/cm*) ratio at the surface, which may also contribute to decreased scaling resistance.

(a)

(b)

Figure 1.3 – Examples of unsatisfactory consolidation. (a) Rapid removal of spud vibrators; (b) walking through consolidated concrete.

Curing is often considered the most important factor in construction affecting the cracking performance of bridge decks (Krauss and Rogalla 1996, Darwin et al. 2012, Rajabipour et al. 2012). According to a survey by Aktan et al. (2003) involving 31 state DOTs, "substandard curing"

was acknowledged by most respondents as the top cause of early-age bridge deck cracking. Curing should start immediately after finishing to avoid plastic shrinkage cracking. When curing with saturated burlap, Darwin et al. (2010 and 2012) recommend that the concrete surface be covered with burlap within 10 to 15 minutes after finishing. An extended curing period also helps improve the overall concrete quality and reduce cracking. Longer curing increases cement hydration, and as a result, the concrete will have a lower permeability, less free water that can be lost to produce shrinkage, and a higher tensile strength to resist shrinkage stresses (Russell 2004). Deshpande et al. (2007), Lindquist et al. (2008), and West et al. (2010) studied the influence of curing time (3, 7, 14, and 28 days) on the drying shrinkage of concretes as a function of air content (air-entrained or non-air entrained), cement type (Type I/II or Type II coarse ground), and paste content (21.6% or 23.3%). They found that extending the curing period consistently reduced drying shrinkage. It is commonly argued that extending the curing time delays the opening of a bridge. Compared to the time required for bridge construction or deck replacement project (months), however, the effect of curing time (usually days) is small.

1.4 FIBER REINFORCED CONCRETE

1.4.1 Introduction

Fibers have been used since ancient times to reinforce brittle materials. Large-scale commercial use of fiber-reinforced cement paste matrices started with asbestos fibers in the 1900s. Due to the health hazards associated with asbestos fibers, alternative fiber types were introduced in the 1960s. Since then, the use of fiber-reinforced concrete (FRC) has steadily increased (ACI Committee 544 2002, Mindess et al. 2003).

1.4.2 Fiber Materials and Properties

Several materials have been used to produce fibers; the most common ones include synthetic polymers and steel (Mindess et al. 2003). Common parameters to describe a fiber include fiber length, equivalent diameter (the diameter of the circle that has the same area as the fiber's cross-section), and aspect ratio (the ratio of fiber length to equivalent diameter).

Synthetic fibers can be made from polypropylene (PP, most common), polyethylene (PE), nylon, polyvinyl alcohol (PVA), carbon, and polyester (PET) (Mindess et al. 2003, ASTM 2015). The length of synthetic fibers range between ¼ and 2½ in. (6 and 64 mm). Synthetic fibers are usually divided into two categories depending on their forms: monofilament (single strands) and fibrillated (bundles). Monofilament fibers can be further categorized into micromonofilament and macromonofilament fibers (ACI Committee 544 2008). With equivalent diameters less than 0.012 in. (0.3 mm), micromonofilament fibers are typically added at a volume fraction of 0.05 to 0.2% of the concrete. At such low dosages, microsynthetic fibers are not intended to strengthen a section. The addition of microfibers, however, significantly improves the early-age cracking resistance of concrete. Macrosynthetic fibers, on the other hand, have equivalent diameters greater than 0.012 in. (0.3 mm) and are typically dosed at higher volume fractions (0.2 to 1.0%). The addition of macrosynthetic fibers has been shown to improve the strength and strain capacity of reinforced concrete members (Roesler et al. 2004, Altoubat et al. 2009). For this reason, macrofibers are sometimes referred to as structural fibers.

Steel fibers can be straight but are more commonly deformed to increase their bond with the cementitious matrix. The most common steel fibers are between 0.5 and 1.25 in. (13 and 32 mm) long and have aspect ratios between 30 and 100 (ACI Committee 544 2008). According to the source material and production procedures used, steel fibers can be divided into five types:

cold-drawn wire (Type I), cut sheet (Type II), melt-extracted (Type III), mill cut (Type IV), and modified cold-drawn wire (Type V). The terms microfiber and macrofiber can also be used to describe steel fibers – those with equivalent diameters less than 0.012 in. (0.3 mm) are microfibers and those with larger equivalent diameters are macrofibers. When using a steel fiber, the fiber type, length, diameter, aspect ratio, and strength are usually specified.

Blending two or more types of fibers to form a hybrid fiber system is an increasingly common practice in the industry. The advantage of a hybrid fiber system is that the positive interactions between fibers produces a synergistic effect and greatly improves the performance of FRC (ACI Committee 554 2008). The most common fiber combinations are: (1) a strong and stiff fiber that improves first crack and ultimate strength with a flexible fiber that improves toughness and strain capacity in the post cracking zone; (2) a small fiber (usually a microfiber) that bridges microcracks and increases the tensile strength of the matrix with a large fiber (usually a macrofiber) that arrests the propagation of macrocracks and improves the toughness of the composite; and (3) one fiber (the primary fiber) that increases the mechanical properties of the composite, such as strength or toughness, with a second fiber (the processing fiber) that improves fresh concrete and early-age properties, such as ease of production and resistance of plastic shrinkage cracking (Qian and Stroeven 2000, Banthia and Gupta 2004, Bentur and Mindess 2007). It should be noted, however, that the proportion of each fiber and the total fiber volume need to be optimized to achieve the best performance (Qian and Stroeven 1999, Tosun-Felekoglu and Felekoglu 2013, Banthia et al. 2014).

1.4.3 Influence of Fibers on Concrete Behavior

The improvement in strength and ductility of concrete members associated with the addition of fiber have been widely reported (Banthia and Sheng 1996, Lawler et al. 2005, Altoubat

et al. 2009, Hamoush et al. 2010). Altoubat et al. (2009) tested the shear behavior of reinforced concrete beams containing no stirrups and various macrosynthetic fiber contents (0, 0.50%, 0.75%, and 1.0% of concrete volume). They found that the addition of macrofibers increased the stress at which the first diagonal shear crack formed by up to 30% and improved the shear strength of the beams by up to 28%. Furthermore, the beam without macrofibers formed only one shear crack and failed in a brittle manner while beams with macrofibers formed multiple shear cracks before failure and were more ductile (the deflection at maximum load was increased up to 138% compared to the beam without fiber addition). Lawler et al. (2005) tested the flexural behavior of unreinforced concrete beam specimens with different combinations of steel macrofibers, steel microfibers, and PVA microfibers. Their results showed that the combinations of (steel microfiber and steel macrofiber) and (PVA microfiber and steel macrofiber) increased the stress at which the first crack formed by up to 20% and the strength of the member by up to 30%. Furthermore, the work of fracture (the area under stress-strain curve) increased from approximately 0.2 N·m (1.8 lbf·in.) for the specimen with no fiber to more than 3 N·m (26.6 lbf·in.) for specimens containing steel microfibers and steel macrofibers and more than 4 N·m (35.4 lbf·in) for the specimen containing PVA microfibers and steel macrofibers, indicating a significant increase in toughness.

It is widely accepted that fibers, especially microfibers, can mitigate plastic shrinkage cracking in concrete (Nanni et al. 1993, Qi et al. 2003, Naaman et al. 2005, Banthia and Gupta 2006). Qi et al. (2003) studied the influences of a fibrillated polypropylene (PP) fiber and a coarse monofilament PP fiber on the width of plastic shrinkage cracks. Concrete mixtures were cast in grooved rigid molds as shown in Figure 1.4 and subjected to a wind velocity of 14.9 mph (24 km/h), an ambient temperature of 100.5 ± 1.5 ºF (38 ± 1 ºC), and a relative humidity of 50 ± 2% for 6 hours. The widths of cracks caused by plastic shrinkage were measured using image

analysis. Results indicate that crack width reduces with increased volume fraction of either fiber and that coarse fibers are less effective in reducing crack width than finer fibers. Naaman et al. (2005) used molds similar to the ones used by Qi et al. (2003) and subjected the specimens to a temperature of 100 ± 5 ºF (37.75 ± 2.75 ºC), a constant high flow air (wind speed not measured), and a relative humidity of 22.5 ± 2.5 %. The results showed that the addition of fibers significantly reduces the total crack length and total surface crack area (summation of the products of crack length by crack width) caused by plastic shrinkage. The volume fraction and diameter of the fiber are the most influential factors in controlling plastic shrinkage cracking. But even at the low fiber dosages (such as 0.1% by volume of concrete), the total crack area, as well as the total crack length, was noticeably reduced compared to the specimen without fibers. A volume content of 0.4% of fibers, the highest value tested in the study, was enough to completely eliminate plastic shrinkage cracking in most cases. At a given fiber volume fraction, specimens made with fibers that had smaller diameters exhibited significantly lowered total crack area. At 0.2% fiber content, specimens containing a fiber with a diameter of 0.0016 in. (0.04 mm) exhibited approximately 10% of the total plastic shrinkage cracking area of the specimens containing a fiber with a diameter of 0.0039 in. (0.1 mm).

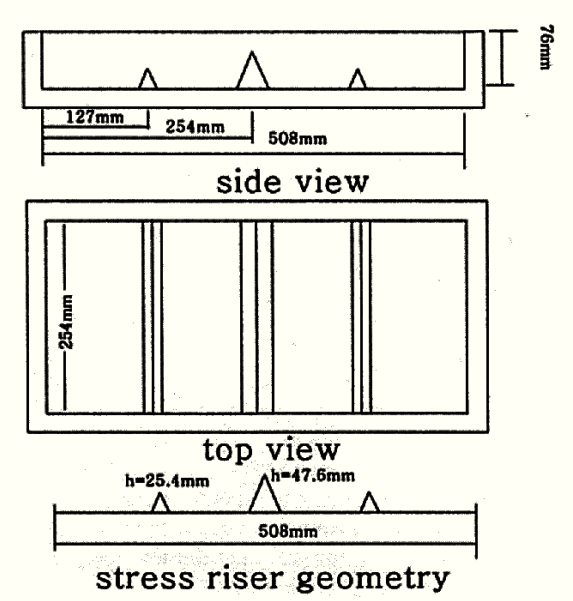

Figure 1.4 – Molds used by Qi et al. (2003). 1 in. = 25.4 mm.

Drying shrinkage cracking can be reduced with macrofibers and with hybrid fibers (Swamy and Stavrides 1979, Voigt et al. 2004, Lawler et al. 2005, Shah and Weiss 2006). Swamy and Stavrides (1979) studied the drying shrinkage cracking behavior of fiber reinforced mortar and concrete using a restrained ring test. An annulus concrete specimen was cast on the perimeter of a steel ring. As the concrete dried, shrinkage was restrained by the steel ring resulting a compressive force being applied to the ring. By monitoring the strain in the steel ring, the average stress in the concrete specimen and time to crack could be determined. The researchers showed that specimens made with fiber reinforced concrete were able to sustain significantly higher shrinkage stresses before formation of the first crack. In addition, specimens with no fiber could not sustain any further shrinkage stresses after formation of the first crack (no strain in the steel ring after concrete cracked), while the specimens with fiber continued to carry stress after the first crack appeared (compressive stress continued to be applied to the steel ring after first crack in concrete). Lawler et al. (2005) performed similar tests on specimens with hybrid fibers (steel macrofiber and steel microfiber or steel macrofiber and PVA microfiber) and found that specimens without fibers

developed only one shrinkage crack whereas the specimens containing hybrid fibers developed two or more cracks. This is because fibers can bridge across cracks and FRC continues to carry tensile stress as further shrinkage occurs. As a result, FRC specimens, albeit with greater numbers of cracks, showed lower total crack width (summation of crack widths). After 44 days of drying, the average total crack width in unreinforced concrete ring specimens was approximately 1 mm, whereas the average total width of cracks in the FRC specimens with either hybrid system were less than 0.2 mm.

The addition of fibers can have a negative effect on the workability of fresh concrete (Bayasi and Zeng 1993, Qi et al. 2003, Hassanpour 2012, Al-Qassag et al. 2015), reducing the contractor's ability to pump, work, and finish the concrete. Bayasi and Zeng (1993) investigated how the slump of concrete mixtures was influenced by fibrillated polypropylene fibers with two different lengths and at different fiber volume fractions (0, 0.1, 0.3, and 0.5%). They found that for the fiber lengths tested [½ and ¾ in. (13 and 19 mm)], slump was not significantly influenced for fiber volumes of 0.3% or less. However, at an addition rate of 0.5%, a mixture with ¾-in. (19 mm) fibers had a slump of 1 in. (25 mm) compared to 8½ in. (215 mm) for the same mixture without fibers. Similar observations were made by Al-Qassag et al. (2015), who studied how the slump of concrete mixtures changed after adding fibers. Four types of synthetic fibers were tested with fiber lengths ranging between 0.75 and 2.25 in. (19 and 57 mm). Eleven or twelve batches of concrete were made for each type of fiber, with initial slumps ranging from 4 to 10 in. (100 to 255 mm). After adding fibers, the mixtures were again tested for slump. At a fiber dosage of 0.2% by volume, the average reduction in the slump ranged from 1½ in. (38 mm) to 2¼ in. (57 mm). Additionally, one of the fibers was tested at two dosages; when the fiber volume fraction increased

from 0.1% to 0.2% of concrete, the average slump reduction after adding fibers increased from 1½ in. (38 mm) to 2 in. (51 mm).

Previous studies on the frost resistance of fiber-reinforced concrete is limited. In general, fiber reinforcement tends to not influence the durability of concrete if proper air-entrainment is present. Balaguru and Ramakrishnan (1986) studied the frost resistance of concrete mixtures containing air contents ranging from 1.2% to 10.8% and steel fiber dosage rates of 0, 75, and 100 lb/yd^3 (0, 44.4, or 59.2 kg/m^3) using ASTM C666, Procedure A. They found that the air content was the most significant parameter for freeze-thaw resistance. At similar air contents, FRC and plain concrete exhibited similar behavior. Similar observations were made by Cantin and Pigeon (1996), who tested the scaling resistance of concrete specimens with and without steel fibers in accordance with ASTM C672. Cantin and Pigeon (1996) found that the addition of fibers did not affect concrete's resistance to salt scaling. Instead, an adequate air-void system and a lower *w/cm* ratio (0.35 compared to 0.45) were found helpful in scaling resistance. It should be noted, however, that some researchers have reported both lowered or improved freeze-thaw durability in fiber-reinforced concrete with no or minimum air entrainment. Persson (2006) tested the freeze-thaw performance of concrete mixtures with and without PP fibers containing similar air contents (around 4%) and spacing factors (around 0.016 in. or 0.4 mm) using ASTM C666-92. He found that, although both mixtures with and without fibers behaved poorly in the test, the mixtures with fiber experienced a greater reduction in their dynamic moduli of elasticity (more than 70%) compared to the mixtures without fibers (approximately 10%) after 300 freeze-thaw cycles. Persson postulated that fibers affected the movement of water in the pores and hence the lowered frost resistance. Based on this, he recommended that a minimum air content of 5% be required to ensure adequate freeze-thaw durability. Berkowski and Kosior-Kazberuk (2015) tested the salt-

scaling resistance of steel fiber-reinforced, non-air-entrained concrete. Two types of steel fibers were tested, a microfiber with a diameter of 0.16 mm (0.006 in.) and a length of 6 mm (0.24 in.) and a macrofiber with a diameter of 0.55 mm (0.022 in.) and a length of 35 mm (1.38 in.). The mass losses due to scaling were significantly reduced in FRC specimens compared to the ones without fiber reinforcement. The scaling resistance of the specimens was improved when the fiber dosage increased from 0.38% to 0.76% by volume of concrete. In this test, the specimens with the micro steel fiber performed better than those with the macro steel fiber, which was attributed to the higher number of microfibers per unit volume of concrete.

1.4.4 Fiber Balling in FRC Production

Balling, the phenomenon where fibers entangle and form clumps or balls, is a common issue with FRC production. Based on longtime experience, Lloyd (2014) suggested that choosing suitable type and length of fibers is the key to reduce balling. For the same volume fraction, it is better to use a higher count of shorter fibers [1 in. (25 mm) or less] with small diameters. In general, lower fiber aspect ratio, shorter fiber length, and finer aggregate gradation will help reduce fiber balls (ACI Committee 544 2008).

In addition to the material considerations just described, it is crucial to ensure that the fibers are dispersed properly and that any clumps that have formed before addition are removed when the fibers are added. Specialized equipment, such as conveyor belts, blowers, or pneumatic tubes, can be used to improve fiber dispersion. Reducing batch size and extending mixing time also help achieve a uniform fiber dispersion (ACI Committee 544 2008).

1.5 SHRINKAGE REDUCING ADMIXTURES

1.5.1 Introduction

Shrinkage-reducing admixtures (SRAs), a group of organic surfactants that reduce the surface tension of pore solutions, provide a means to delay or minimize cracking caused by drying shrinkage (Sato et al. 1983). As shown in Figure 1.5, each surfactant (SRA) molecule consists of a hydrophilic head and a hydrophobic tail. In aqueous solutions (such as pore solutions), the hydrophilic heads are attracted by the solvent whereas the hydrophobic tails are repelled by the liquid (Schramm 2000, Myers 2005). When added to concrete, the surfactant molecules are attracted to the liquid-air interface, with the hydrophilic head in the pore solution and the hydrophobic tail in the air. The adsorption of SRA molecules at the water-air interface reduces the interfacial energy and leads to a reduction of surface tension of the interface.

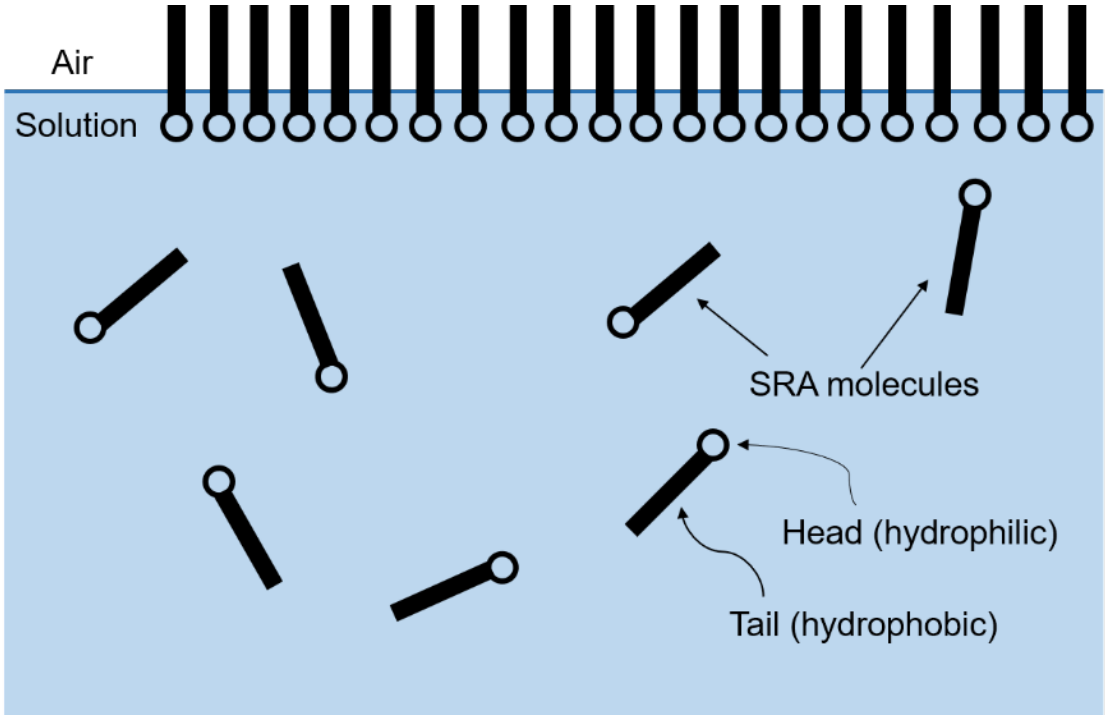

Figure 1.5 – Interaction of surfactant molecules with water. Adapted from Myers (2005)

As discussed in Section 1.3.3, when the water-air interface recedes due to evaporation, the interaction between the pore walls and water induces capillary stresses that cause shrinkage. Reducing the surface tension γ of the pore solution lowers the capillary stress σ_{cap}, which in turn reduces the shrinkage accompanying the loss of water. The strain ε caused by capillary stresses of concrete can be approximated as

$$\varepsilon = \frac{s \cdot \sigma_{cap}}{3} \cdot \left(\frac{1}{K} - \frac{1}{K_s}\right) \tag{1.3}$$

where s is the degree of saturation (%), σ_{cap} is the capillary stress (Pa), K is the bulk modulus of dry concrete (Pa), and K_s is the bulk modulus of the solid framework within concrete (Pa) (Bentz et al. 1998). Combining Eq. (1.1) and (1.3) gives

$$\varepsilon = \frac{2 \cdot s \cdot \gamma}{3 \cdot r} \cdot \left(\frac{1}{K} - \frac{1}{K_s}\right) \tag{1.4}$$

As shown in Eq. (1.5), drying shrinkage strain ε is directly proportional to the surface tension of the pore solution. Therefore, the addition of an SRA can reduce the shrinkage associated with loss of water.

1.5.2 Influence of SRAs on Concrete Properties

The effectiveness of SRAs in reducing the surface tension of concrete pore solution and subsequent drying shrinkage is well-documented. Weiss et al. (2008) measured how the addition of an SRA influenced the surface tension of deionized (DI) water and synthetic pore solution (0.35 M KOH + 0.05 M NaOH in DI water). They found that the surface tension of the solution can be reduced by up to 50% when an SRA is added and that the magnitude of the reduction increases as the concentration of SRA increases before reaching a plateau (critical micelle concentration). The addition of an SRA beyond the critical concentration does not further reduce

the surface tension of the solution because the surfactant molecules start to aggregate and form micelles instead of adsorbing to the surface. Pendergrass and Darwin (2014) evaluated the free shrinkage behavior of mixtures containing two SRAs at the dosages of 0%, 0.5%, 1.0%, or 2.0% by weight of cement. They observed that the drying shrinkage during the first 90 days of exposure was, in general, progressively reduced with increased SRA dosage. The drying shrinkage of the mixtures containing 2% SRA by weight of cement was reduced by as much as 31.8% compared to the mixture with without an SRA.

It has been reported that the addition of an SRA reduces the strength of concrete. For mixtures containing 0, 0.5%, 1.0%, and 2.0% of SRA by weight of cement, Pendergrass and Darwin (2014) found that concrete containing a surfactant-based air entraining admixture and an SRA experienced reduced strength as the SRA dosage increased (up to 14.7% strength reduction when 2% SRA was added). It should be noted, however, that the difference in strength was statistically significant only when the SRA dosage difference between two mixtures was 1.0% or greater. Brooks and Jiang (1997) observed that a 1.5% addition of SRA by weight of cement not only reduced the compressive strength by 28%, but also reduced the direct tensile strength by 30% to 40%. Folliard and Berke (1997) observed a 20% reduction in one-day concrete strength when an SRA was added at 1.5% by weight of cement. After 7 days of curing, however, the strength reduction associated with SRA addition decreased to and stabilized around 7% until the end of the study (90 days of curing). Rajabipour et al. (2008) postulated that SRAs reduce concrete strength by lowering the rate of hydration and strength gain, especially in early ages. They observed a significantly reduced concentration of alkali sulfates in the pore solutions extracted from specimens containing an SRA up to 20 hours of age. Since alkali sulfates in the pore solution

accelerate the hydration of cement, a lower concentration effectively slows hydration at early ages and the strength development is slowed when an SRA is used.

The air-void system in concrete is usually less stable when an SRA is used, and as a result, the concrete may exhibit reduced freeze-thaw durability. The reason is that SRAs and air-entraining admixtures (AEA) are both surfactants (Mindess et al. 2003, Du and Folliard 2005), and when an SRA is added to air-entrained concrete, the combined effects of the SRA and AEA on the surface tension of water in plastic concrete may result in the formation of larger air voids. At the same air content of concrete, mixtures with larger air voids will have greater spacing between the voids, which negatively influences the freeze-thaw performance of concrete. Furthermore, it has been shown that concrete mixtures containing an SRA tend to lose more entrained air after discharge from mixers than mixtures without an SRA, further reducing their frost resistance. Schemmel et al. (2000) measured changes in air content in fresh concrete when an SRA was added. After being discharged from mixer, the concrete was tested for air content every 3 to 5 minutes. During the tests, efforts were made to avoid disturbance to the remaining concrete. Schemmel et al. (2000) reported that approximately 25 minutes after discharge, concrete containing 1.5% SRA by weight of cement lost about 15% of its air content while a similar mixture without an SRA lost only 5%. Cope and Ramey (2001) reported that when an SRA was added at 1.5% by weight of cement, the air content in concrete was reduced resulting in a need to more than double the air-entraining admixture dosage to achieve the standard specified Alabama DOT bridge deck concrete requirement of 3% to 5%. Additionally, despite a similar air content, the mixture containing the SRA exhibited significantly more mass loss compared to the standard Alabama DOT mixture when subjected to freezing and thawing cycles. Pendergrass et al. (2017) observed that for mixtures with the same air content in plastic concrete, the total air content in hardened concrete decreased and

the average distance between air voids (spacing factor) increased as the SRA dosage increased. Subsequent scaling resistance and freeze-thaw durability tests revealed that the loss of air resulted in compromised durability performance.

1.5.3 Application in Concrete Structures

The propensity for concrete to crack due to restrained shrinkage depends on the complex interactions between volume change, creep, tensile strength, modulus of elasticity, and degree of restraint. Thus, results from laboratory tests cannot always provide information that is sufficient to determine the cracking potential of a concrete member or structure. This section describes recent efforts to evaluate the cracking performance of concrete mixtures with SRAs in large-scale specimens or actual bridge decks.

Brown et al. (2007) evaluated the crack-reducing ability of various technologies, including SRAs, using both laboratory and large-scale tests. Restrained ring tests showed that even though a mixture containing 1.5 gallon/yd^3 (7.4 L/m^3) of SRA had 27% lower tensile strength and a similar elastic modulus to the mixture without an SRA, the restrained ring specimens containing the SRA mixture did not crack during the full test period (more than 590 days), while the specimens without an SRA cracked after an average of 38 days. For the large-scale tests, 20 × 9.8 ft (6.1 × 3 m) rectangular, 4 in. (101 mm) thick specimens were used to represent two single-span cast-in-place concrete decks, one with and one without concrete containing an SRA. The specimens were heavily restrained at both two ends and contained no reinforcement in the middle of the span. The specimens were stored outdoors. During the first three weeks of exposure, the ambient temperature ranged between 70 and 97 ºF (21 and 36 ºC) and the relative humidity ranged between 30% and 92%. The specimen without the SRA developed drying shrinkage cracks within 16 days of casting,

while the specimen with the SRA did not crack, demonstrating the improvement in cracking performance with the addition of SRA.

The Washington State Department of Transportation (WSDOT) switched to a performance-based specification in 2011 that allowed the use of an SRA to achieve a specified 28-day shrinkage not exceeding 320 microstrain. Ferluga and Glassford (2015) surveyed 27 bridges, of which 15 were constructed using the performance-based specification and contained an SRA and 12 were constructed using the traditional specification without an SRA. The bridges containing an SRA exhibited significantly fewer cracks underneath the deck than those constructed without an SRA. Of the fifteen bridges constructed with an SRA, six had a crack intensity less than or equal to 1 crack per 100 ft (30 m) of deck length, eight had 2 to 5 cracks per 100 ft (30 m), and one had 18 cracks per 100 ft (30 m). In contrast, of the twelve bridges without an SRA, three had 5 or fewer cracks per 100 ft (30 m), six had 6 to 20 cracks per 100 ft (30 m), and three had 22 to 36 cracks per 100 ft (30 m). It should be noted that the cracks were identified based on efflorescence underneath the deck and the lengths of the cracks were not considered. Also, the traditional mix design had a minimum cementitious material content of 735 lb/yd^3 (436 kg/m^3), and this limit was removed for the performance-based specification. As a result, the cementitious material content in the SRA bridges ranged between 565 and 611 lb/yd^3 (335 and 363 kg/m^3). The significant reduction in cementitious material quantity, and accompanying reduction in paste content, likely contributed to the lower crack intensity, aside from the addition of SRA.

1.6 LOW-CRACKING HIGH-PERFORMANCE CONCRETE

1.6.1 Introduction

Through a series of studies performed at the University of Kansas (Schmitt and Darwin 1995 and 1999, Darwin et al. 2004, Lindquist et al. 2005), specifications for low-cracking high-

performance concrete (LC-HPC) were developed to help minimize cracking and improve the overall durability of bridge decks. Between 2005 and 2011, 16 bridges were constructed in Kansas under the LC-HPC specifications. The specifications are modifications of the Kansas Department of Transportation (KDOT) Standard Specifications for State Road and Bridge Construction and included requirements for aggregate, concrete, and construction procedures known to minimize bridge deck cracking. The LC-HPC specifications have been updated to address lessons learned in the field and, to a lesser extent, incorporate laboratory findings. The latest LC-HPC specifications are included in Appendix A. Eleven bridges constructed during the same period using the standard KDOT specifications served as control decks. The control decks had similar design, traffic volume, and environmental conditions as their associated LC-HPC decks and were included in the study to help evaluate of the effectiveness of LC-HPC specifications.

This section compares some key aspects of the LC-HPC specifications with the specifications used for control decks and compares the cracking performance of LC-HPC bridge decks and their associated control decks.

1.6.2 Specifications

As previously stated, the LC-HPC specifications consist of three individual documents governing aggregate, concrete, and construction. For aspects of construction not covered by the LC-HPC specifications, the standard KDOT specifications govern.

1.6.2.1 Aggregate

Table 1.1 summarizes the requirements for aggregate in the control and LC-HPC decks.

Table 1.1 – Requirements for aggregate in control and LC-HPC decks

Specification	Control	LC-HPC
Maximum absorption for coarse aggregate	2.0% or 0.7%	0.7%
Maximum size of mixed aggregate	¾ in.	1 in.
Proportioning of coarse and fine aggregate	50%-50% by weight	optimized

Note: 1 in. = 25.4 mm.

The upper limit on absorption of coarse aggregate for control decks is 2.0%. Five control decks, however, have a project-specific provision that limits the absorption to 0.7%. The LC-HPC specification requires a maximum absorption for coarse aggregate of 0.7%. The goal of using low absorption was to provide the concrete with an improved durability and reduce slump loss over time and when pumping concrete (Yuan et al. 2011); it was not selected based on its effect on shrinkage.

According to the LC-HPC specification, aggregate gradation must be selected using a proven optimization method, such as the Shilstone Method or the KU Mix Method (Lindquist et al. 2008, Lindquist et al. 2015), to select the proportions of fine and coarse aggregate. In contrast, the specifications for control decks call for a weight ratio of 50%-50% for coarse and fine aggregate (a "50-50 mix"). Optimized aggregate gradations have been shown to improve the workability, pumpability, and cohesiveness of concrete (Quiroga and Fowler 2003, Darwin et al. 2012, Lindquist et al. 2015), allowing the contractor to use concrete with a lower paste content, which can help lower the shrinkage of concrete.

The LC-HPC specification requires that the maximum size of aggregate (MSA) to be 1 in. (25 mm). When a limestone or granite is used as coarse aggregate, the standard KDOT specification limits the maximum size of coarse aggregate to ¾ in. (19 mm). Larger aggregate particles have a lower surface-to-volume ratio. Therefore, for the same aggregate volume fraction, less cement paste is required to cover aggregate surfaces. This allows the contractor to use concretes with lower paste contents while maintaining workability.

1.6.2.2 Concrete

Table 1.2 summarizes the requirements for concrete in the specifications for the control and LC-HPC decks.

Table 1.2 – Requirements for concrete in control and LC-HPC decks

Specification	Control	LC-HPC
Minimum Cementitious Materials Content (lb/yd^3)	602	500
Maximum cement content (lb/yd^3)	not specified	540
w/cm	0.40 or 0.44	0.44 to 0.45
Air content (%)	5 to 8	7 to 9
Allowable concrete temperature (°F)	50 to 90	50 to 75
Minimum 28-day strength (psi)	4500 or 4000	3500
Maximum 28-day strength (psi)	not specified	5500

Note: 1 lb/yd^3 = 0.59 kg/m3, °C = (°F - 32) × 5/9, 1 psi = 6.89 KPa.

The LC-HPC specification for concrete limits the cement content to 500 to 540 lb/yd^3 (297 to 320 kg/m^3). The specifications for control decks require a minimum cement content of 602 lb/yd^3 (357 kg/m^3). In practice, the control decks have cement contents ranging between 600 and 611 lb/yd^3 (356 and 362 kg/m^3) when only cement is used as the cementitious material. Additionally, five control decks contained fly ash as well as cement and have cementitious materials contents of 667 or 668 lb/yd^3 (396 kg/m^3).

The LC-HPC specifications require a *w/c* ratio between 0.44 and 0.45. In comparison, all but one control deck have a *w/cm* ratio of 0.40 (the exception has a *w/cm* ratio of 0.44). The LC-HPC specifications limit both the maximum (5500 psi, 37.9 MPa) and minimum (3500 psi, 24.1 MPa) concrete strengths, while the concrete mixtures in control decks were designed for a *minimum* 28-day concrete compressive strength of 4500 psi (31.0 MPa, 10 decks) or 4000 psi (27.6 MPa, 1 deck). There is no limit on the maximum concrete strength for control decks. An unnecessarily high concrete strength limits creep, which limits relief in tensile stresses caused by restrained shrinkage (Darwin et al. 2012).

The LC-HPC specifications require all mixing water to be added at the plant while the standard KDOT specification allows up to 2 gallons/yd^3 (10 L/m^3) of water to be withheld from the mixture at the plant. In addition, set retarding or accelerating admixtures are prohibited in LC-HPC.

The concretes in control decks are designed with a target air content range of 5% to 8%, while the LC-HPC specifications call for an air content between 7% and 9%. This change was made because higher air contents were associated with reduced cracking. The designated slump range for LC-HPC is 1½ to 3 in. (40 to 75 mm), while the maximum allowable slump for control decks is 7 in. (180 mm). The significantly reduced slump range for LC-HPC was selected to limit settlement cracking. The concrete temperature at the time of placement for LC-HPC must be between 55 and 70 °F (13 and 21 °C). With the approval of the Engineer, this range can be extended by 5 °F (3 °C), both above and below. The standard KDOT specifications allow a concrete temperature range of 50 to 90 °F (10 to 32 °C). The maximum allowable concrete temperature is reduced in the LC-HPC specifications to help reduce plastic shrinkage and thermal cracking.

1.6.2.3 Construction

A qualification slab must be constructed 14 to 45 days prior to placing LC-HPC in the bridge deck to demonstrate that the concrete supplier and the contractor can properly produce, place, finish, and cure LC-HPC. The same personnel, equipment, and methods must be used on both the qualification slab and the bridge deck. The Engineer will evaluate the contractor's performance in placing, consolidating, finishing, and curing the qualification slab and then grant or deny approval to proceed.

During construction, the evaporation rate must be less than 0.2 lb/ft^2/hr (1.0 kg/m^2/hr). To determine the evaporation rate, the air temperature, concrete temperature, wind speed, and relative humidity must be measured just prior to and once per hour during the placement of LC-HPC. When the evaporation rate exceeds 0.2 lb/ft^2/hr (1.0 kg/m^2/hr), actions must be taken to slow down the loss of moisture, such as cooling the concrete and installing wind breaks.

LC-HPC may be placed using a conveyor belt, concrete bucket, or pump. However, pumping is allowed only if the contractor can show proficiency to place the concrete when placing the qualification slab using the same pump to be used for the bridge. Special precautions must be taken to avoid excessive loss of air. The maximum drop of concrete is 5 ft (1.5 m). When a pump is used, it must be equipped with an air cuff or bladder valve.

LC-HPC bridge decks must be consolidated using a mechanical device on which internal concrete vibrators with the same type and size are mounted. Areas that cannot be accessed by the mechanical device must be consolidated using handheld vibrators. The vibrators must be inserted in concrete for 3 to 15 seconds, and the insertions must proceed in the direction of concrete placement in steps less than 12 in. Vibrators should be smoothly extracted so that no voids or holes are left in LC-HPC. Any voids left by workers should be removed by reconsolidation.

LC-HPC must be struck off with a vibrating screed or single-drum roller screed and finished by a burlap drag, a metal pan, or both. A bullfloat may be used behind the burlap drag or metal pan to remove local irregularities. LC-HPC specifications prohibit using water or a finishing aid on the surface while finishing. The standard KDOT specification allows the addition of water as a fog spray upon approval of the Engineer. Tining is not allowed on plastic LC-HPC.

The LC-HPC specifications require that a first layer of burlap be placed on the deck surface within 10 minutes from strike-off followed by a second layer within 5 minutes. The burlap must be soaked for at least 12 hours prior to placement. Concrete must be cured for 14 days, during which time the burlap must be maintained in a fully wet condition, which can be achieved using misting hoses or other fogging equipment before LC-HPC is set and soaker hoses afterwards.

1.6.3 LC-HPC Performance

Of the 16 bridge decks constructed in Kansas between 2005 and 2011, 13 are associated with 11 corresponding control bridges (in two cases, two LC-HPC bridges are paired with the same control bridge). The control decks have similar structural design, traffic flow, and construction date to the LC-HPC decks. Construction records that include material properties, environmental conditions, and construction practices, as well as results from multiple crack surveys on the bridges, are reported by Lindquist et al. (2008), McLeod et al. (2009), Darwin et al. (2010), Yuan et al. (2011), Darwin et al. (2012), Pendergrass and Darwin (2014), and Darwin et al. (2016).

In the final series of surveys (Darwin et al. 2016), the crack densities of bridge decks were compared at an age at or around 96 months. Compared to their paired control bridges, 11 out of 13 LC-HPC bridges had less cracking. In the two cases where the LC-HPC deck exhibited higher crack densities than the control deck, the differences in their cracking performance were small and the control decks were the best-performing among all the control bridges included in this study. Further analyses of the results show that the lowered paste volume, controlled compressive strength, concrete temperature control, and minimized concrete finishing operations help minimize cracking in bridge decks (Khajehdehi et al. 2018).

1.7 OBJECTIVE AND SCOPE

The adverse influence of cracking on bridge durability is well documented. By regulating the aggregate attributes, mixture design, concrete properties, and construction practices, the low-cracking high-performance concrete (LC-HPC) specifications have been shown to reduce bridge deck cracking in multiple studies. The work presented herein evaluates the effectiveness of emerging technologies, including shrinkage-reducing admixtures (SRA), internal curing (IC), and fiber-reinforced concrete (FRC), in reducing bridge deck cracking.

1.7.1 Shrinkage and durability performance of mixtures containing various dosages of internal curing water and with or without shrinkage-reducing admixtures or shrinkage-compensating admixtures

Laboratory tests are performed to evaluate how the quantity of internal curing water affects the shrinkage and durability performance of concrete mixtures containing slag cement and silica fume as partial replacements of cement. The quantities of internal curing water provided by pre-wetted lightweight aggregate were 0%, 5.3%, 6.5%, and 9.7% by weight of cementitious materials. Additional concrete mixtures with internal curing, slag cement, and a shrinkage-reducing admixture or a shrinkage-compensating admixture were also evaluated. The mixtures were evaluated based on drying shrinkage, freeze-thaw resistance, and scaling resistance.

1.7.2 Documentation, evaluation, and analysis of bridge decks constructed with fiber-reinforced concrete or with shrinkage-reducing admixtures

The field evaluation of cracking are presented for 10 bridge deck placements containing fiber-reinforced concrete, six associated control deck placements without fiber reinforcement, four bridge decks containing SRAs, and one control deck without an SRA. The construction procedures and weather conditions, as well as aggregate properties, mixture proportions, and concrete properties, of the FRC and control bridges without FRC are presented. Combining the information obtained prior to and during construction, the factors influencing the cracking behavior of bridge decks are identified based on these comparisons.

1.7.3 Evaluation and analysis of factors affecting bridge deck cracking

The crack density at 36 months of deck age for 74 bridge deck placements are used to analyze the factors that affect bridge deck cracking. The factors analyzed include the paste content of the concrete mixture, the use of crack-reducing technologies (including internal curing, fiber

reinforcement, and shrinkage-reducing admixtures), and the construction practices used by contractors.

CHAPTER 2: SHRINKAGE AND DURABILITY OF CONCRETE MIXTURES WITH INTERNAL CURING, SHRINKAGE-REDUCING ADMIXTURES, AND SHRINKAGE-COMPENSATING ADMIXTURES

2.1 INTRODUCTION

Cracking is a major durability problem that reduces the service life of reinforced concrete bridge decks (Mindess et al. 2003). A main cause of cracking in bridge decks is the restrained drying (Schmitt and Darwin 1999, Darwin et al. 2004).

Over the past decade, internal curing (IC) using pre-wetted lightweight aggregate (LWA) has become a popular tool to reduce shrinkage-induced cracking. Lightweight aggregate is highly porous and has relatively large pores. As drying starts, water is preferentially drawn from the LWA rather than the capillary pores in cement paste (Bentz and Weiss 2011, Choi 2017). As a result, the addition of pre-wetted LWA reduces shrinkage. As shown by Ibrahim et al. (2019), internal curing also reduces settlement cracking. The effectiveness of internal curing with LWA in reducing shrinkage and cracking has been widely reported (Wei and Hansen 2008, Bentz and Weiss 2011, Lafikes et al. 2018, Pendergrass et al. 2018). The influence of the quantity of internal curing water (water absorbed in LWA) on the drying shrinkage of typical bridge deck concretes, however, has not been thoroughly studied. ASTM C1761-17, *Standard Specification for Lightweight Aggregate for Internal Curing of Concrete*, recommends that the quantity of the water contained in LWA be 7% by weight of cementitious material; this recommendation, however, is based on reducing autogenous shrinkage, which is only observed in concretes with low water-cementitious material (*w/cm*) ratios (Mindess et al. 2003). Browning et al. (2011) studied drying shrinkage of concrete mixtures with portland cement as the sole cementitious material using vacuum-saturated LWA providing 5.7%, 7.7%, and 9.4% of internal curing water by weight of cement and found that the

addition of internal curing reduces drying shrinkage that occurred at the early ages (30 days) and in the long-term (365 days). Research is still needed to evaluate how the quantity of internal curing water influences the shrinkage of concrete mixtures with supplementary cementitious materials at moderate water-to-cementitious material (*w/cm*) ratios. Following ASTM C157, Jones (2014) studied the drying shrinkage of concrete mixtures with 20% fly ash by weight of cementitious materials, a *w/cm* ratio of 0.42, and 0%, 6.3%, and 12.6% of IC water by weight of cementitious material. Jones (2014) found that mixtures with IC exhibited lower drying shrinkage than the mixture with no IC water but noted that ASTM C157 cannot account for early age shrinkage and further tests should be performed.

Freeze-thaw durability and scaling resistance of internally cured concrete can be harmed if the *w/cm* (or water-cement, *w/*c) ratio of the concrete mixture is too high or if water is trapped in LWA during freeze-thaw cycles, which can occur or if an excessive quantity of IC water is provided. Jones and Weiss (2015) studied the freeze-thaw durability of concrete mixtures with approximately 6.4% of internal curing water and 20% fly ash by weight of cementitious material, but different *w/cm* ratios, and found that the mixture with the highest *w/cm* ratio (0.56) exhibited noticeable freeze-thaw damage while the mixtures *w/cm* ratios between 0.36 and 0.48 performed satisfactorily in the test. Lafikes et al. (2018) performed field surveys on seven bridge deck placements containing internal curing and observed scaling and freeze-thaw damage on those with 8.5% or more (up to 12%) IC water by weight of cementitious material and *w/cm* ratios of 0.40 to 0.42, despite the relatively young deck ages (11 to 37 months when surveyed). A bridge deck with 7.2% IC water by weight of cementitious material and a *w/c* ratio of 0.39, on the other hand, did not exhibit observable scaling or freeze-thaw damage at an age of 72 months. Laboratory tests are needed to study the freeze-thaw durability and scaling resistance of concrete mixtures containing

various quantities of internal curing water including those containing supplementary cementitious materials, such as slag cement and silica fume.

Combining internal curing with supplementary cementitious materials (SCMs) and shrinkage-reducing admixtures (SRAs) or shrinkage-compensating admixtures (SCAs) can further reduce concrete shrinkage (Zhutovsky et al. 2010, Khajehdehi et al. 2018). Khajehdehi et al. (2018), for example, studied the long-term drying shrinkage of concrete mixtures containing slag cement and silica fume, internal curing, SCAs, or combinations of these. Khajehdehi et al. (2018) observed that, when used separately, SCM, IC, and SCAs can effectively reduce shrinkage after 180 days of drying; the greatest shrinkage reduction, however, was observed in a mixture containing a combination of IC, SCM, and an SCA. Research, however, is needed to evaluate the freeze-thaw durability of concrete mixtures with internal curing, SCMs, and SRAs or SCAs.

In this study, concrete mixtures containing slag cement, silica fume, and various quantities of internal curing were evaluated for shrinkage, scaling resistance, and freeze-thaw durability. Additionally, the scaling resistance and freeze-thaw durability of concrete mixtures containing slag cement, silica fume, internal curing, and a shrinkage-reducing admixture or a shrinkage-compensating admixture were evaluated.

2.2 EXPERIMENTAL WORK

2.2.1 Materials

All mixtures in this study contained Type I/II cement. Grade 100 slag cement and silica fume were used in some mixtures as volume replacements of portland cement. The chemical components and properties of cementitious materials are listed in Table 2.1.

Table 2.1 – Chemical composition and specific gravity of cementitious materials

		Cement	Slag Cement	Silica Fume
Component (%)	SiO_2	20.05	34.92	94.49
	Al_2O_3	4.46	7.64	0.07
	Fe_2O_3	3.33	0.69	0.10
	CaO	62.87	40.94	0.53
	MgO	2.10	10.25	0.62
	SO_3	2.68	2.72	0.11
	Na_2O	0.22	0.30	0.09
	K_2O	0.52	0.55	0.54
	TiO_2	0.27	0.37	-
	P_2O_5	0.09	0.01	0.07
	Mn_2O_3	0.10	0.53	0.02
	SrO	0.25	0.05	0.01
	Cl^-	0.01	0.05	0.05
	BaO	-	0.02	-
	LOI	3.43	0.97	3.21
	Total	100.38	100.01	99.91
Specific Gravity		3.15	2.86	2.20

Two types of granite, with maximum sizes of 1 and ¾ in. (25 and 19 mm), were used as coarse aggregates. The absorption and bulk specific gravity in the saturated-surface dry or SSD condition of the 1 in. (25 mm) granite were 0.50% and 2.61; those for the ¾ in. (19 mm) granite were 0.58% and 2.60. River-run sand and pea-gravel were used as fine aggregates. The sand had a specific gravity (SSD) of 2.62 and an absorption of 0.47%; the pea gravel had a specific gravity (SSD) of 2.63 and an absorption of 1.42%. Internal curing was achieved by replacing normalweight aggregate with lightweight aggregate (LWA). The LWA was soaked for 72 hours prior to batching, which resulted in an absorption of 23.99% and a specific gravity in the pre-wetted surface dry (PSD) condition of 1.72.

A shrinkage-reducing admixture (SRA) or a shrinkage-compensating admixture (SCA) was added to some mixtures. SRAs reduce the surface tension of the pore solution and, therefore, reduce drying shrinkage of concrete. Two types of SCA were used in this study. The active component of SCA 1 is MgO, which forms $Mg(OH)_2$ and expands as it reacts with water. SCA 1 also contains a shrinkage-reducing admixture. SCA 2 mainly consists of CaO, which reacts with

water to form $Ca(OH)_2$, and, like $Mg(OH)_2$, causes expansion. A tall oil-based air-entraining admixture (AEA) was used in all mixtures to achieve the desired air content. A polycarboxylate-based high-range water-reducing admixture (HRWRA) was used when necessary to achieve the desired concrete slump.

2.2.2 Concrete Mixtures

Eleven mixtures were used to evaluate the influence of cementitious materials, chemical admixtures, and the quantity of internal curing on drying shrinkage, freeze-thaw durability, and scaling resistance of concrete. The proportions of the concrete mixtures in this study are listed in Table 2.2. The mixture designated as "Control" contains portland cement as the only cementitious material, with no addition of LWA, SRA, or SCA. The mixture designated as "Slag" contains a 30% volume replacement of cement with slag cement. The mixtures with "SCM" in the designation contain volume replacements of cement by 30% and 3% slag cement and silica fume, respectively. Mixtures with "IC" in the designation contain internal curing provided by the addition of prewetted LWA. Internal curing is quantified by the ratios between the weight of IC water contained in the LWA and the weight of cementitious material in the mixture, expressed as percentages (%). For example, the mixture "6.5% IC-SCM" contains 6.5% internal curing water by weight of cementitious material. In this study, the quantity of internal curing water ranges from 5.3% to 9.7% by weight of cementitious material. The mixtures with "SCA 1" and "SCA 2" in the designation contain 7.5% SCA 1 and 6% SCA 2 by weight of cementitious material, respectively. The mixtures with "SRA" in its designation contain the SRA with a dosage of 1% by weight of cementitious material. Two mixtures containing 6.5% IC, SCM, and SRA were tested; the designation of the second mixture has a suffix (2).

Table 2.2 – Mixture proportions (lb/yd^3)

Mixture	Cement	Silica Fume	Slag Cement	Water	LWA	1 in. Granite	¾ in. Granite	Sand	Pea Gravel	SCA/SRA %*
Control	520	0	0	234	0	477	964	1035	540	-
Slag	384	0	150	231	0	718	746	1138	379	-
SCM	368	12	151	234	0	552	841	1049	569	-
6.5% IC	520	0	0	234	176	529	818	1235	129	-
5.3% IC-SCM	378	11	151	238	147	582	780	1164	206	-
6.5% IC-SCM	378	11	151	238	182	537	848	1147	153	-
9.7% IC-SCM	378	11	151	238	272	604	747	1185	0	-
6.5% IC-SCM-SCA 1	362	11	147	234	176	529	818	1235	129	7.5%
6.5% IC-SCM-SCA 2	362	11	147	234	176	529	818	1235	129	6%
6.5% IC-SCM-SRA	362	11	147	234	176	529	818	1235	129	1%
6.5% IC-SCM-SRA (2)	362	11	147	234	176	529	818	1235	129	1%

Note: 1 lb/yd^3 = 0.59 kg/m^3; 1 in. = 25.4 mm.
* By weight of cementitious material in the mixture.

Concrete properties are summarized in Table 2.3. This study is part of a broader research project at the University of Kansas to develop low-cracking high-performance concrete (LC-HPC) for bridge decks. Therefore, all mixtures except one had relatively high air contents (6.75% to 9%) and moderate slumps (1 to 3¾ in., or 25 to 95 mm). Mixture 6.5% IC-SCM-SRA (2) had an air content of 5.00%. The 28-day compressive strength ranged from 4540 to 5440 psi (31.3 to 37.5 MPa). The water-to-cementitious material (*w/cm*) ratio was 0.44 or 0.45, and the paste content, the volume fraction of cementitious materials and water in the mixture, ranged from 23.7% to 24.7%. The small range of paste content was selected to minimize the influence of paste content on concrete shrinkage.

Table 2.3 – Concrete Properties

Mixture	Air Content %	Slump in.	Temperature °F	Unit Weight lb/ft^3	Strength psi	IC Water %*	Paste Content	*w/cm* Ratio
Control	7.50	3	74	140.8	5060	0	23.7%	0.45
Slag	8.00	3	62	141.7	5050	0	24.1%	0.44
SCM	8.00	3¾	70	-	4660	0	24.3%	0.44
6.5% IC	7.75	1	74	140.4	4580	6.5	23.7%	0.45
5.3% IC-SCM	6.75	2¼	73	140.2	4540	5.3	24.7%	0.44
6.5% IC-SCM	9.00	2¾	69	135.5	4880	6.5	24.7%	0.44
9.7% IC-SCM	8.50	2¾	71	135.4	4920	9.7	24.7%	0.44
6.5% IC-SCM-SCA 1	7.25	1½	74	136.7	5440	6.5	24.1%	0.45
6.5% IC-SCM-SCA 2	7.75	1¾	65	139.6	5000	6.5	24.1%	0.45
6.5% IC-SCM-SRA	7.75	3	74	138.5	5420	6.5	24.1%	0.45
6.5% IC-SCM-SRA (2)	5.00	2.5	74	136.7	5440	6.5	24.1%	0.45

Note: 1 in. = 25.4 mm; °C = (°F - 32) × 5/9; 1 lb/yd^3 = 0.59 kg/m^3; and 10 psi = 0.069 MPa.
- = data not obtained.
* By weight of cementitious material in the mixture.

2.2.3 Free Shrinkage Test

The length change of concrete mixtures during curing and under drying conditions was measured following a procedure based on ASTM C157-17, *Standard Test Method for Length Change of Hardened Hydraulic-Cement Mortar and Concrete*.

Three specimens with dimensions of 3 × 3 × 11.25 in. (76 × 76 × 286 mm) were made for each concrete mixture to measure length change. The only exceptions were mixtures Control and SCM, for which only two specimens were made for the free shrinkage test. After being demolded and measured for initial length 5½ ± ½ hours after casting, a deviation from ASTM C157, the specimens were cured in lime-saturated water until they reached an age of 14 days. After curing, the specimens were stored for 365 days in a controlled environment at a temperature of 73° ± 3°F (23°± 2°C) and a relative humidity of 50 ± 4%. The deformation of the specimens was measured two to seven times the day of casting, daily during the rest of the 14-day curing period and the first 30 days of drying, every second day between the 31st and 90th days of drying, weekly between the 91st and 180th days of drying, and monthly between the 181st and 365th days of drying.

The specimens were demolded 5½ ± ½ hours after casting, instead of 23½ ± ½ hours after the addition of mixing water, as specified in ASTM C157, to capture the deformations, notably expansion, that occur at early ages, which is of particular interest for mixtures that contain SCAs. The procedure was used by Khajehdehi et al. (2018), who found that, for mixtures containing SCA 2, specimens demolded and measured early exhibited more than 200 microstrain of expansion during the first day of curing, a deformation that was not captured with the specimens demolded 23½ ± ½ hours after the addition of mixing water. The specimens containing SCA 2 that were demolded 5½ ± ½ hours after casting exhibited approximately 320 microstrain of expansion at the end of the 14-day curing period; while those demolded following ASTM C157 exhibited only about 150 microstrain of expansion.

2.2.4 Scaling Test

Tests for the resistance of concrete mixtures to surface scaling due to freeze-thaw cycles in the presence of deicing salts were based on Canadian test BNQ NQ 2621-900 Annex B.

Three 16 × 9 × 3 in. (406 × 229 × 76 mm) specimens were cast for each concrete mixture. The specimens were demolded 23½ ± ½ hours after casting and cured in lime-saturated water for 14 days. The specimens were then stored for 14 days in a drying room maintained at 73° ± 3°F (23° ± 2°C) and a relative humidity of 50 ± 4%. During the 14-day drying period, polystyrene foam dikes were attached to the upper surface using a polyurethane sealant to maintain a brine pond on top of the specimen, as shown in Figure 2.1. Starting at the end of the 14-day drying period, the top surface of specimens was covered with approximately ¼ in. (6 mm) of 2.5% NaCl solution and stored in the drying room for another 7 days. The 2.5% NaCl solution was used in place of the BNQ NQ 2621-900 specified value of 3% based on the work by Verbeck and Klieger (1957), who evaluated the effect on scaling of 0, 2%, 4%, 8%, and 16% NaCl solutions and concluded that the

solutions with 2% and 4% NaCl caused the most surface scaling. Based on the slopes of the curve fitting the data reported by Verbeck and Klieger (1957), a solution with a concentration just above 2%, instead of one midway between 2% and 4%, would cause the most severe scaling damage.

At an age of 35 days, the specimens were exposed to freezing-and-thawing cycles consisting of a 16-hour (± 1 hour) freezing phase at 0° ± 5°F (-18° ± 3°C) followed by an 8-hour (± 1 hour) thawing phase at 73° ± 3°F (23° ± 2°C). The mass lost due to surface scaling was measured after 7, 21, 35, and 56 freeze-thaw cycles. At the end of the thawing phase, the saline solution was transferred to a bowl, and the top surface of specimens were flushed to remove any loose particles that had scaled off during freeze-thaw cycles. The brine solution and the materials flushed from the specimens were then wet-sieved over a No. 200 (75 μm) sieve; the particles retained on the sieve were dried in an oven for 24 hours at 221°F (105°C) and then weighed. The mass loss due to scaling was expressed in pound of mass loss per square foot of surface area (lb/ft^2). Mixtures with less than 0.2 lb/ft^2 (1 kg/m^2) of mass loss are considered acceptable by BNQ NQ 2621-900; this value, however, is for specimens tested with 3% NaCl solutions. As discussed, a 2.5% NaCl solution will cause more damage and specimens with mass losses slightly above 0.2 lb/ft^2 (1 kg/m^2) in this study may have been able to pass the test had a 3% NaCl solution been used.

Figure 2.1 – Scaling specimen with polystyrene foam dikes attached

2.2.5 Freeze-Thaw Durability Test

To monitor damage caused by rapid freezing-and-thawing cycles, specimens were cured following the regime in Kansas Department of Transportation (KDOT) Test Method KTMR-22, *Resistance of Concrete to Rapid Freezing and Thawing*, exposed to rapid freeze-thaw cycles as specified in ASTM C666-15, *Standard Test Method for Resistance of Concrete to Rapid Freezing and Thawing*, Procedure B, and tested for dynamic Young's modulus of elasticity following ASTM C215-14, *Standard Test Method for Fundamental Transverse, Longitudinal, and Torsional Resonant Frequencies of Concrete Specimens*, the impact resonance method.

Three 16 × 3 × 4 in. (406 × 76 × 102 mm) specimens from each concrete mixture were used for this test. The specimens were demolded 23½ ± ½ hours after casting and cured for 67 days in lime-saturated water, followed by 21 days in an environmentally-controlled room at 73° ± 3°F (23° ± 2°C) with relative humidity of 50 ± 4%. The specimens were then stored for 24 hours in a tempering tank maintained at 70°F (21°C), followed by 24 hours in a water-filled, thermally-

insulated container at 40°F (4°C). The specimens were then subjected to freeze-thaw cycles in an automated freeze-thaw machine. In each freeze-thaw cycle, the specimens were frozen at 0°F (-18°C) in air and thawed at 40°F (4°C) in water. The dynamic Young's modulus of elasticity was measured before the specimens were exposed to freeze-thaw cycles and during the freeze-thaw exposure at intervals of 30 freeze-thaw cycles or less. Testing continued until the specimens had been subjected to 660 freeze-thaw cycles or until the dynamic modulus of elasticity had dropped below 60% of the initial value (relative dynamic modulus < 60%).

To determine the dynamic modulus of elasticity, the specimens were brought to a surface-dry condition, weighed, and tested for resonant frequency using the impact resonance method described in ASTM C215-14, *Standard Test Method for Fundamental Transverse, Longitudinal, and Torsional Resonant Frequencies of Concrete Specimens*. The dynamic modulus of elasticity is calculated as:

$$\text{Dynamic } E = Cmn^2 \tag{2.1}$$

where C is a constant (m^{-1}), m is the mass of specimen (kg) and n is the resonant transverse frequency (Hz). A concrete mixture is considered durable if the specimens can maintain at least 95% of relative dynamic modulus of elasticity after 660 freeze-thaw cycles.

2.2.6 Student's T-Test

The results reported in this chapter represent the average of three specimens. When comparing the average results of two mixtures (X_1 and X_2), Student's t-test is used to verify whether the difference between X_1 and X_2 is due to the difference between the means of the two underlying populations from which the samples are drawn (μ_1 and μ_2) or merely due to the variations among samples in the same population. The results of t-tests are expressed as p values, which is the probability that the difference between X_1 and X_2 is caused by chance and that there

is, in fact, no difference between μ_1 and μ_2 (that is, the two mixtures will show the same test results if an infinitely large number of specimens were made from each mixture). In this chapter, $p = 0.05$ is used as the threshold. Values of p greater than 0.05 are taken as meaning that the difference between two mean values is not statistically significant.

2.3 RESULTS AND DISCUSSION

2.3.1 Free shrinkage

The length changes of specimens during the 14-day curing period and 365-day drying period are discussed in this section. Strains, expressed in microstrain, at various points in time (such as at the end of curing or at 20 days of drying) with respect to the length of a specimen immediately after demolding and shrinkage during various periods (in the first 20 days or between 20 and 365 days of drying) are discussed separately.

2.3.1.1 Strain

Figure 2.2 shows the strain of mixtures in this study up to 379 days after casting (365 days of drying). Measurements taken on each specimen are included in Appendix B. As shown in Figure 2.2, all specimens expanded during the 14-day curing period, as indicated by the positive strain between 0 and 14 days after casting. Once drying started 14 days after casting, the expansive strain of all specimens decreased. The rate of strain reduction was highest at the beginning of drying, gradually reducing over time; after 180 days of drying, most mixtures exhibited relatively small changes in strain.

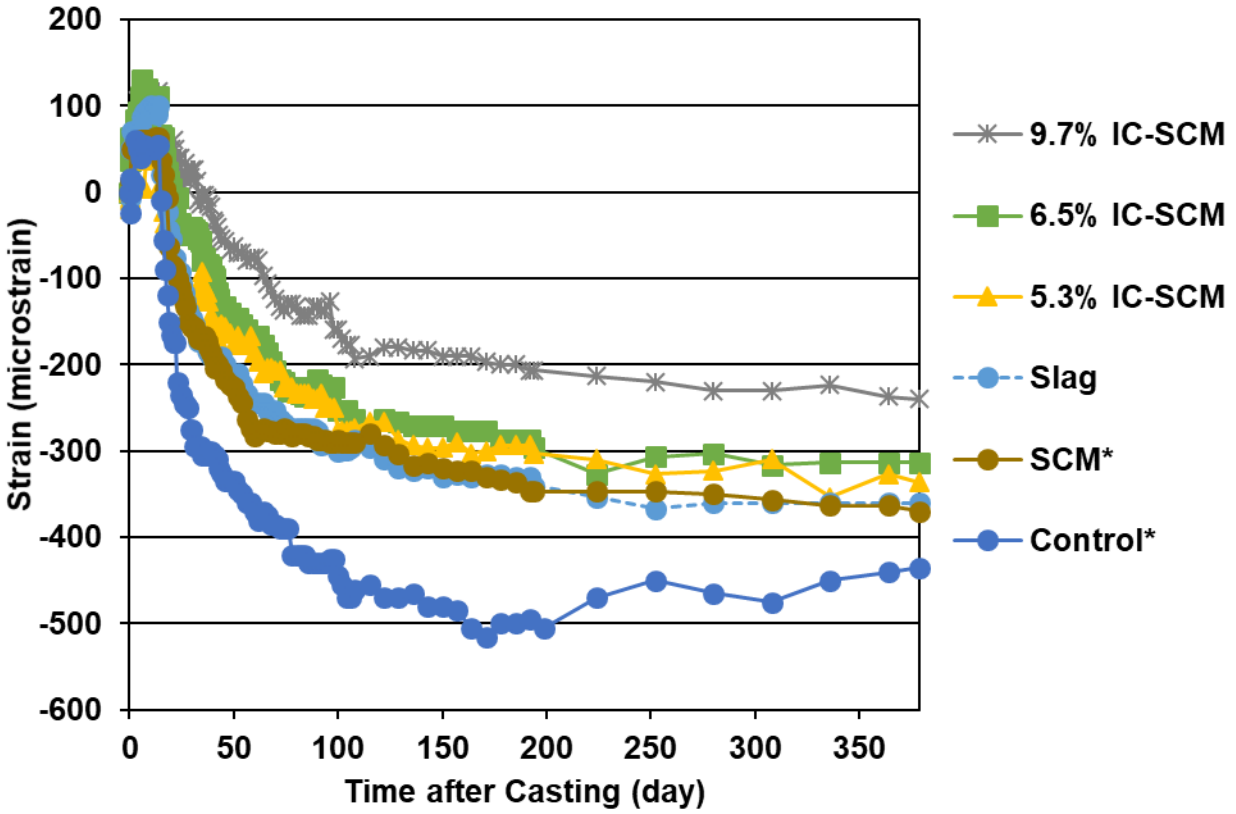

Figure 2.2 – Strain during curing and drying periods. Swelling is positive; shrinkage is negative. *: average of two specimens.

Figure 2.3 summarizes the strains of the mixtures at the end of the 14-day curing period, after 20 days of drying, and after 365 days of drying. The *p* values obtained in Student's t-test between the average strains for pairs of mixtures are listed in Table 2.4 for strains at the end of the curing, in Table 2.5 for strains after 20 days of drying, and in Table 2.6 for strains after 365 days of drying.

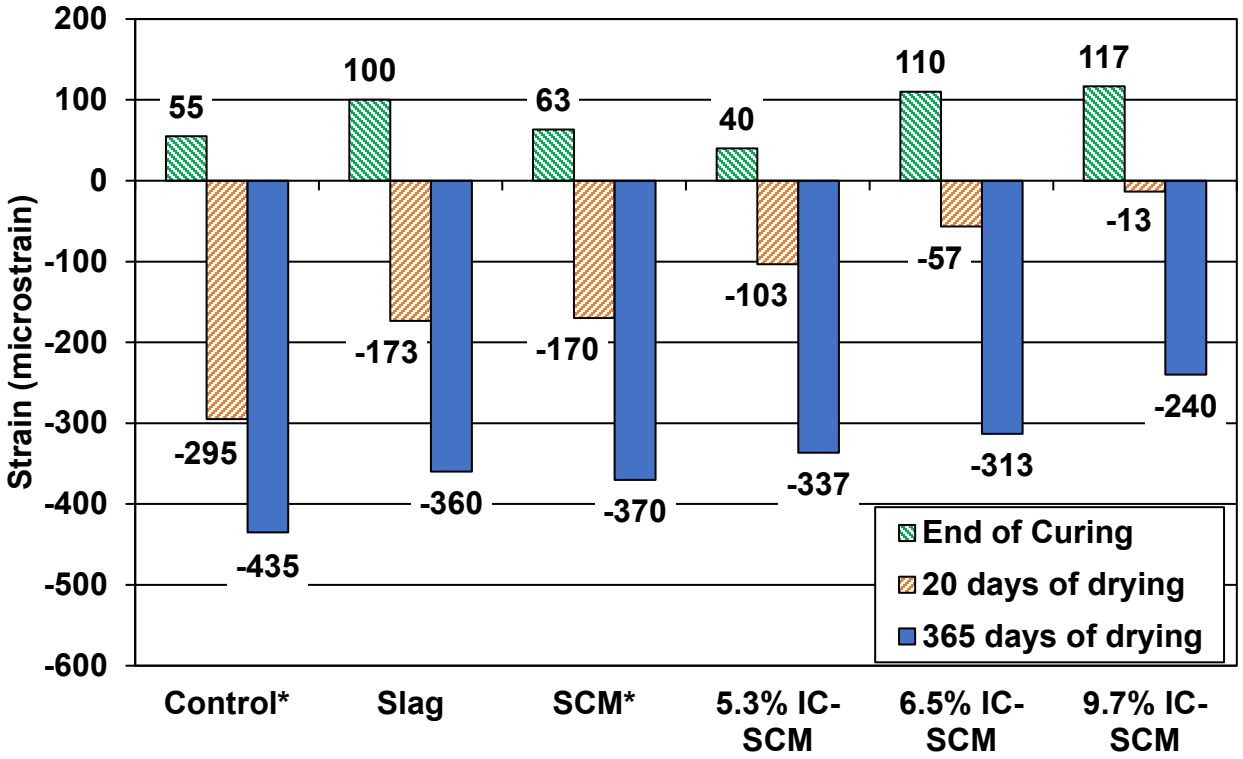

Figure 2.3 – Strains at different points in time. Swelling is positive; shrinkage is negative. *average of two specimens.

Table 2.4 – *p* values obtained in Student's t-test for the differences in strains at the end of curing

	Mixture	Control	Slag	SCM	5.3% IC-SCM	6.5% IC-SCM	9.7% IC-SCM
Mixture	**Strain microstrain**	55	100	63	40	110	117
Control	55		0.14	0.54	0.51	0.14	0.19
Slag	100			0.13	0.06	0.73	0.64
SCM	63				0.26	0.11	0.15
5.3% IC-SCM	40					0.05	0.08
6.5% IC-SCM	110						0.86

Table 2.5 – *p* values obtained in Student's t-test for the differences in strains at 20 days of drying

	Mixture	Control	Slag	SCM	5.3% IC-SCM	6.5% IC-SCM	9.7% IC-SCM
Mixture	**Strain microstrain**	-295	-173	-170	-103	-57	-13
Control	-295		0.04	0.01	0.01	0.01	1.0×10^{-3}
Slag	-173			0.90	0.09	0.02	3.0×10^{-3}
SCM	-170				0.03	0.01	1.2×10^{-4}
5.3% IC-SCM	-103					0.21	0.02
6.5% IC-SCM	-57						0.16

Table 2.6 – *p* values obtained in Student's t-test for the differences in strains at 365 days of drying

	Mixture	Control	Slag	SCM	5.3% IC-SCM	6.5% IC-SCM	9.7% IC-SCM
Mixture	**Strain microstrain**	-435	-360	-370	-337	-313	-240
Control	-435		0.25	0.17	0.26	0.14	0.02
Slag	-360			0.78	0.71	0.41	0.03
SCM	-370				0.54	0.24	3.4×10^{-3}
5.3% IC-SCM	-337					0.73	0.13
6.5% IC-SCM	-313						0.16

At the end of curing, all mixtures exhibited positive strains (expansions) regardless of the use of supplementary cementitious materials or internal curing, with values ranging from 40 to 117 microstrain (Figure 2.2). Further, the differences in strains exhibited by any two mixtures are not statistically significant, with the exception of the relatively large difference between the 5.3% IC-SCM (40 microstrain) and 6.5% IC-SCM (110 microstrain) mixtures, with a *p* value of 0.05 (Table 2.4).

After 20 days of drying, all mixtures exhibited negative strains (shrinkage). The mixtures with internal curing exhibited strains between -13 and -103 microstrain, while the mixtures without IC had strains between -170 and -295 microstrain (Figure 2.3). Further, the differences between the strains of mixtures without internal curing and mixtures with internal curing was statistically significant, with *p* values between 1.2×10^{-4} to 0.03, except for the difference between the Slag and 5.3% IC-SCM mixtures, which had a *p* value of 0.09 (Table 2.5). Among the mixtures with internal curing, negative strain (shrinkage) after 20 days of drying reduced (in absolute values) with increased quantity of internal curing water. As shown in Figure 2.3, the mixtures with 5.3%, 6.5%, and 9.7% of internal curing water by weight of cementitious material had progressively less shrinkage (strains = -103, -57, and -13 microstrain); as shown in Table 2.5, however, only the difference between the mixtures with 5.3% and 9.7% of internal curing water was statistically

significant ($p = 0.02$). Among mixtures without internal curing, the Control mixture had noticeably higher shrinkage (strain = -295 microstrain) than the mixtures with slag cement or slag cement and silica fume (strains = -173 and -170 microstrain, respectively), and the differences were statistically significant, with p values of 0.04 and 0.01. The Slag and SCM (slag and silica fume) mixtures had similar strains after 20 days of drying, indicating that the use of silica fume did not influence the magnitude of shrinkage beyond that resulting from the use of slag cement. Based on the strains at 20 days of drying, the use of supplementary cementitious materials (especially slag cement) and internal curing reduced the shrinkage (negative strain) at early ages.

As observed for strains after 20 days of drying, the incorporation of slag cement or slag cement and silica fume reduced shrinkage through 365 days of drying. Mixtures containing slag cement or both slag cement and silica fume exhibited 75 and 65 microstrain less shrinkage (negative strain) at the end of the 365-day drying period, respectively, than the Control mixture. As at 20 days, the SCM and Slag mixtures exhibited similar strains after 365 days of drying (-370 vs -360 microstrain), indicating that the addition of silica fume did not noticeably alter the strain of concrete mixtures beyond that provided by the addition of slag cement. Used in conjunction with slag cement and silica fume, internal curing further reduced the shrinkage of concrete mixtures after 365 days of drying. The mixtures containing 5.3% and 6.5% of internal curing water by weight of cementitious material exhibited similar strains (-337 and -313 microstrain, respectively), both less than the mixtures without internal curing. A further reduction of shrinkage was observed in the mixture containing 9.7% of internal curing water by weight of cementitious material, highest in this study (strain = -240 microstrain). Among the three mixtures with supplementary cementitious materials and different quantities of internal curing water, the differences in strain after 365 days of drying were not statistically significant (p values between

0.13 and 0.73). Similar observations were made by Reynolds et al. (2009), who studied the strain of concrete mixtures containing portland cement as the only cementitious material and internal curing water equal to 8.6%, 10.3%, and 12.9% by weight of cement and found that the mixtures with 8.6% and 10.3% internal curing water exhibited similar shrinkage (strains = -373 and -370 microstrain, respectively) after 90 days of drying and the mixture with the highest quantity of internal curing water (12.9%) exhibited noticeably less shrinkage (strain = -347 microstrain).

2.3.1.2 Drying Shrinkage Following Curing

Figure 2.4 shows the average shrinkage that occurred in the first 20 days of drying and the additional shrinkage between 20 days and 365 days of drying. The *p* values obtained in Student's t-test between the average shrinkage values of pairs of mixtures are listed in Table 2.7 for the shrinkage that occurred in the first 20 days of drying and in Table 2.8 for the shrinkage occurred between 20 and 365 days of drying.

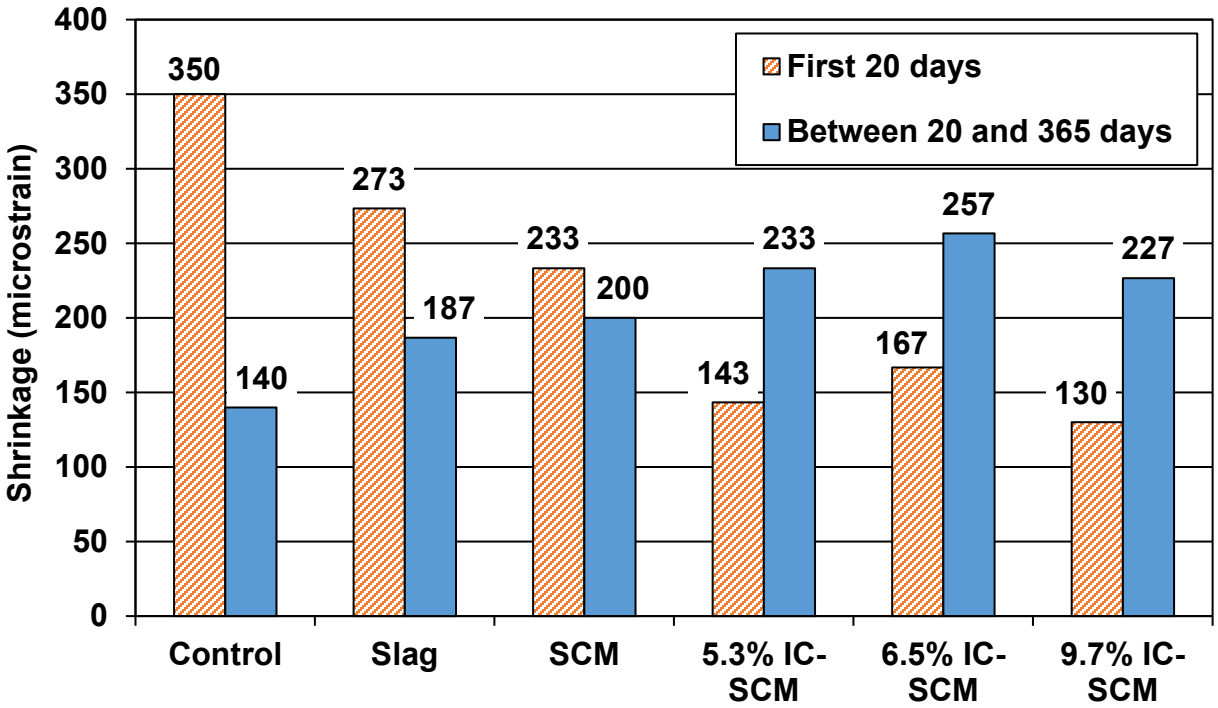

Figure 2.4 – Drying shrinkage during different drying periods

Table 2.7 – *p* values obtained in Student's t-test for the differences in drying shrinkage in the first 20 days of drying

	Mixture	Control	Slag	SCM	5.3% IC-SCM	6.5% IC-SCM	9.7% IC-SCM
Mixture	**Shrinkage microstrain**	350	273	233	143	167	130
Control	350		0.02	0.01	0.01	1.3×10^{-3}	0.01
Slag	273			0.02	0.01	1.4×10^{-4}	2.8×10^{-3}
SCM	233				0.03	2.1×10^{-3}	0.01
5.3% IC-SCM	143					0.43	0.71
6.5% IC-SCM	167						0.16

Table 2.8 – *p* values obtained in Student's t-test for the differences in drying shrinkage between 20 and 365 days of drying

	Mixture	Control	Slag	SCM	5.3% IC-SCM	6.5% IC-SCM	9.7% IC-SCM
Mixture	**Shrinkage microstrain**	350	273	233	143	167	130
Control	350		0.09	0.06	0.14	0.02	0.02
Slag	273			0.37	0.26	0.02	0.03
SCM	233				0.41	0.04	0.12
5.3% IC-SCM	143					0.58	0.86
6.5% IC-SCM	167						0.19

Mixtures with internal curing shrank less than those without internal curing in the first 20 days of drying, as shown in Table 2.4. The mixtures without internal curing (mixtures Control, Slag, and SCM) shrank by 350, 273, and 233 microstrain in the first 20 days of drying, while those with 5.3%, 6.5%, and 9.7% of internal curing water by weight of cementitious materials shrank only 143, 167, and 130 microstrain, respectively. As shown in Table 2.7, the shrinkage differences between any of the mixtures without IC and any of the mixtures with IC were statistically significant with *p* values between 1.4×10^{-4} and 0.03. Among the mixtures without internal curing, the one with slag cement and silica fume (mixture SCM) exhibited the least shrinkage in the first 20 days of drying, while the mixture with 100% portland cement (Control) exhibited the greatest shrinkage. The differences in early-age shrinkage (first 20 days of drying) between any two mixtures without IC were statistically significant with *p* values between 0.01 and 0.02. The early-age shrinkage values of the mixtures with internal curing were similar (between 130 and 167

microstrain) and the differences were not statistically significant, with *p* values between any two mixtures between 0.16 and 0.71. The mixtures with slag cement, slag cement and silica fume, and slag cement, silica fume, and internal curing exhibited progressive reductions in the shrinkage that occurred in the first 20 days of drying; within the range tested, the quantity of internal curing did not appear to affect the magnitude of early-age shrinkage.

Unlike in the first 20 days of drying, mixtures with internal curing exhibited higher shrinkage compared to those without internal curing between 20 and 365 days of drying. As shown in Figure 2.4, the mixtures with 5.3%, 6.5%, and 9.7% of internal curing water by weight of cementitious material shrank 233, 257, and 227 microstrain between 20 and 365 days of drying, noticeably higher than the mixtures without internal curing. Among the mixtures with internal curing, the quantity of internal curing water did not appear to influence the magnitude of shrinkage occurring between 20 and 365 days of drying; the mixture with the highest shrinkage (6.5% IC-SCM) shrank only 30 microstrain more than the mixture with the lowest shrinkage (9.7% IC-SCM), and the differences in shrinkage between pairs of mixtures with internal curing were not statistically significant (*p* between 0.19 and 0.86, Table 2.8). Among the mixtures without internal curing, supplementary cementitious materials appear to increase the shrinkage between 20 and 365 days of drying; the mixture with slag cement and silica fume exhibited the highest shrinkage (200 microstrain) in this period, while the control mixture exhibited the lowest shrinkage (140 microstrain). The differences in shrinkage between mixtures without internal curing, however, were not statistically significant, with *p* values ranging between 0.06 to 0.37 (Table 2.8).

2.3.2 Scaling Resistance

The cumulative mass losses in the scaling test are plotted in Figure 2.5 as a function of freeze-thaw cycles. The results from each test are included in Appendix C. The *p* values obtained in Student's t-test between the average mass losses of any two mixtures are listed in Table 2.9.

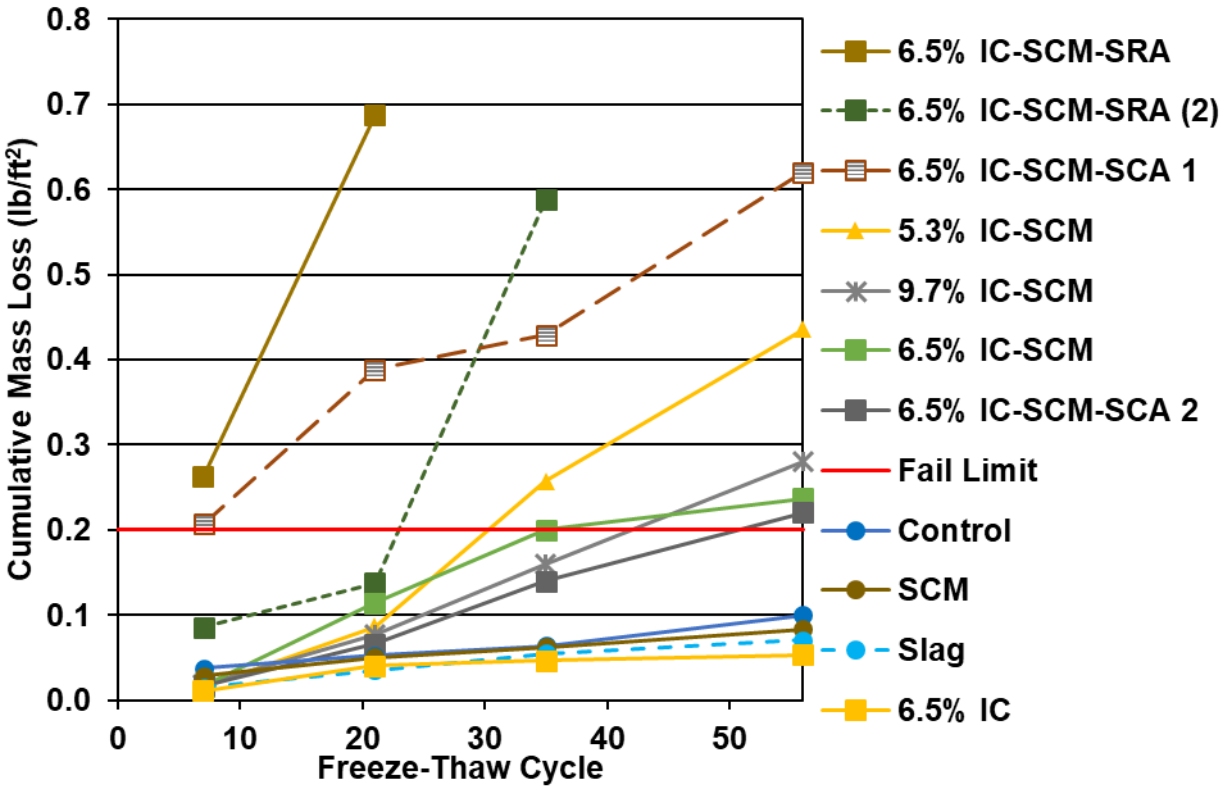

Figure 2.5 – Average cumulative mass loss in scaling test versus freeze-thaw cycles (1 lb/ft^2 = 4.88 kg/m^2)

Table 2.9 – *p* values obtained in Student's t-test for scaling results

	Mixture	Control	Slag	SCM	6.5% IC	5.3% IC-SCM	6.5% IC-SCM	9.7% IC-SCM	6.5% IC-SCM-SCA 1	6.5% IC-SCM-SCA 2	6.5% IC-SCM-SRA	6.5% IC-SCM-SRA (2)
Mixture	**Average Mass Loss lb/ft^2**	0.10	0.07	0.08	0.05	0.44	0.24	0.28	0.62	0.22	0.69	0.59
Control	0.10		0.14	0.37	0.05	1.1×10^{-4}	9.8×10^{-4}	0.03	0.01	1.7×10^{-3}	8.7×10^{-5}	2.9×10^{-4}
Slag	0.07			0.19	0.17	3.5×10^{-5}	4.2×10^{-5}	0.01	0.01	8.4×10^{-5}	5.4×10^{-5}	1.8×10^{-4}
SCM	0.08				0.03	3.7×10^{-5}	4.1×10^{-5}	0.02	0.01	9.1×10^{-5}	5.8×10^{-5}	2.0×10^{-4}
6.5% IC	0.05					3.2×10^{-5}	4.3×10^{-5}	0.01	0.01	8.0×10^{-5}	5.0×10^{-5}	1.7×10^{-4}
5.3% IC-SCM	0.44						3.5×10^{-4}	0.04	0.15	2.8×10^{-4}	2.5×10^{-3}	0.02
6.5% IC-SCM	0.24							0.44	0.02	0.13	1.8×10^{-4}	8.2×10^{-4}
9.7% IC-SCM	0.28								0.04	0.31	2.5×10^{-3}	0.01
6.5% IC-SCM-SCA 1	0.62									0.02	0.57	0.78
6.5% IC-SCM-SCA 2	0.22										1.6×10^{-4}	7.0×10^{-4}
6.5% IC-SCM-SRA	0.69											0.12

The Control mixture and the mixtures with either supplementary cementitious materials or internal curing, but not both, exhibited low mass loss in scaling test. The mixtures with slag cement or slag cement and silica fume exhibited slightly lower (0.07 and 0.08 lb/ft^2) mass loss than the Control mixture (0.10 lb/ft^2), but the differences were not statistically significant (p = 0.14 and 0.37). The difference between the mass losses of the Control and 6.5% IC mixtures was small, although statistically significant (0.10 vs 0.05 lb/ft^2, p = 0.05). Thus, the use of slag cement, slag cement and silica fume, or internal curing alone did not noticeably affect the scaling resistance of concrete mixtures.

When both internal curing and supplementary cementitious materials were used, however, the mass loss increased. The mass losses of the three mixtures with internal curing and supplementary cementitious materials (0.24 to 0.44 lb/ft^2) were higher than those of the mixtures with only internal curing or supplementary cementitious materials (0.05 and 0.08 lb/ft^2), and the

differences were statistically significant with p values between 3.2×10^{-5} and 0.02. The quantity of internal curing water (5.3% to 9.7% by weight of cementitious material) did not affect the mass loss of the mixtures with both internal curing and supplementary cementitious materials; instead, air content (6.50% to 9.00%) appears to have been a major factor in scaling resistance. After 56 freeze-thaw cycles, the mixture with the lowest air content (mixture 5.3% IC-SCM, 6.50% air content) exhibited the highest mass loss (0.44 lb/ft^2); and mixtures with similar air contents (mixtures 6.5% IC-SCM and 9.7% IC-SCM, 9.00% and 8.5% air content, respectively) exhibited similar mass losses (0.24 and 0.28 lb/ft^2, respectively), regardless of the quantity of internal curing water. It should be noted that the mass losses of mixtures with both IC and SCMs exceeded the acceptable mass loss limit (0.2 lb/ft^2 or 1 kg/m^2). As discussed in Section 2.2.4, the test method used in this study was harsher than that specified in BNQ NQ 2621-900; mixtures with SCMs and 6.5% or 9.7% IC would, therefore, likely be able to pass a standard scaling test since their mass losses were close to the failure limit. Further, scaling tests have been reported by many to show varying results on similar (or identical) concrete mixtures and underestimate the durability of concrete mixtures compared to field observations (Bleszynski et al. 2002, Boyd and Hooton 2007, Transportation Research Board 2007, Bilodeau et al. 2008, Jones 2014, ACI Comittee 233 2017). Bilodeau et al. (2008) reported that when specimens from the same batch of concrete were tested by seven laboratories using the BNQ NQ 2621-900 method, the mass loss varied from 0.03 to 0.19 lb/ft^2 (0.17 to 0.94 kg/m^2), with a coefficient of variation of 179%. Boyd and Hooton (2007) studied the scaling resistance of concrete mixtures containing slag cement, fly ash, or combinations of the materials and found that while the mass loss of these mixtures varied remarkably from 0.01 to 0.26 lb/ft^2 (0.05 to 1.28 kg/m^2), in-ground slabs cast with these concrete mixtures showed little to no scaling after 12 years of exposure.

When a shrinkage-reducing admixture was added, the scaling resistance of the mixture containing 6.5% internal curing and SCMs was severely compromised. Mixtures 6.5% IC-SCM-SRA and 6.5% IC-SCM-SRA (2) exhibited the worst scaling resistance among the mixtures in this study, losing 0.69 lb/ft^2 of mass after 21 and 0.59 lb/ft^2 after 35 freeze-thaw cycles when testing was terminated due to their high mass losses. The mixture with SCA 1, which contains a shrinkage-reducing admixture, exhibited the highest mass loss (0.62 lb/ft^2) among mixtures that completed the full 56 freeze-thaw cycles. On the other hand, CaO-based SCA 2 does not appear to influence the scaling resistance of mixtures with internal curing and SCMs: mixture 6.5% IC-SCM-SCA 2 exhibited a mass loss comparable to that of mixture 6.5% IC-SCM (0.22 and 0.24 lb/ft^2, $p = 0.13$). These results indicate that the CaO-based SCA can be added to concrete mixtures with internal curing and supplementary cementitious materials without compromising their scaling resistance; SRAs, however, should be avoided in concrete mixtures with slag cement, silica fume, and IC.

2.3.3 Freeze-Thaw Durability

Values of the average relative dynamic moduli of the concrete mixtures in the freeze-thaw test are shown as functions of the number of freeze-thaw cycles in Figure 2.6. The dynamic moduli of the specimens from each test are listed in Appendix C. Table 2.10 shows the relative dynamic moduli of the mixtures and, if applicable, the number of freeze-thaw cycles finished before reaching 60% of the initial dynamic modulus.

As discussed in Section 2.2.5, testing was terminated when either the number of freeze-thaw cycles reached 660 or the relative dynamic modulus dropped below 60%. As shown in Figure 2.6, four mixtures [9.7% IC-SCM, 6.5% IC-SCM-SCA 1, 6.5% IC-SCM-SRA and 6.5% IC-SCM-SRA (2)] did not complete 660 freeze-thaw cycles before their relative dynamic modulus decreased below 60%. The relative dynamic modulus of mixture 9.7% IC-SCM decreased to 53%

after 571 freeze-thaw cycles, that of mixture 6.5% IC-SCM-SCA 1 dropped to 50% after 180 freeze-thaw cycles, that of mixture 6.5% IC-SCM-SRA reached 44% after 91 freeze-thaw cycles and that of mixture 6.5% IC-SCM-SRA (2) reached 54% after 67 freeze-thaw cycles. Except for mixture 6.5% IC-SCM, which had a durability factor of 94% after 660 freeze-thaw cycles, the mixtures that reached 660 freeze-thaw cycles are acceptable for use in bridge decks since their durability factors were above 95%.

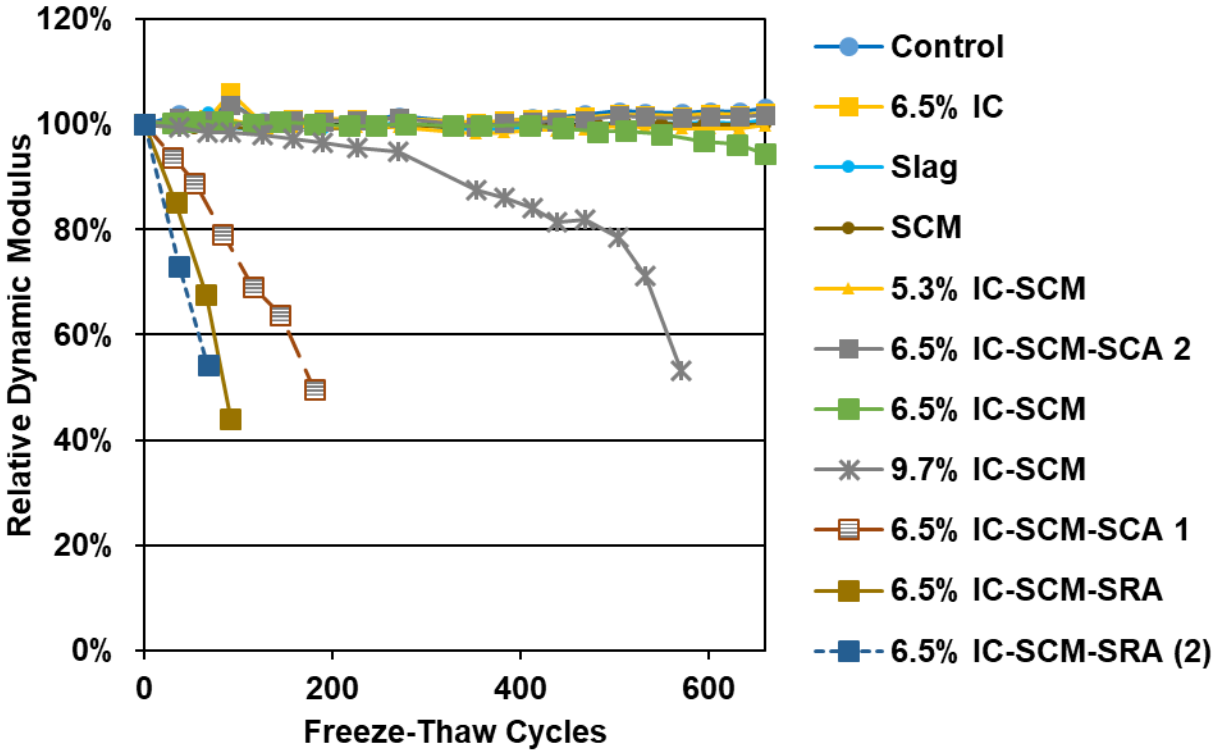

Figure 2.6 – Average relative dynamic modulus of elasticity verses freeze-thaw cycles

Table 2.10 – Average relative dynamic modulus of elasticity at the end of test

Mixture	Relative Dynamic Modulus of Elasticity at End of Test	Cycles Completed when Relative Dynamic Modulus of Elasticity Drops Below 60%
Control	103%	-
Slag	101%	-
SCM	100%	-
6.5% IC	102%	-
5.3% IC-SCM	100%	-
6.5% IC-SCM	94%	-
9.7% IC-SCM	53%	571
6.5% IC-SCM-SCA 1	50%	180
6.5% IC-SCM-SCA 2	102%	-
6.5% IC-SCM-SRA	44%	91
6.5% IC-SCM-SRA (2)	54%	67

"-" denotes mixture reached 660 freeze-thaw cycles prior to dropping to 60% of initial dynamic modulus.

The Control mixture and the mixtures with slag cement, slag cement and silica fume, or 6.5% internal curing water exhibited similar freeze-thaw durability. As shown in Figure 2.6 and Table 2.10, the relative dynamic modulus of elasticity of the Control mixture was 103% at the end 660 freeze-thaw cycles, while those for mixtures Slag, SCM, and 6.5% IC ranged from 100% to 102%.

When supplementary cementitious materials and internal curing were used together, the freeze-thaw durability of concrete mixtures decreased with an increased quantity of internal curing water. As shown in Figure 2.6 and Table 2.10, among the mixtures containing slag cement, silica fume, and internal curing, the two with lower quantities of internal curing water (5.3% IC-SCM and 6.5% IC-SCM) exhibited the highest relative dynamic moduli (100% and 94%, respectively) at the end 660 freeze-thaw cycles; while the mixture with the highest quantity of internal curing water (9.7% IC-SCM) had a relative dynamic modulus of 53% after 571 freeze-thaw cycles. Similar results were observed by Jones and Weiss (2015), who studied the freeze-thaw durability of mixtures with fly ash and 0, approximately 6%, or approximately 12% IC water by weight of cementitious material and found that the mixtures with lower quantities of IC water (0% and

approximately 6%) exhibited good freeze-thaw durability while the mixture with increased quantity of IC water (approximately 12%) exhibited significantly compromised freeze-thaw durability. Concrete mixtures with SCMs and IC had satisfactory freeze-thaw durability when the quantity of IC water was relatively low; when an excessive quantity of IC water is added, however, internally cured concrete can be susceptible to freeze-thaw damage. The freeze-thaw performance of internally cured concrete should be studied at greater details on mixtures with different paste contents, quantities of IC water, and combinations of SCMs.

For concrete mixtures with supplementary cementitious materials and internal curing, the addition of a shrinkage-reducing admixture, either by itself or as a part of another admixture, reduced freeze-thaw durability. As shown in Figure 2.6 and Table 2.10, compared to the mixture with slag cement, silica fume, and 6.5% internal curing water, the addition an SRA or SCA 1, which contains an SRA, resulted in very poor freeze-thaw performance. Mixture 6.5% IC-SCM-SCA 1 lost 50% of its initial dynamic modulus after 180 freeze-thaw cycles, while mixtures 6.5% IC-SCM-SRA and 6.5% IC-SCM-SRA (2) lost 56% and 46% of their initial dynamic moduli after 91 and 67 freeze-thaw cycles, respectively. On the other hand, the addition of CaO-based SCA 2 did not affect the freeze-thaw durability of the mixture; the relative dynamic modulus of mixture 6.5% IC-SCM-SCA 2 was 102% after 660 freeze-thaw cycles, which was, in fact, greater than that of the mixture without SCA 2 (6.5% IC-SCM, 94%). Overall, the current results indicate that SRAs should be avoided to ensure adequate freeze-thaw durability when supplementary cementitious materials and internal curing are used.

2.4 Summary and Conclusions

Using a modified ASTM C157 test method that involves measuring the length change of concrete specimens starting at 5½ ± ½ hours after casting. Drying shrinkage was measured for

concrete mixtures with 100% portland cement and 0% or 6.5% internal curing water by weight of cement provided by pre-wetted lightweight aggregate, a mixture with a 30% volume replacement of cement with slag cement, a mixture with 30% and 3% volume replacements of cement with slag cement and silica fume, respectively, and mixtures with slag cement, silica fume, and 5.3%, 6.5%, or 9.7% internal curing water by weight of cementitious material. Further, the scaling resistance (based on test method BNQ NQ 2621-900) and freeze-thaw durability (following ASTM C666, Procedure B) were evaluated for these concrete mixtures plus four mixtures containing slag cement, silica fume, 6.5% internal curing water, and a shrinkage-reducing admixture or one of two shrinkage-compensating admixtures (one of which contains an SRA).

Based on the observations in this study, the following conclusions can be made:

1. The combination of slag cement, silica fume, and internal curing reduces the shrinkage (negative strain) after 20 and 365 days of drying; and the shrinkage at 20 and 365 days of drying decreases as the quantity of internal curing water increases.
2. The mixtures with slag cement, silica fume, and internal curing shrank notably less in the first 20 days of drying but more between 20 and 365 days of drying compared to the mixture with 100% portland cement or the mixtures with slag cement or slag cement and silica fume.
3. The mixtures with 100% portland cement and 0% or 6.5% internal curing water by weight of cement, as well as those with slag cement or slag cement and silica fume without internal curing water, performed satisfactorily in the scaling resistance and freeze-thaw durability tests.
4. The mixtures with slag cement, silica fume, and 5.3% or 6.5% internal curing water by weight of cementitious material performed satisfactorily in the freeze-thaw durability

test but showed mass losses exceeding the failure limit in the scaling resistance test, while the mixture with slag cement, silica fume, and 9.7% internal curing water (highest in this study) performed poorly in both tests. The scaling resistance test procedure used in this study was harsher than the standard method; given that the mass losses of mixtures with slag cement, silica fume, and 6.5% or 9.7% internal curing water [0.24 and 0.28 lb/ft^2 (1.2 and 1.4 kg/m^2), respectively] were close to the failure limit (0.2 lb/ft^2, or 1.0 kg/m^2), the mixtures may have performed adequately in a standard scaling test. The high mass loss observed on the mixture with slag cement, silica fume, and 5.3% internal curing water is likely explained by the mixture's relatively low air content.

5. When a shrinkage-reducing admixture, either by itself or as a component of a shrinkage-compensating admixture, is added to mixtures with slag cement, silica fume, and 6.5% internal curing water, the scaling resistance and freeze-thaw durability can be drastically reduced; the CaO-based shrinkage-compensating admixture that did not contain an SRA did not noticeably affect the scaling resistance or freeze-thaw durability of concrete mixtures, and the mixture with the CaO-based shrinkage-compensating admixture, slag cement, silica fume, and internal curing performed satisfactorily in this study.

CHAPTER 3: CRACKING PERFORMANCE OF BRIDGE DECKS CONTAINING SYNTHETIC FIBERS OR SHRINKAGE-REDUCING ADMIXTURES

3.1 GENERAL

This chapter describes the cracking performance of eleven bridge decks cast with concrete containing either synthetic fibers or shrinkage-reducing admixtures (SRAs), along with six decks that serve as controls. Specifically, seven decks in Kansas were constructed with fiber-reinforced concrete (FRC) and four decks in Virginia were constructed with concrete mixtures containing an SRA. Five of the FRC decks have a companion control deck constructed without fiber reinforcement. The four decks with SRA share a control deck that was constructed without SRA.

The descriptions include the concrete properties, construction practices, and crack survey results. The seven bridge decks with FRC are designated Fiber-1 through Fiber-7 in order of the dates of construction. The paired control bridge decks are labeled Control-4 through Control-7. The four decks with SRAs are designated SRA-1 through SRA-4 in order of dates of construction, and the control deck is designated VA-Control. In the cases where the bridge decks consist of two placements, the placement number is added to the end of the placement name.

3.2 CRACK SURVEY METHOD

3.2.1 Crack Density

A standard procedure has been established to perform crack surveys with the goal of ensuring consistent results. The survey procedures are outlined in this section. The specification covering those procedures is included in Appendix D.

Prior to a survey, the weather forecast is checked to ensure that the air temperature during the survey is 60° F (15.5° C) or higher. The sky condition should be at least mostly sunny for most

of the day. The deck must be completely dry regardless of the weather. A survey is deemed invalid and is repeated on another day unless these conditions are satisfied.

A map of the bridge deck in plan view with a scale of 1 in. = 10 ft (1:120) is printed prior to leaving for the bridge. A second copy of the map that includes grid lines spaced at 5 ft × 5 ft (1.52 m × 1.52 m) on the deck is also printed. During a survey, the map with grid lines is aligned with and placed under the map without grid lines so that the surveyor can use the former as a reference to locate any point of the bridge deck when marking cracks on the map without grid lines. A north arrow is also shown on the map to help the surveyor orient while on the bridge deck.

Traffic control during surveys is provided by state departments of transportation (DOTs) to ensure the safety of surveyors. At least one lane is closed to traffic at a time. Grid points spaced at 5 ft × 5 ft (1.52 m × 1.52 m), matching the grid lines on the maps, are drawn on the deck surface using sidewalk chalk.

To find cracks on the deck surface, surveyors bend their back to lower their eyes to the waist level and walk in a zigzag pattern to ensure the entire deck is checked. Each section of the bridge deck is checked by at least two surveyors to minimize error. Cracks visible at the waist level are marked using sidewalk chalks on the deck. When marking a crack, the surveyor may bend closer or crouch down to mark the crack to its ends, including the portions that are too narrow to be seen at waist height. When crouching down to mark a crack, the surveyor can sometimes see other cracks. If such cracks are not connected to the crack currently being marked, they are not be marked unless can be seen when the surveyor is bending at waist height. A surveyor then draws the marked crack on the scaled bridge map, using the grid lines on both the bridge deck and the map to keep track of the location and length of cracks.

To calculate crack density, the maps are scanned and imported into AutoCAD, a computer-aided drafting software developed by Autodesk, where the summation of crack lengths can be calculated for the entire deck, each span, and, in the cases where the deck was constructed in multiple placements, each placement. The total crack lengths are then divided by the area of the deck, span, or placement to obtain the crack density, which is reported in m/m^2.

3.2.2 Crack Width

Crack width measurements have been made during crack surveys beginning in 2016. A group of randomly selected cracks are measured for crack width. Cautions were taken to include cracks with different lengths (short or long), orientations (transverse, parallel, or diagonal to traffic), and shapes (straight or crazing). When measuring the width of a crack, the widest point of the crack was visually located and measured. A bank card-sized crack width comparator is used for the measurements. The accuracy of the comparator was verified using a caliper with an accuracy of 0.001 in. (0.026 mm).

For surveys performed within the same year (such as all surveys in 2016), the same surveyor measured crack widths whenever possible. The surveyor responsible for crack width measurements, however, changed between years. To avoid variations in the measurements, crack widths obtained from the same year are compared with each other. For Fiber-1 through Fiber-4, Control-3, and Control-4, crack widths measured in 2016 are used; for Fiber-5 through Fiber-7 and Control-5 through Control-7, crack widths measured in 2017 are used; for SRA-1 through SRA-4 and VA-Control, crack widths from 2016 are used.

When comparing the average crack widths on two bridge deck placements (X_1 and X_2), Student's t-test is used to verify whether the difference between X_1 and X_2 is due to the difference between the means of the two underlying populations from which the samples are drawn (μ_1 and

μ_2) or merely due to the variations among samples in the same population. The results of t-tests are expressed as *p* values, which is the probability that the difference between X_1 and X_2 is caused by chance and that there is, in fact, no difference between μ_1 and μ_2 (that is, the two bridge deck placements will show the same test results if an infinitely large number of crack width measurements were made from each placement). In this chapter, $p = 0.05$ is used as the threshold. Values of *p* greater than 0.05 are taken as meaning that the difference between two mean values is not statistically significant.

3.3 BRIDGES

3.3.1 Bridge Decks

Table 3.1 summarizes the structure numbers assigned by the Kansas Department of Transportation (KDOT) or Virginia Department of Transportation (VDOT), locations, dimensional information, and girder types for the bridges in this study. The bridges are in three counties in Kansas (Wyandotte, Shawnee, and Douglas) and five counties in Virginia (Rockingham, Alleghany, Stafford, King William, and Spotsylvania). The bridges in Kansas have three spans with skews between 0° and 47°, while those in Virginia have between one and four spans with skews of 0° to 19°. The lengths of the bridges range from 99 to 640 ft (30.2 to 195.1 m) and the widths ranged from 26 to 66 ft (7.9 to 20.1 m). Except for Control 3, all of the bridges have one-course (monolithic) decks. Control 3 has a 1.5-in. 5% silica fume overlay on a concrete subdeck. All but one deck is supported by steel girders. The deck for SRA-1 is supported by prestressed box beams. The reinforcement in Fiber-2 consists of glass fiber-reinforced polymer (GFRP) bars, while that in others consists of epoxy-coated reinforcing bars.

Table 3.1 – Bridge decks

Bridge Deck	Structure Number	Location	County	Deck Type [1]
Fiber-1	635-105-5.12(049)	NB I-635 over State Ave.	Wyandotte, KS	Monolithic
Fiber-2*	635-105-5.11(048)	SB I-635 over State Ave.	Wyandotte, KS	Monolithic
Fiber-3	24-89-17.68(297)	EB US-24 over Menoken Rd.	Shawnee, KS	Monolithic
Control-3	24-89-17.67(296)	WB US-24 over Menoken Rd.	Shawnee, KS	5% SFO
Fiber-4	24-89-17.23(283)	EB US-24 over UPRR	Shawnee, KS	Monolithic
Control-4	24-89-17.22(282)	WB US-24 over UPRR	Shawnee, KS	Monolithic
Fiber-5	10-23-12.44(177)	WB K-10 over North Canal	Douglas, KS	Monolithic
Control-5	10-23-12.45(178)	EB K-10 over North Canal	Douglas, KS	Monolithic
Fiber-6	10-23-12.93(179)	WB K-10 over 31st St.	Douglas, KS	Monolithic
Control-6	10-23-12.94(180)	EB K-10 over 31st St.	Douglas, KS	Monolithic
Fiber-7	10-23-10.71(169)	WB K-10 over Haskell Ave.	Douglas, KS	Monolithic
Control-7	10-23-10.72(170)	EB K-10 over Haskell Ave.	Douglas, KS	Monolithic
SRA-1	VA 6154	Route 1421 over Linville Creek	Rockingham, VA	Monolithic
SRA-2	VA 1149	Route 633 over Cowpasture River	Alleghany, VA	Monolithic
SRA-3	VA 6065	Telegraph Rd. over I-95	Stafford, VA	Monolithic
SRA-4	VA 6002	Route 600 over Herring Creek	King William, VA	Monolithic
VA-Control	VA 1022	Route 208 over TA River	Spotsylvania, VA	Monolithic

Bridge Deck	Spans	Skew	Length		Width		Girder Type
		degree	ft	m	ft	m	
Fiber-1	3	7	232	70.7	66	20.1	Steel
Fiber-2*	3	7	232	70.7	66	20.1	Steel
Fiber-3	3	0	250	76.2	40	12.2	Steel
Control-3	3	0	250	76.2	40	12.2	Steel
Fiber-4	3	0	640	195.1	40	12.2	Steel
Control-4	3	0	640	195.1	40	12.2	Steel
Fiber-5	3	45	354	107.9	40	12.2	Steel
Control-5	3	45	354	107.9	40	12.2	Steel
Fiber-6	3	47	284	86.6	40	12.2	Steel
Control-6	3	47	284	86.6	40	12.2	Steel
Fiber-7	3	7	293	89.3	50	15.2	Steel
Control-7	3	7	293	89.3	50	15.2	Steel
SRA-1	4	15	260	79.2	30	9.1	Prestressed box beam
SRA-2	3	0	340	103.6	26	7.9	Steel
SRA-3	2	19	313	95.4	40	12.2	Steel
SRA-4	1	12	99	30.2	40	12.2	Steel
VA-Control	1	11	129	39.2	44	13.4	Steel

[1] Monolithic = one-course bridge decks; 5% SFO = subdeck is topped by a 1.5-in overlay of 5% silica fume mixture.
*: Fiber-2 uses glass fiber reinforced polymer (GFRP) reinforcing bars.

3.3.2 Fibers and SRAs

Table 3.2 lists the fibers used in the bridge decks in Kansas. Fiber-1 through Fiber-4 used microfibers, and Fiber-5 through Fiber-7 used a macrofiber. The fiber lengths were 0.75 in. (19 mm) for both types of microfiber and 1.55 in. (39 mm) for the macrofiber. The equivalent

diameter was not provided for the microfiber used in decks Fiber-1 and Fiber-2. The microfiber used in Fiber-3 and Fiber-4 has an equivalent diameter of 0.026 in. (0.66 mm) and the macrofiber used in Fiber-5 through Fiber-7 has an equivalent diameter of 0.017 in. (0.43 mm). Both types of microfibers are made from polypropylene and have a specific gravity of 0.91, while the macrofiber is a blend of polypropylene and polyethylene and has a specific gravity of 0.92.

Table 3.2 – Properties of fiber reinforcement

Bridge Deck	Fiber Designation	Type	Length in.	Equivalent Diameter in.	Specific Gravity	Material
Fiber-1	F-5	Fibrillated microfiber	0.75	- [a]	0.91	Polypropylene
Fiber-2	F-5	Fibrillated microfiber	0.75	- [a]	0.91	Polypropylene
Fiber-3	F-4	Fibrillated microfiber	0.75	0.026	0.91	Polypropylene
Fiber-4	F-4	Fibrillated microfiber	0.75	0.026	0.91	Polypropylene
Fiber-5	F-3	Monofilament macrofiber	1.55	0.017	0.92	Polypropylene/polyethylene blend
Fiber-6	F-3	Monofilament macrofiber	1.55	0.017	0.92	Polypropylene/polyethylene blend
Fiber-7	F-3	Monofilament macrofiber	1.55	0.017	0.92	Polypropylene/polyethylene blend

a: Data is not available from the manufacturer.
Note: 1 in. = 25.4 mm.

Table 3.3 lists the SRAs used in the bridge decks in Virginia. Two types of SRAs were used; the active components of both are surfactants, which reduces the surface tension of concrete pore solution.

Table 3.3 – Properties of SRAs

Bridge Deck	SRA Designation	Effective Component
SRA-1	Admixture SRA-3	2-methylpentane-2,4-diol
SRA-2	Admixture SRA-2	2,2-dimethylpropane-1,3-diol
SRA-3	Admixture SRA-3	2-methylpentane-2,4-diol
SRA-4	Admixture SRA-2	2,2-dimethylpropane-1,3-diol

3.3.3 Concrete Proportions and Properties

The concrete mixture proportions, based on saturated surface-dry (SSD) aggregates, are listed in Table 3.4. Four bridge decks (Fiber-3, Fiber-4, Control-3, and Control-4) contained cement as the only cementitious material, seven decks (Fiber-6, Fiber-7, Control-6, Control-7, SRA-1, SRA-3, and VA-Control) used binary mixtures with cement and slag cement, four (Fiber-1, Fiber-2, SRA-2, and SRA-4) used binary mixtures with cement and fly ash, and two (Fiber-5 and Control-5) used ternary mixtures with cement, slag cement, and fly ash as the cementitious material. The total weight of cementitious material ranged from 510 to 564 lb/yd^3 (302.5 to 334.5 kg/m^3) for the Kansas decks (Fibers and Controls) and from 580 to 676 lb/yd^3 (344.0 to 401.0 kg/m^3) for the Virginia decks (SRAs and VA-Control). With water-to-cementitious material (*w/cm*) ratios ranging from 0.40 to 0.45 for the decks, the paste contents (volume fractions of cementitious materials and mixing water) ranged from 22.2% to 24.7% for the Kansas decks and from 27.0% to 29.4% for the Virginia decks.

Table 3.4 – Design concrete proportions of all bridges in this chapter (lb/yd^3, SSD basis)

Bridge Deck	Cement	Slag	Fly Ash	Water	*w/cm* Ratio	Paste Content	Coarse Aggregate	Fine Aggregate	Intermediate Aggregate
Fiber-1	405	0	105	230	0.45	23.8%	1704	1377	0
Fiber-2	405	0	105	230	0.45	23.8%	1704	1377	0
Fiber-3	521	0	0	208	0.40	22.2%	1590	1590	0
Control-3	521	0	0	208	0.40	22.2%	1590	1590	0
Fiber-4	521	0	0	208	0.40	22.2%	1590	1590	0
Control-4	521	0	0	208	0.40	22.2%	1586	1593	0
Fiber-5	351	135	54	238	0.44	24.7%	1370	1370	304
Control-5	351	135	54	238	0.44	24.7%	1370	1370	304
Fiber-6	423	141	0	231	0.41	24.6%	1816	1211	0
Control-6	423	141	0	231	0.41	24.6%	1816	1211	0
Fiber-7	423	141	0	231	0.41	24.6%	1816	1211	0
Control-7	423	141	0	231	0.41	24.6%	1816	1211	0
SRA-1	325	325	0	260	0.40	28.2%	1985	1022	0
SRA-2	464	0	116	261	0.45	27.1%	1832	1217	0
SRA-3	300	300	0	258	0.43	27.0%	1986	1178	0
SRA-4	480	0	120	258	0.43	27.3%	1715	1320	0
VA-Control	338	338	0	270	0.40	29.4%	1944	1096	0

Note: 1 lb/yd^3 = 0.6 kg/m^3.

Fiber and SRA dosages for the mixtures are listed in Table 3.5. The fiber dosage by weight was 0.75 or 1.5 lb/yd^3 (0.45 or 0.89 kg/m^3) when a microfiber was used and 4.5 lb/yd^3 (2.67 kg/m^3) when the macrofiber was used. In decks Fiber-1 and Fiber-2, the fibers occupied 0.05% of concrete volume. In decks Fiber-3 and Fiber-4, the fibers occupied 0.10% of the concrete volume. In decks Fiber-5 through Fiber-7, the volume fraction of macrofibers was 0.29%. Following common practice, mixture proportions were not modified to account for the volume of fibers. The SRA dosages ranged from 1 gal/yd^3 to 1.5 gal/yd^3 (5.0 to 7.4 L/m^3).

Table 3.5 – Addition rates of fibers and SRAs

Bridge Deck	Dosage	Fiber Volume Fraction %
Fiber-1	0.75 lb/yd^3	0.05
Fiber-2	0.75 lb/yd^3	0.05
Fiber-3	1.5 lb/yd^3	0.10
Fiber-4	1.5 lb/yd^3	0.10
Fiber-5	4.5 lb/yd^3	0.29
Fiber-6	4.5 lb/yd^3	0.29
Fiber-7	4.5 lb/yd^3	0.29
SRA-1	1.0 gal/yd^3	Not applicable
SRA-2	1.0 gal/yd^3	Not applicable
SRA-3	1.5 gal/yd^3	Not applicable
SRA-4	1.5 gal/yd^3	Not applicable

Note: 1 lb/yd^3 = 0.6 kg/m^3, 1 gal/yd^3 = 4.95 L/m^3.

The average concrete properties of the bridge deck placements are summarized in Table 3.6. Decks Fiber-1, Fiber-2, Fiber-4, and Control-4 were cast in two placements on different days. The other decks were cast in a single placement. Average air contents for the deck placements ranged from 5.2% to 7.6%, average slumps ranged from 3 to 6½ in. (80 to 165 mm), average concrete temperatures ranged from 61° to 84°F (16.0° to 29.0°C), and 28-day compressive strengths ranged from 3780 to 7030 psi (26.1 to 48.5 MPa). No concrete test results are available for the subdeck of Control-3. No strength results are available for Control-4 placement 1.

Table 3.6 – Average properties of concrete in each bridge

Placement	Air Content %	Slump in.	Concrete Temperature °F	°C	28-day Strength psi
Fiber-1 Placement 1	5.6	3¾	84	29.0	5590
Fiber-1 Placement 2	6.4	4½	61	16.0	6810
Fiber-2 Placement 1	7.5	5	83	28.0	5740
Fiber-2 Placement 2	5.3	5	61	16.0	5950
Fiber-3	6.5	3¼	66	19.0	5230
Control-3 [a]	-	-	-	-	-
Fiber-4 Placement 1	6.5	3	83	28.5	5330
Fiber-4 Placement 2	6.7	3¼	84	29.0	5530
Control-4 Placement 1	5.5	3¼	72	22.0	-[b]
Control-4 Placement 2	5.7	3¼	78	25.5	5700
Fiber-5	7.0	4½	76	24.5	6700
Control-5	7.4	6½	66	19.0	6340
Fiber-6	7.5	5¼	67	19.5	5900
Control-6	6.5	5¾	75	24.0	6780
Fiber-7	7.1	5¼	75	24.0	6660
Control-7	6.2	4¾	76	24.5	7030
SRA-1	7.6	4	68	20.0	4340
SRA-2	5.7	3¾	70	21.0	4600
SRA-3	5.9	4¼	76	24.5	4760
SRA-4	5.2	3	77	25.0	3780
VA-Control	5.9	3¾	64	17.5	5610

[a]: concrete properties are not available.
[b]: no data available.
Note: 1 in. = 25.4 mm; 10 psi = 0.07 MPa.

3.3.4 Construction

Table 3.7 lists the construction dates, contractors, and issues that occurred during construction of the bridge decks. The seven fiber and five control decks in Kansas were constructed between 2013 and 2015 by three contactors, while the four SRA and single control deck in Virginia were constructed between 2011 and 2013, each by a different contractor. Decks without personnel from the University of Kansas (KU) present during construction are marked “Not observed.”

Table 3.7 – Construction date and contractor for FRC, SRA, and control decks

Bridge Number	Construction Date	Contractor	Construction Issue
Fiber-1 Placement 1	9/5/2013	Contractor-KS-E	No issue
Fiber-1 Placement 2	11/6/2013		No issue
Fiber-2 Placement 1	9/25/2013		No issue
Fiber-2 Placement 2	11/14/2013		No issue
Fiber-3	4/11/2014	Contractor-KS-D	Loss of consolidation
Control-3	3/13/2014		Loss of consolidation
Fiber-4 Placement 1	8/19/2014		Loss of consolidation Rain during construction
Fiber-4 Placement 2	8/26/2014		Loss of consolidation
Control-4 Placement 1	6/13/2014		Loss of consolidation
Control-4 Placement 2	6/20/2014		Loss of consolidation
Fiber-5	11/10/2014	Contractor-KS-F	No issue
Control-5	11/25/2014		No issue
Fiber-6	5/12/2015		No issue
Control-6	5/5/2015		No issue
Fiber-7	6/1/2015		No issue
Control-7	5/27/2015		No issue
SRA-1	12/4/2012	Contractor-VA-A	Not observed
SRA-2	12/19/2012	Contractor-VA-B	Not observed
SRA-3	8/30/2013	Contractor-VA-C	Not observed
SRA-4	8/30/2013	Contractor-VA-D	Not observed
VA-Control	12/13/2011	Contractor-VA-E	Not observed

The concrete in Fiber-3, Fiber-4, Control-3, and Control-4 did not receive adequate consolidation. Throughout construction of both placements of Fiber-4, construction workers with Contractor-KS-D walked through the concrete in the space between the vibrators and the screed to work the concrete [Figure 3.1(a)]. Walking in the initially consolidated concrete damaged the compaction and left voids (footprints) in the concrete. These voids were later covered when the finishing machine passed the sections, instead of being removed by revibration. Not reconsolidating the concrete can leave a substantial amount of entrapped air in the concrete, making the bridge deck susceptible to settlement cracking over and parallel to the top reinforcement (transverse to the direction of traffic). KDOT construction specifications require that voids left by workers be removed by reconsolidation (KDOT 2007). Because Contractor-KS-D has for many years permitted construction workers to walk through consolidated concrete

[Figure 3.1(b), taken during a construction in 2009], the same problem (loss of consolidation) is expected to have occurred on the other decks constructed by the company, including Fiber-3, Control-3, and Control-4.

(a)

(b)

Figure 3.1 – Construction personnel with Contractor-KS-D walking through consolidated concrete. (a) During construction of Fiber-4 in 2014, (b) during a construction in 2009. Red circles indicate the workers disturbing consolidated concrete

During the construction of Fiber-4 Placement 1, it rained when concrete finishing had progressed approximately 100 ft (30.5 m) (west end deck). Construction was not stopped due to the rain, and the concrete already in place was not protected from the rain water. Despite the low quantity of precipitation, water accumulated on the concrete surface and ponding was observed (Figure 3.2). This increases the local *w/cm* ratio and can lead to reduced concrete strength and an increased likelihood for scaling.

Figure 3.2 – Ponding of rainwater during construction of Fiber-4 Placement 1

3.4 CRACK SURVEY RESULTS

3.4.1 Fiber-1

Fiber-1 deck was constructed in two placements. Placement 1 was constructed on September 5, 2013, and Placement 2 was constructed on November 6, 2013. This deck has been surveyed four times. Survey 1 was performed at a deck age of 9.9 months for Placement 1 and 7.9 months for Placement 2. The crack map from this survey is shown in Figure 3.3. Survey 2 was

performed at a deck age of 21.6 months for Placement 1 and 19.6 months for Placement 2, the crack map from this survey is shown in Figure 3.4. Survey 3 (Figure 3.5) was performed at ages of 33.7 months and 31.7 months for Placement 1 and Placement 2, respectively. Lastly, Survey 4 was performed when Placement 1 was 45.5 months old and Placement 2 was 43.5 months old, the crack map is shown in Figure 3.6.

The crack densities for the entire deck (both placements) were 0.010, 0.121, 0.166, 0.130 m/m^2 in the four surveys, respectively, 0.009, 0.189, 0.112, 0.088 m/m^2 for Placement 1 and 0.011, 0.056, 0.220, and 0.172 m/m^2 for Placement 2. Ignoring short crazing cracks, it can be seen in Figures 3.3 through 3.6 that cracking consists primarily of transverse cracks that are parallel to the top reinforcement in most areas of the deck, except near the abutments, where the majority of cracks are longitudinal. The length of both transverse and longitudinal cracks tended to increase as the bridge deck aged. The density of crazing cracks reached a peak in Survey 2 and decreased in subsequent surveys, leading to a decreased crack density in Survey 4 compared to Survey 3. The main reason for the decrease is scaling of the deck surface, making short cracks more difficult to identify. A similar observation can be made for Fiber-2, as discussed in Section 3.4.2.

In Survey 3 (2016), 58 measurements of crack width were made on Fiber-1 Placement 1, with crack widths ranging between 0.003 and 0.020 in. (0.08 and 0.51 mm) and averaging 0.006 in. (0.15 mm); 77 crack width measurements were made on Placement 2, with crack widths ranging between 0.002 and 0.012 in. (0.05 and 0.30 mm) and averaging 0.005 in. (0.13 mm).

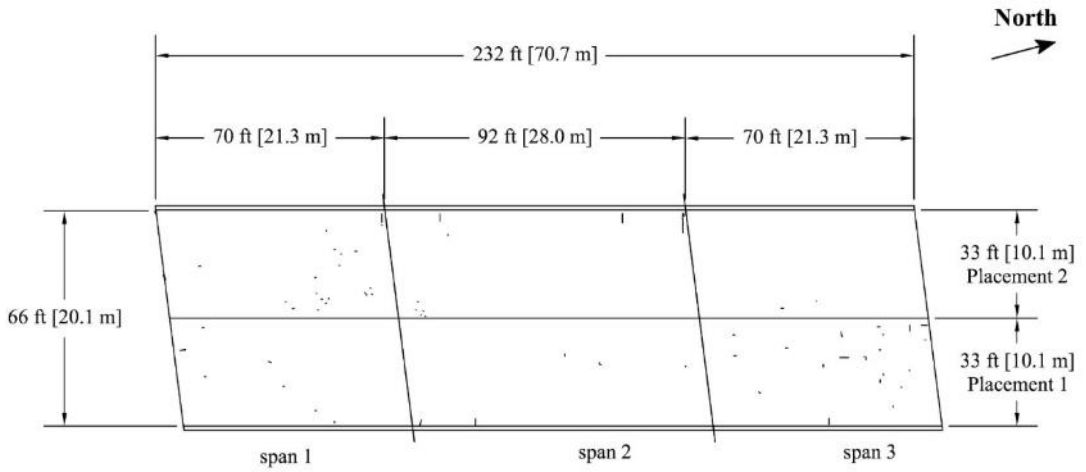

Bridge Number: 635-105-5.12
Bridge Location: NB I-635 over State Avenue
Construction Date:
Placement 1: 9/5/2013
Placement 2: 11/6/2013
Crack Survey Date: 7/2/2014

Bridge Length: 232 ft (70.7 m)
Bridge Width: 66 ft (20.1 m)
Skew: 7.3°
Number of Spans: 3
Span 1: 70.0 ft (21.3 m)
Span 2: 92.0 ft (28.0 m)
Span 3: 70.0 ft (21.3 m)
Number of Placements: 2

Bridge Age:
Placement 1: 9.9 months
Placement 2: 7.9 months
Crack Density:
Overall: 0.010 m/m^2
Span 1: 0.009 m/m^2
Span 2: 0.010 m/m^2
Span 3: 0.013 m/m^2
Placement 1: 0.009 m/m^2
Placement 2: 0.011 m/m^2

Figure 3.3 – Fiber-1 (Survey 1)

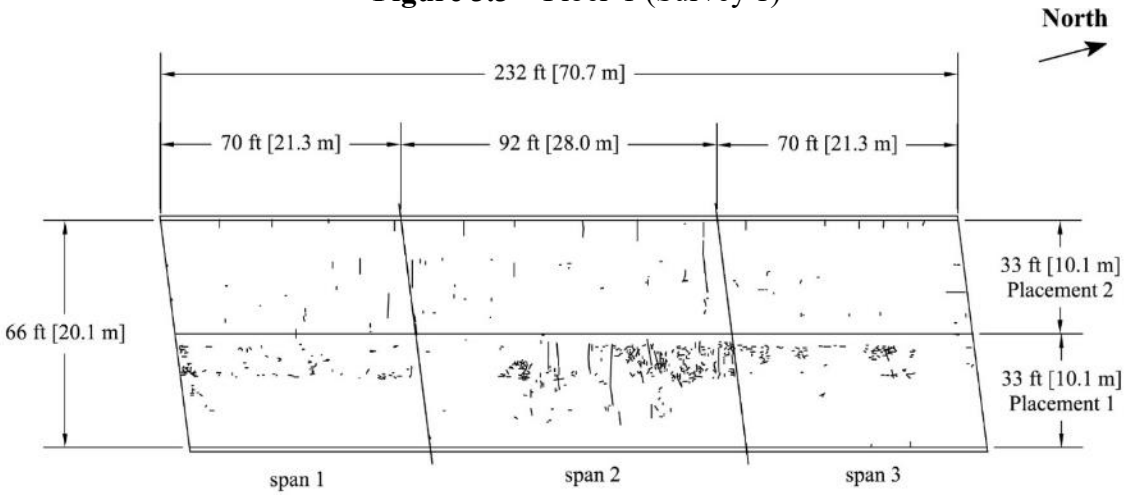

Bridge Number: 635-105-5.12
Bridge Location: NB I-635 over State Avenue
Construction Date:
Placement 1: 9/5/2013
Placement 2: 11/6/2013
Crack Survey Date: 6/23/2015

Bridge Length: 232 ft (70.7 m)
Bridge Width: 66 ft (20.1 m)
Skew: 7.3°
Number of Spans: 3
Span 1: 70 ft (21.3 m)
Span 2: 92 ft (28 m)
Span 3: 70 ft (21.3 m)
Number of Placements: 2

Bridge Age:
Placement 1: 21.6 months
Placement 2: 19.6 months
Crack Density:
Overall: 0.121 m/m^2
Span 1: 0.074 m/m^2
Span 2: 0.193 m/m^2
Span 3: 0.071 m/m^2
Placement 1: 0.189 m/m^2
Placement 2: 0.056 m/m^2

Figure 3.4 – Fiber-1 (Survey 2)

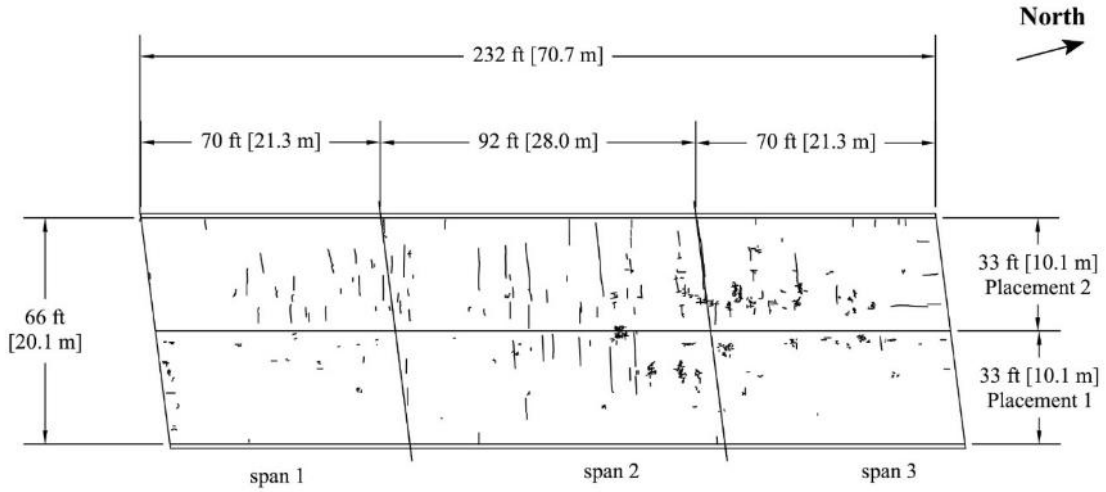

Bridge Number: 635-105-5.12
Bridge Location: NB I-635 over State Avenue
Construction Date:
Placement 1: 9/5/2013
Placement 2: 11/6/2013
Crack Survey Date: 6/27/2016

Bridge Length: 232 ft (70.7 m)
Bridge Width: 66 ft (20.1 m)
Skew: 7.3°
Number of Spans: 3
Span 1: 70 ft (21.3 m)
Span 2: 92 ft (28.0 m)
Span 3: 70 ft (21.3 m)
Number of Placements: 2

Bridge Age:
Placement 1: 33.7 months
Placement 2: 31.7 months
Crack Density: 0.166 m/m^2
Span 1: 0.082 m/m^2
Span 2: 0.211 m/m^2
Span 3: 0.189 m/m^2
Placement 1: 0.112 m/m^2
Placement 2: 0.220 m/m^2

Figure 3.5 – Fiber-1 (Survey 3)

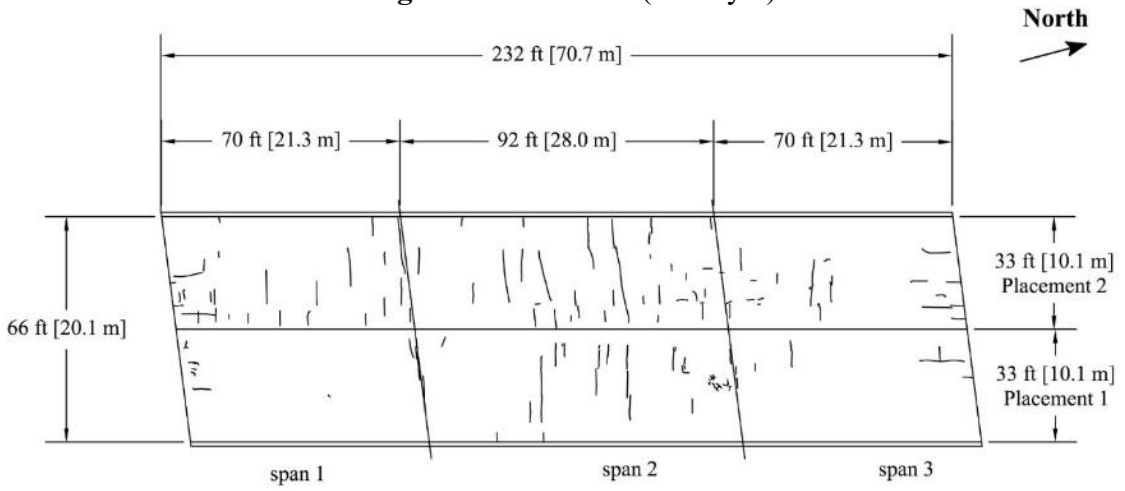

Bridge Number: 635-105-5.12
Bridge Location: NB I-635 over State Avenue
Construction Date:
Placement 1: 9/5/2013
Placement 2: 11/6/2013
Crack Survey Date: 6/20/2017

Bridge Length: 232 ft (70.7 m)
Bridge Width: 66 ft (20.1 m)
Skew: 7.3°
Number of Spans: 3
Span 1: 70 ft (21.3 m)
Span 2: 92 ft (28.0 m)
Span 3: 70 ft (21.3 m)
Number of Placements: 2

Bridge Age:
Placement 1: 45.5 months
Placement 2: 43.5 months
Crack Density:
Overall: 0.130 m/m^2
Span 1: 0.119 m/m^2
Span 2: 0.170 m/m^2
Span 3: 0.088 m/m^2
Placement 1: 0.088 m/m^2
Placement 2: 0.172 m/m^2

Figure 3.6 – Fiber-1 (Survey 4)

3.4.2 Fiber-2

The Fiber-2 deck was constructed in two placements. The first placement was constructed on September 25, 2013 and the second November 14, 2013. Four surveys have been performed on Fiber-2. The first survey was in the summer of 2014 when Placement 1 was 9.2 months old and Placement 2 was 7.6 months old. Survey 2 was performed at an age of 22.4 months for Placement 1 and 20.7 months for Placement 2. Survey 3 was performed at an age of 34.0 months for Placement 1 and 32.4 months for Placement 2. The most recent survey was performed in the summer of 2017 at an age of 44.9 months for Placement 1 and 43.2 months for Placement 2.

In the four surveys, the crack densities for the entire deck were 0.027, 0.153, 0.291, and 0.208 m/m^2, 0.014, 0.049, 0.127, and 0.126 m/m^2 for Placement 1, and 0.042, 0.269, 0.456, and 0.290 m/m^2 for Placement 2. The deck exhibited primarily short and randomly oriented cracks in the first two surveys, while in the latter two surveys, more transverse cracks (parallel to the top reinforcement) were observed over most of the deck, and more longitudinal cracks were observed near the abutments. A notable number of crazing cracks were found during Surveys 2 and 3, especially near the pier between Span 1 and Span 2 and in the middle of Span 2 in Placement 2. The number of crazing cracks decreased in Survey 4. As with Fiber-1, the decrease in crazing cracks, and the resulting decrease in crack density, was likely due to scaling of the concrete surface, which made it difficult to identify short cracks during the crack surveys. Figure 3.11 compares the appearance of the deck surface during the surveys performed in 2016 and 2017. Surface scaling is clearly observable in 2017, as indicated by the appearance of coarse aggregate [limestone, shown as white particles in Figure 3.11 (b)] and lower definition to the edges of grooves.

In Survey 3, 40 crack width measurements were taken on Fiber-2 Placement 1, with crack widths ranging from 0.003 to 0.008 in. (0.08 to 0.20 mm) and averaging 0.006 in. (0.15 mm); 119 measurements were taken on Placement 2, with crack widths ranging between 0.004 and 0.012 (0.10 and 0.30 mm) and averaging 0.005 in. (0.13 mm).

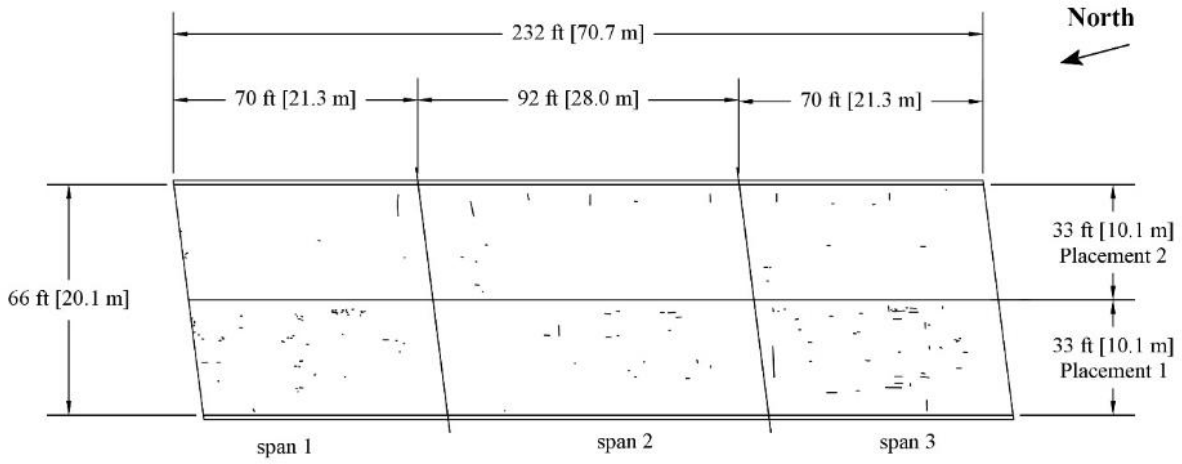

Bridge Number: 635-105-5.12
Bridge Location: SB I-635 over State Avenue
Construction Date:
Placement 1: 9/25/2013
Placement 2: 11/14/2013
Crack Survey Date: 7/2/2014

Bridge Length: 232 ft (70.7 m)
Bridge Width: 66 ft (20.1 m)
Skew: 7.2°
Number of Spans: 3
Span 1: 70 ft (21.3 m)
Span 2: 92 ft (28.0 m)
Span 3: 70 ft (21.3 m)
Number of Placements: 2

Bridge Age:
Placement 1: 9.2 months
Placement 2: 7.6 months
Crack Density:
Overall: 0.027 m/m^2
Span 1: 0.021 m/m^2
Span 2: 0.017 m/m^2
Span 3: 0.047 m/m^2
Placement 1: 0.014 m/m^2
Placement 2: 0.042 m/m^2

Figure 3.7 – Fiber-2 (Survey 1)

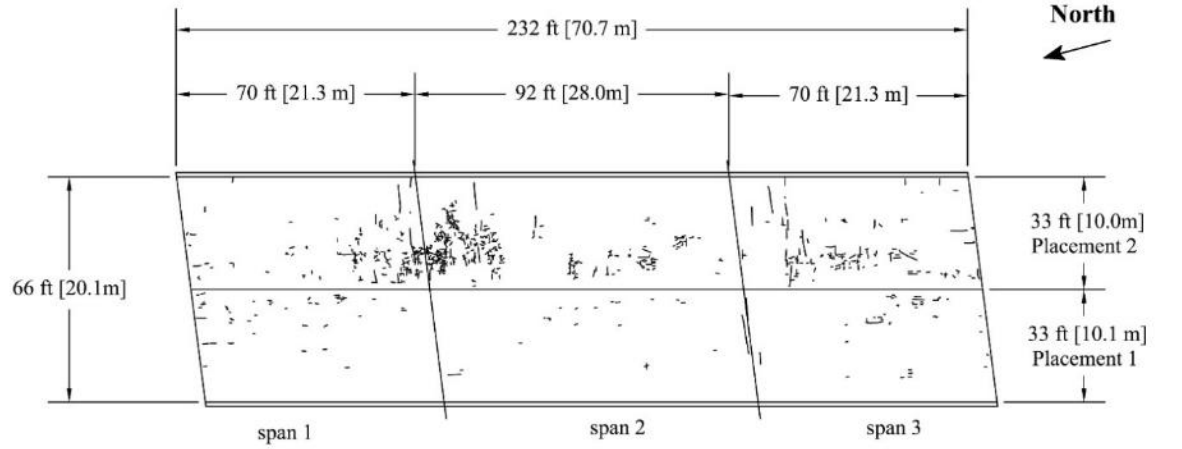

Bridge Number: 635-105-5.12
Bridge Location: SB I-635 over State Avenue
Construction Date:
Placement 1: 9/25/2013
Placement 2: 11/14/2013
Crack Survey Date: 7/28/2015

Bridge Length: 232 ft (70.7 m)
Bridge Width: 66 ft (20.1 m)
Skew: 7.2°
Number of Spans: 3
Span 1: 70 ft (21.3 m)
Span 2: 92 ft (28.0 m)
Span 3: 70 ft (21.3 m)
Number of Placements: 2

Bridge Age:
Placement 1: 22.4 months
Placement 2: 20.7 months
Crack Density:
Overall: 0.153 m/m^2
Span 1: 0.134 m/m^2
Span 2: 0.174 m/m^2
Span 3: 0.145 m/m^2
Placement 1: 0.049 m/m^2
Placement 2: 0.269 m/m^2

Figure 3.8 – Fiber-2 (Survey 2)

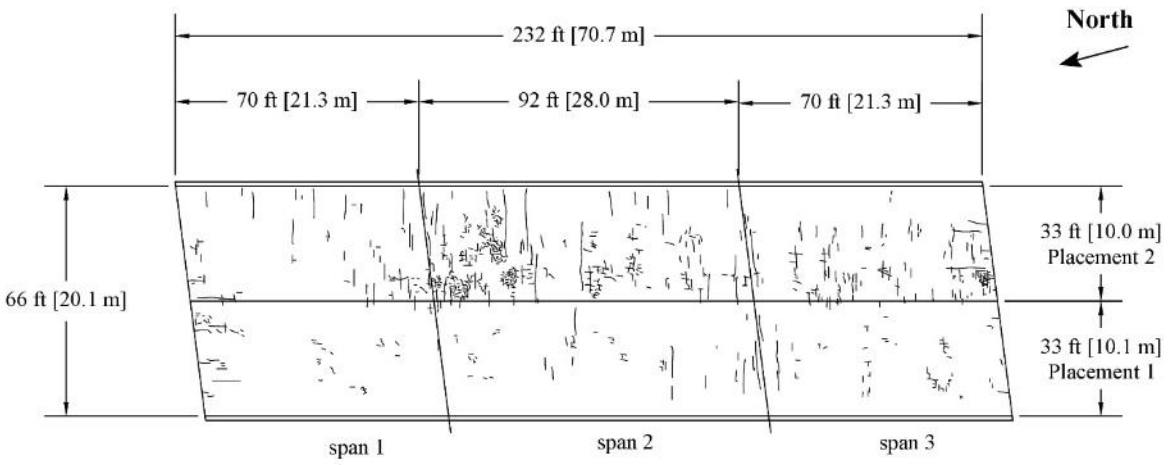

Bridge Number: 635-105-5.12
Bridge Location: SB I-635 over State Avenue
Construction Date:
Placement 1: 9/25/2013
Placement 2: 11/14/2013
Crack Survey Date: 7/26/2016

Bridge Length: 232 ft (70.7 m)
Bridge Width: 66 ft (20.1 m)
Skew: 7.2°
Number of Spans: 3
Span 1: 70 ft (21.3 m)
Span 2: 92 ft (28.0 m)
Span 3: 70 ft (21.3 m)
Number of Placements: 2

Bridge Age:
Placement 1: 34.0 months
Placement 2: 32.4 months
Crack Density:
Overall: 0.291 m/m^2
Span 1: 0.186 m/m^2
Span 2: 0.383 m/m^2
Span 3: 0.255 m/m^2
Placement 1: 0.127 m/m^2
Placement 2: 0.456 m/m^2

Figure 3.9 – Fiber-2 (Survey 3)

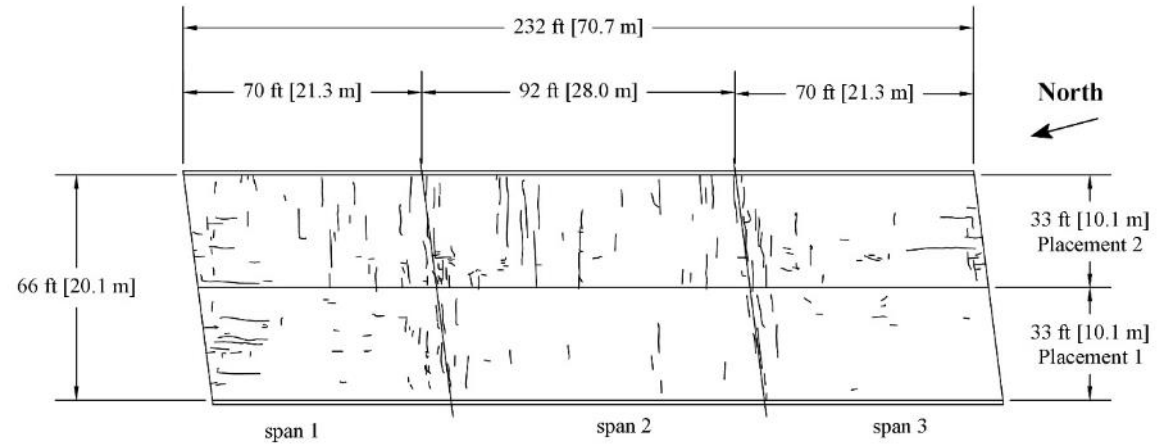

Bridge Number: 635-105-5.12
Bridge Location: SB I-635 over State Avenue
Construction Date:
Placement 1: 9/25/2013
Placement 2: 11/14/2013
Crack Survey Date: 6/20/2017

Bridge Length: 232 ft (70.7 m)
Bridge Width: 66 ft (20.1 m)
Skew: 7.2°
Number of Spans: 3
Span 1: 70 ft (21.3 m)
Span 2: 92 ft (28.0 m)
Span 3: 70 ft (21.3 m)
Number of Placements: 2

Bridge Age:
Placement 1: 44.9 months
Placement 2: 43.2 months
Crack Density:
Overall: 0.208 m/m^2
Span 1: 0.253 m/m^2
Span 2: 0.204 m/m^2
Span 3: 0.168 m/m^2
Placement 1: 0.126 m/m^2
Placement 2: 0.290 m/m^2

Figure 3.10 – Fiber-2 (Survey 4)

(a) (b)

Figure 3.11 – Comparison of deck surface of Fiber-2 during (a) 2016 and (b) 2017 surveys.

3.4.3 Fiber-1 and Fiber-2 Comparison

Figure 3.12 compares the crack densities of the placements on Fiber-1 and Fiber-2 as a function of age. Fiber-1 Placement 1 had the second highest crack density in Survey 2 but had the lowest crack density in the last two surveys; as discussed earlier, this is likely due to the development of surface scaling, which made it hard to identify crazing cracks. By comparing the placements with GFRP reinforcement (both placements of Fiber-2) and those without (both placements of Fiber-1), it can be seen that GFRP reinforcement did not noticeably change the cracking behavior of bridge decks, as indicated by the similar crack densities of this group of decks. Fiber-2 Placement 2 has noticeably higher crack densities in all four surveys; it is not clear, however, what the cause is.

The average crack widths measured in 2016 surveys and the *p* values obtained in Student's t-test for the differences in the average crack widths of Fiber-1 and Fiber-2 are shown in Table 3.8. GFRP reinforcement did not appear to affect the crack width of bridge decks, indicated by the similar average crack widths of the four placements [0.005 in. or 0.006 in. (0.13 mm or 0.15 mm)].

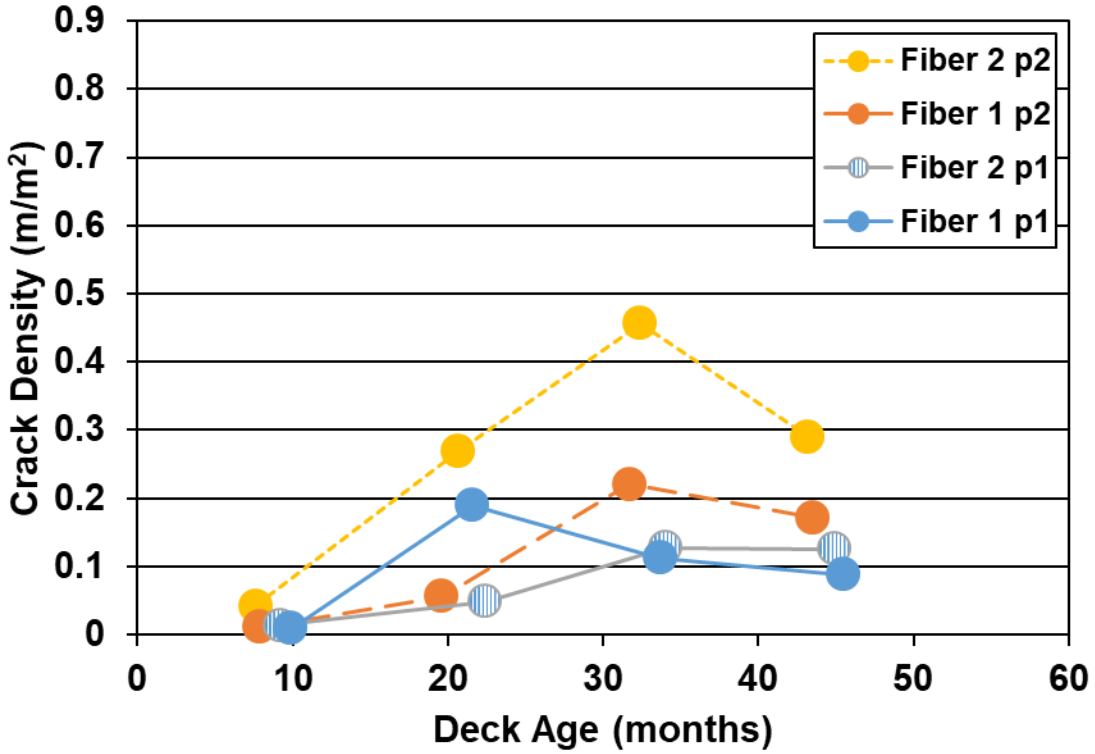

Figure 3.12 – Fiber-1 and Fiber-2 crack density versus deck age

Table 3.8 – *p* values obtained in Student's t-test for the differences in average crack widths of Fiber-1 and Fiber-2

	Bridge Deck Placement	Fiber-1 Placement 1	Fiber-1 Placement 2	Fiber-2 Placement 1	Fiber-2 Placement 2
Bridge Deck Placement	Average Crack Width in.	0.006	0.005	0.006	0.005
Fiber-1 Placement 1	0.006		0.02	0.06	0.01
Fiber-1 Placement 2	0.005			0.44	0.70
Fiber-2 Placement 1	0.006				0.25

3.4.4 Fiber-3

Fiber-3 was constructed on April 11, 2014 and has been surveyed four times. Survey 1 was performed in 2015 when the deck was 16.0 months old; Survey 2 was completed at an age of 26.8 months; Survey 3 was completed at an age of 37.8 months; and Survey 4 was performed in 2018 at an age of 50.9 months.

The crack maps for the four surveys on Fiber-3 are shown in Figures 3.13 through 3.16. The crack density steadily increased with deck age, going up from 0.157 m/m^2 in Survey 1 (Figure 3.13) to 0.272 m/m^2 in Survey 2 (Figure 3.14), 0.287 m/m^2 in Survey 3 (Figure 3.16), and 0.394 m/m^2 in Survey 4 (Figure 3.17). Most cracks were transverse to the direction of traffic and between the middle of Span 1 and middle of Span 3; cracks near the abutments were mainly longitudinal. As will be shown in Section 3.3.8, the crack pattern of Fiber-3 is similar to that of Fiber-4, suggesting that the same procedure for consolidation and finishing was used for both decks and that Fiber-3, like Fiber-4, experienced a loss of consolidation (described in Section 3.3.4). Short, randomly oriented cracks were found throughout the deck, and the extent of such cracking increased as the deck aged. In Survey 1, the short cracks were concentrated around the pier between Spans 1 and 2; in Survey 2, such cracks were observed around both piers and in Span 2; in Surveys 3 and 4, such cracks were observed throughout the deck. Minimal scaling was observed on Fiber-3.

In Survey 2 (2016), 125 crack width measurements were made on Fiber-3, yielding values ranging between 0.004 and 0.012 in. (0.10 and 0.30 mm) and averaging 0.006 in. (0.15 mm).

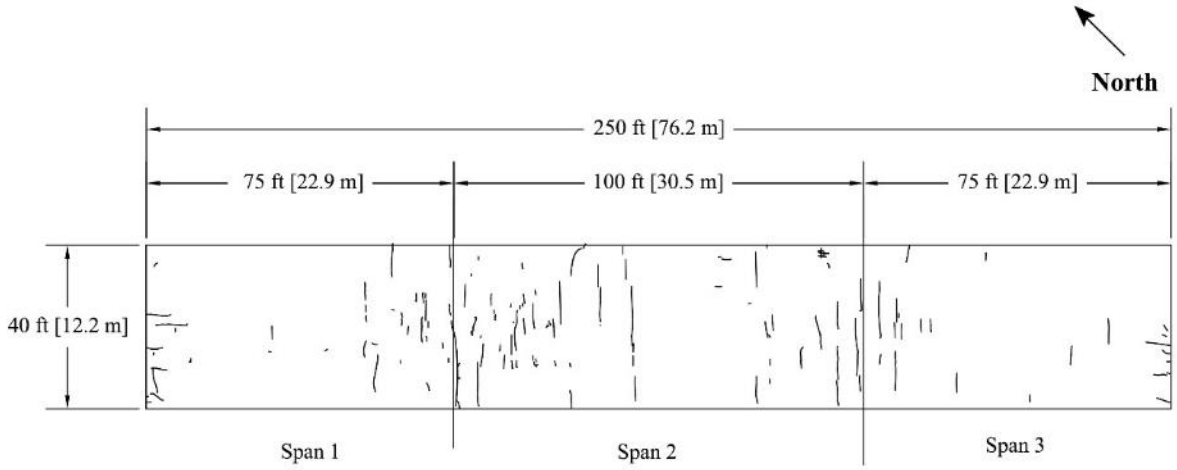

Bridge Number: 24-89-17.68 (297)
Bridge Location: EB US-24 over Menoken Rd.
Construction Date: 4/11/2014
Crack Survey Date: 8/11/2015

Bridge Length: 250 ft (76.2 m)
Bridge Width: 40 ft (12.2 m)
Skew: 0°
Number of Spans: 3
Span 1: 75 ft (22.9 m)
Span 2: 100 ft (30.5 m)
Span 3: 75 ft (22.9 m)
Number of Placements: 1

Bridge Age: 16.0 months
Crack Density: 0.157 m/m^2
Span 1: 0.122 m/m^2
Span 2: 0.230 m/m^2
Span 3: 0.096 m/m^2

Figure 3.13 – Fiber-3 (Survey 1)

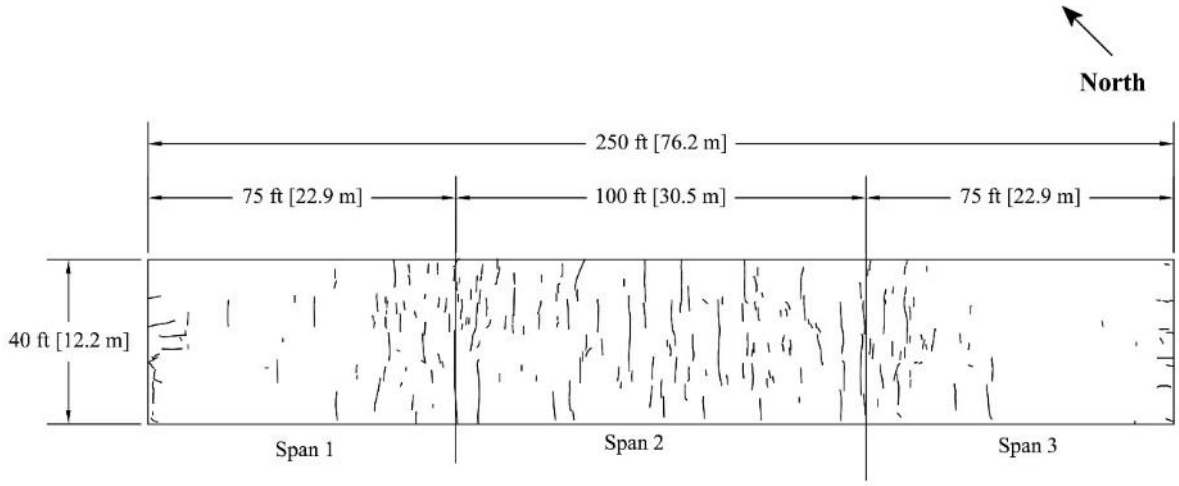

Bridge Number: 24-89-17.68 (297)
Bridge Location: EB US-24 over Menoken Rd.
Construction Date: 4/11/2014
Crack Survey Date: 6/24/2016

Bridge Length: 250 ft (76.2 m)
Bridge Width: 40 ft (12.2 m)
Skew: 0°
Number of Spans: 3
Span 1: 75 ft (22.9 m)
Span 2: 100 ft (30.5 m)
Span 3: 75 ft (22.9 m)
Number of Placements: 1

Bridge Age: 26.8 months
Crack Density: 0.272 m/m^2
Span 1: 0.218 m/m^2
Span 2: 0.399 m/m^2
Span 3: 0.157 m/m^2

Figure 3.14 – Fiber-3 (Survey 2)

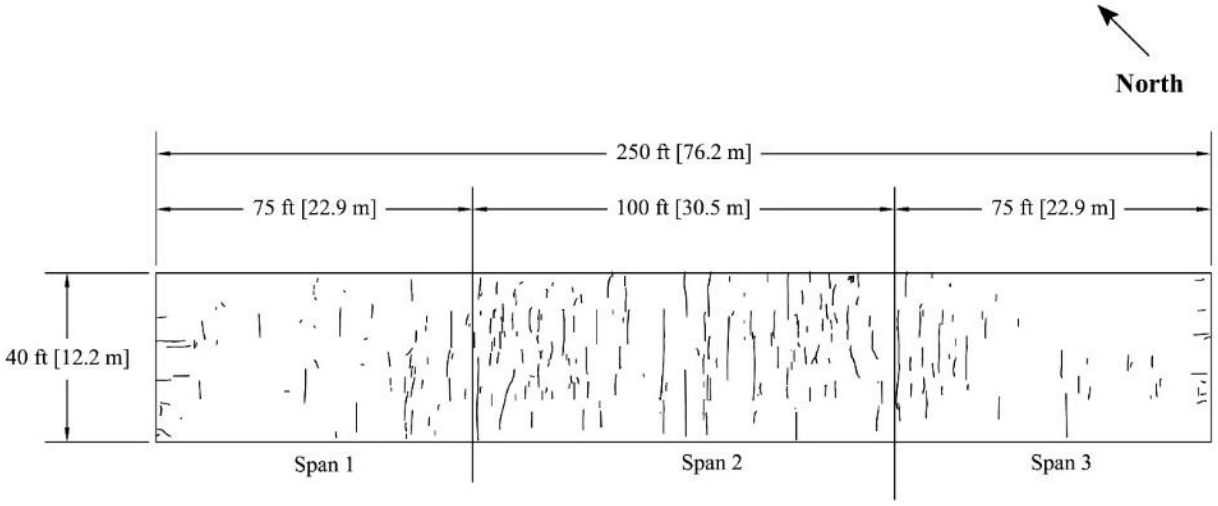

Bridge Number: 24-89-17.68 (297)
Bridge Location: EB US-24 over Menoken Rd.
Construction Date: 4/11/2014
Crack Survey Date: 6/5/2017

Bridge Length: 250 ft (76.2 m)
Bridge Width: 40 ft (12.2 m)
Skew: 0°
Number of Spans: 3
Span 1: 75 ft (22.9 m)
Span 2: 100 ft (30.5 m)
Span 3: 75 ft (22.9 m)
Number of Placements: 1

Bridge Age: 37.8 months
Crack Density: 0.287 m/m^2
Span 1: 0.181 m/m^2
Span 2: 0.440 m/m^2
Span 3: 0.192 m/m^2

Figure 3.15 – Fiber-3 (Survey 3)

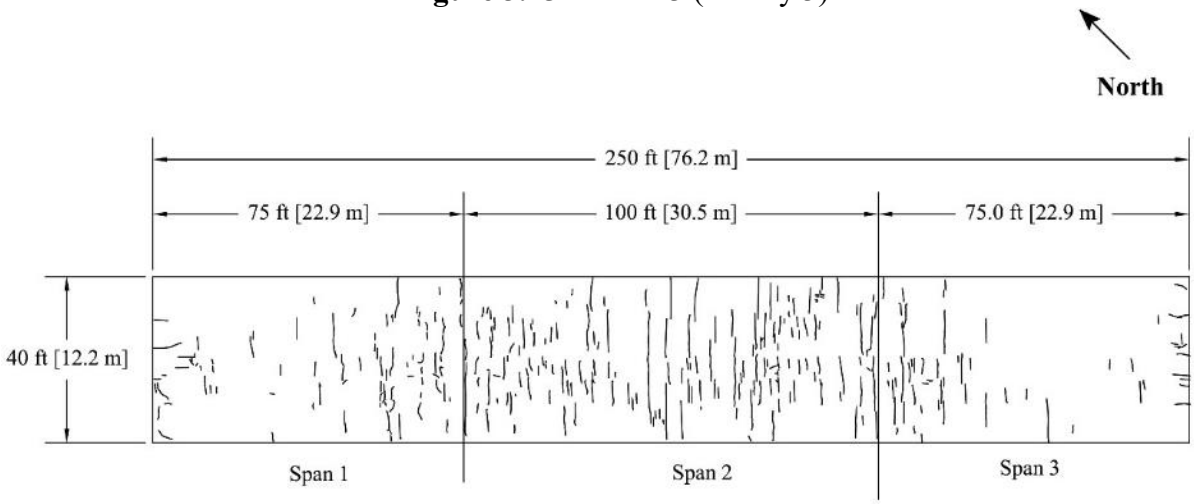

Bridge Number: 24-89-17.68 (297)
Bridge Location: EB US-24 over Menoken Rd.
Construction Date: 4/11/2014
Crack Survey Date: 7/9/2018

Bridge Length: 250 ft (76.2m)
Bridge Width: 40 ft (12.2 m)
Skew: 0°
Number of Spans: 3
Span 1: 75 ft (22.9 m)
Span 2: 100 ft (30.5 m)
Span 3: 75 ft (22.9 m)
Number of Placements: 1

Bridge Age: 50.9 months
Crack Density: 0.394 m/m^2
Span 1: 0.272 m/m^2
Span 2: 0.602 m/m^2
Span 3: 0.239 m/m^2

Figure 3.16 – Fiber-3 (Survey 4)

3.4.5 Control-3

Bridge deck Control-3 was constructed on June 6, 2014 and has been surveyed four times. The first survey was completed in 2015 at a deck age of 14.3 months (Figure 3.17). The subsequent surveys were performed at ages of 24.9, 36.0, and 49.1 months. The crack maps for the four surveys on Control-3 are shown in Figures 3.17 through 3.20.

A crack density of 0.141 m/m^2 was observed in Survey 1 (Figure 3.17), increasing notably to 0.322 m/m^2 in Survey 2 (Figure 3.18). The crack density decreased to 0.233 m/m^2 in Survey 3 (Figure 3.19) and increased again to 0.290 m/m^2 in Survey 4 (Figure 3.20). Both the number and length of transverse cracks increased with deck age, even as the total crack density fluctuated. In Survey 1, transverse cracks were found only in Span 2 and near the two piers; in later surveys, such cracks were found in all three spans of the deck. The number of crazing cracks increased from Survey 1 to Survey 2, but decreased in Surveys 3 and 4, most notably at the west abutment. The reduction of crazing cracks in Surveys 3 and 4 is most likely caused by surface scaling, shown in Figure 3.21.

In Survey 2 (2016), 111 crack width measurements were taken, with values ranging from 0.004 to 0.025 in. (0.10 to 0.64 mm) and averaging 0.009 in. (0.23 mm).

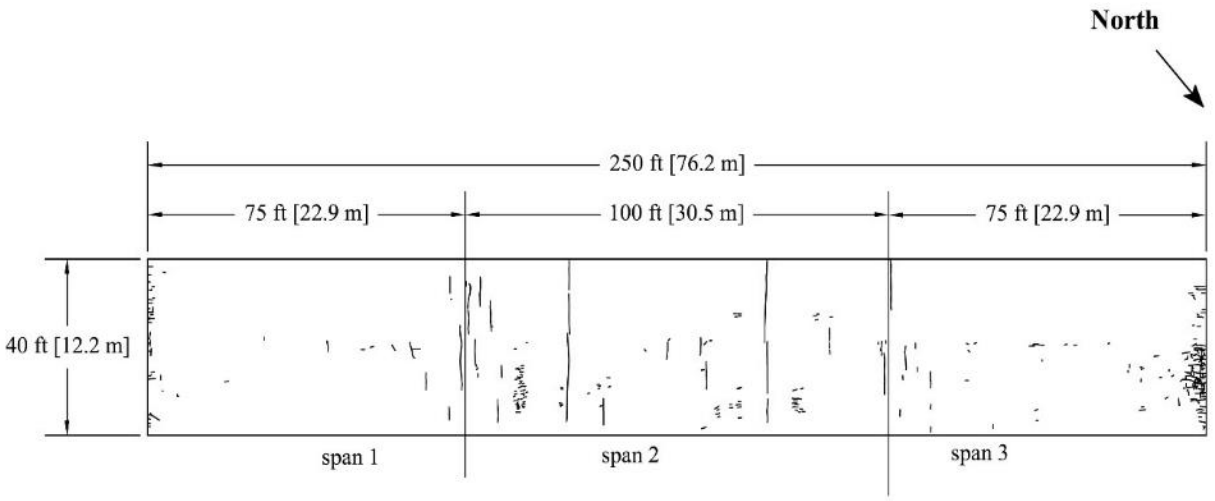

Bridge Number: 24-89-17.67 (296)
Bridge Location: WB US-24 over Menoken Rd.
Construction Date: 6/6/2014
Crack Survey Date: 8/11/2015

Bridge Length: 250 ft (76.2 m)
Bridge Width: 40 ft (12.2 m)
Skew: 0°
Number of Spans: 3
Span 1: 75 ft (22.9 m)
Span 2: 100 ft (30.5 m)
Span 3: 75 ft (22.9 m)
Number of Placements: 1

Bridge Age: 14.3 months
Crack Density: 0.141 m/m^2
Span 1: 0.075 m/m^2
Span 2: 0.168 m/m^2
Span 3: 0.170 m/m^2

Figure 3.17 – Control-3 (Survey 1)

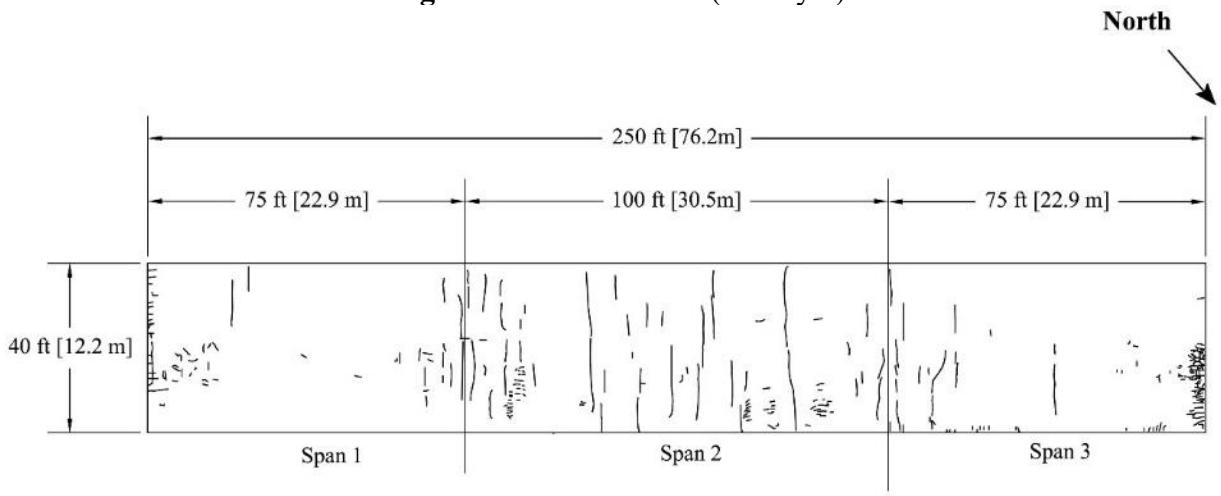

Bridge Number: 24-89-17.67 (296)
Bridge Location: WB US-24 over Menoken Rd.
Construction Date: 6/6/2014
Crack Survey Date: 6/22/2016

Bridge Length: 250 ft (76.2 m)
Bridge Width: 40 ft (12.2 m)
Skew: 0°
Number of Spans: 3
Span 1: 75 ft (22.9 m)
Span 2: 100 ft (30.5 m)
Span 3: 75 ft (22.9 m)
Number of Placements: 1

Bridge Age: 24.9 months
Crack Density: 0.322 m/m^2
Span 1: 0.246 m/m^2
Span 2: 0.431 m/m^2
Span 3: 0.257 m/m^2

Figure 3.18 – Control-3 (Survey 2)

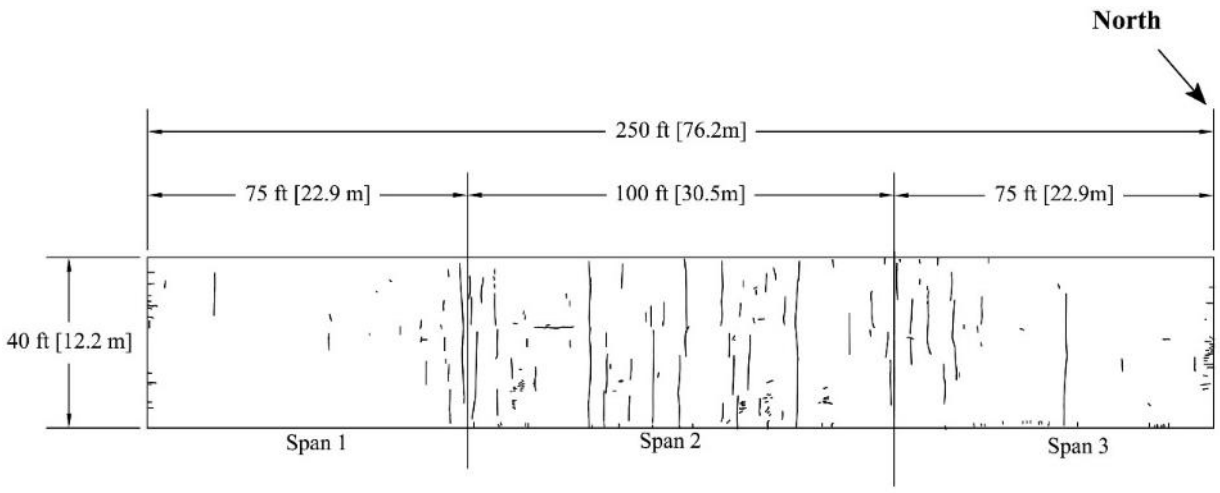

Bridge Number: 24-89-17.67 (296)
Bridge Location: WB US-24 over Menoken Rd.
Construction Date: 6/6/2014
Crack Survey Date: 6/5/2017

Bridge Length: 250 ft (76.2 m)
Bridge Width: 40 ft (12.2 m)
Skew: 0°
Number of Spans: 3
Span 1: 75 ft (22.9 m)
Span 2: 100 ft (30.5 m)
Span 3: 75 ft (22.9 m)
Number of Placements: 1

Bridge Age: 36.0 months
Crack Density: 0.233 m/m^2
Span 1: 0.108 m/m^2
Span 2: 0.369 m/m^2
Span 3: 0.178 m/m^2

Figure 3.19 – Control-3 (Survey 3)

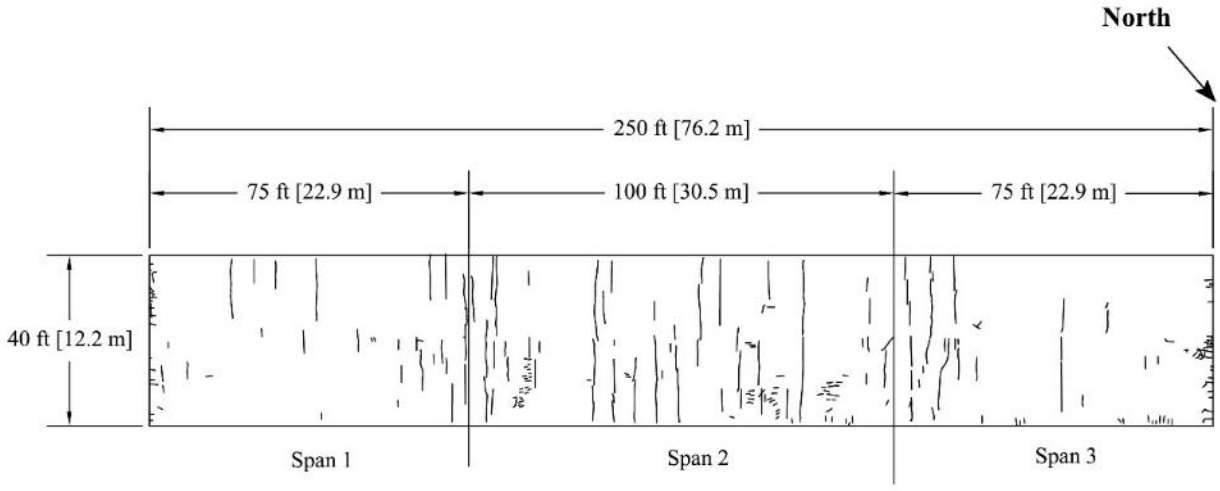

Bridge Number: 24-89-17.67 (296)
Bridge Location: WB US-24 over Menoken Rd.
Construction Date: 6/6/2014
Crack Survey Date: 7/9/2018

Bridge Length: 250 ft (76.2 m)
Bridge Width: 40 ft (12.2 m)
Skew: 0°
Number of Spans: 3
Span 1: 75 ft (22.9 m)
Span 2: 100 ft (30.5 m)
Span 3: 75 ft (22.9 m)
Number of Placements: 1

Bridge Age: 49.1 months
Crack Density: 0.290 m/m^2
Span 1: 0.203 m/m^2
Span 2: 0.389 m/m^2
Span 3: 0.244 m/m^2

Figure 3.20 – Control-3 (Survey 4)

Figure 3.21 – Surface scaling on Control-3 during Survey 3

3.4.6 Fiber-3 and Control-3 Comparison

Figure 3.22 shows the crack densities of Fiber-3 and Control-3 as a function of deck age. Overall, the two decks have similar crack densities. The crack density of Fiber-3 increased steadily over the years, while that of Control-3 reached a peak in Survey 2, decreased in Survey 3, and increased again in Survey 4. As discussed in Section 3.4.5, Control-3 exhibited scaling, which reduces the number of crazing cracks that can be observed, and in turn, the measured crack density, which may explain its lower crack density compared to Fiber-3 in Surveys 3 and 4.

The average crack width on Fiber-3, at 0.006 in. (0.15 mm), was approximately one-third narrower than on Control-3, with an average of 0.009 in. (0.22 mm), a difference that is statistically significant ($p = 2.45 \times 10^{-8}$).

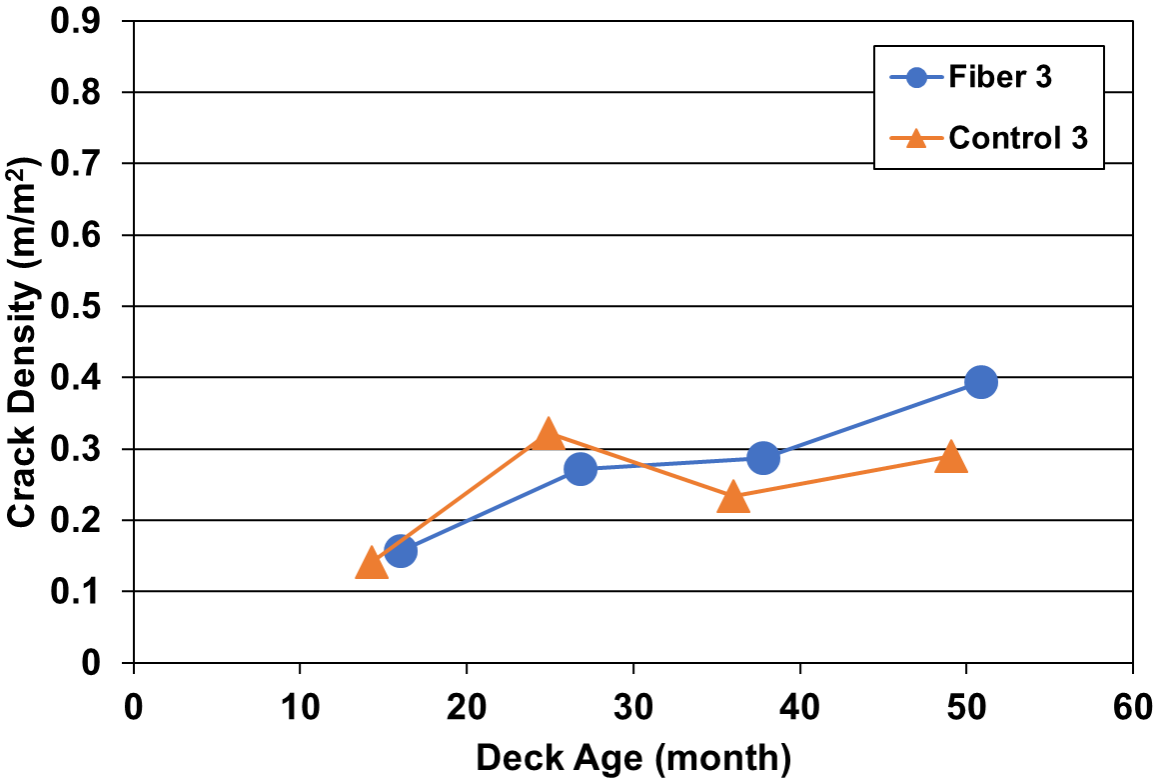

Figure 3.22 – Fiber-3 and Control-3 crack density versus deck age

3.4.7 Fiber-4

Fiber-4 had two placements. Placement 1 was constructed on August 19, 2014 and Placement 2 was constructed on August 26, 2014. Fiber-4 has been surveyed 3 times. Survey 1 was performed in 2015 at ages of 12.2 and 12.1 months for Placements 1 and 2, respectively. Survey 2 was completed in 2016 at ages of 24.2 and 24.1 months for Placements 1 and 2. Survey 3 was performed in 2017 at ages of 33.6 and 33.4 months for Placements 1 and 2. The crack maps for these surveys are shown in Figures 3.23 through 3.25.

The overall crack density found in Survey 1 was 0.432 m/m^2, 0.608 m/m^2 for Placement 1 and 0.173 m/m^3 for Placement 2 was (Figure 3.23). In Survey 2, the crack density was 0.522 m/m^2 for the entire deck, 0.645 m/m^2 for Placement 1 and 0.300 m/m^2 for Placement 2 (Figure 3.24). In Survey 3, the crack density was 0.594 m/m^2 for the entire bridge, 0.709 m/m^2 for Placement 1 and 0.431 m/m^2 for Placement 2 (Figure 3.25). The majority of the cracks on Fiber-4 are transverse to

the direction of traffic, except for some diagonal cracks at the abutments. Surveying on Fiber-4 was discontinued after Survey 3 due to the high crack density.

In all three surveys, Span 2 consistently exhibited a higher crack density than the other two spans. As shown in the crack maps, most of the cracks in Span 2 occur in Placement 1. Given that the two placements were constructed seven days apart, the high crack density in Span 2 may have been caused by the loading from construction.

Scaling was observed in the approximately first 100 ft (30.5 m) of the deck at the west end [Figure 3.26 (a)]. As discussed in Section 3.3.4, rainfall occurred during concrete placement in this section, which increased the local *w/c* ratio at the surface and increased the vulnerability of concrete to scaling. The remainder of the deck had minimal scaling [Figure 3.26 (b)].

In Survey 2 (2016), 93 crack width measurements were made on Placement 1, with values ranging from 0.004 to 0.020 in. (0.10 to 0.51 mm) and averaging 0.008 in. (0.20 mm); 47 measurements were made on Placement 2 with values ranging from 0.004 to 0.016 (0.10 and 0.41 mm) and averaging 0.007 in. (0.18 mm).

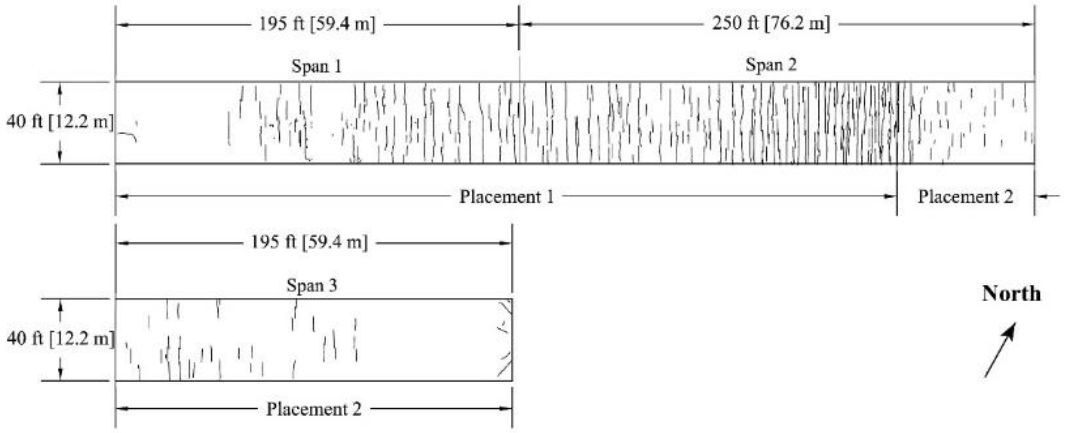

Bridge Number: 24-89-17.23 (283)
Bridge Location: EB US-24 over UPRR
Construction Date:
Placement 1: 8/19/2014
Placement 2: 8/26/2014
Crack Survey Date: 8/17/2015

Bridge Length: 640 ft (195.1m)
Bridge Width: 40 ft (12.2 m)
Skew: 0°
Number of Spans: 3
Span 1: 195 ft (59.4 m)
Span 2: 250 ft (76.2 m)
Span 3:195 ft (59.4 m)
Number of Placements: 2

Bridge Age:
Placement 1: 12.2 months
Placement 2: 12.1 months
Crack Density:
Overall: 0.432 m/m^2
Span 1: 0.340 m/m^2
Span 2: 0.746 m/m^2
Span 3: 0.124 m/m^2
Placement 1: 0.608 m/m^2
Placement 2: 0.173 m/m^2

Figure 3.23 – Fiber-4 (Survey 1)

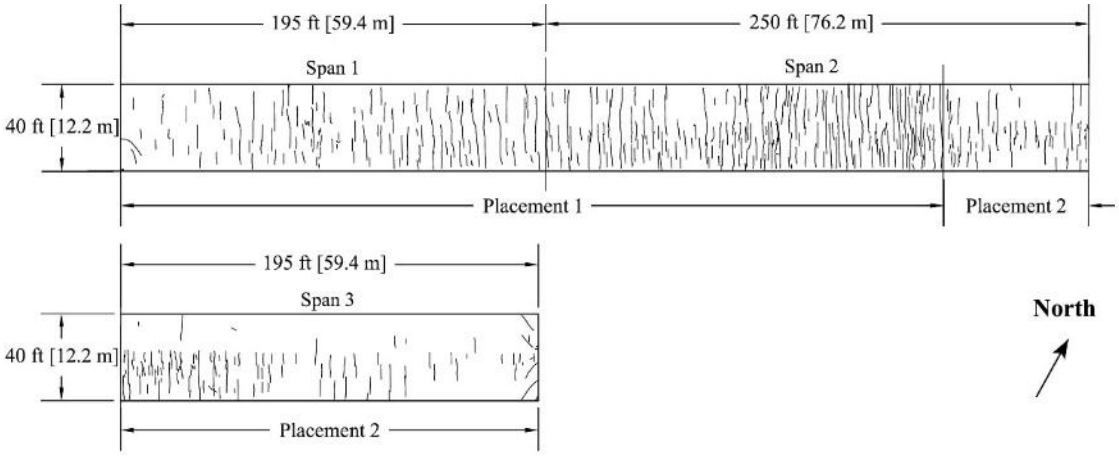

Bridge Number: 24-89-17.23 (283)
Bridge Location: EB US-24 over UPRR
Construction Date:
Placement 1: 8/19/2014
Placement 2: 8/26/2014
Crack Survey Date: 8/18/2016

Bridge Length: 640 ft (195.1 m)
Bridge Width: 40 ft (12.2 m)
Skew: 0°
Number of Spans: 3
Span 1: 195 ft (59.4 m)
Span 2: 250 ft (76.2 m)
Span 3: 195 ft (59.4 m)
Number of Placements: 2

Bridge Age:
Placement 1: 24.2 months
Placement 2: 24.1 months
Crack Density:
Overall: 0.522 m/m^2
Span 1: 0.420 m/m^2
Span 2: 0.780 m/m^2
Span 3: 0.293 m/m^2
Placement 1: 0.645 m/m^2
Placement 2: 0.300 m/m^2

Figure 3.24 – Fiber-4 (Survey 2)

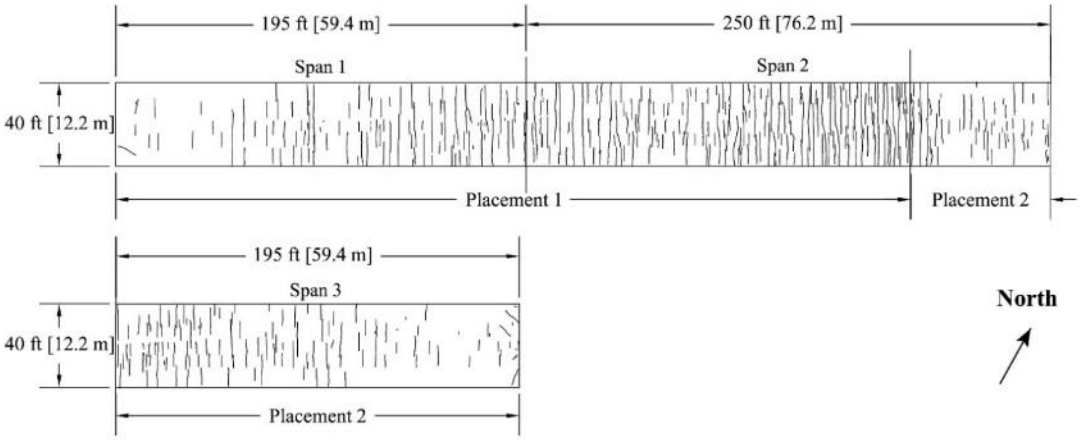

Bridge Number: 24-89-17.23 (283)
Bridge Location: EB US-24 over UPRR
Construction Date:
Placement 1: 8/19/2014
Placement 2: 8/26/2014
Crack Survey Date: 6/7/2017

Bridge Length: 640 ft (195.1 m)
Bridge Width: 40 ft (12.2 m)
Skew: 0°
Number of Spans: 3
Span 1: 195 ft (59.4 m)
Span 2: 250 ft (76.2 m)
Span 3: 195 ft (59.4 m)
Number of Placements: 2

Bridge Age:
Placement 1: 33.6 months
Placement 2: 33.4 months
Crack Density:
Overall: 0.594 m/m^2
Span 1: 0.447 m/m^2
Span 2: 0.872 m/m^2
Span 3: 0.386 m/m^2
Placement 1: 0.709 m/m^2
Placement 2: 0.431 m/m^2

Figure 3.25 – Fiber-4 (Survey 3)

(a)

(b)

Figure 3.26 – Scaling observed on Fiber-4 during Survey 3. (a) a typical section within 100 ft (30.5 m) from the west end of the deck; (b) a typical section for the remainder of the deck

3.4.8 Control-4

Control-4 was constructed in two placements. Placement 1 was completed on June 13, 2014 and Placement 2 on June 20, 2014. Like Fiber-4, Control-4 has been surveyed three times. Survey 1 was performed in 2015 at ages of 14.2 months and 13.9 months for Placements 1 and 2, respectively. Survey 2 was completed in 2016 at ages of 27.0 and 26.8 months for Placements 1 and 2. Survey 3 was performed in 2017 at ages of 35.8 and 35.6 months for Placements 1 and 2. The crack maps from these surveys are shown in Figures 3.27 through 3.29.

For all three surveys, the crack density was high and nearly constant. An overall crack density of 0.601 m/m^2 was found in Survey 1, 0.739 m/m^2 on Placement 1 and 0.395 m/m^2 on Placement 2 (Figure 3.27). The overall crack density did not noticeably change in Survey 2, with a value of 0.598 m/m^2 (Figure 3.28); the two placements also exhibited similar crack densities to those observed in Survey 1 (0.725 m/m^2 for Placement 1 and 0.411 m/m^2 for Placement 2). The crack density of the deck increased slightly to 0.615 m/m^2 in Survey 3, 0.766 m/m^2 for Placement 1 and 0.393 m/m^2 for Placement 2 (Figure 3.29). The pattern of cracks in Control-4 was similar to that of Fiber-4. Most of the cracks on Control-4 were transverse to the direction of traffic and many crossed the full width of the deck. Some short cracks were also found, mostly in Span 1 and Span 3. In all three surveys, Span 2 consistently had higher crack density than the other two spans. Like Fiber-4, most of the cracks in Span 2 of Control-4 were in the first placement. Control-4 has exhibited minimal scaling.

In Survey 2 (2016), 122 crack width measurements were taken on Placement 1, with values ranging from 0.002 to 0.030 in. (0.05 to 0.76 mm) and averaging 0.010 in. (0.25 mm); 58 measurements were taken on Placement 2, with values ranging from 0.004 to 0.019 in. (0.10 to 0.48 mm) and averaging of 0.007 in. (0.33 mm).

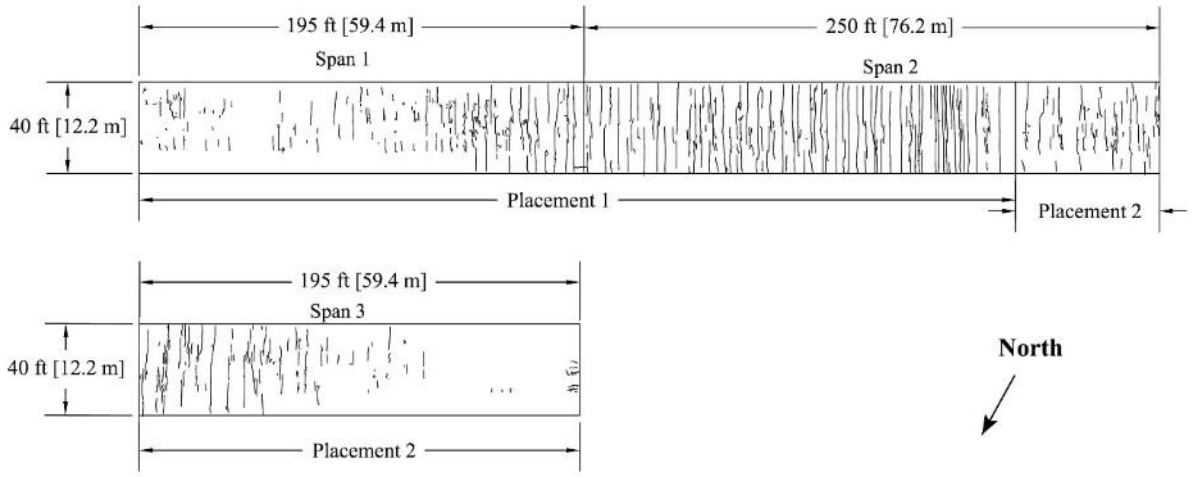

Bridge Number: 24-89-17.22 (282)
Bridge Location: WB US-24 over UPRR
Construction Date:
Placement 1: 6/13/2014
Placement 2: 6/20/2014
Crack Survey Date: 8/12/2015

Bridge Length: 640 ft (195.1 m)
Bridge Width: 40 ft (12.2 m)
Skew: 0°
Number of Spans: 3
Span 1: 195 ft (59.4 m)
Span 2: 250 ft (76.2 m)
Span 3: 195 ft (59.4 m)
Number of Placements: 2

Bridge Age:
Placement 1: 14.2 months
Placement 2: 13.9 months
Crack Density:
Overall: 0.601 m/m^2
Span 1: 0.426 m/m^2
Span 2: 0.981 m/m^2
Span 3: 0.288 m/m^2
Placement 1: 0.739 m/m^2
Placement 2: 0.395 m/m^2

Figure 3.27 – Control-4 (Survey 1)

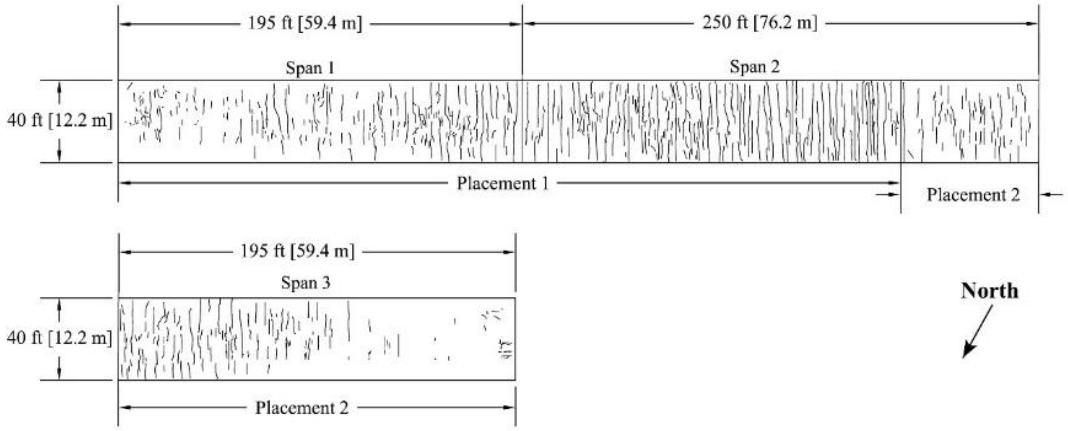

Bridge Number: 24-89-17.22 (282)
Bridge Location: WB US-24 over UPRR
Construction Date:
Placement 1: 6/13/2014
Placement 2: 6/20/2014
Crack Survey Date: 9/1/2016

Bridge Length: 640 ft (195.1 m)
Bridge Width: 40 ft (12.2 m)
Skew: 0°
Number of Spans: 3
Span 1: 195 ft (59.4 m)
Span 2: 250 ft (76.2 m)
Span 3: 195 ft (59.4 m)
Number of Placements: 2

Bridge Age:
Placement 1: 27.0 months
Placement 2: 26.8 months
Crack Density:
Overall: 0.598 m/m^2
Span 1: 0.547 m/m^2
Span 2: 0.869 m/m^2
Span 3: 0.361 m/m^2
Placement 1: 0.725 m/m^2
Placement 2: 0.411 m/m^2

Figure 3.28 – Control-4 (Survey 2)

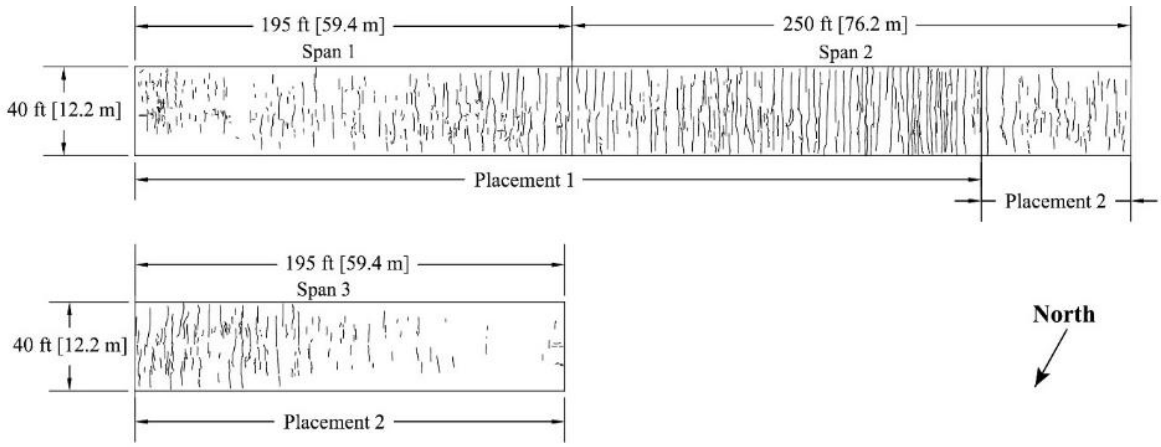

Bridge Number: 24-89-17.22 (282)
Bridge Location: WB US-24 over UPRR
Construction Date:
Placement 1: 6/13/2014
Placement 2: 6/20/2014
Crack Survey Date: 6/6/2017

Bridge Length: 640 ft (195.1 m)
Bridge Width: 40 ft (12.2 m)
Skew: 0°
Number of Spans: 3
Span 1: 195 ft (59.4 m)
Span 2: 250 ft (76.2 m)
Span 3: 195 ft (59.4 m)
Number of Placements: 2

Bridge Age:
Placement 1: 35.8 months
Placement 2: 35.6 months
Crack Density:
Overall: 0.615 m/m^2
Span 1: 0.543 m/m^2
Span 2: 0.887 m/m^2
Span 3: 0.345 m/m^2
Placement 1: 0.766 m/m^2
Placement 2: 0.393 m/m^2

Figure 3.29 – Control-4 (Survey 3)

3.4.9 Fiber-4 and Control-4 Comparison

Figure 3.31 compares the crack density of Fiber-4 and Control-4 as a function of deck age. As shown, both decks had high crack densities. The crack density of Fiber-4 Placement 2 increased with deck age, from 0.173 m/m^2 at 12.2 months to 0.431 m/m^2 at 33.4 months. The crack density of the other three placements did not change noticeably with time. For both decks, the first placement exhibited higher crack density than the second. Overall, there is no distinction in the crack densities of the two decks.

The average crack widths of the four placements of Fiber-4 and Control-4, and the *p* value for their differences, are listed in Table 3.9. Control-4 Placement 1 showed a higher average crack width (0.010 in., 0.25 mm) compared to both placements of Fiber-4 [0.008 in. (0.20 mm) and 0.007 in. (0.18 mm) for Placements 1 and 2, respectively], and the differences are statistically

significant ($p = 0.01$ and 2.17×10^{-5}). The average crack width of Control-4 Placement 2 (0.007 in., 0.18 mm) was narrower than Fiber-4 Placement 1 ($p = 0.05$) and the same as Fiber-4 Placement 2.

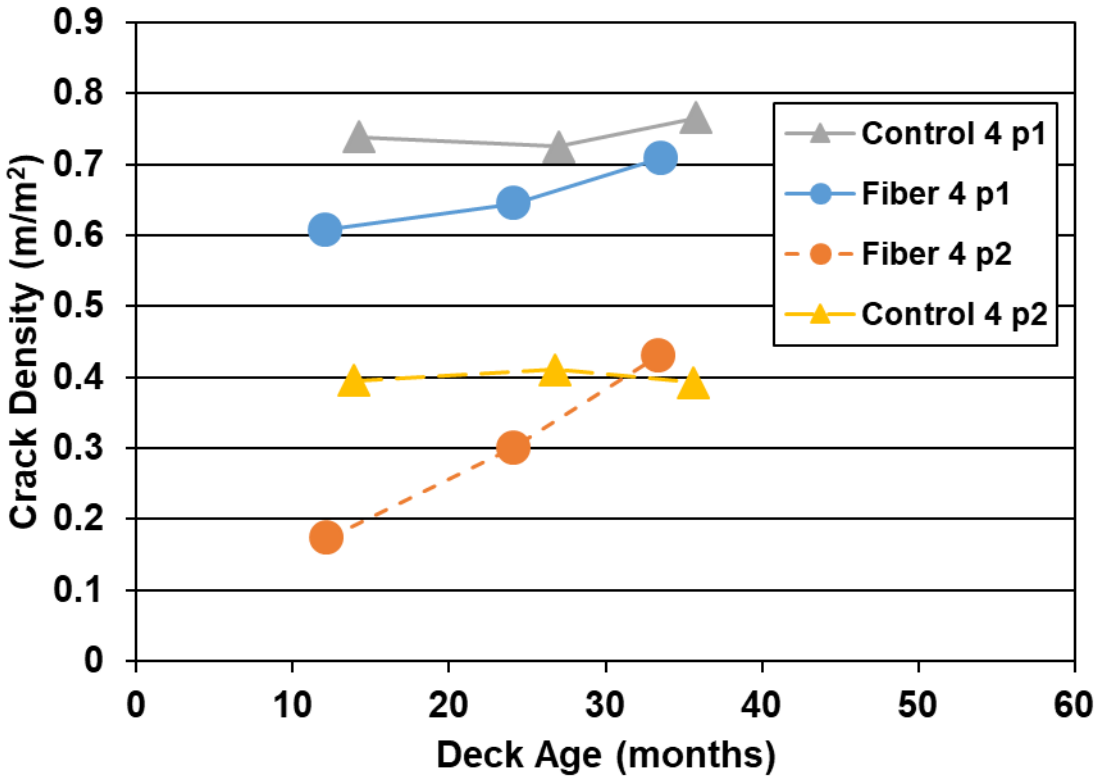

Figure 3.30 – Fiber-4 and Control-4 crack density versus deck age

Table 3.9 – *p* values obtained in Student's t-test for the differences in average crack widths of Fiber-1 and Fiber-2

	Bridge Deck Placement	Fiber-4 Placement 1	Fiber-4 Placement 2	Control-4 Placement 1	Control-4 Placement 2
Bridge Deck Placement	**Average Crack Width in.**	0.008	0.007	0.010	0.007
Fiber-4 Placement 1	0.008		0.02	0.01	0.05
Fiber-4 Placement 2	0.007			2.17×10^{-5}	0.70
Control-4 Placement 1	0.010				4.19×10^{-4}

3.4.10 Fiber-5

Fiber-5 was constructed in one placement on November 10, 2014. The deck has been surveyed three times. Survey 1 was in 2016 when the deck was 18.9 months old; Survey 2 was completed in 2017 at a deck age of 31.1 months; and Survey 3 was performed in 2018 at a deck age of 44.7 months. The crack maps for the surveys are shown in Figure 3.31 to 3.33.

Overall, the cracking has been low on this deck. The crack density was 0.010 m/m^2 in Survey 1 (Figure 3.31), increasing to 0.044 m/m^2 in Survey 2 and 0.091 m/m^2 in Survey 3. Transverse cracks were found along the south side of the deck in all three surveys, and the number and length of such cracks have increased as the deck aged. In Survey 2, short and randomly oriented cracks were observed in the middle of Span 2; in Survey 3, the extent of such cracking increased: short cracks were observed in all three spans and the number of the cracks in Span 2 increased. Cracks perpendicular to the end of the deck were found at the east abutment. The number and length of the longitudinal cracks have increased as the deck has aged.

In Survey 2 (2017), 37 crack width measurements were made, with values ranging from 0.004 to 0.020 in. (0.10 to 0.51 mm) and averaging 0.006 in. (0.15 mm).

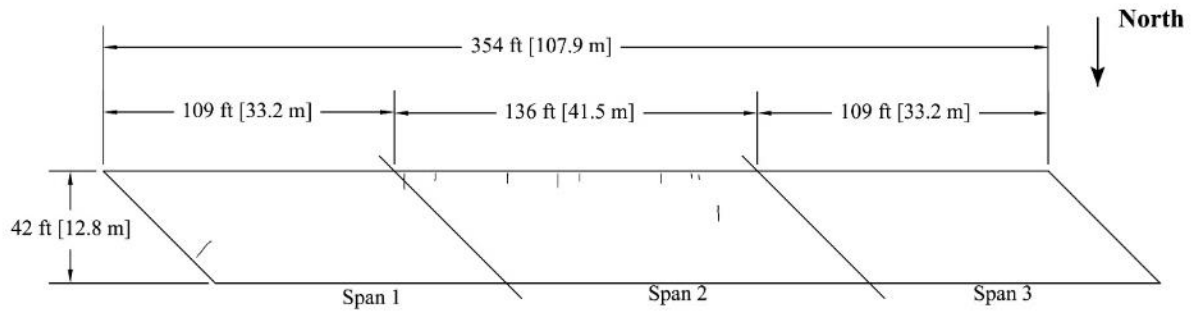

Bridge Number: 10-23-12.44
Bridge Location: WB K-10 over North Canal
Construction Date: 11/10/2014
Crack Survey Date: 6/6/2016

Bridge Length: 354 ft (107.9 m)
Bridge Width: 40 ft (12.2 m)
Skew: 45°
Number of Spans: 3
Span 1: 109 ft (33.2 m)
Span 2: 136 ft (41.5 m)
Span 3: 109 ft (33.2 m)
Number of Placements: 1

Bridge Age: 18.9 months
Crack Density:
Overall: 0.010 m/m^2
Span 1: 0.000 m/m^2
Span 2: 0.018 m/m^2
Span 3: 0.008 m/m^2

Figure 3.31 – Fiber-5 (Survey 1)

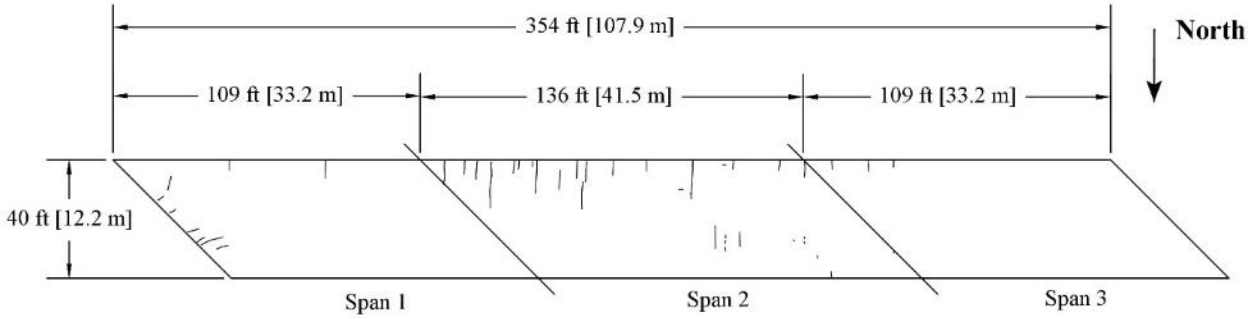

Bridge Number: 10-23-12.44
Bridge Location: WB K-10 over North Canal
Construction Date: 11/10/2014
Crack Survey Date: 6/12/2017

Bridge Length: 354 ft (107.9 m)
Bridge Width: 40 ft (12.2 m)
Skew: 45°
Number of Spans: 3
Span 1: 109 ft (33.2 m)
Span 2: 136 ft (41.5 m)
Span 3: 109 ft (33.2 m)
Number of Placements: 1

Bridge Age: 31.1 months
Crack Density:
Overall: 0.044 m/m^2
Span 1: 0.030 m/m^2
Span 2: 0.084 m/m^2
Span 3: 0.007 m/m^2

Figure 3.32 – Fiber-5 (Survey 2)

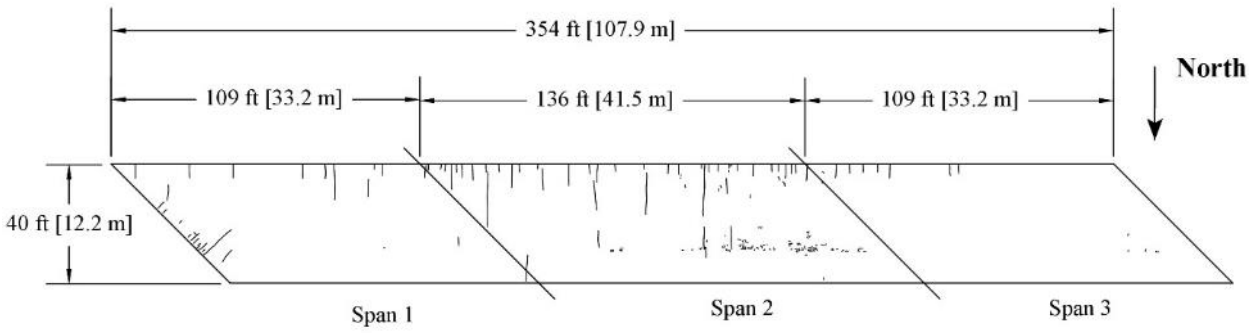

Bridge Number: 10-23-12.44
Bridge Location: WB K-10 over North Canal
Construction Date: 11/10/2014
Crack Survey Date: 7/31/2018

Bridge Length: 354 ft (107.9 m)
Bridge Width: 40 ft (12.2 m)
Skew: 45°
Number of Spans: 3
Span 1: 109 ft (33.2 m)
Span 2: 136 ft (41.5 m)
Span 3: 109 ft (33.2 m)
Number of Placements: 1

Bridge Age: 44.7 months
Crack Density:
Overall: 0.091 m/m^2
Span 1: 0.024 m/m^2
Span 2: 0.157 m/m^2
Span 3: 0.077 m/m^2

Figure 3.33 – Fiber-5 (Survey 3)

3.4.11 Control-5

Bridge deck Control-5 was constructed on November 7, 2014. The deck has been surveyed three times. Survey 1 was performed in 2016 when the deck was 19.0 months old. Survey 2 was completed at an age of 31.2 months. The most recent survey (Survey 3) was performed in 2018 at an age of 44.8 months. The crack maps for the three surveys are shown in Figures 3.34 through 3.36.

The crack density of Control-5 was 0.008 m/m^2 in Survey 1 (Figure 3.34), increasing to 0.038 m/m^2 in Survey 2 (Figure 3.35) and 0.077 m/m^2 in Survey 3 (Figure 3.36). The cracks in Control-5 are mostly transverse, initiating along the north or the south side of the deck; the number and length of the cracks has increased as the deck has aged. In Surveys 2 and 3, an increasing number of transverse cracks were observed in Span 2.

In Survey 2, 31 crack width measurements were made, with crack widths ranging from 0.004 to 0.009 in. (0.10 to 0.23 mm) and averaging of 0.006 in. (0.15 mm).

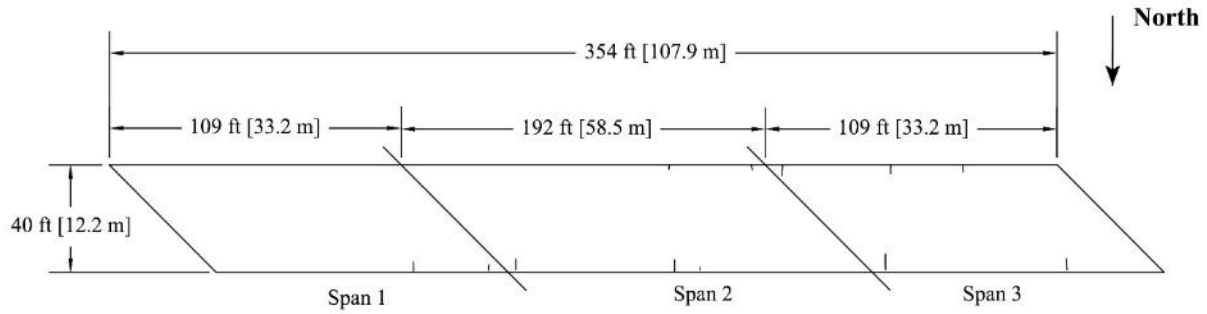

Bridge Number: 10-23-12.44
Bridge Location: EB K-10 over North Canal
Construction Date: 11/7/2014
Crack Survey Date: 6/6/2016

Bridge Length: 354 ft (107.9 m)
Bridge Width: 40 ft (12.2 m)
Skew: 45°
Number of Spans: 3
Span 1: 109 ft (33.2 m)
Span 2: 136 ft (41.5 m)
Span 3: 109 ft (33.2 m)
Number of Placements: 1

Bridge Age: 19.0 months
Crack Density:
Overall: 0.008 m/m^2
Span 1:0.004 m/m^2
Span 2: 0.008 m/m^2
Span 3: 0.015 m/m^2

Figure 3.34 – Control-5 (Survey 1)

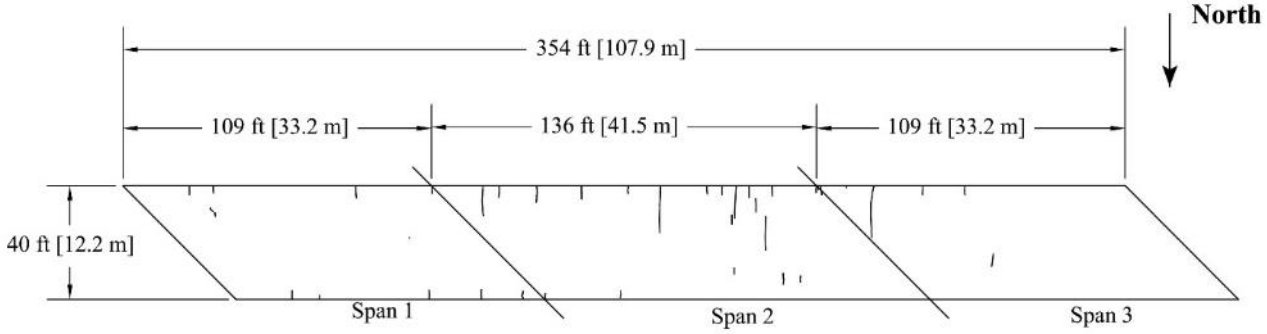

Bridge Number: 10-23-12.44
Bridge Location: EB K-10 over North Canal
Construction Date: 11/7/2014
Crack Survey Date: 6/13/2017

Bridge Length: 354 ft (107.9 m)
Bridge Width: 40 ft (12.2 m)
Skew: 45°
Number of Spans: 3
Span 1: 109 ft (33.2 m)
Span 2: 136 ft (41.5 m)
Span 3: 109 ft (33.2 m)
Number of Placements: 1

Bridge Age: 31.2 months
Crack Density:
Overall: 0.038 m/m^2
Span 1:0.021 m/m^2
Span 2: 0.063 m/m^2
Span 3: 0.023 m/m^2

Figure 3.35 – Control-5 (Survey 2)

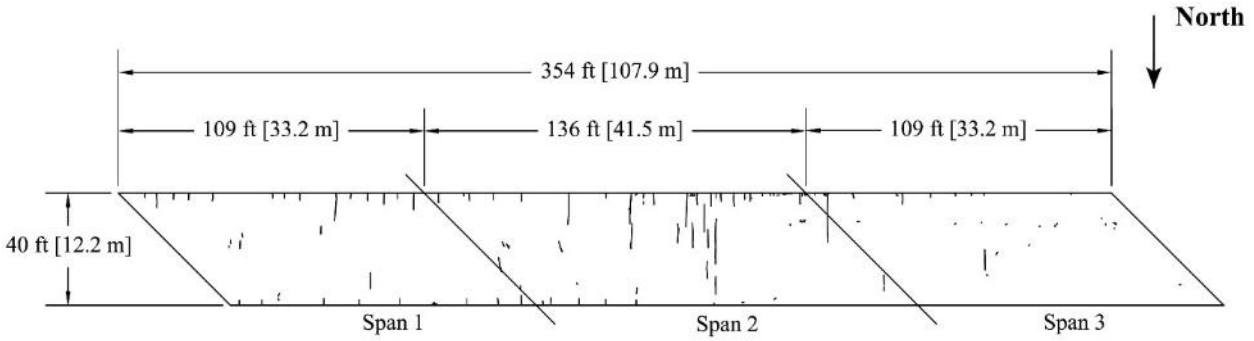

Bridge Number: 10-23-12.44
Bridge Location: EB K-10 over North Canal
Construction Date: 11/7/2014
Crack Survey Date: 8/1/2018

Bridge Length: 354 ft (107.9 m)
Bridge Width: 40 ft (12.2 m)
Skew: 45°
Number of Spans: 3
Span 1: 109 ft (33.2 m)
Span 2: 136 ft (41.5 m)
Span 3: 109 ft (33.2 m)
Number of Placements: 1

Bridge Age: 44.8 months
Crack Density:
Overall: 0.077 m/m^2
Span 1: 0.061 m/m^2
Span 2: 0.128 m/m^2
Span 3: 0.028 m/m^2

Figure 3.36 – Control-5 (Survey 3)

3.4.12 Fiber-5 and Control-5 Comparison

Figure 3.37 compares the crack densities of Fiber-5 and Control-5 over time. The crack densities of both decks have increased with deck age, but remained low. As with the previous pairs of bridge decks, the addition of fiber does not appear to influence the crack density of a bridge deck.

Although the use of fibers was associated with narrower cracks in the more highly cracked decks in this study, fiber-reinforced concrete did not influence the average crack width in this pair of decks. In the surveys performed in 2017, both Fiber-5 and Control-5 had an average crack width of 0.006 in. (0.15 mm).

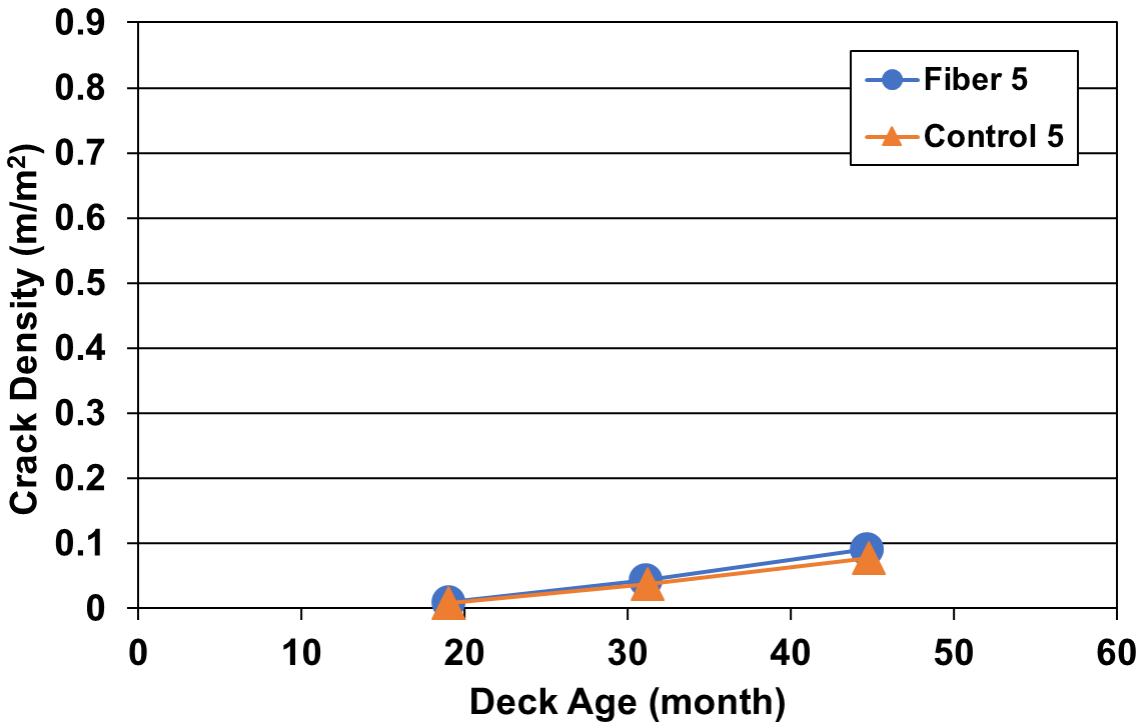

Figure 3.37 – Fiber-5 and Control-5 crack density versus deck age

3.4.13 Fiber-6

Fiber-6 was constructed on May 12, 2015. The deck has been surveyed three times. Survey 1 was performed in 2016 at an age of 12.8 months. Survey 2 was completed the following year at an age of 25.0 months. The most recent survey was performed in 2018 at an age of 38.6 months. The crack maps for the three surveys are shown in Figures 3.38 through 3.40.

No cracks were found on the deck in Survey 1 (Figure 3.38). In Survey 2, some short widely-spaced cracks were found, mostly in Spans 2 and 3. The crack density was 0.005 m/m^2 (Figure 3.39). In Survey 3, more cracks were found on the deck, resulting in a crack density of 0.013 m/m^2 (Figure 3.40). All cracks on Fiber-6 were short and randomly oriented.

In Survey 2, 13 crack width measurements were taken, with values ranging from 0.004 to 0.007 (0.10 to 0.18 mm) and averaging 0.006 in. (0.15 mm).

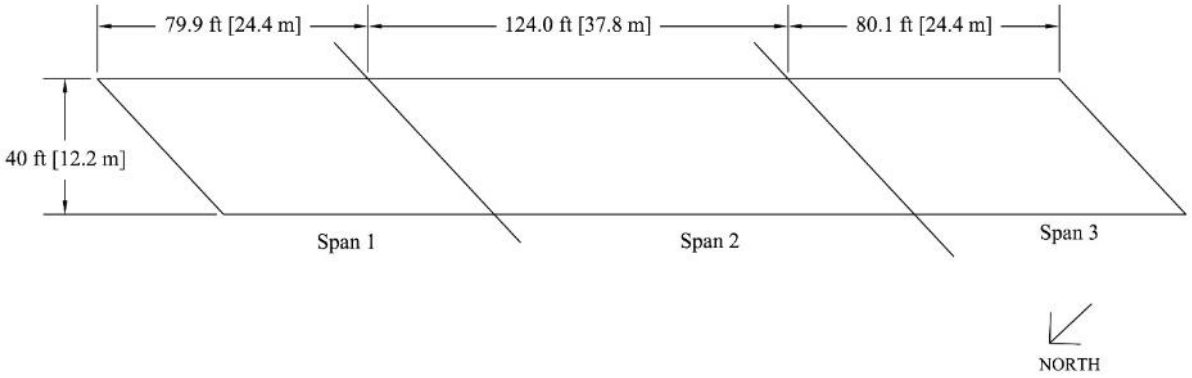

Bridge Number: 10-23 12.94 (179)
Bridge Location: WB K-10 over 31st St.
Construction Date: 5/12/2015
Crack Survey Date: 6/6/2016

Bridge Length: 284 ft (86.6 m)
Bridge Width: 40 ft (12.2 m)
Skew: 47°
Number of Spans: 3
Span 1: 80 ft (24.4 m)
Span 2: 124 ft (37.8 m)
Span 3: 80 ft (24.4 m)
Number of Placements: 1

Bridge Age: 12.8 months
Crack Density:
Overall: 0.000 m/m^2
Span 1: 0.000 m/m^2
Span 2: 0.000 m/m^2
Span 3: 0.000 m/m^2

Figure 3.38 – Fiber-6 (Survey 1)

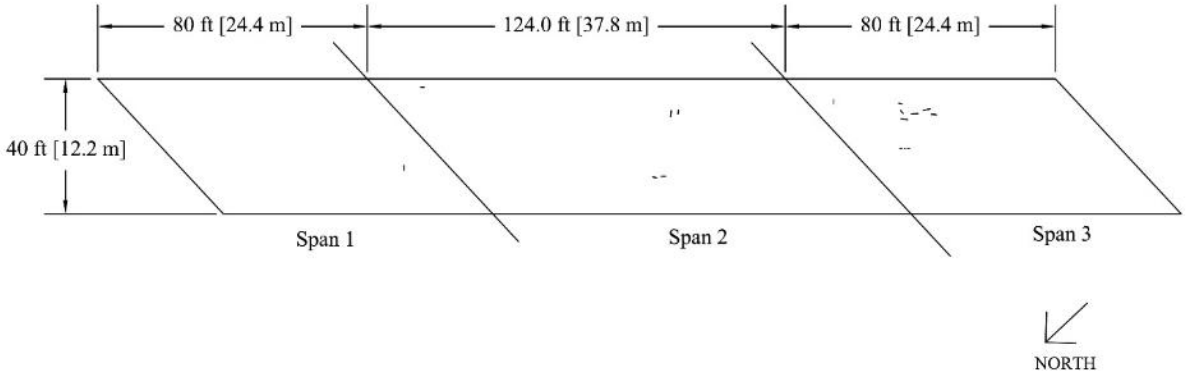

Bridge Number: 10-23 12.94 (179)
Bridge Location: WB K-10 over 31st St.
Construction Date: 5/12/2015
Crack Survey Date: 6/12/2017

Bridge Length: 284 ft (86.6 m)
Bridge Width: 40 ft (12.2 m)
Skew: 47°
Number of Spans: 3
Span 1: 80 ft (24.4 m)
Span 2: 124 ft (37.8 m)
Span 3: 80 ft (24.4 m)
Number of Placements: 1

Bridge Age: 25.0 months
Crack Density:
Overall: 0.005 m/m^2
Span 1: 0.001 m/m^2
Span 2: 0.004 m/m^2
Span 3: 0.010 m/m^2

Figure 3.39 – Fiber-6 (Survey 2)

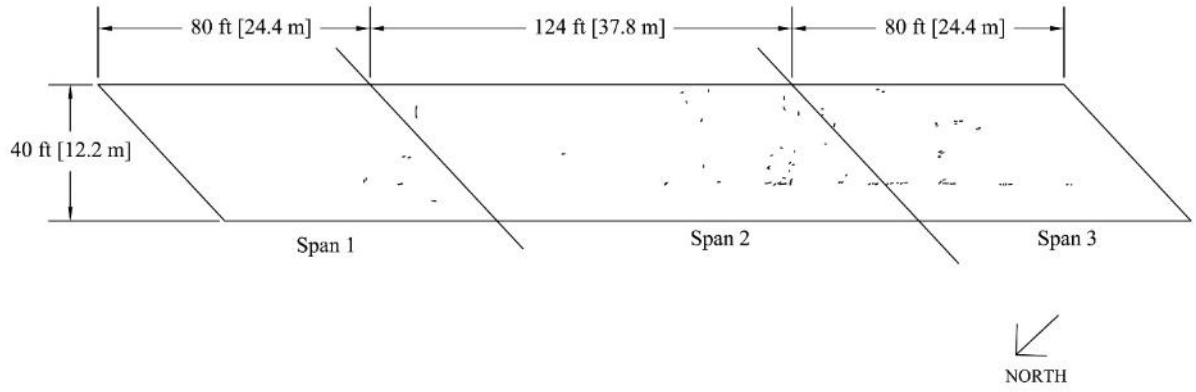

Bridge Number: 10-23 12.94 (179)
Bridge Location: WB K-10 over 31st St.
Construction Date: 5/12/2015
Crack Survey Date: 7/31/2018

Bridge Length: 284 ft (86.6 m)
Bridge Width: 40 ft (12.2 m)
Skew: 47°
Number of Spans: 3
- **Span 1:** 80 ft (24.4 m)
- **Span 2:** 124 ft (37.8 m)
- **Span 3:** 80 ft (24.4 m)

Number of Placements: 1

Bridge Age: 38.6 months
Crack Density:
- **Overall:** 0.013 m/m^2
- **Span 1:** 0.005 m/m^2
- **Span 2:** 0.014 m/m^2
- **Span 3:** 0.020 m/m^2

Figure 3.40 – Fiber-6 (Survey 3)

3.4.14 Control-6

Control-6 was constructed on May 5, 2015. The deck has been surveyed three times. Survey 1 took place in 2016 at an age of 13.0 months. Survey 2 was performed the next summer at an age of 25.3 months. The last survey was completed in 2018 at an age of 38.9 months. The crack maps are shown in Figures 3.41 through 3.43.

No cracks were found in Survey 1 (Figure 3.41). In Survey 2, some short cracks were found along the south side of the deck, resulting in a crack density of 0.002 m/m^2 (Figure 3.42). In Survey 3, the crack density increased slightly to 0.013 m/m^2 (Figure 3.43). The cracks on Control-6 were short and randomly oriented and were mostly along the south side in Spans 1 and 2.

Four crack width measurements were taken in Survey 2, all with the same result, 0.004 in. (0.10 mm).

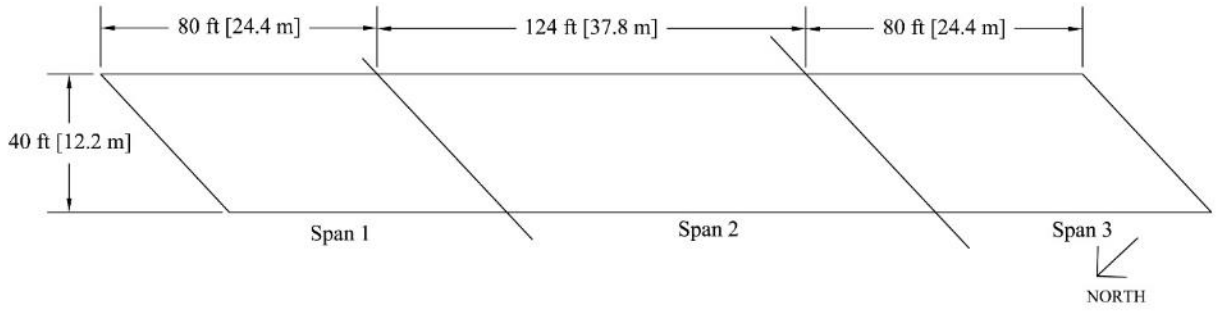

Bridge Number: 10-23 12.94 (180)
Bridge Location: EB K-10 over 31st St.
Construction Date: 5/5/2015
Crack Survey Date: 6/6/2016

Bridge Length: 284 ft (87.8 m)
Bridge Width: 40 ft (12.2 m)
Skew: 47°
Number of Spans: 3
Span 1: 80 ft (24.4 m)
Span 2: 124 ft (37.8 m)
Span 3: 80 ft (24.4 m)
Number of Placements: 1

Bridge Age: 13.0 months
Crack Density:
Overall: 0.000 m/m^2
Span 1: 0.000 m/m^2
Span 2: 0.000 m/m^2
Span 3: 0.000 m/m^2

Figure 3.41 – Control-6 (Survey 1)

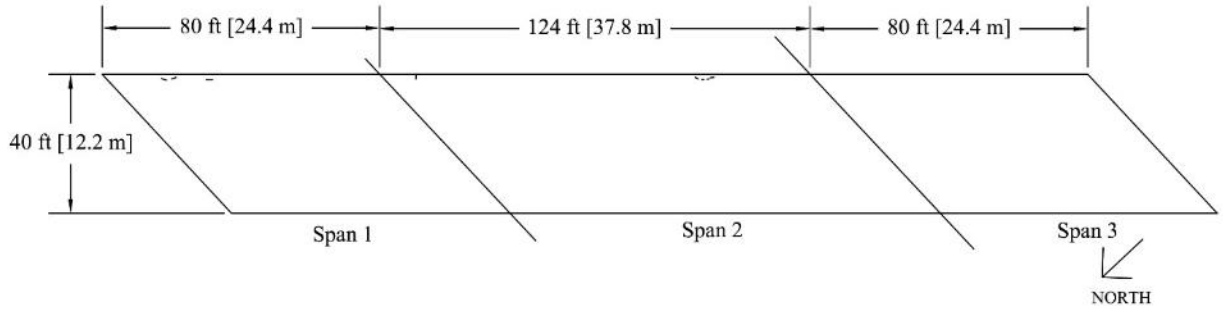

Bridge Number: 10-23 12.94 (180)
Bridge Location: EB K-10 over 31st St.
Construction Date: 5/5/2015
Crack Survey Date: 6/13/2017

Bridge Length: 284 ft (87.8 m)
Bridge Width: 40 ft (12.2 m)
Skew: 47°
Number of Spans: 3
Span 1: 80 ft (24.4 m)
Span 2: 124 ft (37.8 m)
Span 3: 80 ft (24.4 m)
Number of Placements: 1

Bridge Age: 25.3 months
Crack Density:
Overall: 0.002 m/m^2
Span 1: 0.003 m/m^2
Span 2: 0.003 m/m^2
Span 3: 0.000 m/m^2

Figure 3.42 – Control-6 (Survey 2)

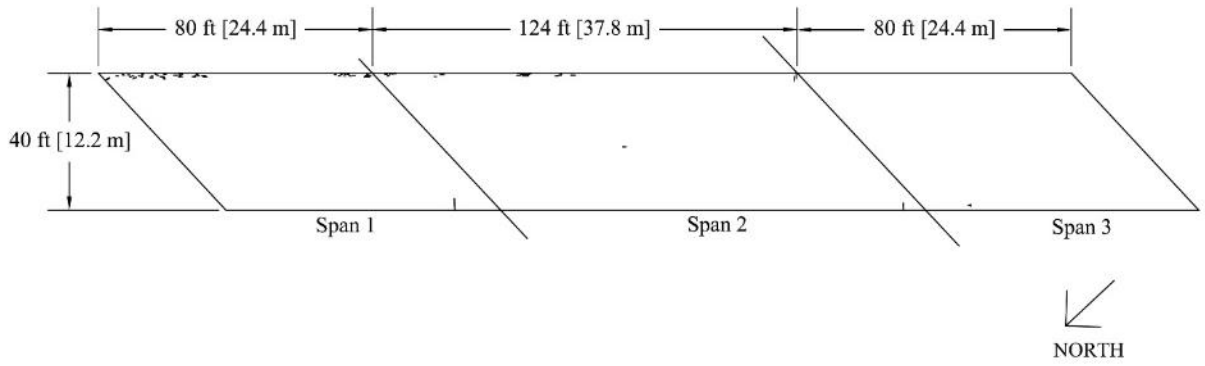

Bridge Number: 10-23 12.94 (180)
Bridge Location: EB K-10 over 31st St.
Construction Date: 5/5/2015
Crack Survey Date: 8/1/2018

Bridge Length: 284 ft (87.8 m)
Bridge Width: 40 ft (12.2 m)
Skew: 47°
Number of Spans: 3
- **Span 1:** 80 ft (24.4 m)
- **Span 2:** 124 ft (37.8 m)
- **Span 3:** 80 ft (24.4 m)

Number of Placements: 1

Bridge Age: 38.9 months
Crack Density:
- **Overall:** 0.013 m/m^2
- **Span 1:** 0.029 m/m^2
- **Span 2:** 0.011 m/m^2
- **Span 3:** 0.001 m/m^2

Figure 3.43 – Control-6 (Survey 3)

3.4.15 Fiber-6 and Control-6 Comparison

Figure 3.44 compares the crack densities of Fiber-6 and Control-6 with deck age. As shown in the figure, both decks have very low crack densities that are the same or nearly the same.

The average crack width of Fiber-6, 0.006 in. (0.15 mm), was slightly higher than that of Control-6, 0.004 in. (0.10 mm), and the difference, although small, is statistically significant ($p = 4.98 \times 10^{-3}$).

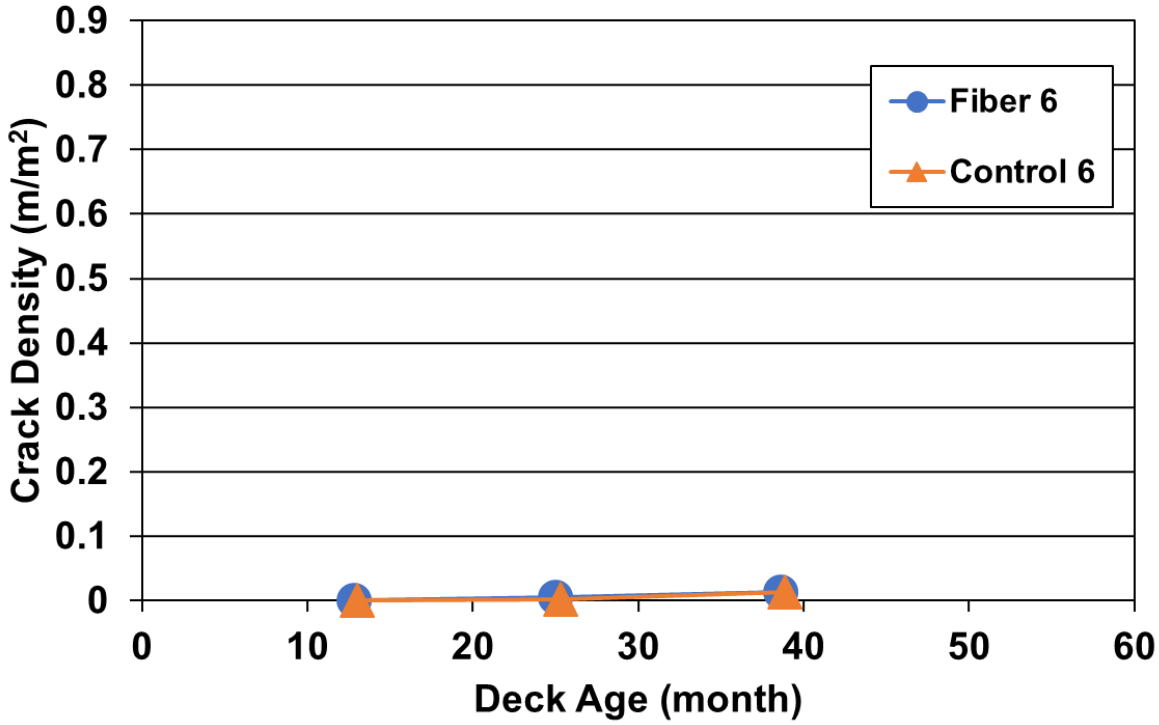

Figure 3.44 – Fiber-6 and Control-6 crack density versus deck age

3.4.16 Fiber-7

Fiber-7 was constructed on June 1, 2015 and has been surveyed three times. Survey 1 was performed in 2016 at an age of 12.2 months. Survey 2 was completed at an age of 24.6 months. The last survey was performed in 2018 at an age of 38.0 months. The crack maps for these surveys are shown in Figures 3.45 through 3.47.

Only one crack was found, in Span 3, during Survey 1, and the crack density of the deck can be closely approximated as 0.000 m/m^2 (Figure 3.45). During Survey 2, a group of short cracks were found in Span 2, resulting in a crack density of 0.002 m/m^2 for Span 2 but the overall crack density of the deck was still essentially 0.000 m/m^2 (Figure 3.46). In Survey 3, some short cracks were found in Spans 1 and 2, increasing the crack density of the deck to 0.005 m/m^2 (Figure 3.47).

One crack width measurement was taken in Survey 2, and the result was 0.006 in. (0.15 mm).

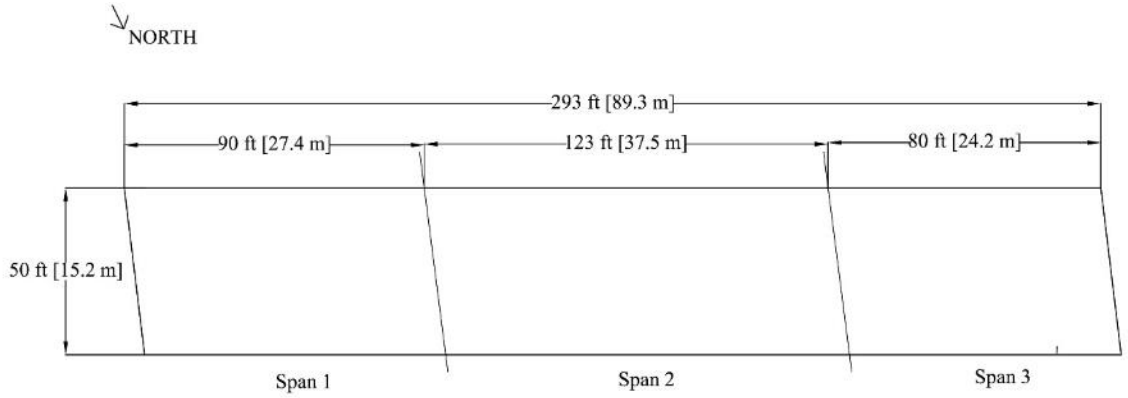

Bridge Number: 10-23 K-8392-04
Bridge Location: WB K-10 over Haskell Ave.
Construction Date: 6/1/2015
Crack Survey Date: 6/6/2016

Bridge Length: 293 ft (89.3 m)
Bridge Width: 50 ft (15.2 m)
Skew: 7°
Number of Spans: 3
Span 1: 90 ft (27.4 m)
Span 2: 123 ft (37.5 m)
Span 3: 80 ft (24.4 m)
Number of Placements: 1

Bridge Age: 12.2 months
Crack Density:
Overall: 0.000 m/m^2
Span 1: 0.000 m/m^2
Span 2: 0.000 m/m^2
Span 3: 0.002 m/m^2

Figure 3.45 – Fiber-7 (Survey 1)

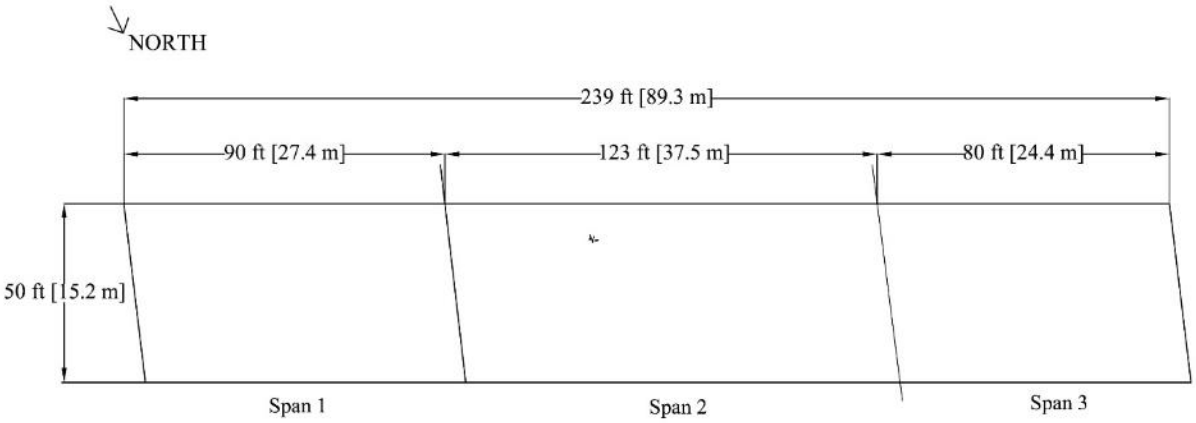

Bridge Number: 10-23 K-8392-04
Bridge Location: WB K-10 over Haskell Ave.
Construction Date: 6/1/2015
Crack Survey Date: 6/19/2017

Bridge Length: 293 ft (89.3 m)
Bridge Width: 50 ft (15.2 m)
Skew: 7°
Number of Spans: 3
Span 1: 90 ft (27.4 m)
Span 2: 123 ft (37.5 m)
Span 3: 80 ft (24.4 m)
Number of Placements: 1

Bridge Age: 24.6 months
Crack Density:
Overall: 0.000 m/m^2
Span 1: 0.000 m/m^2
Span 2: 0.002 m/m^2
Span 3: 0.000 m/m^2

Figure 3.46 – Fiber-7 (Survey 2)

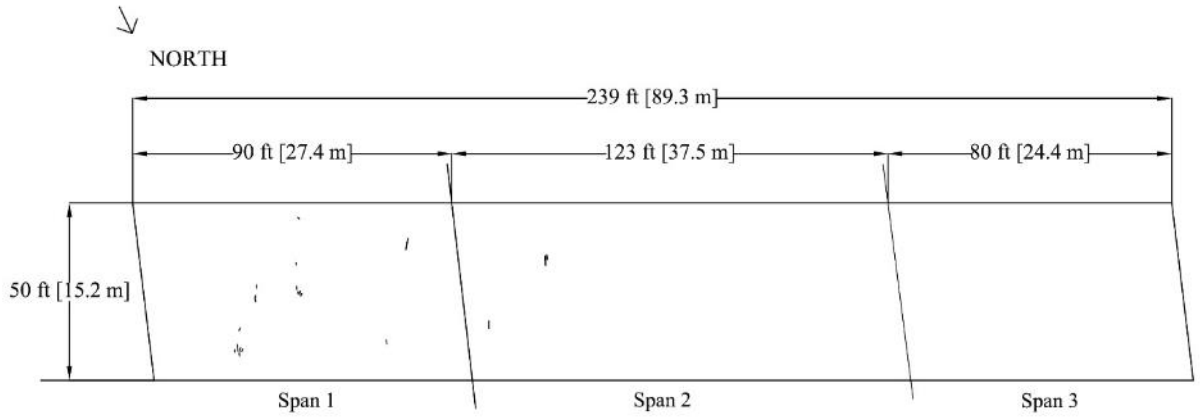

Bridge Number: 10-23 K-8392-04
Bridge Location: WB K-10 over Haskell Ave.
Construction Date: 6/1/2015
Crack Survey Date: 8/2/2018

Bridge Length: 293 ft (89.3 m)
Bridge Width: 50 ft (15.2 m)
Skew: 7°
Number of Spans: 3
Span 1: 90 ft (27.4 m)
Span 2: 123 ft (37.5 m)
Span 3: 80 ft (24.4 m)
Number of Placements: 1

Bridge Age: 38.0 months
Crack Density:
Overall: 0.005 m/m^2
Span 1: 0.012 m/m^2
Span 2: 0.003 m/m^2
Span 3: 0.000 m/m^2

Figure 3.47 – Fiber-7 (Survey 3)

3.4.17 Control-7

Control-7 was constructed on May 27, 2015. The deck has been surveyed three times. Survey 1 took place in 2016 at an age of 12.3 months. Survey 2 was performed the following year at an age of 25.8 months. Survey 3 was completed in 2018 at an age of 38.3 months. The crack maps for these surveys are shown in Figures 3.48 through 3.50.

No cracks were found in Survey 1 (Figure 3.48). In Survey 2, some short cracks were found at random orientations in Spans 2 and 3. The crack density of the entire deck was 0.014 m/m^2 (Figure 3.49). In Survey 3, the number of cracks increased noticeably, with most of the cracks in Spans 2 and 3. Some longitudinal cracks were found along the south side of the deck in Span 2, but most of the cracks were randomly oriented. The crack density in Survey 3 was 0.037 m/m^2 (Figure 3.50).

In Survey 2, 18 crack width measurements were made, with values ranging from 0.004 to 0.007 in. (0.10 to 0.18 mm) and averaging 0.005 in. (0.13 mm).

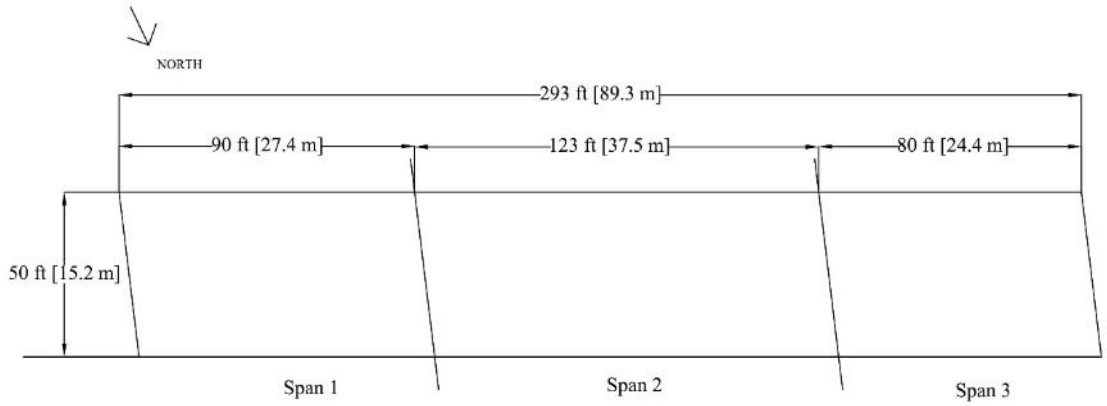

Bridge Number: 10-23-10.72 (170)
Bridge Location: WB K-10 over Haskell Ave.
Construction Date: 5/27/2015
Crack Survey Date: 6/6/2016

Bridge Length: 293 ft (89.3 m)
Bridge Width: 50 ft (15.2 m)
Skew: 7°
Number of Spans: 3
Span 1: 90 ft (27.4 m)
Span 2: 123 ft (37.5 m)
Span 3: 80 ft (24.4 m)
Number of Placements: 1

Bridge Age: 12.3 months
Crack Density:
Overall: 0.000 m/m^2
Span 1: 0.000 m/m^2
Span 2: 0.000 m/m^2
Span 3: 0.000 m/m^2

Figure 3.48 – Control-7 (Survey 1)

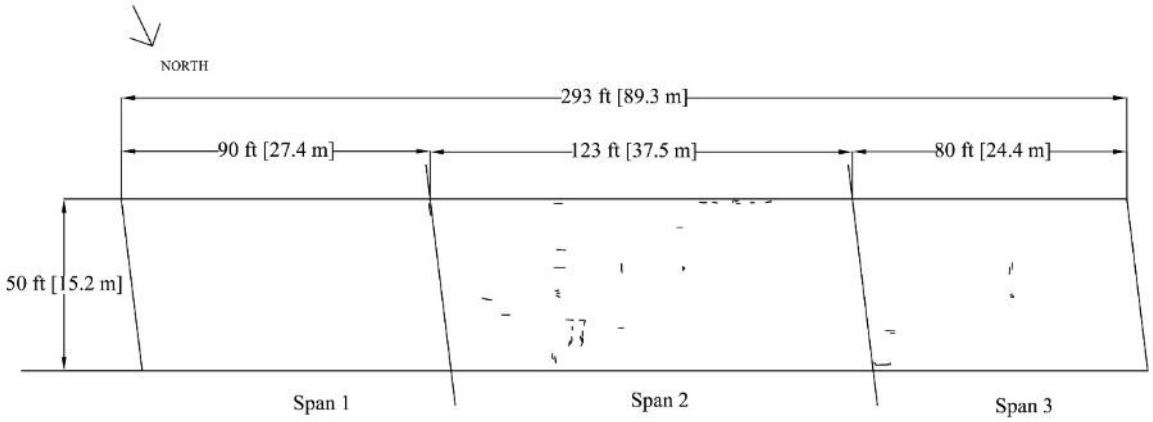

Bridge Number: 10-23-10.72 (170)
Bridge Location: WB K-10 over Haskell Ave.
Construction Date: 5/27/2015
Crack Survey Date: 7/20/2017

Bridge Length: 293 ft (89.3 m)
Bridge Width: 50 ft (15.2 m)
Skew: 7°
Number of Spans: 3
Span 1: 90 ft (27.4 m)
Span 2: 123 ft (37.5 m)
Span 3: 80 ft (24.4 m)
Number of Placements: 1

Bridge Age: 25.8 months
Crack Density:
Overall: 0.014 m/m^2
Span 1: 0.002 m/m^2
Span 2: 0.027 m/m^2
Span 3: 0.008 m/m^2

Figure 3.49 – Control-7 (Survey 2)

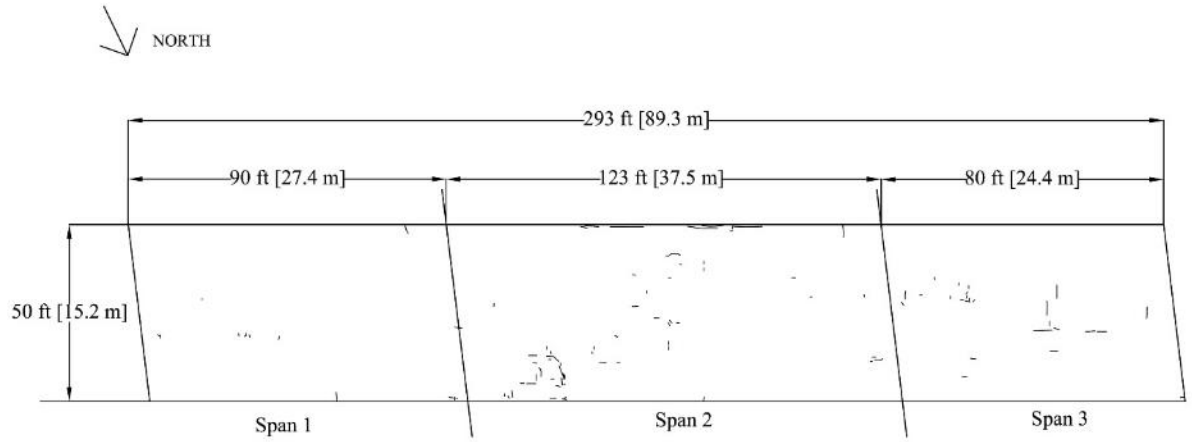

Bridge Number: 10-23-10.72 (170)
Bridge Location: WB K-10 over Haskell Ave.
Construction Date: 5/27/2015
Crack Survey Date: 8/6/2018

Bridge Length: 293 ft (89.3 m)
Bridge Width: 50 ft (15.2 m)
Skew: 7°
Number of Spans: 3
Span 1: 90 ft (27.4 m)
Span 2: 123 ft (37.5 m)
Span 3: 80 ft (24.4 m)
Number of Placements: 1

Bridge Age: 38.3 months
Crack Density:
Overall: 0.037 m/m^2
Span 1: 0.010 m/m^2
Span 2: 0.059 m/m^2
Span 3: 0.035 m/m^2

Figure 3.50 – Control-7 (Survey 3)

3.4.18 Fiber-7 and Control-7 Comparison

The crack densities of Fiber-7 and Control-7 are compared in Figure 3.51 as a function of deck age. Although the crack density of Control-7 increased slightly over time, the crack densities of Fiber-7 and Control-7 were both low (0.005 and 0.037 m/m^2, respectively).

The average crack widths of Fiber-7 and Control-7 were similar, with values of 0.006 in. (0.15 mm, based on one measurement) for Fiber-7 and 0.005 in. (0.13 mm) for Control-7.

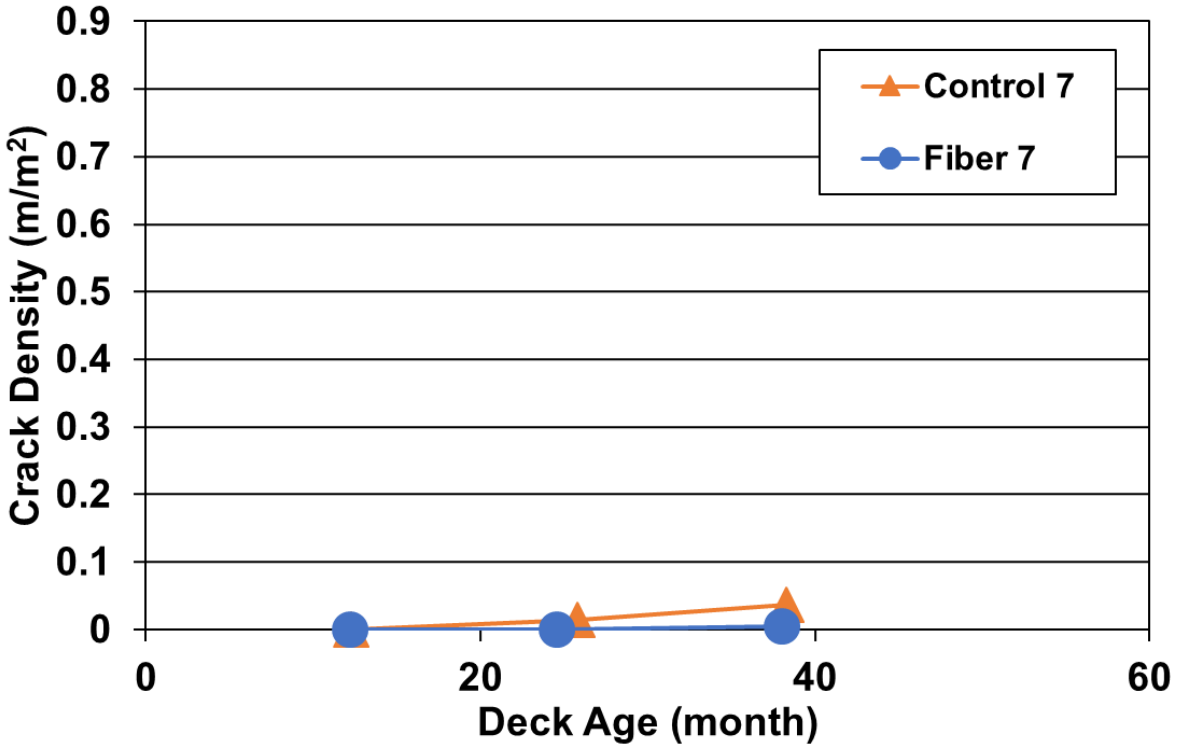

Figure 3.51 – Fiber-7 and Control-7 crack density versus deck age

3.4.19 SRA-1

SRA-1 was constructed on December 2, 2012. The deck has been surveyed twice. Survey 1 was performed on July 11, 2014 at an age of 19.1 months, and Survey 2 was performed on June 15, 2016 at an age of 43.0 months. Figures 3.52 and 3.53 show the crack maps from the two surveys.

The crack density found in Survey 1 was 0.455 m/m^2, which decreased to 0.333 m/m^2 in Survey 2. In both surveys, long longitudinal cracks were found in Spans 1, 3, and 4; one crack, parallel to the skew, was observed above each of the three piers, although in Figure 3.53 (Survey 2), the crack above the pier between Spans 2 and 3 is difficult to see in the figure because it is directly over the pier. In Survey 2, the number of short randomly oriented cracks decreased noticeably in all four spans, which resulted in a decrease in crack density. Similar to Fiber-1, Fiber-2, Fiber-3, and Control-3, the decrease in cracking was due to surface scaling. As shown in Figure

3.54, the deck surface showed more scaling during Survey 2, as indicated by the exposed aggregate particles and lower definition of the edges of the grooves.

Based on the 165 measurements made during Survey 2, the cracks on SRA-1 had widths between 0.003 and 0.020 in. (0.08 and 0.51 mm) with an average of 0.007 in. (0.18 mm).

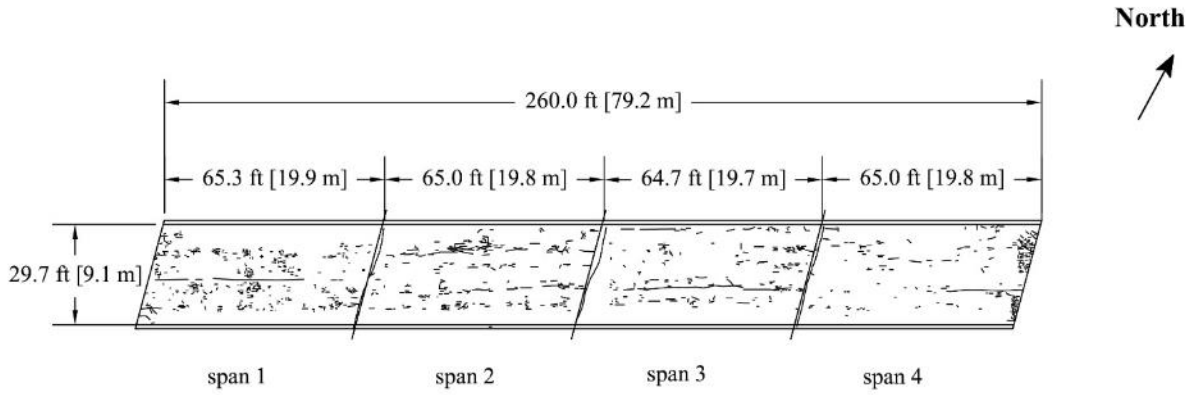

Bridge Number: B682
Bridge Location: Rte. 1421 over Linville Creek
Construction Date: 12/4/2012
Crack Survey Date: 7/11/2014

Bridge Length: 260 ft (79.2 m)
Bridge Width: 30 ft (9.1 m)
Skew: 15°
Number of Spans: 4
Span 1: 65.0 ft (19.8 m)
Span 2: 65.0 ft (19.8 m)
Span 3: 65.0 ft (19.8 m)
Span 4: 65.0 ft (19.8 m)
Number of Placements: 1

Bridge Age: 19.1 months
Crack Density: 0.455 m/m^2
Span 1: 0.492 m/m^2
Span 2: 0.503 m/m^2
Span 3: 0.443 m/m^2
Span 4: 0.383 m/m^2

Figure 3.52 – SRA-1 (Survey 1)

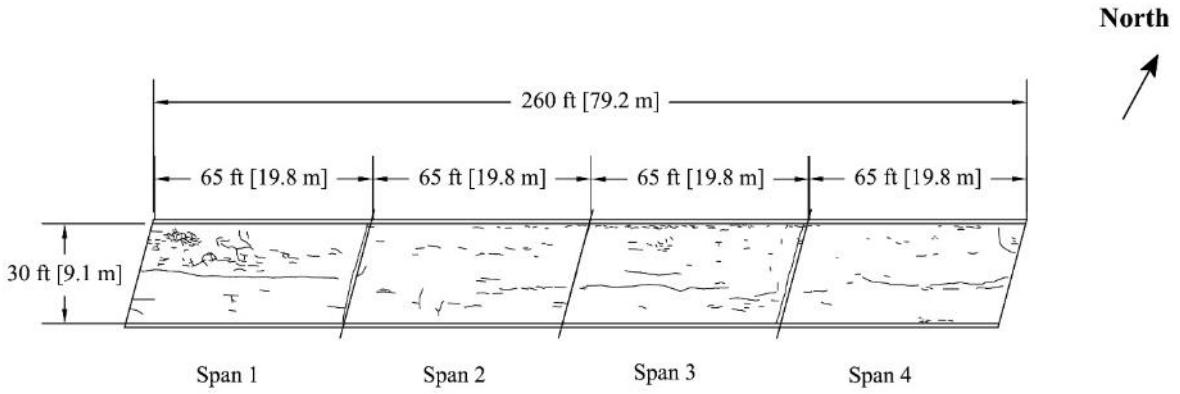

Bridge Number: B682
Bridge Location: Rte. 1421 over Linville Creek
Construction Date: 12/4/2012
Crack Survey Date: 6/15/2016

Bridge Length: 260 ft (79.2 m)
Bridge Width: 30 ft (9.1 m)
Skew: 15°
Number of Spans: 4
Span 1: 65.0 ft (19.8 m)
Span 2: 65.0 ft (19.8 m)
Span 3: 65.0 ft (19.8 m)
Span 4: 65.0 ft (19.8 m)
Number of Placements: 1

Bridge Age: 43.0 months
Crack Density: 0.333 m/m^2
Span 1: 0.511 m/m^2
Span 2: 0.205 m/m^2
Span 3: 0.413 m/m^2
Span 4: 0.204 m/m^2

Figure 3.53 – SRA-1 (Survey 2)

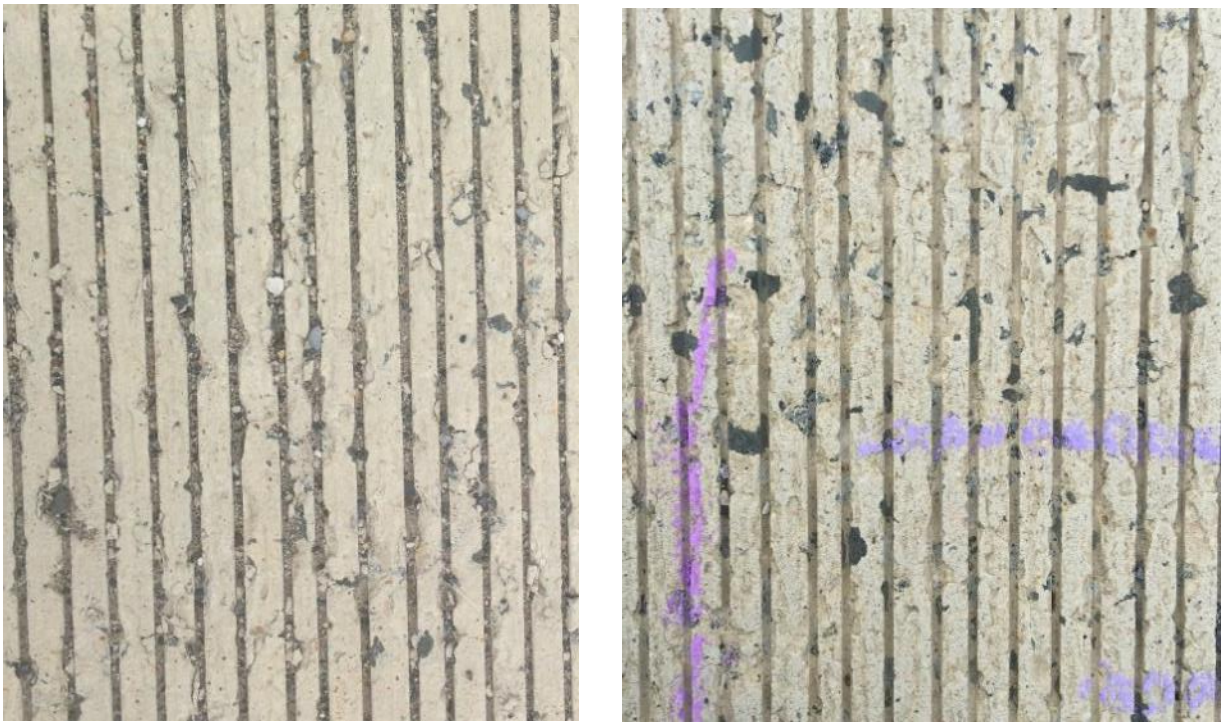

(a) (b)

Figure 3.54 – Changes in surface condition between the two surveys on SRA-1. (a) deck surface during Survey 1; (b) deck surface during Survey 2

3.4.20 SRA-2

Bridge deck SRA-2 was constructed on December 19, 2012. The deck has been surveyed twice. Survey 1 was performed on July 10, 2014 at the deck age of 18.6 months, and the crack density was 0.344 m/m^2 for the entire deck (Figure 3.55). Survey 2 (Figure 3.56) was performed on June 16, 2016, and the crack density was 0.217 m/m^2.

Both surveys found cracks transverse to the traffic, most notably near the two piers and in Span 2 and Span 3, while short randomly oriented cracks were more prevalent in Survey 1, especially in Spans 2 and 3. The reduction of observed short cracks in Survey 2 is, similar to many other bridges reported in this chapter, due to surface scaling. As shown in Figure 3.57, noticeable scaling occurred on the deck, evidenced by the exposed coarse aggregate and the nearly complete loss of grooves.

In Survey 2, 111 cracks were measured, with widths ranging from 0.003 to 0.016 in. (0.08 to 0.41 mm) and averaging 0.006 in. (0.15 mm).

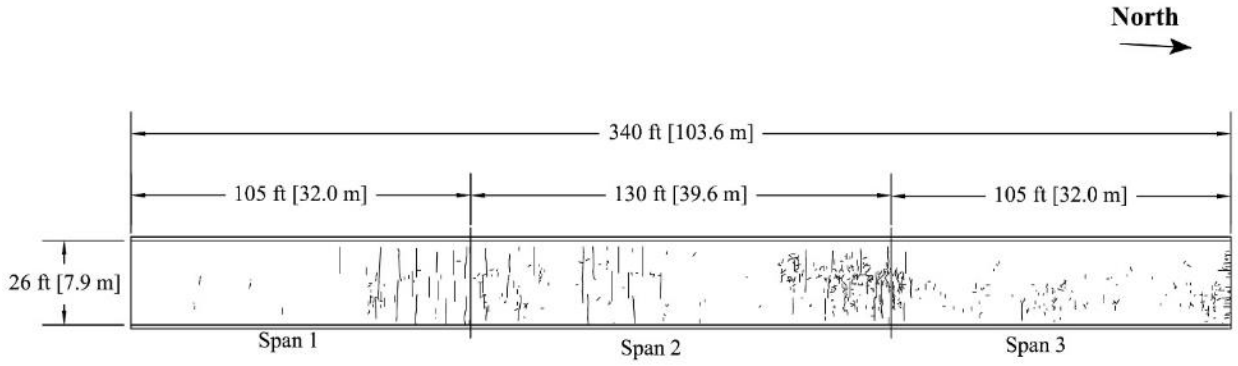

Bridge Number: B626
Bridge Location: RTE. 633 over Cowpasture River
Construction Date: 12/19/2012
Crack Survey Date: 7/10/2014

Bridge Length: 340 ft (103.6 m)
Bridge Width: 26 ft (7.9 m)
Skew: 0°
Number of Spans: 3
Span 1: 105 ft (32.0 m)
Span 2: 130 ft (39.6 m)
Span 2: 105 ft (32.0 m)
Number of Placements: 1

Bridge Age: 18.6 months
Crack Density: 0.344 m/m^2
Span 1: 0.263 m/m^2
Span 2: 0.502 m/m^2
Span 3: 0.228 m/m^2

Figure 3.55 – SRA-2 (Survey 1)

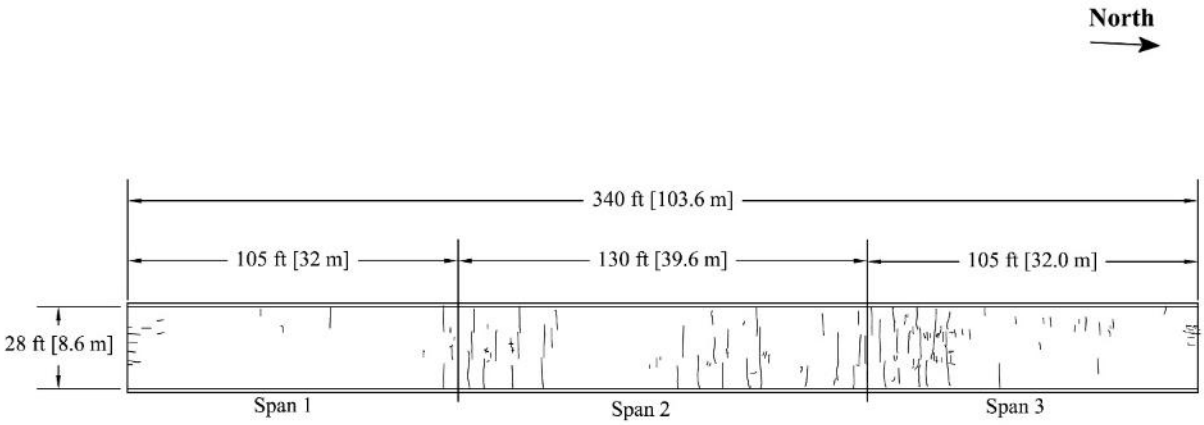

Bridge Number: 0663-003-155, B626
Bridge Location: RTE. 633 over Cowpasture River
Construction Date: 12/19/2012
Crack Survey Date: 6/16/2016

Bridge Length: 340 ft (103.6 m)
Bridge Width: 28 ft (8.6 m)
Skew: 0°
Number of Spans: 3
Span 1: 105 ft (32.0 m)
Span 2: 130 ft (39.6 m)
Span 2: 105 ft (32.0 m)
Number of Placements: 1

Bridge Age: 42.5 months
Crack Density: 0.217 m/m^2
Span 1: 0.070 m/m^2
Span 2: 0.282 m/m^2
Span 3: 0.284 m/m^2

Figure 3.56 – SRA-2 (Survey 2)

Figure 3.57 – Surface scaling on SRA-2 during Survey 2

3.4.21 SRA-3

Bridge deck SRA-3 was constructed on August 30, 2013 and has been surveyed twice. The deck was first surveyed on July 15, 2014 at an age of 10.5 months. The crack density was 0.027 m/m^2 (Figure 3.58). The second survey was completed on June 13, 2016 at an age of 33.9 months. The crack density was 0.083 m/m^2 (Figure 3.59).

Several short cracks parallel to the skew were found in the middle of Span 1 during Survey 1, which grew and connected between the two surveys, resulting in longer cracks in the second survey at the same locations. One longitudinal crack was found along the north side of the deck in Span 2, which likely developed from short cracks found at the same location during Survey 1. Cracks parallel to the skew were found near the pier in Survey 2. SRA-3 showed minimal scaling during Survey 2.

In Survey 2, 74 crack width measurements were made, with values ranging from 0.003 to 0.016 in. (0.08 to 0.41 mm) and averaging 0.007 in. (0.18 mm).

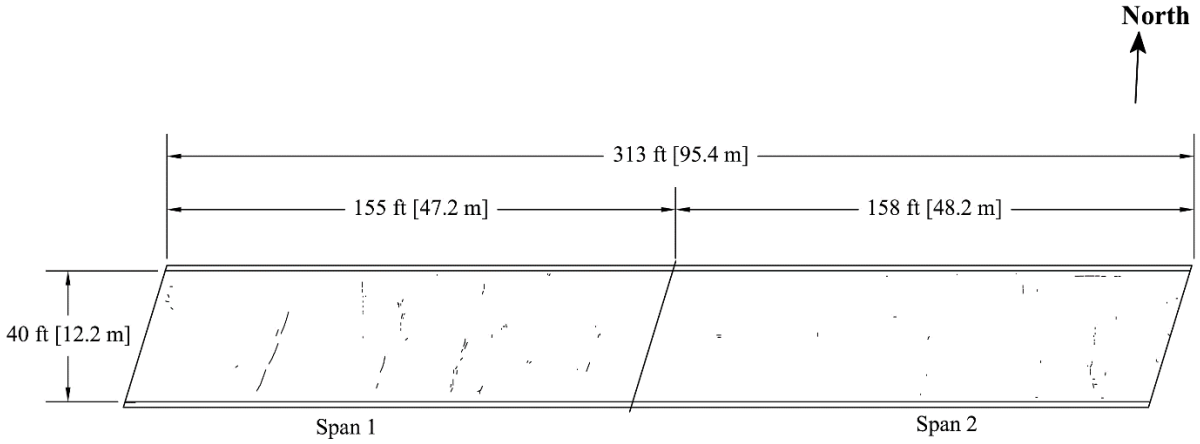

Bridge Number: B607
Bridge Location: Telegraph Road over I-95
Construction Date: 8/30/2013
Crack Survey Date: 7/15//2014

Bridge Length: 310 ft (95.4 m)
Bridge Width: 40 ft (12.2 m)
Skew: 19°
Number of Spans: 2
Span 1: 155 ft (47.2 m)
Span 2: 158 ft (48.2 m)
Number of Placements: 1

Bridge Age: 10.5 months
Crack Density: 0.027 m/m^2
Span 1: 0.037 m/m^2
Span 2: 0.016 m/m^2

Figure 3.58 – SRA-3 (Survey 1)

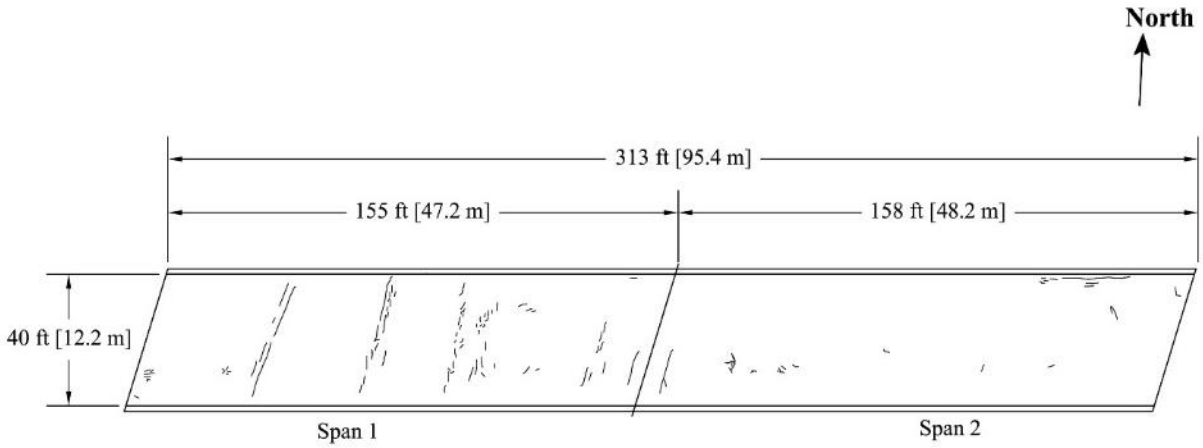

Bridge Number: B607
Bridge Location: Telegraph Road over I-95
Construction Date: 8/30/2013
Crack Survey Date: 6/13/2016

Bridge Length: 313 ft (95.4 m)
Bridge Width: 40 ft (12.2 m)
Skew: 19°
Number of Spans: 2
Span 1: 155 ft (47.2 m)
Span 2: 158 ft (48.2 m)
Number of Placements: 1

Bridge Age: 33.9 months
Crack Density: 0.083 m/m^2
Span 1: 0.121 m/m^2
Span 2: 0.046 m/m^2

Figure 3.59 – SRA-3 (Survey 2)

3.4.22 SRA-4

Bridge deck SRA-4 was constructed on August 30, 2013 and has been surveyed twice. The first survey was performed on July 16, 2014 at an age of 10.5 months. The crack density was 0.025 m/m^2 (Figure 3.60). The second survey was performed on June 16, 2016 at an age of 34.0 months. The crack density was 0.056 m/m^2 (Figure 3.61). In both surveys, all cracks were found only near the two abutments of the bridge.

Figure 3.62 shows the surface condition of SRA-4 during the second survey. The deck surface in general was in good condition. Some scaling, however, was observed on the deck, which occurred in strips perpendicular to the direction of traffic.

During Survey 2, 14 crack width measurements were made, with values ranging from 0.003 to 0.009 in. (0.08 and 0.23 mm) and averaging 0.006 in. (0.15 mm).

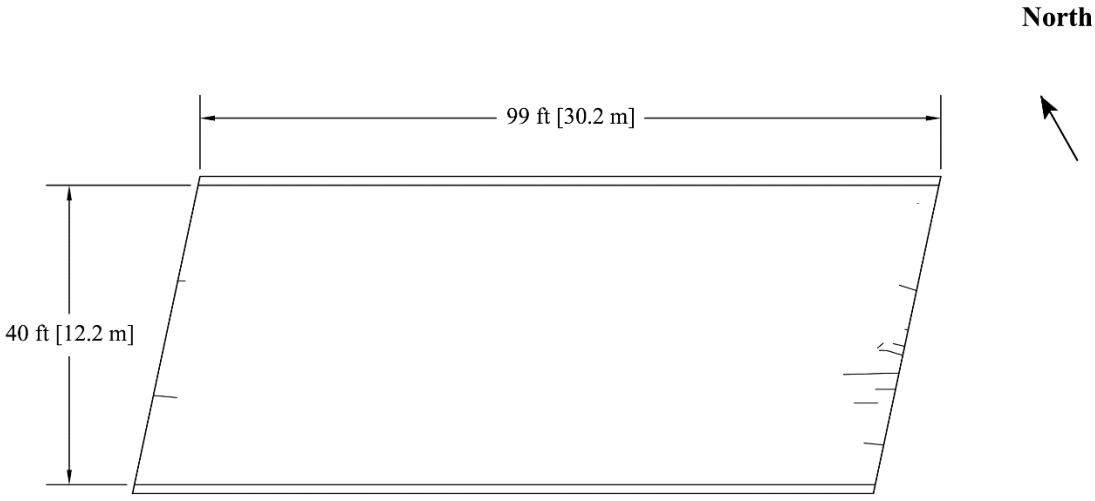

Bridge Number: B615
Bridge Location: Rte. 600 over Herring Creek
Construction Date: 8/30/2013
Crack Survey Date: 7/16/2014

Bridge Length: 99 ft (30.2 m)
Bridge Width: 40 ft (12.2 m)
Skew: 12°
Number of Spans: 1
Number of Placements: 1

Bridge Age: 10.5 months
Crack Density: 0.025 m/m^2

Figure 3.60 – SRA-4 (Survey 1)

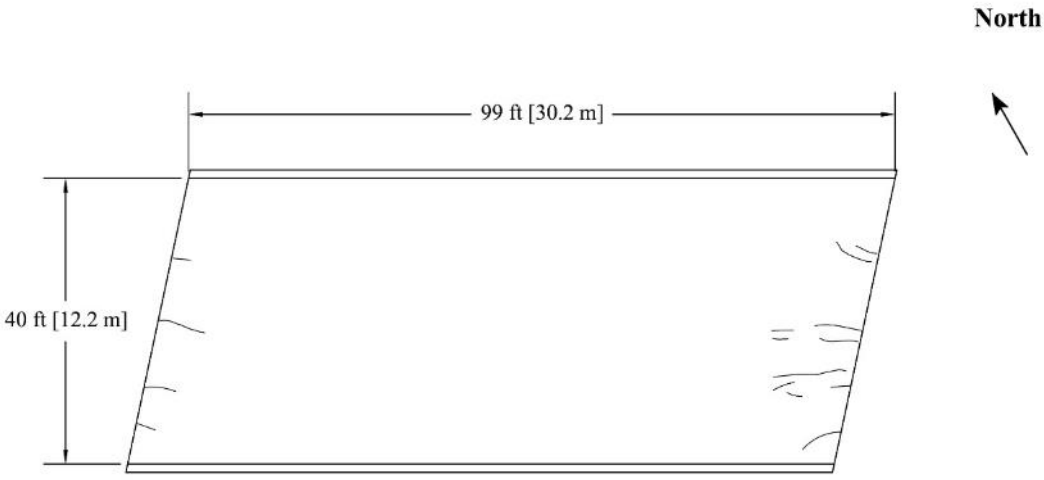

Bridge Number: B615
Bridge Location: Rte. 600 over Herring Creek
Construction Date: 8/30/2013
Crack Survey Date: 6/16/2016

Bridge Length: 99 ft (30.2 m)
Bridge Width: 40 ft (12.2 m)
Skew: 12°
Number of Spans: 1
Number of Placements: 1

Bridge Age: 34.0 months
Crack Density: 0.056 m/m^2

Figure 3.61 – SRA-4 (Survey 2)

(a) (b)

Figure 3.62 – Surface condition of SRA-4 during Survey 2. (a) an overview of the deck where a strip of the surface had scaling; (b) a close-up view of scaled section.

3.4.23 VA-Control

Bridge deck VA-Control was constructed on December 13, 2011. The deck has been surveyed twice. Survey 1 was performed on July 16, 2014 (Figure 3.63) at an age of 31.0 months, and the crack density was 0.222 m/m^2. Survey 2 was completed on July 17, 2014 at a deck age of 31.0 months (Figure 3.64), and the crack density was 0.266 m/m^2. The second survey was performed under rainy conditions and the deck was partially wet. The survey was not rescheduled owing to continued rainy weather in the region and time constraints that the survey crew were under. The result from the second survey, however, is deemed valid because the crack pattern found in the second survey (Figure 3.64) is consistent with that recorded in the first survey (Figure 3.63) as exemplified by the large longitudinal crack initiated at the east abutment, short

longitudinal cracks at both abutments, and crazing cracks at approximately one third the length of the deck from both ends.

Figure 3.65 shows the surface condition of VA-Control during Survey 2. As shown, some scaling was observed, as indicated by the exposed coarse aggregate.

During Survey 2, 89 crack width measurements were made, with values ranging from 0.003 to 0.016 in. (0.08 and 0.41 mm) and averaging 0.006 in. (0.15 mm).

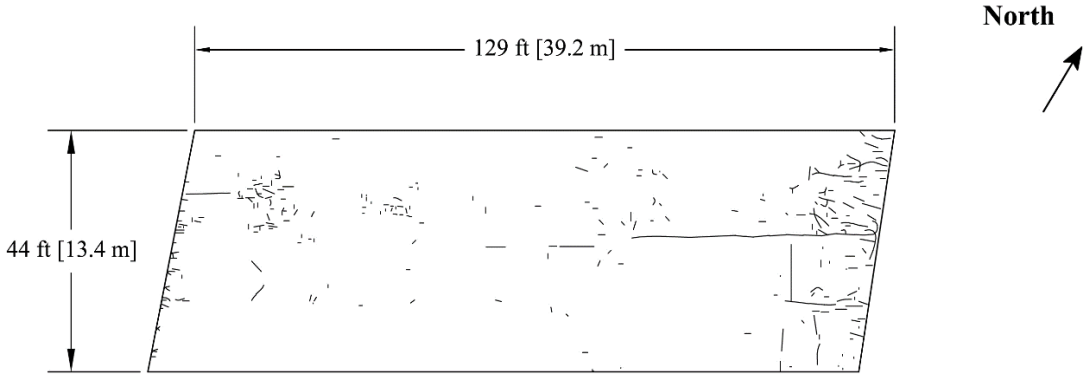

Bridge Number: B601
Bridge Location: Rte. 208 over TA River
Construction Date: 12/13/2011
Crack Survey Date: 07/16/2014

Bridge Length: 129 ft (39.2 m)
Bridge Width: 44 ft (13.4 m)
Skew: 11°
Number of Spans: 1
Number of Placements: 1

Bridge Age: 31.0 months
Crack Density: 0.222 m/m^2

Figure 3.63 – VA-Control (Survey 1)

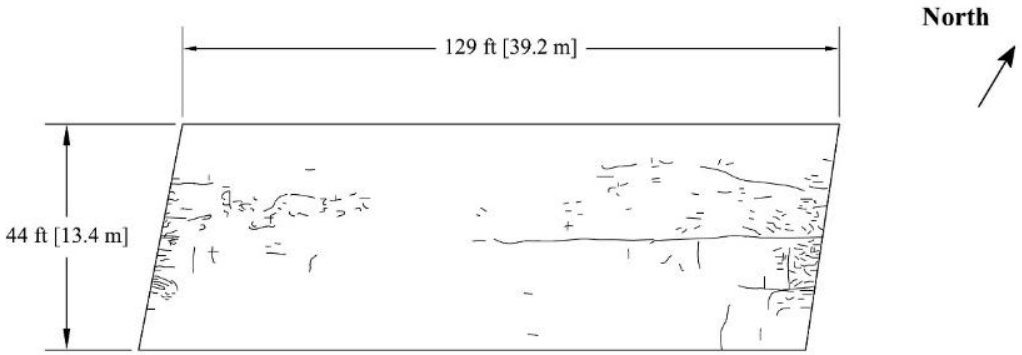

Bridge Number: B601
Bridge Location: Rte. 208 over TA River
Construction Date: 12/13/2011
Crack Survey Date: 6/17/2016

Bridge Length: 129 ft (39.2 m)
Bridge Width: 44 ft (13.4 m)
Skew: 11°
Number of Spans: 1
Number of Placements: 1

Bridge Age: 54.1 months
Crack Density: 0.266 m/m^2

Figure 3.64 – VA-Control (Survey 2)

Figure 3.65 – Deck surface of VA-Control during Survey 2

3.4.24 SRA and VA-Control Comparison

Figure 3.66 compares the crack densities of bridge decks with and without an SRA as a function of deck age. The use of an SRA in these decks did not consistently reduce cracking. SRA-3 and SRA-4 had lower crack densities than the control deck, SRA-2 had a similar crack density compared to the control deck, and SRA-1 had a higher crack density compared to the control deck.

The average crack widths of the decks in Virginia and the *p* values for their differences are shown in Table 3.10 based on the measurements made during 2016 surveys. Bridge decks with and without SRAs had similar crack widths, with average values of 0.007 in. (0.18 mm) for SRA-1 and SRA-3 and 0.006 in. (0.15 mm) for SRA-2, SRA-4, and VA-Control.

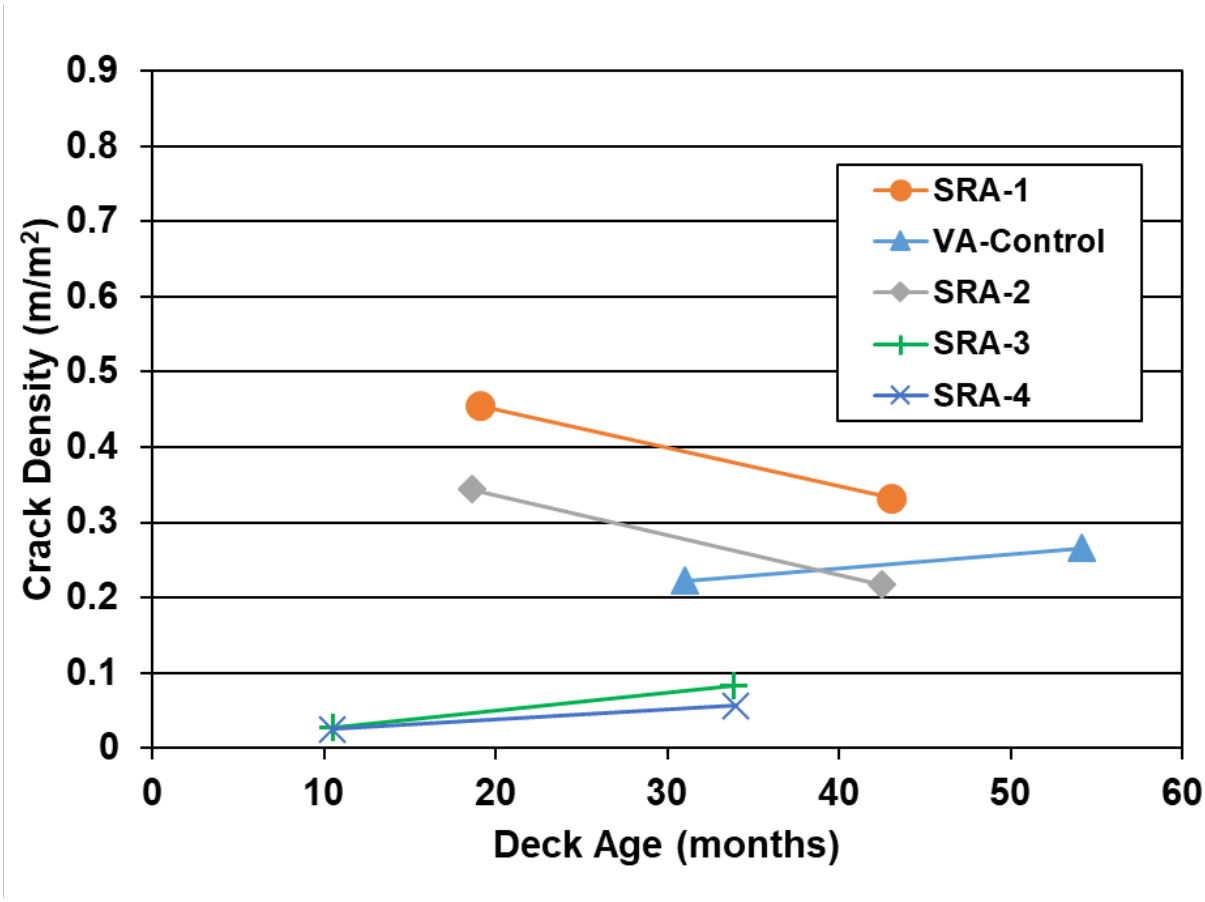

Figure 3.66 – SRA and VA-Control crack density versus deck age

Table 3.10 – *p* values obtained in Student's t-test for the differences in average crack widths of Fiber-1 and Fiber-2

	Bridge Deck Placement	SRA-1	SRA-2	SRA-3	SRA-4	VA-Control
Bridge Deck Placement	**Average Crack Width in.**	0.007	0.006	0.007	0.006	0.006
SRA-1	0.007		0.37	0.04	0.40	0.09
SRA-2	0.006			2.95×10^{-3}	0.58	0.37
SRA-3	0.007				0.03	1.58×10^{-4}
SRA-4	0.006					0.92

3.5 DISCUSSION

Table 3.11 summarizes the crack densities for bridge decks surveyed from 2014 to 2018, as well as crack densities at 36 months of age linearly interpolated from available survey results. Figure 3.67 shows crack density versus deck age for the decks.

The following procedures are used to calculate the 36-month crack density of each deck using the survey results. For decks surveyed both before and after 36 months of deck age, the crack density at 36 months is linearly interpolated using the two consecutive survey results. For decks whose latest survey was before 36 and no earlier than 30 months of deck age, the last survey result is used to approximate the 36-month crack density; this was done for Fiber-4, Control-4, SRA-3, and SRA-4. As discussed previously, Fiber-1, Fiber-2, Control-1, Control-2, SRA-1, and SRA-2 showed reduced crack densities in their latest surveys due to scaling; the crack densities found in the second to last survey for those decks, at ages between 18.6 to 34.0 months, are used to approximate the 36-month crack densities.

Table 3.11 – Crack density comparison

Bridge Deck	Deck Age	Crack Density	36-month Crack Density	Bridge Deck	Deck Age	Crack Density	36-month Crack Density
	month	m/m²	m/m²		month	m/m²	m/m²
Fiber-1 Placement 1	9.9	0.009	0.112	Control-4 Placement 2	13.9	0.395	0.393
	21.6	0.189			26.8	0.411	
	33.7	0.112*			35.6	0.393	
	45.5	0.088		Fiber-5	18.9	0.010	0.061
Fiber-1 Placement 2	7.9	0.011	0.220		31.1	0.044	
	19.6	0.056			44.7	0.091	
	31.7	0.220*		Control-5	19.0	0.008	0.052
	43.5	0.172			31.2	0.038	
Fiber-2 Placement 1	9.2	0.014	0.127		44.8	0.077	
	22.4	0.049		Fiber-6	12.8	0.000	0.011
	34.0	0.127*			25.0	0.005	
	44.9	0.126			38.6	0.013	
Fiber-2 Placement 2	7.6	0.042	0.456	Control-6	13.0	0.000	0.011
	20.7	0.269			25.3	0.002	
	32.4	0.456*			38.9	0.013	
	43.2	0.290		Fiber-7	12.2	0.000	0.004
Fiber-3	16.0	0.157	0.285		24.6	0.000	
	26.8	0.272			38.0	0.005	
	37.8	0.287		Control-7	12.3	0.000	0.033
	50.9	0.394			25.8	0.014	
Control-3	14.3	0.141	0.233		38.3	0.037	
	24.9	0.322		SRA-1	19.1	0.455*	0.455
	36.0	0.233			43.0	0.333	
	49.1	0.290		SRA-2	18.6	0.344*	0.344
Fiber-4 Placement 1	12.2	0.608	0.709		42.5	0.217	
	24.2	0.645		SRA-3	10.5	0.027	0.083
	33.6	0.709			33.9	0.083	
Fiber-4 Placement 2	12.1	0.173	0.431	SRA-4	10.5	0.025	0.056
	24.1	0.300			34.0	0.056	
	33.4	0.431		VA-Control	31.0	0.222	0.232
Control-4 Placement 1	14.2	0.739	0.766		54.1	0.266	
	27.0	0.725					
	35.8	0.766					

*: Crack density used to approximate the 36-month crack density.

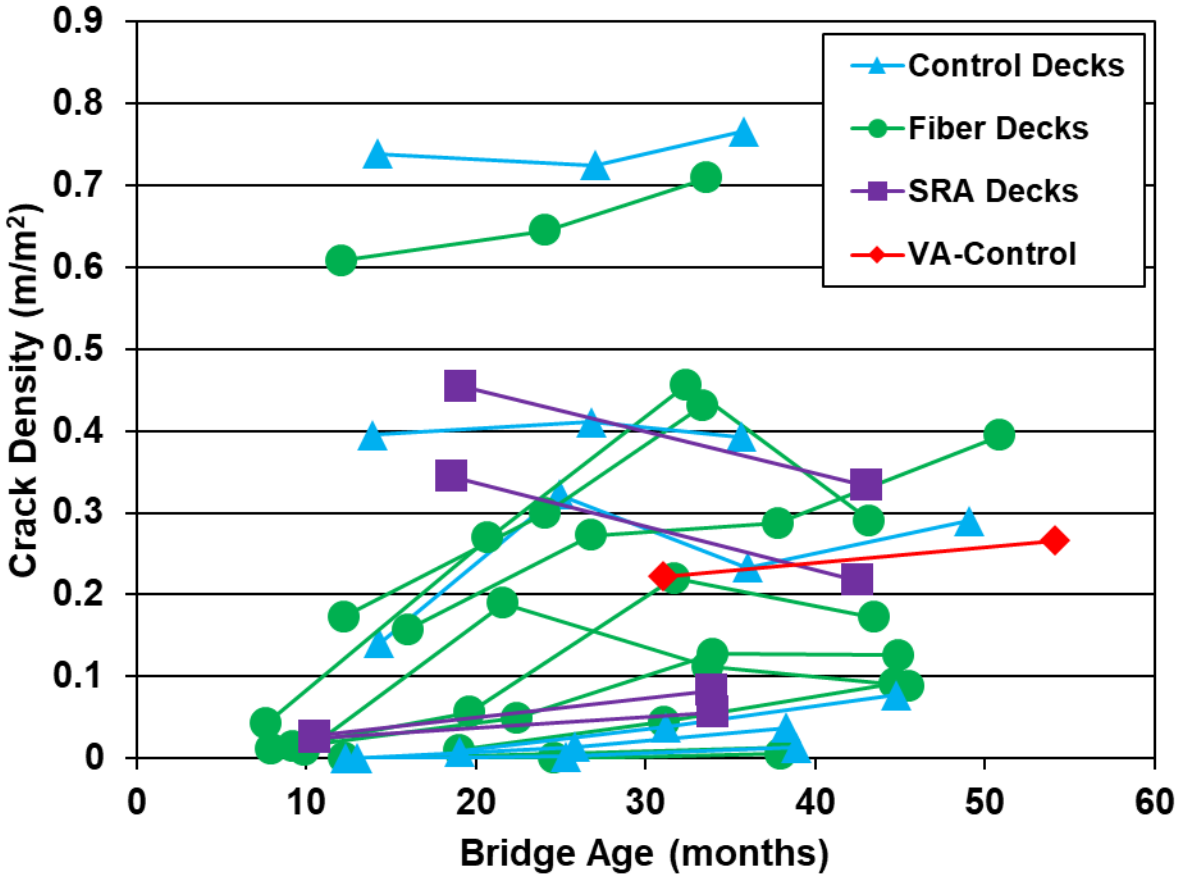

Figure 3.67 – Crack densities versus age for decks with fiber reinforcement, SRAs, and control decks

Figure 3.68 compares the 36-month crack densities of the fiber and control deck in each pair (for example, Fiber-3 and Control-3). In general, crack densities increased with age. At similar ages, the crack densities of bridge decks containing FRC and plain concrete were similar. This is best exemplified by comparing the cracking performance of Fiber-5, Fiber-6, and Fiber-7 with their associated control decks. The 36-month crack densities of decks Fiber-5 through Fiber-7 are between 0.004 and 0.061 m/m^2, while those of Control-5 thought Control-7 are between 0.011 and 0.052 m/m^2. Further, the decks constructed by the same contractor tended to exhibit similar cracking performance. Fiber-3, Fiber-4 (both placements), Control-3, and Control-4 (both placements), constructed by Contractor-KS-D, had similar and relatively high crack densities;

while Fiber-5 through Fiber-7 and Control-5 through Control-7, Constructed by Contractor-KS-F, showed similar and noticeably lower crack densities. Although numerous publications have shown that fiber reinforcement reduces concrete cracking caused by settlement and shrinkage (Ideker and Bañuelos 2014, Al-Qassag et al. 2015, Mazzoli et al. 2015, Ibrahim et al. 2019 to name a few), when construction is executed properly and concrete mixtures with low paste contents are used, cracking due to settlement and shrinkage is minimal (Khajehdehi and Darwin 2018) and the addition of fibers does not further improve the cracking performance of bridge decks.

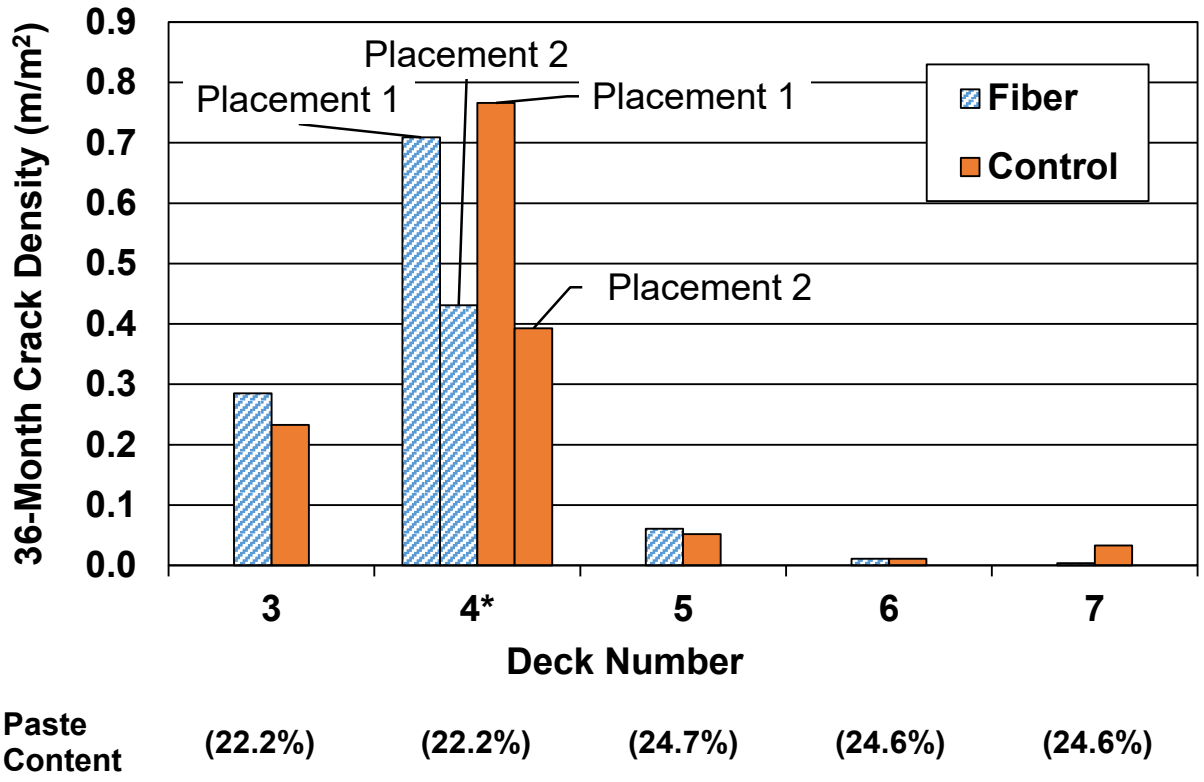

Figure 3.68 – Comparison of 36-month crack densities of decks with and without fiber reinforcement in each pair. *the column on the left represents Placement 1 and the one on the right represents Placement 2.

When poor construction practices are used, as in the case of Fiber-3, Fiber-4, Control-3, and Control-4, where inadequate consolidation was observed, bridge decks can exhibit drastically

higher crack densities, and adding fiber reinforcement cannot mitigate the negative effects of poor construction. The 36-month crack densities of the placements on Fiber-3 and Fiber 4 ranged from 0.285 to 0.709 m/m^2, similar to the crack densities of Control-3 and Control-4 (between 0.233 and 0.766 m/m^2) and noticeably higher than the majority of the decks included in this chapter at similar ages. Good construction practices are crucial to achieve low cracking in bridge decks; when construction practices are poor, bridge decks will exhibit increased cracking, and adding crack-reducing technologies cannot mitigate the negative effects.

The crack density of bridge decks containing SRA varied considerably. Of the four SRA decks, the deck with the highest paste content, SRA-1 (paste content of 28.2% by volume) exhibited the highest 36-month crack density (0.455 m/m^2), even higher than the control deck, VA-Control (paste content of 29.4% by volume), which had a crack density of 0.232 m/m^2. The other three SRA decks, with paste contents between 27.0% and 27.3%, exhibited noticeably lower 36-month crack densities compared to SRA-1, ranging from 0.056 to 0.344 m/m^2. Khajehdehi and Darwin (2018) analyzed the crack densities of 40 bridge decks at 96 months of age and found that paste content is the only material factor that notably influences the cracking performance of bridge decks: bridges with paste contents exceeding 27.2% are noticeably more likely to have high crack densities than the decks with lower paste contents. A similar trend appears to be true for decks containing SRAs: those with paste contents below a threshold are more likely to have low cracking; the threshold is less than that of SRA-1 (28.2%). Further research is needed to study with greater precision how the cracking performance of bridge decks containing SRAs changes with paste content.

The use of fiber reinforcement or SRAs does not consistently reduce crack widths. Among the paired decks cast with fiber-reinforced concrete (FRC) or plain concrete, only Control-3 and

Control-4 Placement 1 showed higher average crack widths than their associated decks cast with FRC and the differences are statistically significant; in all other comparisons, the control decks either had lower average crack widths or there is no statistically significant differences between the decks cast with FRC or plain concrete. The four decks with SRAs showed similar crack widths compared to their associated control deck (VA-Control).

3.6 COMPARISON WITH LC-HPC DECKS

Figures 3.69 and 3.70 compare the crack densities as a function of age for the sixteen bridge decks constructed in Kansas following the Low-Cracking High-Performance (LC-HPC) specifications with those of the decks with fiber reinforcement and SRAs, respectively. The LC-HPC decks have shown superior cracking performance compared to similar bridge decks constructed following the standard Kansas Department of Transportation specifications (Bohaty et al. 2013, Pendergrass and Darwin 2014, Alhmood et al. 2015, to name a few).

In general, the crack densities of most decks with fiber reinforcement and their paired control decks in this study had comparable crack densities with the LC-HPC decks, mainly due to their low paste contents (24.7% or lower). The fiber and control decks with construction issues (Fiber-3, Fiber-4, Control-3, and Control-4), on the other hand, exhibited higher crack densities than most of the LC-HPC decks at similar ages. The deck containing an SRA and a paste content of 28.2% (SRA-1) had a crack density noticeably higher than most of the LC-HPC decks. The three decks with SRAs and paste contents between 27.0% to 27.3% behaved differently, with one showing a crack density higher than most of the LC-HPC decks and two showing crack densities lower than most of the LC-HPC decks.

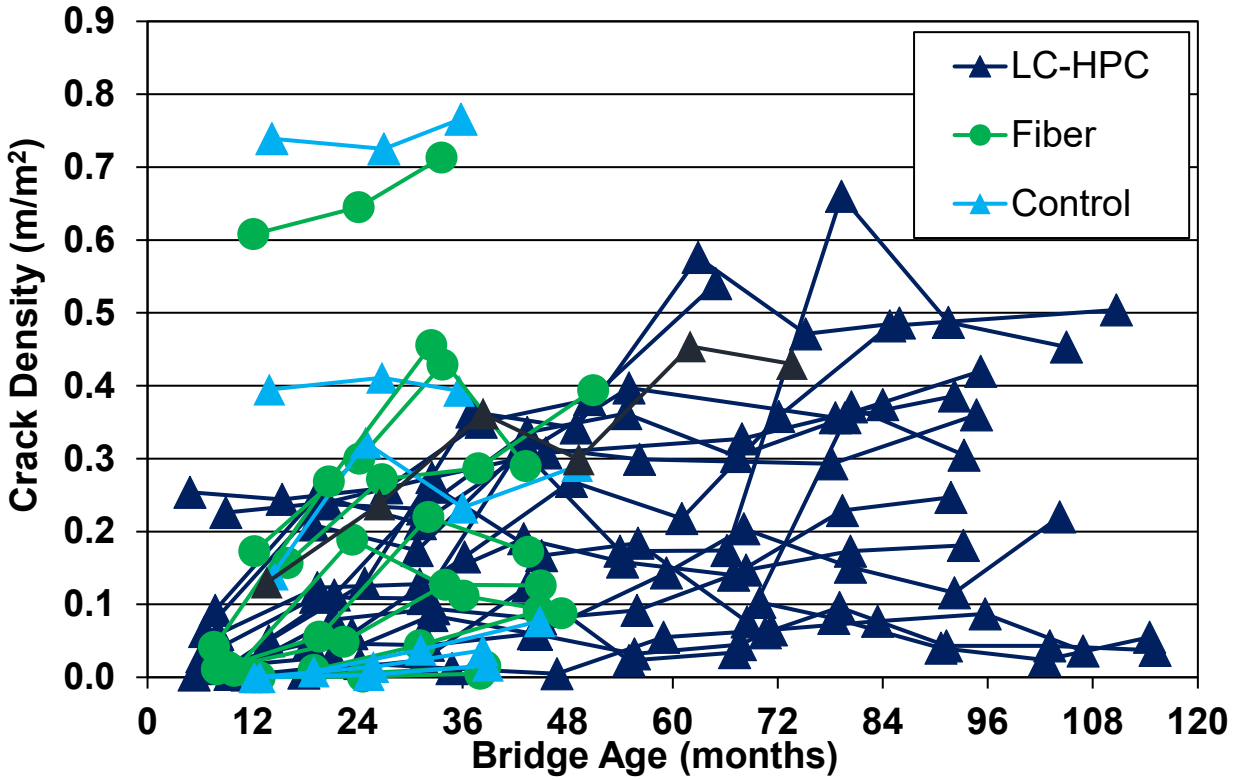

Figure 3.69 – Crack densities versus deck age for LC-HPC decks, decks with fiber reinforcement, and control decks

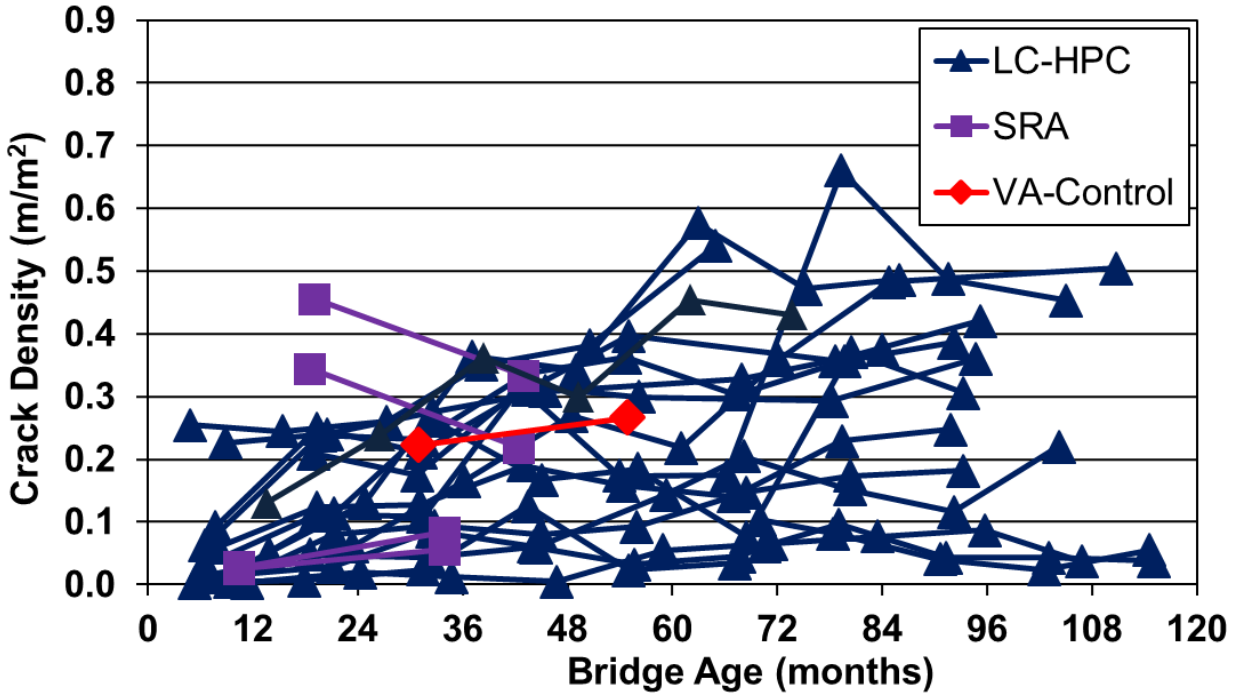

Figure 3.70 – Crack densities versus deck age for LC-HPC decks, decks with SRAs, and control deck in Virginia

3.7 SUMMARY AND CONCLUSIONS

Between 2014 and 2018, crack surveys were performed on seven bridge decks containing fiber-reinforced concrete (FRC), five associated control decks without fibers, four bridge decks containing shrinkage-reducing admixtures (SRAs), and one control deck without an SRA. The density of cracks visible, expressed in m/m^2, and average crack widths are used to quantify the cracking performance of bridge decks.

Based on the crack densities and crack width measurements, the following conclusions can be drawn:

1. The crack density of a bridge deck, in general, increases with age.
2. Cracks transverse to the direction of traffic are the most common. Near abutments, however, cracks usually initiate from and run perpendicular to the abutment.
3. When concrete mixtures with low paste contents and proper construction methods are used, the resulting bridge decks will show minimal cracking.
4. When poor construction practices are used, the resulting bridge decks will exhibit increased cracking.
5. If poor construction practices are used, the addition of fiber reinforcement may provide a slight reduction in cracking, but cannot overcome the negative effects of poor construction.
6. Shrinkage-reducing admixtures can reduce cracking in bridge decks if the paste content of the concrete mixture does not exceed 27.3%. SRAs cannot reduce cracking in bridge decks if the paste content is 28.2% or higher. No data are available for bridge decks with SRAs and paste contents between 27.3% and 28.2%.

7. In this study, the average widths of cracks ranged from 0.004 to 0.010 in. (0.10 to 0.25 mm).
8. The use of FRC and SRAs does not consistently reduce crack width.

CHAPTER 4: FACTORS AFFECTING BRIDGE DECK CRACKING: CRACK-REDUCING TECHNOLOGIES, PASTE CONTENT, AND CONSTRUCTION PRACTICES

4.1 INTRODUCTION

Cracking of reinforced concrete in bridge decks accelerates corrosion of reinforcing steel and freeze-thaw damage of concrete, reducing the service life and increasing the maintenance costs of bridge decks (Mindess et al. 2003). According to a national survey led by the Federal Highway Administration, bridge deck cracking, corrosion of reinforcing steel, and freeze-thaw damage of concrete were among the top forms of distress in bridge decks recognized by state departments of transportation (Triandafilou 2005).

Methods to reduce bridge deck cracking include lowering the paste content in the concrete (the volume percentage of cementitious material and water) and enforcing good construction practices, such as minimal finishing, thorough consolidating, and prompt application of curing (Schmitt and Darwin 1995, Darwin et al. 2004, Transportation Research Board 2006, Deshpande et al. 2007, Radlińska and Weiss 2012, Khajehdehi and Darwin 2018). These methods, however, are not always used (McLeod et al. 2009, Khajehdehi and Darwin 2018, Lafikes et al. 2018). Additionally, innovative technologies that promise to reduce cracking in bridge decks, including shrinkage-reducing admixtures (SRAs), fiber reinforcement, and internal curing (IC), have been developed and become increasingly popular in recent decades.

Theoretically, SRAs and IC reduce bridge deck cracking by reducing concrete shrinkage (Berke et al. 2003, Browning et al. 2011) while fiber reinforcement does so by increasing the toughness of concrete (Gopalaratnam et al. 1991). The effectiveness of these crack-reducing technologies is supported by numerous studies; the majority of these, however, are based on

laboratory tests (Voigt et al. 2004, Naaman et al. 2005, Brown et al. 2007, Bentz and Weiss 2011, Delatte and Crowl 2012, Pendergrass and Darwin 2014, Al-Qassag et al. 2015, Khajehdehi et al. 2018). The evaluation of the crack-reducing technologies based on long-term observations of in-service bridge decks, on the other hand, is limited and sometimes contradicts laboratory findings. Based on a survey involving 116 bridge decks, Delatte and Crowl (2012) reported that synthetic fibers do not prevent cracking in bridge decks; the cracking performance of individual bridge decks, however, is not published. Streeter et al. (2012) evaluated the cracking performance of three decks containing fine lightweight aggregate for internal curing and two decks without internal curing and found that, with or without IC, all the five decks performed similarly and exhibited none or minimal cracking (one crack per deck) when inspected at an age of one year or less. Polley et al. (2015) compared the cracking performance of six bridge decks with SRAs and found that, at similar ages (10 to 19 months), decks with SRAs exhibited similar or even higher cracking compared to the decks without SRAs.

The significance of construction practices used by contractors, especially the methods used to consolidate, finish, and cure concrete, on the cracking performance of bridge decks is largely underappreciated. The need for proper construction practices has been highlighted by researchers at the University of Kansas (KU), including McLeod et al. (2009), Darwin et al. (2016), and Khajehdehi and Darwin (2018), who illustrated quantitatively that when contractors fail to properly consolidate, finish, and cure the concrete, the resulting bridge decks will exhibit high crack densities.

To further examine the long-term effects of crack-reducing technologies, paste content, and construction practices on bridge deck cracking, cracking performance was evaluated quantitatively following a consistent on-site survey method (described in Chapter 3) for 20 bridge

deck placements with crack-reducing technologies, specifically SRA, IC, or fiber reinforcement, as well as 54 deck placements without these technologies. All but two of the deck placements have been surveyed at least twice at different deck ages. Because the crack density of bridge decks increases with age (Darwin et al. 2004, Lindquist et al. 2005, Yuan et al. 2011, Pendergrass and Darwin 2014), crack densities at 36 months of age are compared for all the decks to provide a consistent measure of cracking. An age of 36 months is chosen because this is when the long-term cracking performance of bridge decks starts to show (Lindquist et al. 2008, Yuan et al. 2011, Pendergrass and Darwin 2014).

4.2 BRIDGE DECKS INCLUDED FOR ANALYSIS

Besides the bridge decks constructed with and without fiber-reinforced concrete or shrinkage-reducing admixtures described in Chapter 3 and Appendix D, additional bridge decks from previous studies are also included in the comparisons in this chapter. For bridge decks constructed in multiple placements, each placement is analyzed separately.

Table 4.1 summarizes the paste contents and construction issues that occurred for the decks with and without fiber reinforcement or SRAs discussed in Chapter 3. Decks whose construction was not observed by personnel from the University of Kansas are marked as “Not observed.” As discussed in Chapter 3, during the construction of Fiber-4, the construction workers walked in the consolidated concrete, causing a loss of consolidation, which increased the likelihood of settlement cracking, as evidenced by the crack survey results in Chapter 3. Given that the same contractor constructed Fiber-3, Control-3, Fiber-4, and Control-4 within a short period (between 3/13/2014 and 8/26/2014), and these decks exhibited similar cracking patterns (described in Chapter 3), it is deduced that the same construction procedures were followed for Fiber-3, Control-3, Fiber-4, and Control-4 and all these decks experienced a loss of consolidation.

Table 4.1 – Paste content and construction issues of fiber and SRA decks

Bridge Deck Placement	Paste Content	Construction Issue	Bridge Deck Placement	Paste Content	Construction Issue
Fiber-1 p1*	23.8%	No issue	Control-5	24.7%	No issue
Fiber-1 p2*	23.8%	No issue	Fiber-6	24.6%	No issue
Fiber-2 p1*	23.8%	No issue	Control-6	24.6%	No issue
Fiber-2 p2*	23.8%	No issue	Fiber-7	24.6%	No issue
Fiber-3	22.2%	Loss of consolidation	Control-7	24.6%	No issue
Control-3	22.2%	Loss of consolidation	VA-SRA-1	28.2%	Not observed
Fiber-4 p1*	22.2%	Loss of consolidation	VA-SRA-2	27.1%	Not observed
Fiber-4 p2*	22.2%	Loss of consolidation	VA-SRA-3	27.0%	Not observed
Control-4 p1*	22.2%	Loss of consolidation	VA-SRA-4	27.3%	Not observed
Control-4 p2*	22.2%	Loss of consolidation	VA-Control	29.4%	Not observed
Fiber-5	24.7%	No issue			

*: p = placement

The paste contents of six bridge deck placements constructed with internally cured concrete (IN-IC-1 through IN-IC-5) and one without IC (IN-Control) in Indiana are listed in Table 4.2. IN-Control has a paste content of 27.6%, while the paste contents of the decks with IC ranged from 25.2% to 27.6%. Crack survey results for the Indiana decks are reported by Lafikes et al. (2018). IN-Control and IN-IC-1 are supported by prestressed box girders and all other IC decks are supported by steel girders. IN-IC-5 was constructed in 2 placements; Placement 1 is the northbound lane and Placement 2 is the southbound lane (Figure 4.1). A coal mine operated just south of the deck (Wild Boar Mine) and trucks carrying coal travelled frequently on Placement 1. As a result, the first placement of IN-IC-5 exhibited unusually high cracking and is excluded for the analysis (Figure 4.1).

Table 4.2 – Paste content of decks in Indiana with or without IC

Bridge Deck Placement	Paste Content	Bridge Deck Placement	Paste Content
IN-Control	27.6%	IN-IC-3	25.3%
IN-IC-1	27.6%	IN-IC-4	25.9%
IN-IC-2 p1*	24.6%	IN-IC-5 p2*	25.7%
IN-IC-2 p2*	25.2%		

*: p = placement

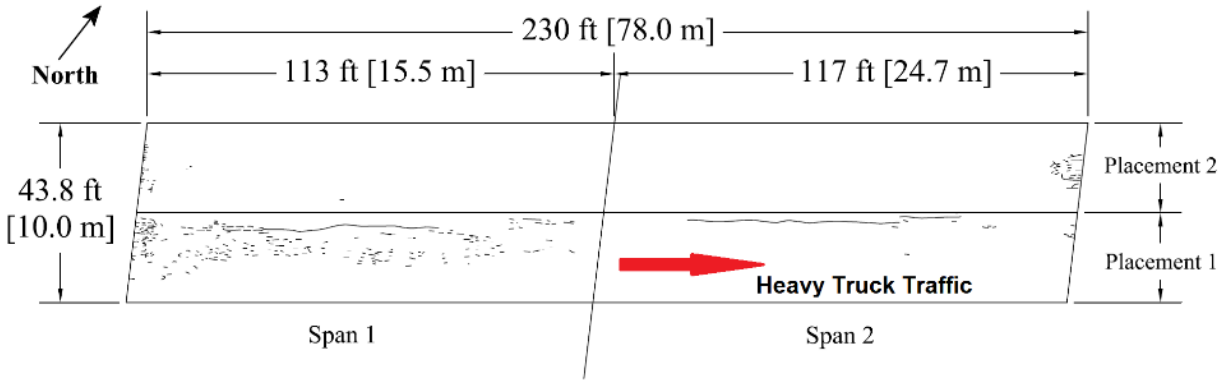

Figure 4.1 – Direction of truck traffic and uneven cracking on IN-IC-5

Twenty-seven bridge decks surveyed by Schmitt and Darwin (1995), Miller and Darwin (2000), and Lindquist et al. (2005) are included to represent decks constructed without a crack-reducing technology. Referred to as Conventional decks in this chapter, this group of decks were constructed following the Kansas Department of Transportation (KDOT) specifications. The paste contents of the Conventional decks ranged from 25.7% to 28.8%. This wide range allows the comparison of cracking performance among decks with various paste contents. Table 4.3 lists the paste contents of the Conventional decks. All Conventional decks are supported by steel girders.

Table 4.3 – Paste content of conventional decks

Bridge Deck Placement	Paste Content	Bridge Deck Placement	Paste Content
3-046 East Deck	26.4%	70-095 Deck	27.2%
3-046 West Deck	26.4%	70-103 Right	27.2%
3-046 Ctr. Deck	25.7%	70-103 Left	27.2%
75-044 Deck	27.9%	70-104 Deck	27.2%
75-045 Deck	27.9%	70-107 Deck	27.2%
89-204 Deck	28.8%	99-076 p4*	28.7%
3-045 West Deck	26.4%	99-076 p5*	28.7%
3-045 East Deck	26.4%	99-076 North (West Ln.)	28.7%
3-045 W. Ctr. Deck	26.4%	99-076 North (East Ln.)	28.7%
3-045 Ctr. Deck	26.4%	99-076 p2*	27.9%
3-045 E. Ctr. Deck	26.4%	99-076 p3*	27.9%
56-142 Pos. Moment	26.5%	89-208 Deck	27.1%
56-142 Neg. Moment	26.5%	56-49 Deck	25.7%
56-148 Deck	27.2%		

*: p = placement

Nineteen decks constructed in Kansas following the low-cracking high-performance concrete (LC-HPC) specifications introduced in Chapter 1 are included (Table 4.4). Similar to the Conventional decks, the LC-HPC decks did not use any crack-reducing technology other than specifications calling for low paste contents and quality construction procedures. The crack survey results of the LC-HPC decks were reported by Lindquist et al. (2008), McLeod et al. (2009), Yuan et al. (2011), Pendergrass and Darwin (2014), Bohaty et al. (2013), and Alhmood et al. (2015). The LC-HPC decks included in this chapter are supported by steel girders and have paste contents between 22.8% and 24.6% (Table 4.4). The first placement of LC-HPC-4 is not included in the analysis because the mixture proportions were changed during placement and the actual paste content is unknown (Lindquist et al. 2008). LC-HPC-8 and -10 are excluded because these decks are supported by prestressed girders. The right east-bound driving lane of LC-HPC-11 is excluded from the analysis because, like Placement 1 of IN-IC-5, heavy truck traffic travels on this lane and this portion of the deck exhibited unusually high crack densities (Darwin et al. 2016).

Table 4.4 – Paste content and construction issues of LC-HPC decks

Bridge Deck Placement	Paste Content	Construction Issue	Bridge Deck Placement	Paste Content	Construction Issue
LC-HPC-1 p1*	24.6%	No issue	LC-HPC-12 p1*	24.3%	Loss of consolidation
LC-HPC-1 p2*	24.6%	No issue	LC-HPC-12 p2*	24.3%	Loss of consolidation
LC-HPC-2	24.6%	No issue	LC-HPC-13	24.1%	Loss of consolidation
LC-HPC-3	24.4%	No issue	LC-HPC-14 p1*	24.4%	Insufficient consolidation Excessive finishing
LC-HPC-4 p2*	23.4%	No issue	LC-HPC-14 p2*	24.4%	Insufficient consolidation Excessive finishing
LC-HPC-5	23.9%	No issue	LC-HPC-14 p3*	24.4%	Insufficient consolidation Excessive finishing
LC-HPC-6	24.4%	No issue	LC-HPC-15	22.8%	No issue
LC-HPC-7	24.6%	No issue	LC-HPC-16	22.8%	No issue
LC-HPC-9	24.2%	No issue	LC-HPC-17	24.6%	No issue
LC-HPC-11[a]	23.4%	No issue			

*: p = placement

[a]: The right east-bound driving lane of LC-HPC-11 is excluded from analysis.

Researchers from the University of Kansas observed the construction of all LC-HPC decks; the influence of construction practices can be evaluated by comparing the crack densities of the LC-HPC decks with and without issues. Similar to Fiber-4 (described in Chapter 3), during the construction of LC-HPC-12 and -13, workers walked through consolidated concrete, leaving holes (footprints) in the surface, as shown in Figure 4.2. The holes were merely covered by the finishing machine instead of removed by re-consolidation. This loss of consolidation increased the likelihood of settlement cracking, as observed during the surveys of LC-HPC-12 at ages of 38.1 and 49.5 months, shown in Figure 4.3. The same contractor constructed Fiber-3, Control-3, Fiber-4, Control-4, and LC-HPC-12.

Figure 4.2 – Construction workers walking in previously vibrated concrete and causing a loss in consolidation during construction of LC-HPC-12 Placement 1 (direction of placement is from left to right in the picture)

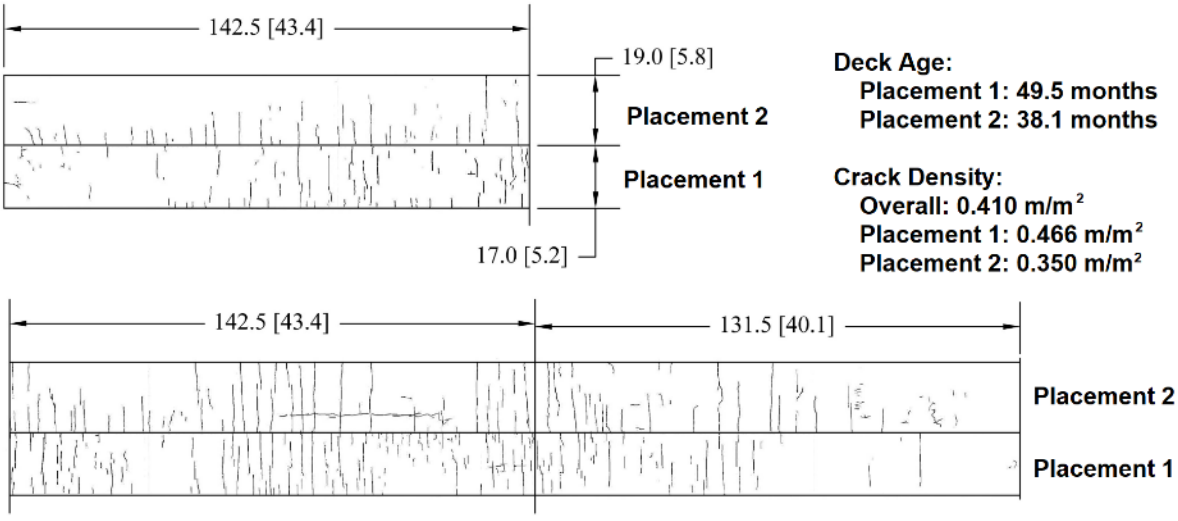

Figure 4.3 – Crack survey results of LC-HPC-12 at 49.5 and 38.1 months of age for Placement 1 and 2, respectively (Bohaty et al. 2013)

Problematic construction practices were also observed during the construction of LC-HPC-14. The contractor used spring-loaded gang vibrators for consolidation; after consolidating the

concrete, the vibrators were extracted from concrete abruptly, leaving a series of holes in the deck surface (Figure 4.4). These holes were later covered by the finishing machine instead of by reconsolidation and resulted in insufficient consolidation in LC-HPC-14. Similar to LC-HPC-12 and -13, this increased the likelihood of settlement cracking. Furthermore, the contractor devoted extra effort to bullfloating and hand-finishing the deck surface; excessive finishing can bring a significant amount of cement paste to the surface and delays the application of curing, which increases the likelihood of shrinkage cracking.

The issues observed during the construction of LC-HPC-12, -13, and -14 are described in greater detail by McLeod et al. (2009), Pendergrass and Darwin (2014), and Khajehdehi and Darwin (2018).

Figure 4.4 – Holes left by vibrators on LC-HPC-14 Placement 1 (McLeod et al. 2009)

4.3 CRACK DENSITIES AT 36 MONTHS

The crack density of bridge decks increases with age. To eliminate the influence of deck age for the comparisons that follow, crack densities at 36 months of deck age are used for the analyses in this chapter.

To establish the 36-month crack density of the decks using the survey results, for decks surveyed both before and after 36 months of deck age, the crack density at 36 months is linearly interpolated using the two consecutive survey results. For decks whose latest survey was before 36 but no earlier than 30 months of age, the last survey result is approximated as the 36-month crack density. Similarly, for decks whose earliest survey was after 36 but no later than 42 months of deck age, the first survey result is used to approximate the 36-month crack density. For decks whose first survey was after 42 months of age and those whose most recent survey was before 30 months of age, their 36-month crack densities are linearly extrapolated based on the two available survey results closest to 36 months, thus assuming crack density is a linear function of deck age.

Exceptions were made for the following decks. As described in Chapter 3, Fiber-1 and Fiber-2 showed reduced cracking in their most recent survey (Survey 4) due to scaling of the decks; the crack densities obtained in Survey 3 for these decks are, therefore, treated as the crack densities at 36 months. VA-SRA-1, VA-SRA-2, and 75-045 deck have been surveyed twice but showed lower crack densities in the second survey; the crack densities found in the first survey are used as the 36-month crack densities.

The 36-month crack densities of the bridge decks included in this chapter are listed in Table 4.5. The survey results used to calculate 36-month crack densities are shown in Appendix E. More detailed crack survey results are presented in Chapter 3 and by Polley et al. (2015) for the decks in Kansas containing fiber reinforcement, the decks in Virginia containing SRAs, and their

associated control decks; by Lafikes et al. (2018) for the Indiana decks with and without IC; by Schmitt and Darwin (1995), Miller and Darwin (2000), and Lindquist et al. (2006) for the Conventional decks in Kansas; and by Yuan et al. (2011), Bohaty et al. (2013), and Alhmood et al. (2015) for the LC-HPC decks.

When analyzing the influence of crack-reducing technologies, paste contents, and construction practices, bridge decks with similar combinations of these variables are grouped and the average crack densities of the groups are used for comparison. When comparing the average crack densities of two groups of bridge decks (X_1 and X_2), Student's t-test is used to verify whether the difference between X_1 and X_2 is due to the difference between the means of the two underlying populations from which the samples are drawn (μ_1 and μ_2) or merely due to the variations among samples in the same population. The results of the t-tests are expressed as *p* values, which is the probability that the difference between X_1 and X_2 is caused by chance and that there is, in fact, no difference between μ_1 and μ_2 (that is, the two groups of decks will show the same crack density if an infinitely large number of specimens were made from each mixture). In this chapter, $p = 0.05$ is used as the threshold. Values of *p* less than or equal to 0.05 are taken as meaning that the difference between two means is statistically significant.

Table 4.5 – Crack density of bridge decks at 36 months of age

Placement	36-Month Crack Density (m/m^2)	Placement	36-Month Crack Density (m/m^2)
Fiber-1 p1*	0.112	Fiber-1 p2*	0.220
Fiber-2 p1*	0.127	Fiber-2 p2*	0.456
Fiber-3	0.285	Control-3	0.233
Fiber-4 p1*	0.709	Fiber-4 p2*	0.431
Control-4 p1*	0.766	Control-4 p2*	0.393
Fiber-5	0.061	Control-5	0.052
Fiber-6	0.011	Control-6	0.011
Fiber-7	0.004	Control-7	0.033
VA-SRA-1	0.455	VA-SRA-2	0.252
VA-SRA-3	0.083	VA-SRA-4	0.056
VA-Control	0.232	IN-Control	0.236
IN-IC-1	0.181	IN-IC-2 p1*	0.000
IN-IC-2 p2*	0.020	IN-IC-3	0.017
IN-IC-4	0.057	IN-IC-5 p2*	0.032
3-046 West Deck	0.254	3-046 Ctr. Deck	0.042
3-046 East Deck	0.392	75-044 Deck	0.165
75-045 Deck	0.468	89-204 Deck	0.736
3-045 West Deck	0.074	3-045 East Deck	0.078
3-045 W. Ctr. Deck	0.178	3-045 Ctr. Deck	0.174
3-045 E. Ctr. Deck	0.043	56-142 Pos. Moment	0.071
56-142 Neg. Moment	0.064	56-148 Deck	0.259
70-095 Deck	0.025	70-103 Right	0.253
70-103 Left	0.396	70-104 Deck	0.069
70-107 Deck	0.326	99-076 p4*	0.872
99-076 p5*	0.861	99-076 North (West)	0.801
99-076 North (East)	0.412	99-076 p2*	1.536
99-076 p3*	0.739	89-208 Deck	0.009
56-49 Deck	0.246	LC-HPC-1 p1*	0.049
LC-HPC-1 p2*	0.024	LC-HPC-2	0.048
LC-HPC-3	0.121	LC-HPC-4 p2*	0.090
LC-HPC-5	0.154	LC-HPC-6	0.271
LC-HPC-7	0.012	LC-HPC-9	0.325
LC-HPC-11	0.163	LC-HPC-12 p1*	0.301
LC-HPC-12 p2*	0.332	LC-HPC-13	0.344
LC-HPC-14 p1*	0.543	LC-HPC-14 p2*	1.223
LC-HPC-14 p3*	0.695	LC-HPC-15	0.228
LC-HPC-16	0.250	LC-HPC-17	0.283

*: p = placement

4.4 COMPARISONS AND DISCUSSION

4.4.1 Influence of Paste Content

Khajehdehi and Darwin (2018) analyzed the crack densities of 40 bridge deck placements at 96 months of age and found that paste content has a dominant effect on cracking. Bridge decks with paste contents above 27.2% are associated with high cracking, while decks with paste contents of 26.4% or less consistently exhibit low cracking. For bridge decks with similar paste contents, crack density is affected only slightly, if at all, by other material properties, such as concrete slump, strength, and air content.

At 36 months of age, bridge decks with low paste contents are also noticeably more likely to have low crack densities. Figure 4.5 shows the 36-month crack density of bridge decks as a function of the paste content. Decks with construction issues are not included in the figure. As shown, decks with paste contents of 27.2% and less, in general, exhibited low crack densities at 36 months of age. For example, 30 of the 34 (88%) decks with a paste content of 27.2% or less and no crack-reducing technologies had a crack density below 0.3 m/m^2. The probability of low cracking is further increased for those with paste contents of 26.5% or less: 25 out of the 27 (93%) these decks had crack densities below 0.3 m/m^2. Decks without crack-reducing technologies with paste contents greater than 27.3%, on the other hand, had a much higher probability of exhibiting high crack densities at 36 months of age. For example, 8 out of the 11 (73%) decks without crack-reducing technologies with paste contents higher than 27.3% had crack densities above 0.4 m/m^2. Th paste content of the concrete mixture used in bridge decks clearly appears to be a major, if not the major, governing factor on bridge deck cracking. A paste content of 26.5% or less greatly increases the likelihood that the deck will exhibit low crack density.

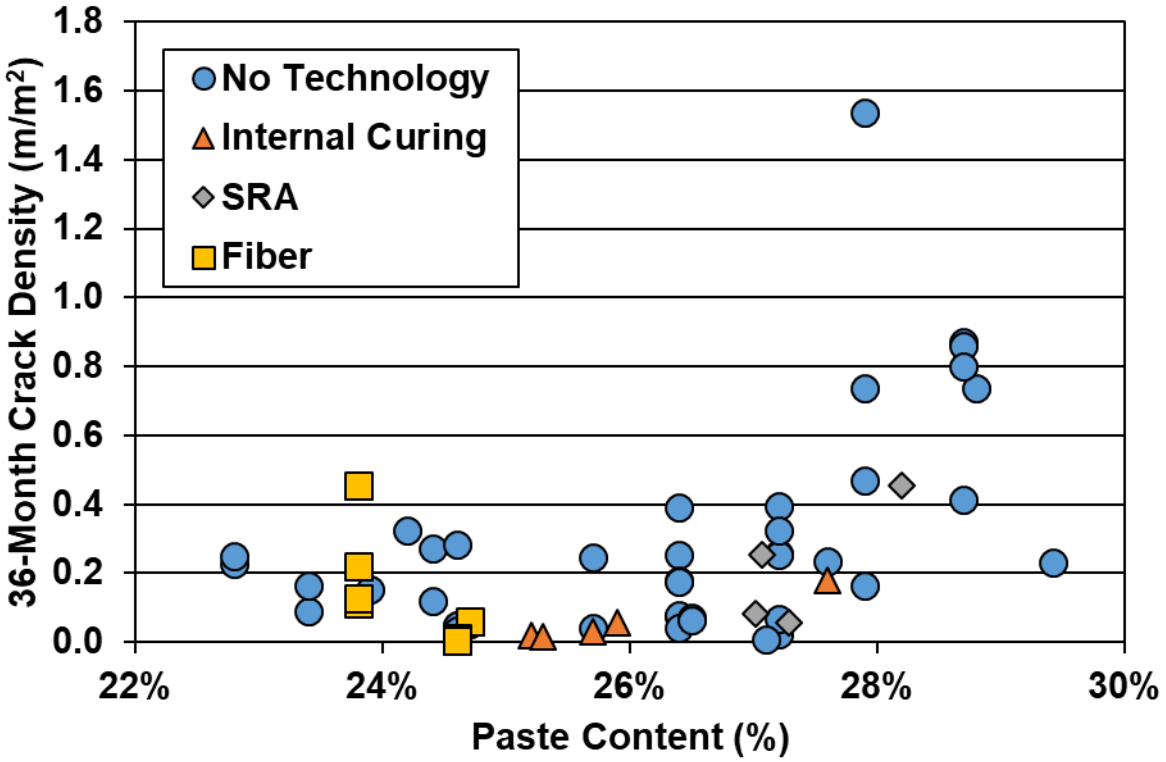

Figure 4.5 – Paste content versus 36-month crack density for all bridges involved in this study

4.4.2 Influence of Crack-Reducing Technologies

Compared to paste content, the use of crack-reducing technologies is a secondary factor in bridge deck cracking. As shown in Figure 4.5, in general, the crack densities of bridge decks with IC, SRAs, or fiber reinforcement are generally, but not totally, comparable to those of decks without these technologies with similar paste contents, indicating that these technologies have less effect on the cracking performance of bridge decks. The influence of each crack reducing technology on bridge deck cracking is analyzed separately in this section.

4.4.2.1 Shrinkage-Reducing Admixtures

Figure 4.6 compares the average 36-month crack densities of bridge decks with and without an SRA. The decks with SRAs are divided into two groups: three decks with paste contents between 27.0% and 27.3% [VA-SRA (Low Paste)] and one deck with a high paste content of

28.2% (VA-SRA-1). The deck without an SRA in Virginia (VA-Control) has a high paste content, 29.4%. The average 36-month crack density of the decks in Kansas with no SRA are also included; the decks with paste contents higher than 27.3% are categorized as high paste content [KS-W/O SRA (High Paste)] and those with 27.3% or lower paste contents are designated as low paste content [KS-W/O SRA (Low Paste)]. Error bars indicate the ranges of the crack densities for each bridge deck type.

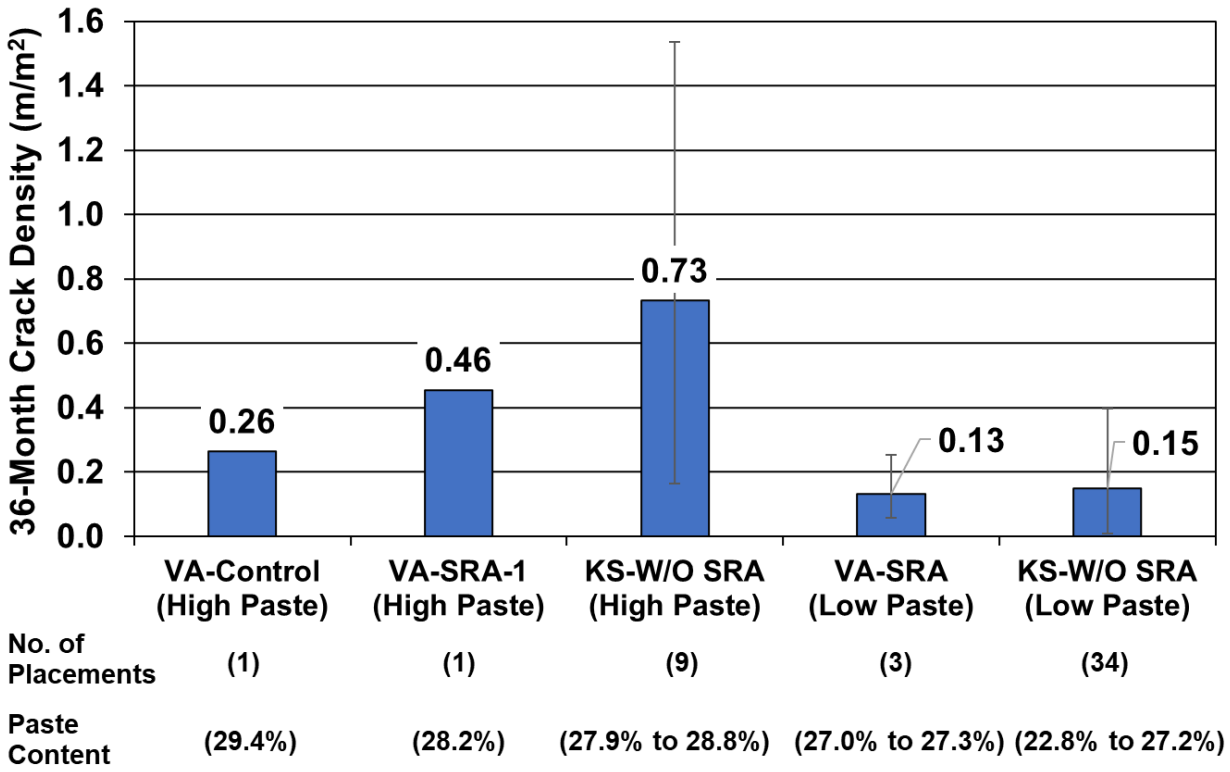

Figure 4.6 – Crack densities of bridges decks with and without SRAs. [a] includes the nine Conventional decks with paste contents of 27.9% or higher in Table 4.3. [b] includes the three deck placements in Virginia with SRAs and paste contents of 27.3% or lower in Table 4.1. [c] includes the 18 Conventional deck placements with paste contents of 27.2% or lower in Table 4.3, the 13 LC-HPC deck placements with no construction issues in Table 4.4, and the three control decks paired with fiber decks with no construction issues in Table 4.1.

The bridge decks with high paste contents (higher than 27.3%), including those with SRAs, showed remarkably higher average crack densities at 36 months of age compared to those with

27.3% or lower paste contents. The average 36-month crack densities of the decks with 27.3% or lower paste contents, VA-SRA (Low Paste) and KS-W/O SRA (Low Paste), were 0.13 and 0.15 m/m^2, respectively, noticeably lower than those of the decks with paste contents higher than 27.3%, VA-Control, VA-SRA-1, and KS-W/O SRA (High Paste), which were 0.26, 0.46, and 0.73 m/m^2, respectively. Using concrete mixtures with low paste contents proves to be the most effective way to reduce bridge deck cracking.

Among bridge decks with similar paste contents, those with SRAs tend to show lower crack densities, although the differences in their crack densities are small. As shown in Figure 4.6, while the SRA deck with a high paste content showed a higher crack density than the deck without SRA in Virginia (0.46 vs. 0.26 m/m^2), its crack density was lower than the average of the decks with paste contents higher than 27.3% and without an SRA in Kansas [KS-W/O SRA (High Paste), 0.73 m/m^2]. Similarly, among the two groups of decks with paste contents of 27.3% or lower, the group with an SRA had a lower average 36-month crack density (0.13 m/m^2) compared to the group without SRAs (0.15 m/m^2); this difference, however, is not statistically significant (p = 0.82).

It has been reported that SRAs can reduce drying shrinkage of concrete by over 50%, delaying the initiation of cracking and reducing the crack width by over 80% in restrained shrinkage tests (Shah et al. 1992, Folliard and Berke 1997, Nmai et al. 1998, Lindquist et al. 2008). The survey results presented in this study, however, show that the effectiveness of SRAs in reducing cracking of bridge decks is much subtler than what has been shown in laboratory tests, and the influence of SRAs on the cracking performance of bridge decks is minor compared to that of paste content.

4.4.2.2 Internal Curing

The crack densities of bridge decks with or without internal curing are compared in Figure 4.7. The decks in Indiana with internal curing are divided into two groups: five with 25.9% or lower paste contents [IN-IC (Low Paste)] and one with a higher paste content (27.6%, IN-IC-1). Three groups of decks without internal curing are included: one deck in Indiana with a high paste content (27.6%, IN-Control), nine decks in Kansas with high paste contents [27.9% to 28.8%, labelled "KS-W/O IC (High Paste)"], and 34 decks in Kansas with a low paste content [22.8% to 27.2%, labelled "KS-W/O IC (Low Paste)"].

As for comparison of decks with or without SRAs, paste content is the dominant factor affecting the crack density of bridge decks in these comparisons. The two Indiana decks with a high paste content (27.6%), one with and one without IC, have crack densities (0.18 and 0.24 m/m^2) higher than the average crack densities of the decks with low paste contents [IN-IC- (Low Paste), 0.03 m/m^2, and KS-W/O IC (Low Paste), 0.15 m/m^2]. The two Indiana decks with high paste contents, however, have lower crack densities than the decks with high paste contents in Kansas, likely due to their lower paste content compared with the Kansas decks (27.6% vs. 27.9% to 28.8%). In addition, between the two, the deck with IC had the lower crack density, and they both had densities below 0.30 m/m^2.

When comparing bridge decks with similar paste contents, the decks with internal curing consistently had lower 36-month crack densities than these without IC. Among the three groups of decks with high paste contents, the one with internal curing (IN-IC-1) had a crack density of 0.18 m/m^2, lower than that of the deck without IC in Indiana (IN-Control, 0.24 m/m^2) (note that both have densities below 0.30 m/m^2) and the average of the decks without IC and with high paste contents in Kansas [KS-W/O IC (High Paste), 0.73 m/m^2]. The same observation can be made in

reference to the two groups with low paste contents; decks with internal curing and low paste contents [IN-IC (Low Paste)] had an average 36-month crack density of 0.03 m/m^2, clearly lower than that of the decks without IC [KS-W/O IC (Low Paste), 0.15 m/m^2], a difference that is statistically significant (p = 0.03).

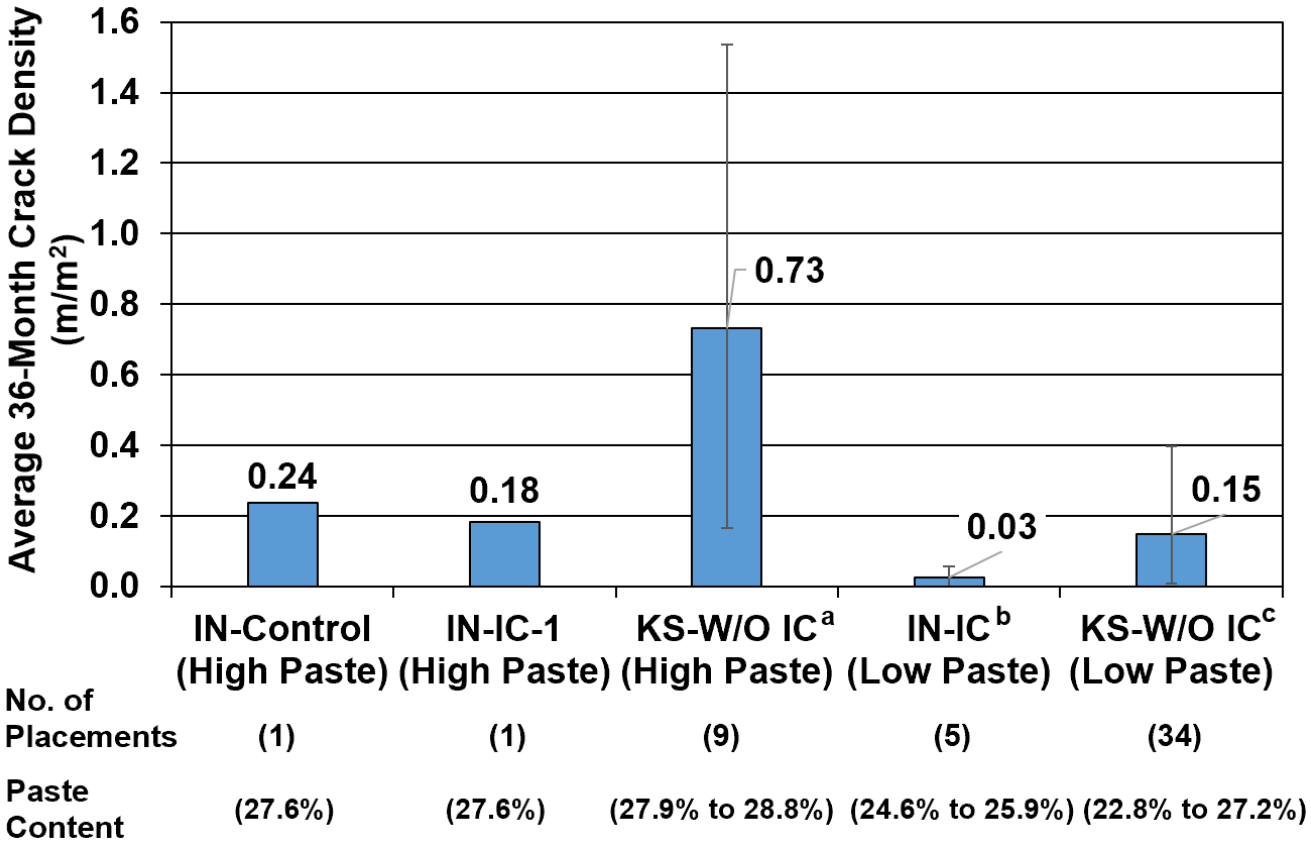

Figure 4.7 – Crack densities of bridge decks with or without internal curing. [a] includes the nine Conventional decks with paste contents of 27.9% or higher in Table 4.3. [b] includes the five deck placements in Indiana with internal curing and paste contents of 25.9% or lower in Table 4.2. [c] includes the 18 Conventional deck placements with paste contents of 27.2% or lower in Table 4.3, the 13 LC-HPC deck placements with no construction issues in Table 4.4, and the three control decks paired with fiber decks with no construction issues in Table 4.1.

4.4.3 Influence of Construction Practices

Figure 4.8 compares the average 36-month crack densities of bridge decks, including the decks with FRC, their associated control decks, and the LC-HPC decks (Tables 4.1 and 4.4), all

without FRC, whose construction was observed by KU researchers. All of the decks have low paste contents (22.2% to 24.7%), and if not for the use of poor construction practices, should exhibit low cracking. The decks labelled "good construction" were built without noticeable issues during construction (decks labelled "no issue" in Tables 4.1 and 4.4); the decks labelled "poor construction" were constructed using problematic procedures (decks labelled "loss of consolidation," "insufficient consolidation," or "excessive finishing" in Tables 4.1 and 4.4).

As shown in Figure 4.8, poor construction practices are associated with substantially increased cracking (likely caused by settlement of concrete, as discussed in Section 4.2). This is true for bridge decks constructed both with and without fiber reinforcement. For bridge decks with fiber reinforcement, those with bad construction practices exhibited a much higher average crack density than the fiber decks without construction issues (0.48 m/m^2 vs 0.14 m/m^2, p = 0.02). A similar observation can be made about the decks without fiber reinforcement: poor construction practices resulted in a drastically increased average crack density (0.54 m/m^2 vs 0.13 m/m^2, p = 9.3×10^{-5}).

Additionally, the negative impact of poor construction practices cannot be fully overcome by either a low paste content or fiber reinforcement. This is illustrated by the similar crack densities of the decks with poor construction practices and with or without FRC (0.48 m/m^2 for the decks constructed with FRC and 0.54 m/m^2 for the decks constructed without FRC). Although the decks constructed with FRC have a lower average crack density, the difference between the two values is not statistically insignificant (p = 0.76). Laboratory tests (which usually involve proper consolidation) have shown that fiber reinforcement reduces the settlement of fresh concrete and the cracking due to settlement (Qi 2003, Al-Qassag et al. 2015); the survey results reported herein, however, showed that, when used in bridge decks, fiber reinforcement cannot overcome the

increased likelihood of settlement cracking due to poor construction practices. To reduce bridge deck cracking, it is, therefore, imperative that state departments of transportation work with contractors to improve construction practices.

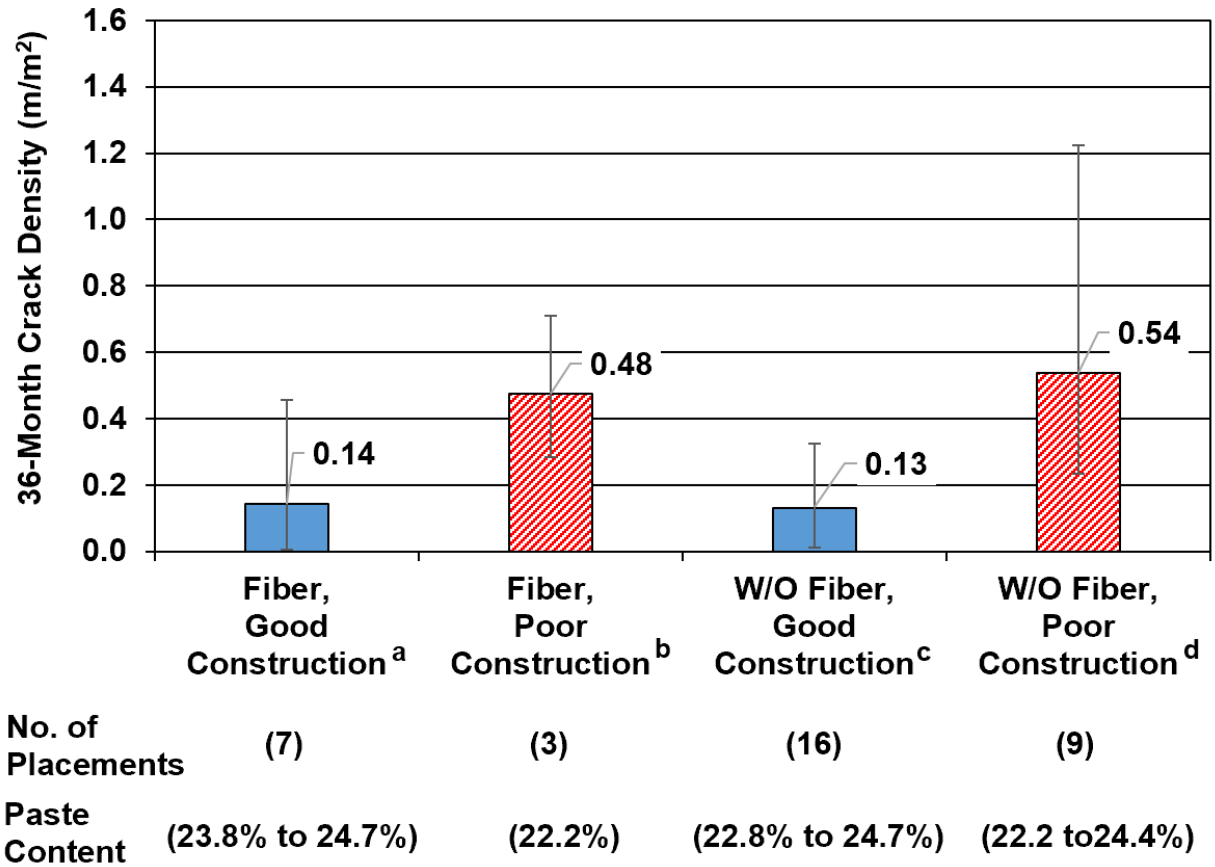

Figure 4.8 – Average crack densities of bridge decks with and without fiber and with good or bad construction. [a] includes the seven decks with FRC and no construction issues in Table 4.1. [b] includes the three decks with FRC and construction issues in Table 4.1. [c] includes the three decks without FRC and without construction issues in Table 4.1 and the 13 LC-HPC decks without construction issues in Table 4.4. [d] includes the three decks without FRC and with construction issues in Table 4.1 and the six LC-HPC decks with construction issues.

4.5 CONCLUSIONS

Crack densities at 36 months obtained from on-site surveys are studied for 74 bridge deck placements containing concrete mixtures with paste contents between 22.8% and 29.4%. Of the bridge deck placements studied, 20 were constructed with a crack-reducing technology (internal

curing, shrinkage-reducing admixtures, or fiber reinforcement) and 54 without; further, three of the decks with fiber reinforcement and nine of the decks without crack-reducing technologies had poor construction practices. The influence of paste content, crack-reducing technologies, and construction practices on bridge deck cracking at 36 months are quantitatively studied.

Based on the crack survey results, the following conclusions can be made:

1. The paste content of concrete mixtures is the paramount material factor affecting cracking in bridge decks. A paste content of 26.5% or lower noticeably increases the probability that a bridge deck will have good cracking performance. When a paste content higher than 27.3% is used, the bridge deck is more likely to exhibit a high crack density.
2. When used in conjunction with a low paste content, SRAs and IC can reduce cracking in bridge decks.
3. When contractors fail to follow proper procedures to consolidate, finish, or cure concrete, bridge decks will exhibit substantially greater cracking, even when a low paste content is used. Despite the use of concretes with low paste contents and crack-reducing technologies, departments of transportation should strictly regulate the procedures that contractors follow during construction to achieve low cracking in bridge decks.
4. While laboratory tests can provide some insight in the effectiveness of crack-reducing technologies, those tests do not fully reflect the cracking behavior of in-service bridge decks and cannot account for the impact of poor construction practices.

CHAPTER 5: SUMMARY, CONCLUSIONS, AND RECOMMENDATIONS

5.1 SUMMARY

The effects of crack-reducing technologies on the drying shrinkage and the durability in freezing and thawing environments of concrete mixtures are evaluated based on laboratory tests. The effectiveness of crack-reducing technologies in reducing cracking in bridge decks and the influence of construction practices on cracking are evaluated based on experience gained from construction and evaluation of bridge decks.

The laboratory portion of this study includes eleven concrete mixtures that are evaluated based on free shrinkage (using a modified version of ASTM C157 that involves measuring the length change of concrete specimens starting at 5½ ± ½ hour after casting), freeze-thaw durability (following ASTM C215, C666, and KTMR-22), and scaling resistance (following a modified version of the Quebec Test BNQ NQ 2621-900 that involves using an NaCl solution with a concentration of 2.5% instead of the standard 3%, making the test harsher). The free shrinkage test was performed on concrete mixtures with 100% portland cement and 0% or 6.5% internal curing water by weight of cement provided by pre-wetted lightweight aggregate, a mixture with a 30% volume replacement of cement with slag cement, a mixture with 30% and 3% volume replacements of cement with slag cement and silica fume, respectively, and mixtures with slag cement, silica fume, and 5.3%, 6.5%, or 9.7% internal curing water by weight of cementitious material; and the freeze-thaw durability and scaling resistance tests were performed on these mixtures plus four mixtures containing slag cement, silica fume, 6.5% internal curing water, and a shrinkage-reducing admixture (SRA) or one of two shrinkage-compensating admixtures (one of which contains an SRA).

The second portion of this study involves the field evaluation of cracking in bridge decks constructed with crack-reducing technologies [SRAs, fiber reinforcement, or internal curing (IC)] and bridge decks cast with or without proper construction procedures for consolidation, finishing, or curing. The field surveys were conducted between 2014 and 2018 on 21 bridge deck placements, 10 containing fiber-reinforced concrete (FRC), six associated control deck placements without fiber reinforcement, four bridge decks containing SRAs, and one control deck without an SRA. Additionally, crack densities 36 months after construction are used to evaluate 74 bridge deck placements, including the aforementioned 21 placements plus six placements containing internal curing (IC) and 47 without a crack-reducing technology. The bridge decks contained concrete mixtures with paste contents between 22.8% and 29.4%, and three of the decks with fiber reinforcement and nine of the decks without crack-reducing technologies had poor construction practices. The influence of paste content, crack-reducing technologies, and construction practices on bridge deck cracking at 36 months are studied quantitatively based on crack density.

5.2 CONCLUSIONS

The following conclusions are based on the results and analyses presented in this report.

5.2.1 Laboratory evaluations of shrinkage and durability of concrete mixtures with internal curing, shrinkage-reducing admixtures, and shrinkage-compensating admixtures

1. The combination of slag cement, silica fume, and internal curing reduces the shrinkage (negative strain) after 20 and 365 days of drying; and the shrinkage at 20 and 365 days of drying decreases as the quantity of internal curing water increases.
2. The mixtures with slag cement, silica fume, and internal curing shrank less in the first 20 days of drying but more between 20 and 365 days of drying compared to the mixture

with 100% portland cement or the mixtures with slag cement or slag cement and silica fume.

3. The mixtures with 100% portland cement and 0% or 6.5% internal curing water by weight of cement, as well as those with slag cement or slag cement and silica fume without internal curing water, performed satisfactorily in the scaling resistance and freeze-thaw durability tests.
4. The mixtures with slag cement, silica fume, and 5.3% or 6.5% internal curing water by weight of cementitious material performed satisfactorily in the freeze-thaw durability test but had mass losses exceeding the failure limit in the scaling resistance test, while the mixture with slag cement, silica fume, and 9.7% internal curing water (highest in this study) performed poorly in both tests. The scaling resistance test procedure used in this study was harsher than used in the standard method; given that the mass losses of mixtures with slag cement, silica fume, and 6.5% or 9.7% internal curing water [0.24 and 0.28 lb/ft^2 (1.2 and 1.4 kg/m^2), respectively] were close to the failure limit (0.2 lb/ft^2, or 1.0 kg/m^2), the mixtures may have performed adequately in a standard scaling test. The high mass loss observed for the mixture with slag cement, silica fume, and 5.3% internal curing water is likely explained by the mixture's relatively low air content (6.75% compared to 9.00 and 8.50% for the mixtures with 6.5% or 9.7% internal curing water, respectively).
5. When a shrinkage-reducing admixture, either by itself or as a component of a shrinkage-compensating admixture, is added to mixtures with slag cement, silica fume, and 6.5% internal curing water, the scaling resistance and freeze-thaw durability was drastically reduced; use of the CaO-based shrinkage-compensating admixture, which

did not contain an SRA, did not noticeably affect the scaling resistance or freeze-thaw durability of concrete mixtures, and the mixture with the CaO-based shrinkage-compensating admixture, slag cement, silica fume, and internal curing performed satisfactorily in this study.

5.2.2 Field Evaluations

5.2.2.1 Cracking performance of bridge decks containing synthetic fibers or shrinkage-reducing admixtures

1. The crack density of a bridge deck, in general, increases with age.
2. Cracks transverse to the direction of traffic are the most common. Near abutments, however, cracks usually initiate from and run perpendicular to the abutment.
3. When concrete mixtures with low paste contents and proper construction methods are used, the resulting bridge decks will show minimal cracking.
4. When poor construction practices are used, the resulting bridge decks will exhibit increased cracking.
5. If poor construction practices are used, the addition of fiber reinforcement may provide a slight reduction in cracking, but cannot overcome the negative effects of poor construction.
6. Shrinkage-reducing admixtures can reduce cracking in bridge decks if the paste content of the concrete mixture does not exceed 27.3%. SRAs cannot reduce cracking in bridge decks if the paste content is 28.2% or higher. No data are available for bridge decks with SRAs and paste contents between 27.3% and 28.2%.
7. In this study, the average widths of cracks ranged from 0.004 to 0.010 in. (0.10 to 0.25 mm).

8. The use of FRC and SRAs does not consistently reduce crack widths.

5.2.2.2 Factors affecting bridge deck cracking: crack-reducing technologies, paste content, and construction practices

5. The paste content of concrete mixtures is the paramount material factor affecting cracking in bridge decks. A paste content of 26.5% or lower increases the probability that a bridge deck will have good cracking performance. When a paste content higher than 27.3% is used, the bridge deck is more likely to exhibit a high crack density.
6. When used in conjunction with a low paste content, SRAs and IC can reduce cracking in bridge decks.
7. When contractors fail to follow proper procedures to consolidate, finish, or cure concrete, bridge decks will exhibit substantially greater cracking, even when a low paste content is used. Despite the use of concretes with low paste contents and crack-reducing technologies, departments of transportation should strictly regulate the procedures that contractors follow during construction to achieve low cracking in bridge decks.
8. While laboratory tests can provide some insight in the effectiveness of crack-reducing technologies, those tests do not fully reflect the cracking behavior of in-service bridge decks and cannot account for the impact of poor construction practices.

5.3 RECOMMENDATIONS

1. Concrete with the lowest paste content that is pumpable, workable, and can be easily consolidated should be used to minimize shrinkage-induced cracking. The paste content of concrete should not exceed 27.3%.

2. A low paste content in the concrete is necessary even when crack-reducing technologies (such as shrinkage-reducing admixtures and internal curing) are used. When the paste content is 27.3% or lower, crack-reducing technologies can be added to further reduce cracking in bridge decks.
3. Proper procedures to consolidate, finish, and cure concrete are necessary to achieve low cracking in bridge decks in addition to the use of low paste contents and crack-reducing technologies. Departments of transportation should closely regulate the construction practices used by contractors.
4. Concrete should be thoroughly consolidated to minimize cracking. Walking in concrete after consolidation should be strictly prohibited.
5. Excessive finishing and delayed application of curing should not be permitted.
6. Supplementary cementitious materials (such as slag cement and silica fume), internal curing, or shrinkage-compensating admixtures can be used, alone or in combinations, to reduce cracking. Laboratory tests, however, must be used to establish proper addition rates that ensure satisfactory freeze-thaw durability and scaling resistance of the resulting concrete mixtures. Shrinkage-reducing admixtures should not be used when supplementary cementitious materials and internal curing are used.

REFERENCES

ACI Committee 209. (2005). *Report on Factors Affecting Shrinkage and Creep of Hardened Concrete*, ACI 209.1R-05, American Concrete Institute, Farmington Hills, MI, 12 pp.

ACI Comittee 233 (2017). *Guide to the Use of Slag Cement in Concrete and Mortar*, ACI 233R-17, American Concrete Institute, Farmington Hills, MI, 36 pp.

ACI Comittee 305. (2010). *Guide to Hot Weather Concreting*, ACI 305R-10, American Concrete Institute, Farmington Hills, MI, 23 pp.

ACI Comittee 308. (2016). *Guide to External Curing of Concrete*, ACI 308R-16, American Concrete Institute, Farmington Hills, MI, 36 pp.

ACI Comittee 345. (2011). *Guide for Concrete Highway Bridge Deck Construction*, ACI 345R-11, American Concrete Institute, Farmington Hills, MI, 42pp.

ACI Committee 544. (2009). *State-of-the-Art Report on Fiber Reinforced Concrete*, ACI 544.1R-96 (Reapproved 2009), American Concrete Institute, Farmington Hills, MI, 66 pp.

ACI Committee 544. (2008). *Guide for Specifying, Proportioning, and Production of Fiber-Reinforced Concrete*, ACI 544.3R-08, American Concrete Institute, Farmington Hills, MI, 12pp.

ACI Committee 544. (2010). *Report on the Physical Properties and Durability of Fiber-Reinforced Concrete*, ACI 544.5R-10, American Concrete Institute, Farmington Hills, MI, 31 pp.

Aktan, H. M., Fu, G., Dekelbab, W., and Attanayaka, U. (2003). "Investigate Causes and Develop Methods to Minimize Early-Age Deck Cracking on Michigan Bridge Decks," *Research Report*, RC-1437, Wayne State University Center for Structural Duability, Detroit, MI, December, 364 pp.

Alhmood, A., Darwin, D., and O'Reilly, M. (2015). "Crack Surveys of Low-Cracking High-Performance Concrete Bridge Decks in Kansas 2014-2015," *SL Report*, No. 15-3, University of Kansas Center for Research, Inc., Lawrence, KS, September, 118 pp.

Al-Qassag, O., Darwin, D., and O'Reilly, M. (2015). "Effect of Synthetic Fibers and a Rheology Modifier on Settlement Cracking of Concrete," *SM Report*, No. 116, University of Kansas Center for Research, Inc., Lawrence, KS, December, 130 pp.

Altoubat, S., Yazdanbakhsh, A., Rieder, K. A. (2009). "Shear Behavior of Macro-Synthetic Fiber-Reinforced Concrete Beams without Stirrups," *ACI Materials Journal*, Vol. 106, Issue 4, July-August, pp. 381-389.

ASCE. (2018a). "The 2017 Report Card for America's Infrastructure," https://web.archive.org/web/20190319204635/https://www.infrastructurereportcard.org/cat-item/bridges/ (accessed March 19,2019).

ASCE. (2018b). "Report Card for Kansas' Infrastructure 2018," http://web.archive.org/web/20190319205124/https://www.infrastructurereportcard.org/wp-content/uploads/2016/10/ASCE-Report-Card-Kansas-FINAL-061318.pdf (accessed March 19, 2019).

Ardeshirilajimi, A., Wu, D.,Chaunsali, P., Mondal, P., Chen, Y. T., Rahman, M. M., Ibrahim, A., Lindquist, W., and Hindi, R. (2016). "Bridge Decks: Mitigation of Cracking and Increased Durability," *Research Report*, FHWA-ICT-16-016, Illinois Center for Transportation, Urbana, IL, June, 103 pp.

ASTM C1116/C1116M-10a (2015). "*Standard Specification for Fiber-Reinforced Concrete1*," ASTM International, West Conshohocken, PA, 7 pp.

ASTM C157/C157M-17 (2017). "*Standard Test Method for Length Change of Hardened Hydraulic-Cement Mortar and Concrete*," ASTM International, West Conshohocken, PA, 7 pp.

ASTM C1761/C1761M−17 (2017). "*Standard Specification for Lightweight Aggregate for Internal Curing of Concrete,*" ASTM International, West Conshohocken, PA, 8 pp.

ASTM C215-14 (2014). "*Standard Test Method for Fundamental Transverse, Longitudinal, and Torsional Resonant Frequencies of Concrete Specimens*," ASTM International, West Conshohocken, PA, 7 pp.

ASTM C666/C666M-15 (2015). "*Standard Test Method for Resistance of Concrete to Rapid Freezing and Thawing*," ASTM International, West Conshohocken, PA, 7 pp.

Babaei, K., and Fouladgar, A. M. (1997). "Solutions to Concrete Bridge Deck Cracking," *Concrete International*, Vol. 19, Issue 7, July, pp. 34-37.

Balaguru, P. N., and Ramakrishnan, V. (1986). "Freeze-Thaw Durablity of Fiber Reinforced Concrete," *ACI Journal Proceedings*, Vol. 83, Issue 3, May, pp. 374-382.

Banthia, N., and Gupta, R. (2004). "Hybrid Fiber Reinforced Concrete (HyFRC): Fiber Synergy in High Strength Matrices," *Materials and Structures*, Vol. 37, Issue 10, December, pp. 707-716.

Banthia, N., Majdzadeh, F., Wu, J., and Bindiganavile, V. (2014). "Fiber Synergy in Hybrid Fiber Reinforced Concrete (HyFRC) in Flexure and Direct Shear," *Cement and Concrete Composites*, Vol. 48, April, pp. 91-97.

Banthia, N. and Sheng, J. (1996). "Fracture Toughness of Micro-Fiber Reinforced Cement Composites," *Cement and Concrete Composites*, Vol. 18, Issue 4, April, pp. 251-269.

Bayasi, Z., and Zeng, J. (1993). "Properties of Polypropylene Fiber Reinforced Concrete," *ACI Materials Journal*, Vol. 90, No. 6, November-December, pp. 605-610.

Bella, C. D., Villani, C., Hausheer, E., and Weiss, J. (2012). "Chloride Transport Measurements for a Plain and Internally Cured Concrete Mixture," *ACI Special Publication*, Vol. 290, September, pp. 1-16.

Bentur, A., and Mindess, S. (2014). *Fibre Reinforced Cementitious Composites*, second edition, CRC Press, Boca Raton, FL, 624 pp.

Bentz, D. P., Garboczi, E. J., and Quenard, D. A. (1998). "Modelling Drying Shrinkage in Reconstructed Porous Materials: Application to Porous Vycor Glass," *Modelling and Simulation in Materials Science and Engineering*, Vol. 6, No. 3, pp. 211-236.

Bentz, D. P., Sant, G., and Weiss, J. (2008). "Early-Age Properties of Cement-Based Materials. I: Influence of Cement Fineness," *Journal of Materials in Civil Engineering*, Vol. 20, No. 7, July, pp. 502-508.

Bentz, D. P. (2009). "Influence of Internal Curing Using Lightweight Aggregates on Interfacial Transition Zone Percolation and Chloride Ingress in Mortars," *Cement and Concrete Composites*, Vol. 31, No. 5, pp. 285-289.

Bentz, D. P., & Weiss, W. J. (2011). "Internal Curing: A 2010 State-of-the-Art Review," NISTIR 7765, US Department of Commerce, National Institute of Standards and Technology, Gaithersburg, MD, Feburary, 82 pp.

Berke, N. S., Li, L., Hicks, M. C., and Bae, J. (2003). "Improving Concrete Performance with Shrinkage-Reducing Admixtures," *ACI Special Publication*, Vol. 217, pp. 37-50.

Berkowski, P., and Kosior-Kazberuk, M. (2015). "Effect of Fiber on the Concrete Resistance to Surface Scaling Due to Cyclic Freezing and Thawing," *Procedia Engineering*, Vol. 111, pp. 121-127.

Bilodeau, A., Fournier, B., Hooton, D., Gagné, R., Jolin, M., and Bouzoubaâ, N. (2008). "Deicing salt scaling resistance of concrete incorporating supplementary cementing materials: Laboratory and field test data," *Canadian Journal of Civil Engineering*, Vol. 35, pp. 1261-1275.

Bisschop, J., L. Pel, and J. G. M. Van Mier. (2001). "Effect of Aggregate Size and Paste Volume on Drying Shrinkage Microcracking in Cement-Based Composites," *Creep, Shrinkage & Durability Mechanics of Concrete and other Quasi-Brittle Materials*, Elsevier, pp. 75-80.

Bleszynski, R., Hooton, R. D., Thomas, M. D. A., and Rogers, C. A. (2002). "Durability of ternary blend concrete with silica fume and blast-furnace slag: Laboratory and outdoor exposure site studies," *ACI Materials Journal*, Vol. 99, Issue 5, September-October, pp. 499-508.

BNQ NQ2621-900 (2012). *Betons de masse volumique normale et constituants (Guide for Normal Density Concrete)*, Bureau de Normalisation du Québec (Bureau of Standardization of Quebec), Québec City, QC, Canada.

Bohaty, B., Elizabeth, R., and David, D. (2013). "Crack Surveys of Low-Cracking High-Performance Concrete Bridge Decks in Kansas 2011-2013," *SL Report*, No. 13-6, University of Kansas Center for Research, Inc., Lawrence, KS, December, 153 pp.

Boyd, A. J., and Hooton, R. D. (2007). "Long-Term Scaling Performance of Concretes Containing Supplementary Cementing Materials," *Journal of Materials in Civil Engineering*, Vol. 19, Issue 10, October, pp. 820-825.

Brooks, J. J., and Jiang, X. (1997). "The Influence of Chemical Admixtures on Restrained Drying Shrinkage of Concrete," *ACI Special Publication,* Vol. 173, September, pp. 249-266.

Brooks, J. J., and Johari, M. M. (2001). "Effect of Metakaolin on Creep and Shrinkage of Concrete," *Cement and concrete composites*, Vol. 23, Issue 6, December, pp. 495-502.

Brown, M. D., Smith, C. A., Sellers, J. G., Folliard, K. J., and Breen, J. E. (2007). "Use of Alternative Materials to Reduce Shrinkage Cracking in Bridge Decks," *ACI Materials Journal*, Vol. 104, Issue 6, November-December, pp. 629-637.

Browning, J., Darwin, D., Reynolds, D., and Pendergrass, B. (2011). "Lightweight Aggregate as Internal Curing Agent to Limit Concrete Shrinkage," *ACI Materials Journal*, Vol. 108, Issue 6, November-December, pp. 638-644.

Brown, M. D., Smith, C. A., Sellers, J. G., Folliard, K. J., and Breen, J. E. (2007). "Use of alternative materials to reduce shrinkage cracking in bridge decks," *ACI Materials Journal*, Vol. 104, Issue 6, November, pp. 629-637.

Cantin, R., and Pigeon, M. (1996). "Deicer Salt Scaling Resistance of Steel-Fiber-Reinforced Concrete," *Cement and Concrete Research*, Vol. 26, Issue 11, pp. 1639-1648.

Chindaprasirt, P., Homwuttiwong, S., and Sirivivatnanon, V. (2004). "Influence of Fly Ash Fineness on Strength, Drying Shrinkage and Sulfate Resistance of Blended Cement Mortar," *Cement and Concrete Research*, Vol. 34, Issue 7, July, pp. 1087-1092.

Choi, S. (2017). "Internal Relative Humidity and Drying Shrinkage of Hardening Concrete Containing Lightweight and Normal-Weight Coarse Aggregates: a Comparative Experimental Study and Modeling," *Construction and Building Materials*, Vol. 148, September, pp. 288-296.

Cope, B. L., and Ramey, G. E. (2001). "Reducing Drying Shrinkage of Bridge-Deck Concrete," *Concrete International*, Vol. 23, Issue 08, August, pp. 76-82.

Dakhil, F. H., Cady, P. D., and Carrier, R. E. (1975). "Cracking of Fresh Concrete as Related to Reinforcement," *ACI Journal Proceedings*, Vol. 72, Issue 8, August, pp. 421-428.

Darwin, D., Browning, J., Lindquist, W., McLeod, H., Yuan, J., Toledo, M., and Reynolds, D. (2010). "Low-Cracking, High-Performance Concrete Bridge Decks: Case Studies over First 6 Years," *Transportation Research Record: Journal of the Transportation Research Board*, No. 2022, January, pp. 61-69.

Darwin, D., Browning, J., and Lindquist, W. D. (2004). "Control of Cracking in Bridge Decks: Observations from the Field," *Cement, Concrete and Aggregates*, Vol. 26, No. 2, December, pp. 1-7.

Darwin, D., Browning, J., McLeod, H., Lindquist, W., and Yuan, J. (2012). "Implementing Lessons Learned From Twenty Years of Bridge-Deck Crack Surveys," *ACI Special Publication*, Vol. 284, March, pp. 1-18.

Darwin, D., Khajehdehi, R., Alhmood, A., Feng, M., Lafikes, J., Ibrahim, E., and O'Reilly, M. (2016). "Construction of Crack-Free Bridge Decks: Final Report," *SM Report*, No. 121, University of Kansas Center for Research, Inc., Lawrence, KS, December, 160 pp.

Delatte, N., and Crowl, D. (2012). "Case Studies of Internal Curing of Bridge Decks in the Greater Cleveland Area," *ACI Special Publication*, Vol. 290, September, pp. 1-12.

Deshpande, S., Darwin, D., and Browning, J. (2007). "Evaluating Free Shrinkage of Concrete for Control of Cracking in Bridge Decks," *SM Report*, No. 89, University of Kansas Center for Research, Inc., Lawrence, KS, January,290 pp.

Donahey, R. C., and Darwin, D. (1985). "Bond of Top-Cast Bars in Bridge Decks," *ACI Journal Proceedings*, Vol. 82, Issue 1, January, pp. 57-66.

Du, L., and Folliard, K. J. (2005). "Mechanisms of Air Entrainment in Concrete," *Cement and Concrete Research*, Vol. 35, Issue 8, August, pp. 1463-1471.

Espinoza-Hijazin, G., and Lopez, M. (2011). "Extending Internal Curing to Concrete Mixtures with *w/c* Higher than 0.42," *Construction and Building Materials*, Vol. 25, Issue 3, March, pp. 1236-1242.

Fagerlund, G. (1975). "The Signifcance of Critical Degrees of Saturation at Freezing of Porous and Brittle Materials," *ACI Special Publication*, Vol. 47, January, pp. 13-66.

Fagerlund, G. (2004). "A Service Life Model for International Frost Damage in Concrete," *Report TVBM*, Vol. 3119, Division of Building Technology, Lund Institute of Technology, Lund, Sweden, 138 pp.

Ferluga, E., and Glassford, P. (2015). "Evaluation of Performance Based Concrete for Bridge Decks," *WSDOT Research Report*, WA-RD 845-1, Washington State Department of Transportation, Tumwater, WA, June, 295 pp.

Folliard, K. J., and Berke, N. S. (1997). "Properties of High-Performance Concrete Containing Shrinkage-Reducing Admixture," *Cement and Concrete Research*, Vol. 27, Issue 9, September, pp. 1357-1364.

Gopalaratnam, V. S., Shah, S. P., Batson, G., Criswell, M., Ramakishnan, V., and Wecharatana, M. (1991). "Fracture Toughness of Fiber Reinforced Concrete," *ACI Materials Journal*, Vol. 88, Issue 4, July, pp. 339-353.

Grasley, Z. C., Lange, D. A., and D'Ambrosia, M. D. (2006). "Internal Relative Humidity and Drying Stress Gradients in Concrete," *Materials and Structures*, Vol. 39, No. 9, Novenmber, pp. 901-909.

Güneyisi, E., Gesoğlu, M., Karaoğlu, S., and Mermerdaş, K. (2012). "Strength, Permeability, and Shrinkage Cracking of Silica Fume and Metakaolin Concretes," *Construction and Building Materials*, Vol. 34, September, pp. 120-130.

Hamoush, S., Taher, A. L., and Toney, C. (2010). "Deflection Behavior of Concrete Beams Reinforced with PVA Micro-Fibers," *Construction and Building Materials*, Vol. 24, Issue 11, November, pp. 2285-2293.

Hassanpour, M., Shafigh, P., and Mahmud, H. B. (2012). "Lightweight Aggregate Concrete Fiber Reinforcement–A Review," *Construction and Building Materials*, Vol. 37, December, pp. 452-461.

Hooton, R. D., Stanish, K., and Prusinski, J. (2009), "The Effect of Ground Granulated Blast Furnace Slag (Slag Cement) on the Drying Shrinkage of Concrete–A Critical Review of the Literature," *ACI Special Publication*, Vol. 263, October, pp. 79-94.

Hwang, S.-D., Khayat, K. H., and Youssef, D. (2013). "Effect of Moist Curing and Use of Lightweight Sand on Characteristics of High-Performance Concrete," *Materials and Structures*, Vol. 46, Issue 1, January, pp. 35-46.

Ibrahim, E., Darwin, D., and O'Reilly, M. (2019). "Effect of Crack-Reducing Technologies and Supplementary Cementitious Materials on Settlement Cracking of Plastic Concrete and Durability Performance of Hardened Concrete," *SM Report*, No. 134, University of Kansas Center for Research, Inc., Lawrence, KS, September, 294 pp.

Ideker, J. H. and Bañuelos, J. (2014). "The Use of Synthetic Blended Fibers to Reduce Cracking Risk in High Performance Concrete," *Final Report*, SRS 500-620, Oregon Department of Transportation Research Section, Salem, OR, September 2014, 68 pp.

Imamoto, K., and Arai, M. (2008). "Specific Surface Area of Aggregate and Its Relation to Concrete Drying Shrinkage," *Materials and Structures*, Vol. 41, Issue 2, March, pp. 323-333.

Jones, W., and Weiss, W. (2015). "Freezing and Thawing Behavior of Internally Cured Concrete," *Advances in Civil Engineering Materials*, Vol. 4, Issue 1, pp. 144-155.

Jones, W. (2014). "Examining the Freezing and Thawing Behavior of Concretes with Improved Performance Through Internal Curing and Other Methods," *Thesis for Master of Science in Civil Engineering*, Purdue University, West Lafayette, Indiana, April, 170 pp.

Kansas Department of Transportation (2007). "Standard Specifications for State Road and Bridge Construction," Topeka, Kansas.

Khajehdehi, R. and Darwin, D. (2018). "Controlling Cracks in Bridge Decks," *SM Report*, No. 129, University of Kansas Center for Research, Inc., Lawrence, KS, December, 236 pp.

Khajehdehi, R., Feng, M., Darwin, D., Lafikes, J., Ibrahim, E., and O'Reilly, M. (2018). "Combined Effects of Internal Curing, SCMs, and Expansive Additives on Concrete Shrinkage," *Advances in Civil Engineering Materials*, Vol. 7, Issue 4, 7 pp.

Khayat, K. H., and Mehdipour, I. (2017). "Economical and Crack-Free High-Performance Concrete for Pavement and Transportation Infrastructure Construction," *Final Report*, cmr 17-007, Missouri University of Science and Technology, Rolla, MO, May, 219 pp.

Khayat, K. H., Meng, W., Valipour, M., and Hopkins, M. (2018). "Use of Lightweight Sand for Internal Curing to Improve Performance of Concrete Infrastructure," *Final Report,* cmr 18-005, Missouri University of Science and Technology, Rolla, MO, March, 92 pp.

Krauss, P. D., and Rogalla, E. A. (1996). "Transverse Cracking in Newly Constructed Bridge Decks," *National Cooperative Highway Research Program Report*, No. 380, Transportation Research Board, Washington, D.C., 126 pp.

KTMR-22 (2012). "*Resistance of Concrete to Rapid Freezing and Thawing*," Kansas Department of Transportation, Topeka, KS, 9pp.

Lafikes, J., Khajehdehi, R., Feng, M., O'Reilly, M., and Darwin, D. (2018). "Internal Curing and Supplementary Cementitious Materials in Bridge Decks," *SL Report*, No. 18-2, University of Kqnsas Center for Research, Inc., Lawrence, KS, April, 76 pp.

Lawler, J. S., Zampini, D., and Shah, S. P. (2005). "Microfiber and Macrofiber Hybrid Fiber-Reinforced Concrete," *Journal of Materials in Civil Engineering*, Vol. 17, No. 5, September-October, pp. 595-604.

Li, W., Pour-Ghaz, M., Castro, J., and Weiss, J. (2012). "Water Absorption and Critical Degree of Saturation Relating to Freeze-Thaw Damage in Concrete Pavement Joints," *Journal of Materials in Civil Engineering*, Vol. 24, No. 3, March-June, pp. 299-307.

Lindquist, W. D., Darwin, D., and Browning, J. (2008). "Development and Construction of Low-Cracking High-Performance Concrete (LC-HPC) Bridge Decks: Free Shrinkage, Mixture Optimization, and Concrete Production," *SM Report*, No. 92, University of Kansas Center for Research, Inc., Lawrence, KS, November, 540 pp.

Lindquist, W. D., Darwin, D., and Browning, J. P. (2005). "Cracking and Chloride Contents in Reinforced Concrete Bridge Decks," *SM Report*, No. 78, University of Kansas Center for Research, Inc., Lawrence, KS, Feburary, 482 pp.

Lindquist, W. D., Darwin, D., Browning, J., McLeod, H. A. K., Yuan, J., and Reynolds, D. (2015). "Implementation of Concrete Aggregate Optimization," *Construction and Building Materials*, Vol. 74, January, pp. 49-56.

Lindquist, W. D., Darwin, D., Browning, J. P., and Miller, G. G. (2006). "Effect of Cracking on Chloride Content in Concrete Bridge Decks," *ACI Materials Journal*, Vol. 103, Issue 6, November-December, pp. 467-473.

Litvan, G. G. (1970). "Freezing of Water in Hydrated Cement Paste," *Research Paper*, No. 446, National Research Council of Canada, Ottawa, ON, Canada, July, 8 pp.

Lloyd, S. (2014). "Steel Fibers in Concrete Floor Slabs," *Concrete International*, Vol. 36, Issue 2, Feburary, pp. 47-49.

Mazzoli, A., Monosi, S., and Plescia, E. S. (2015). "Evaluation of the early-age-shrinkage of Fiber Reinforced Concrete (FRC) using image analysis methods," *Construction and Building Materials*, Vol. 101, December, pp. 596-601.

McLeod, H. A. K., Darwin, D., and Browning, J. (2009). "Development and Construction of Low-Cracking High-Performance Concrete (LC-HPC) Bridge Decks: Construction Methods, Specifications, and Resistance to Chloride Ion Penetration," *SM Report*, No. 94, University of Kansas Center for Research, Inc., Lawrence, KS, September, 848 pp.

Medjigbodo, G., Rozière, E., Charrier, K., Izoret, L., and Loukili, A. (2018). "Hydration, Shrinkage, and Durability of Ternary Binders Containing Portland Cement, Limestone Filler and Metakaolin," *Construction and Building Materials*, Vol. 183, September, pp. 114-126.

Mehta, P. K. and Monteiro, P. J. M. (2006). *Concrete: Microstructure, Properties, and Materials*, third edition, McGraw-Hill Companies, Inc., New York, NY, 704 pp.

Menzel, C. A. (1954). "Causes and Prevention of Crack Development in Plastic Concrete," *Proceedings, Portland Cement Association Annual Meeting*, SP-249-8, pp. 130-136.

Miller, G. G., and Darwin, D. (2000). "Performance and Constructability of Silica Fuse Bridge Deck Overlays," *SM Report*, No. 57, University of Kansas Center for Research, Inc., Lawrence, KS, January, 444 pp.

Mindess, S., Young, J. F., and Darwin, D. (2003). *Concrete*, second edition, Prentice-Hall, Inc., Englewood Cliffs, NJ, 644 pp.

Minnesota Department of Transportation (2018). "Standard Specifications for Construction," St. Paul, Minnesota.

Myers, D. (2005). *Surfactant Science and Technology*, third edition, John Wiley & Sons, Inc., New Jersy, NJ, 393 pp.

Naaman, A. E., Wongtanakitcharoen, T., and Hauser, G. (2005). "Influence of Different Fibers on Plastic Shrinkage Cracking of Concrete," *ACI Materials Journal*, Vol. 102, Issue 1, January-Feburary, pp. 49-58.

Nanni, A., Ludwig, D. A., and McGillis, M. T. (1993). "Plastic Shrinkage Cracking of Restrained Fiber-Reinforced Concrete," *Transportation Research Record*, Issue 1382, Washington, D.C., July, pp. 69-72.

Neville, A. (1964). "Creep of Concrete as a Function of its Cement Paste Content," *Magazine of concrete Research*, Vol. 16, Issue 46, May, pp. 21-30.

Nmai, C., Tomita, R., F., H., and Buffenbarger, J. (1998). "Shrinkage-Reducing Admixtures," *Concrete International*, Vol. 20, Issue 4, April, pp. 31-37.

NRMCA (1960). "Plastic Cracking of Concrete," *Engineering Information*, CIP-5, National Ready Mixed Concrete Association, Silver Spring, MD, July, 2 pp.

Ohio Department of Transportation (2016). "Construction and Materials Specification," Columbus, Ohio

Pease, B. (2010). "Influence of Concrete Cracking on Ingress and Reinforcement Corrosion," *PhD Thesis*, Technical University of Denmark, Department of Civil Engineering, December, 298 pp.

Pendergrass, B., and Darwin, D. (2014). "Low-Cracking High-Performance Concrete (LC-HPC) Bridge Decks: Shrinkage-Reducing Admixtures, Internal Curing, and Cracking Performance," *SM Report*, No. 107, University of Kansas Center for Research, Inc., Lawrence, KS, Feburary, 664 pp.

Pendergrass, B., Darwin, D., Feng, M., and Khajehdehi, R. (2017). "Compatibility of Shrinkage-Reducing and Air-Entraining Admixtures," *ACI Materials Journal*, Vol. 114, Issue 5, September-October, pp. 809-818.

Pendergrass, B., Darwin, D., Khajehdehi, R., and Feng, M. (2018). "Effects of Internal Curing, Slag, and Silica Fume on Concrete Shrinkage," *ACI Materials Journal*, Vol. 115, No. 4, pp. 585-593.

Pickett, G. (1956). "Effect of Aggregate on Shrinkage of Concrete and a Hypothesis Concerning Shrinkage," *ACI Journal Proceedings*, Vol. 52, Issue. 1, January, pp. 581-590.

Polley, G., Feng, M., Khajehdehi, R., Alhmood, A., Al-Qassag, O., and Darwin, D. (2015). "Use of Shrinkage Reducing Admixtures and Lightweight Concrete in Virginia Bridge Decks - 2014," *SL Report*, No. 15-1, The University of Kansas Center for Research, Inc., Lawrence, KS, January, 74 pp.

Powers, T. C. and Helmuth, R. A. (1953). "Theory of Volume Changes in Hardened Portland-Cement Paste During Freezing," *Proceedings, Highway Research Board Annual Meeting*, Vol. 32, Highway Research Board, August, pp. 285-297.

Purvis, R., Babei, K., Udani, N., Qanbari, A., and Williams, W. (1995). "Premature Cracking of Concrete Bridge Decks: Causes and Methods of Prevention," *Proceedings of the 4th International Bridge Engineering Conference*, Washington, DC, 13 pp.

Qi, C. (2003). "Quantitative assessment of plastic shrinkage cracking and its impact on the corrosion of steel reinforcement," *Thesis for Doctor of Philosophy*, Purdue University, West Lafayette, Indiana, May, 24 pp

Qi, C., Weiss, J., and Olek, J. (2003). "Characterization of Plastic Shrinkage Cracking in Fiber Reinforced Concrete Using Image Analysis and a Modified Weibull Function," *Materials and Structures*, Vol. 36, No. 6, July, pp. 386-395.

Qian, C. X., and Stroeven, P. (2000). “Development of Hybrid Polypropylene-Steel Fibre-Reinforced Concrete,” *Cement and Concrete Research*, Vol. 30, Issue 1, January, pp. 63-69.

Quiroga, P. N., and Fowler, D. W. (2003). “The Effects of the Aggregates Characteristics on the Performance of Portland Cement Concrete,” *Research Report*, ICAR 104-1F, University of Texas at Austin International Center for Aggregates Research, Austin, TX, December, 383 pp.

Radlińska, A., and Weiss, J. (2012). “Toward the Development of a Performance-Related Specification for Concrete Shrinkage,” *Journal of Materials in Civil Engineering*, Vol 24, Issue 1, Janurary, pp. 64-71.

Rajabipour, F., Sant, G., and Weiss, J. (2008). "Interactions between Shrinkage Reducing Admixtures (SRA) and Cement Paste's Pore Solution," *Cement and Concrete Research*, Vol. 38, Issue 5, May, pp. 606-615.

Rajabipour, F., Wright, J., Laman, J., Radlińska, A., Morian, D., Jahangirnejad, S., and Cartwright, C. (2012). “Longitudinal Cracking in Concrete at Bridge Deck Dams on Structural Rehabilitation Projects,” *Final Project Report*, FHWA-PA-2012-006-100303. Pennsylvania State University Thomas D. Larson Pennsylvania Transportation Institute, University Park, PA, October, 223 pp.

Raoufi, K., Schlitter, J., Bentz, D., and Weiss, J. (2011). “Parametric Assessment of Stress Development and Cracking in Internally Cured Restrained Mortars Experiencing Autogenous Deformations and Thermal Loading,” *Advances in Civil Engineering*, Vol. 2011, Article ID 870128, 16 pp.

Reynolds, D., Browning, J., and Darwin, D. (2009). “Lightweight Aggregates as an Internal Curing Agent for Low-Cracking High-Performance Concrete,” *SM Report*, No. 97, University of Kansas Center for Research, Inc., Lawrence, KS, December, 159 pp.

Rodriguez, O. G., and Hooton, R. D. (2003). “Influence of Cracks on Chloride Ingress into Concrete,” *ACI Materials Journal*, Vol. 100, Issue 2, March-April, pp. 120-126.

Roesler, J. R., Altoubat, S. A., Lange, D. A., Rieder, K. A., and Ulreich, G. R. (2006). “Effect of Synthetic Fibers on Structural Behavior of Concrete Slabs-on-Ground,” *ACI Materials Journal*, Vol. 103, Issue 1, January-Feburary, pp. 3-10.

Russell, H. G. (2004). “Concrete Bridge Deck Performance,” *National Cooperative Highway Research Program Synthesis* 333, Transportation Research Board, Washington, D.C., October, 109 pp.

Şahmaran, M., Özbay, E., Yücel, H. E., Lachemi, M., and Li, V. C. (2012). “Frost Resistance and Microstructure of Engineered Cementitious Composites: Influence of Fly Ash and Micro Poly-Vinyl-Alcohol Fiber,” *Cement and Concrete Composites*, Vol. 34, Issue 2, Feburary, pp. 156-165.

Schemmel, J. J., Ray, J. C., and Kuss, M. L. (2000). "Impact of Shrinkage Reducing Admixture on Properties and Performance of Bridge Deck Concrete," *ACI Special Publication*,Vol. 189, January, pp. 367-386.

Schmitt, T. R., and Darwin, D. (1995). "Cracking in Concrete Bridge Decks," *SM Report*, No. 39, University of Kansas Center for Research, Inc., Lawrence, KS, April,164 pp.

Schmitt, T. R., and Darwin, D. (1999). "Effect of Material Properties on Cracking in Bridge Decks," *Journal of Bridge Engineering*, Vol. 4, Issue 1, Feburary, pp. 8-13.

Schramm, L. L. (2000). *Surfactants: Fundamentals and Applications in the Petroleum Industry*, first edition, Cambridge University Press, Cambridge, United Kingdom, 615 pp.

Scotta, R., and Giorgi, P. (2016). "Comparative Cyclic Tests of Exterior Flat Slab–Column Connections in Normal Concrete and Fiber-Reinforced Lightweight Aggregate Concrete," *Materials and Structures*, Vol. 49, Issue 10, October, pp. 4049-4067.

Shah, H. R., and Weiss, J. (2006). "Quantifying Shrinkage Cracking in Fiber Reinforced Concrete Using The Ring Test," *Materials and structures*, Vol. 39, No. 9, September, pp. 887-899.

Shah, S. P., Krguller, M. E., and Sarigaphuti, M. (1992). "Effects of Shrinkage-Reducing Admixtures on Restrained Shrinkage Cracking of Concrete," *ACI Materials Journal*, Vol. 89, Issue 3, May, pp. 289-295.

Silfwerbrand, J. L., and Farhang, A. A. (2014). "Reducing Crack Risk in Industrial Concrete Floors," *ACI Materials Journal*, Vol 111, Issue 6, November-December, pp. 681-690.

Streeter, D. A., Wolfe, W. H., and Vaughn, R. E. (2012). "Field Performance of Internally Cured Concrete Bridge Decks in New York State," *ACI Special Publication*, Vol. 290, September, pp. 1-16.

Swamy, R. N., and Stavrides, H. (1979). "Influence of Fiber Reinforcement on Restrained Shrinkage and Cracking," *Journal of American Concrete Institute*, Vol. 76, Issue 3, March, pp. 443-460.

Tosun-Felekoglu, K., and Felekoglu, B. (2013). "Effects of Fibre Hybridization on Multiple Cracking Potential of Cement-Based Composites Under Flexural Loading," *Construction and Building Materials*, Vol. 41, April, pp. 15-20.

Transportation Research Board (2006). "Control of Cracking in Concrete: State of the Art," *Transportation Research Circular*, E-C107, Basic Research and Emerging Technologies Related to Concrete Committee, Washington, DC, October, 56 pp.

Transportation Research Board (2007). *Guidelines for Concrete Mixtures Containing Supplementary* Cementitious Materials to Enhance Durability of Bridge Decks, The National Academies Press, Washington, DC, 130 pp.

Triandafilou, L. (2005). "Implementation of high-performance materials: When will they become standard?," *Transportation Research Record: Journal of the Transportation Research Board*, CD11-s, pp. 33-48.

Verbeck, G. J., and Klieger, P. (1957). "Studies of 'salt' scaling of concrete," *Highway Research Board Bulletin*, Vol. 150, pp. 13.

Virginia Department of Transportation (2016). "Road and Bridge Specification Book," Richmond, Virginia

Voigt, T., Bui, V. K., and Shah, S. P. (2004). "Drying Shrinkage of Concrete Reinforced with Fibers and Welded-Wire Fabric," *ACI Materials Journal*, Vol. 101, Issue 3, May-June, pp. 233-241.

Wei, Y., and Hansen, W. (2008). "Pre-soaked Lightweight Fine Aggregates as Additives for Internal Curing in Concrete," *ACI Special Publication*, Vol. 256, October, pp. 35-44.

Weiss, J., Couch, J., Pease, B., Laugesen, P., and Geiker, M. (2017). "Influence of Mechanically Induced Cracking on Chloride Ingress in Concrete," *Journal of Materials in Civil Engineering*, Vol. 29, No. 9, 04017128, 9 pp.

Weiss, J., Lura, P., Rajabipour, F., and Sant, G. (2008). "Performance of Shrinkage-Reducing Admixtures at Different Humidities and at Early Ages," *ACI Materials Journal*, Vol. 105, Issue 5, September-October, pp. 478-486.

West, M., Darwin, D., and Browning, J. (2010). "Effect of Materials and Curing Period on Shrinkage of Concrete," *SM Report*, No. 98, University of Kansas Center for Research, Inc., Lawrence, KS, January, 269 pp.

Yuan, J., Darwin, D., and Browning, J. (2011). "Development and Construction of Low-Cracking High-Performance Concrete (LC-HPC) Bridge Decks: Free Shrinkage Tests, Restrained Ring Tests, Construction Experience, and Crack Survey Results," *SM Report*. No. 103, University of Kansas Center for Research, Inc., Lawrence, KS, September, 505 pp.

Yuan, J., Lindquist, W., Darwin, D., and Browning, J. (2015). "Effect of Slag Cement on Drying Shrinkage of Concrete," *ACI Materials Journal*, Vol. 112, No. 2, March-April, pp. 267-276.

Zhutovsky, S., Kovler, K., and Brameshuber, W. "Combined Effect of Internal Curing and Shrinkage-Reducing Admixture on Cracking Potential of High-Strength Concrete," *Proc., International RILEM Conference on Material Science*, RILEM Publications SARL, pp. 165-174.

APPENDIX A: LOW-CRACKING HIGH-PERFORMANCE CONCRETE (LC-HPC) SPECIFICATIONS – AGGREGATES, CONCRETE, AND CONSTRUCTION

KANSAS DEPARTMENT OF TRANSPORTATION
SPECIAL PROVISION TO THE
STANDARD SPECIFICATIONS, 2007 EDITION

Add a new SECTION to DIVISION 1100:

LOW-CRACKING HIGH-PERFORMANCE CONCRETE – AGGREGATES

1.0 DESCRIPTION

This specification is for coarse aggregates, fine aggregates, and mixed aggregates (both coarse and fine material) for use in bridge deck construction.

2.0 REQUIREMENTS

a. Coarse Aggregates for Concrete.

(1) Composition. Provide coarse aggregate that is crushed or uncrushed gravel, chat, or crushed stone. (Consider calcite cemented sandstone, rhyolite, basalt and granite as crushed stone

(2) Quality. The quality requirements for coarse aggregate for bridge decks are in **TABLE 1-1**:

TABLE 1-1: QUALITY REQUIREMENTS FOR COARSE AGGREGATES FOR BRIDGE DECK

Concrete Classification	Soundness (min.)	Wear (max.)	Absorption (max.)	Acid Insol. (min.)
Grade 3.5 (AE) (LC-HPC) [1]	0.90	40	0.7	55

[1] Grade 3.5 (AE) (LC-HPC) – Bridge Deck concrete with select coarse aggregate for wear and acid insolubility.

(3) Product Control.

(a) Deleterious Substances. Maximum allowed deleterious substances by weight are:

- Material passing the No. 200 sieve (KT-2)..... 2.5%
- Shale or Shale-like material (KT-8)..... 0.5%
- Clay lumps and friable particles (KT-7) 1.0%
- Sticks (wet) (KT-35)..... 0.1%
- Coal (AASHTO T 113)..... 0.5%

(b) Uniformity of Supply. Designate or determine the fineness modulus (grading factor) according to the procedure listed in the Construction Manual Part V, Section 17 before delivery, or from the first 10 samples tested and accepted. Provide aggregate that is within ±0.20 of the average fineness modulus.

(4) Do not combine siliceous fine aggregate with siliceous coarse aggregate if neither meet the requirements of **subsection 2.0c.(2)(a)**. Consider such fine material, regardless of proportioning, as a Basic Aggregate that must conform to **subsection 2.0c**.

(5) Handling Coarse Aggregates.

(a) Segregation. Before acceptance testing, remix all aggregate segregated by transportation or stockpiling operations.

(b) Stockpiling.

- Stockpile accepted aggregates in layers 3 to 5 feet thick. Berm each layer so that aggregates do not "cone" down into lower layers.
- Keep aggregates from different sources, with different gradings, or with a significantly different specific gravity separated.
- Transport aggregate in a manner that insures uniform gradation.
- Do not use aggregates that have become mixed with earth or foreign material.

- Stockpile or bin all washed aggregate produced or handled by hydraulic methods for 12 hours (minimum) before batching. Rail shipment exceeding 12 hours is acceptable for binning provided the car bodies permit free drainage.
- Provide additional stockpiling or binning in cases of high or non-uniform moisture.

b. Fine Aggregates for Basic Aggregate in MA for Concrete.

(1) Composition.

(a) Type FA-A. Provide either singly or in combination natural occurring sand resulting from the disintegration of siliceous or calcareous rock, or manufactured sand produced by crushing predominately siliceous materials.

(b) Type FA-B. Provide fine granular particles resulting from the crushing of zinc and lead ores (Chat).

(2) Quality.

(a) Mortar strength and Organic Impurities. If the District Materials Engineer determines it is necessary, because of unknown characteristics of new sources or changes in existing sources, provide fine aggregates that comply with these requirements:

- Mortar Strength (Mortar Strength Test, KTMR-26). Compressive strength when combined with Type III (high early strength) cement:
  - At age 24 hours, minimum……..100%*
  - At age 72 hours, minimum……..100%*

  *Compared to strengths of specimens of the same proportions, consistency, cement and standard 20-30 Ottawa sand.
- Organic Impurities (Organic Impurities in Fine Aggregate for Concrete Test, AASHTO T 21). The color of the supernatant liquid is equal to or lighter than the reference standard solution.

(b) Hardening characteristics. Specimens made of a mixture of 3 parts FA-B and 1 part cement with sufficient water for molding will harden within 24 hours. There is no hardening requirement for FA-A.

(3) Product Control.

(a) Deleterious Substances.

- Type FA-A: Maximum allowed deleterious substances by weight are:
  - Material passing the No. 200 sieve (KT-2)……..……. 2.0%
  - Shale or Shale-like material (KT-8) ……. 0.5%
  - Clay lumps and friable particles (KT-7)……..……. 1.0%
  - Sticks (wet) (KT-35)……...…….…… 0.1%
- Type FA-B: Provide materials that are free of organic impurities, sulfates, carbonates, or alkali. Maximum allowed deleterious substances by weight are:
  - Material passing the No. 200 sieve (KT-2)…….……..... 2.0%
  - Clay lumps & friable particles (KT-7)……. 0.25%

(c) Uniformity of Supply. Designate or determine the fineness modulus (grading factor) according to the procedure listed in the Construction Manual Part V, Section 17 before delivery, or from the first 10 samples tested and accepted. Provide aggregate that is within ±0.20 of the average fineness modulus.

(4) Proportioning of Coarse and Fine Aggregate. Use a proven optimization method such as the Shilstone Method or the KU Mix Method.

Do not combine siliceous fine aggregate with siliceous coarse aggregate if neither meet the requirements of **subsection 2.0c.(2)(a)**. Consider such fine material, regardless of proportioning, as a Basic Aggregate and must conform to the requirements in **subsection 2.0c**.

(5) Handling and Stockpiling Fine Aggregates.

- Keep aggregates from different sources, with different gradings or with a significantly different specific gravity separated.
- Transport aggregate in a manner that insures uniform grading.
- Do not use aggregates that have become mixed with earth or foreign material.

- Stockpile or bin all washed aggregate produced or handled by hydraulic methods for 12 hours (minimum) before batching. Rail shipment exceeding 12 hours is acceptable for binning provided the car bodies permit free drainage.
- Provide additional stockpiling or binning in cases of high or non-uniform moisture.

c. Mixed Aggregates for Concrete.

(1) Composition.

(a) Total Mixed Aggregate (TMA). A natural occurring, predominately siliceous aggregate from a single source that meets the Wetting & Drying Test (KTMR-23) and grading requirements.

(b) Mixed Aggregate. A combination of basic and coarse aggregates that meet **TABLE 1-2**.

- Basic Aggregate (BA). Singly or in combination, a natural occurring, predominately siliceous aggregate that does not meet the grading requirements of Total Mixed Aggregate.

(c) Coarse Aggregate. Granite, crushed sandstone, chat, and gravel. Gravel that is not approved under **subsection 2.0c.(2)** may be used, but only with basic aggregate that meets the wetting and drying requirements of TMA.

(2) Quality.

(a) Total Mixed Aggregate.

- Soundness, minimum (KTMR-21) …….……0.90
- Wear, maximum (KTMR-25) ……..……50%
- Wetting and Drying Test (KTMR-23) for Total Mixed Aggregate
  Concrete Modulus of Rupture:
  - At 60 days, minimum…….550 psi
  - At 365 days, minimum…..……..……550 psi

  Expansion:
  - At 180 days, maximum…….……0.050%
  - At 365 days, maximum…….…….0.070%
- Aggregates produced from the following general areas are exempt from the Wetting and Drying Test:
  - Blue River Drainage Area.
  - The Arkansas River from Sterling, west to the Colorado state line.
  - The Neosho River from Emporia to the Oklahoma state line.

(b) Basic Aggregate.

- Retain 10% or more of the BA on the No. 8 sieve before adding the Coarse Aggregate. Aggregate with less than 10% retained on the No. 8 sieve is to be considered a Fine Aggregate described in **subsection 2.0b**. Provide material with less than 5% calcareous material retained on the ⅜" sieve.
- Soundness, minimum (KTMR-21)……..0.90
- Wear, maximum (KTMR-25)…….……50%
- Mortar strength and Organic Impurities. If the District Materials Engineer determines it is necessary, because of unknown characteristics of new sources or changes in existing sources, provide mixed aggregates that comply with these requirements:
  - Mortar Strength (Mortar Strength Test, KTMR-26). Compressive strength when combined with Type III (high early strength) cement:
    - At age 24 hours, minimum……..100%*
    - At age 72 hours, minimum……..100%*

      *Compared to strengths of specimens of the same proportions, consistency, cement and standard 20-30 Ottawa sand.
  - Organic Impurities (Organic Impurities in Fine Aggregate for Concrete Test, AASHTO T 21). The color of the supernatant liquid is equal to or lighter than the reference standard solution.

(3) Product Control.

(a) Size Requirement. Provide mixed aggregates that comply with the grading requirements in **TABLE 1-2**.

TABLE 1-2: GRADING REQUIREMENTS FOR MIXED AGGREGATES FOR CONCRETE BRIDGE DECKS												
Type	**Usage**	**Percent Retained on Individual Sieves - Square Mesh Sieves**										
		1½"	**1"**	**3/4"**	**1/2"**	**3/8"**	**No. 4**	**No. 8**	**No. 16**	**No. 30**	**No. 50**	**No. 100**
MA-4	Optimized for LC-HPC Bridge Decks*	0	2-6	5-18	8-18	8-18	8-18	8-18	8-18	8-15	5-15	0-5

*Use a proven optimization method, such as the Shilstone Method or the KU Mix Method.

Note: Manufactured sands used to obtain optimum gradations have caused difficulties in pumping, placing or finishing. Natural coarse sands and pea gravels used to obtain optimum gradations have worked well in concretes that were pumped.

(b) Deleterious Substances. Maximum allowed deleterious substances by weight are:

- Material passing the No. 200 sieve (KT-2)……..….. 2.5%
- Shale or Shale-like material (KT-8)……..……. 0.5%
- Clay lumps and friable particles (KT-7)…… 1.0%
- Sticks (wet) (KT-35)……..…… 0.1%
- Coal (AASHTO T 113)…..……..……. 0.5%

(c) Uniformity of Supply. Designate or determine the fineness modulus (grading factor) according to the procedure listed in the Construction Manual Part V, Section 17 before delivery, or from the first 10 samples tested and accepted. Provide aggregate that is within ±0.20 of the average fineness modulus.

(4) Handling Mixed Aggregates.

(a) Segregation. Before acceptance testing, remix all aggregate segregated by transit or stockpiling.

(b) Stockpiling.

- Keep aggregates from different sources, with different gradings or with a significantly different specific gravity separated.
- Transport aggregate in a manner that insures uniform grading.
- Do not use aggregates that have become mixed with earth or foreign material.
- Stockpile or bin all washed aggregate produced or handled by hydraulic methods for 12 hours (minimum) before batching. Rail shipment exceeding 12 hours is acceptable for binning provided the car bodies permit free drainage.
- Provide additional stockpiling or binning in cases of high or non-uniform moisture.

3.0 TEST METHODS

Test aggregates according to the applicable provisions of **SECTION 1117**.

4.0 PREQUALIFICATION

Aggregates for concrete must be prequalified according to **subsection 1101.2**.

5.0 BASIS OF ACCEPTANCE

The Engineer will accept aggregates for concrete base on the prequalification required by this specification, and **subsection 1101.4**.

KANSAS DEPARTMENT OF TRANSPORTATION
SPECIAL PROVISION TO THE
STANDARD SPECIFICATIONS 2007 EDITION

Add a new SECTION to DIVISION 400:

LOW-CRACKING HIGH-PERFORMANCE CONCRETE

1.0 DESCRIPTION

Provide the grades of low-cracking high-performance concrete (LC-HPC) specified in the Contract Documents.

2.0 MATERIALS

Coarse, Fine & Mixed Aggregate ..... **07-PS0165, latest version**
Admixtures ..... **DIVISION 1400**
Cement ..... **DIVISION 2000**
Water ..... **DIVISION 2400**

3.0 CONCRETE MIX DESIGN

a. General. Design the concrete mixes specified in the Contract Documents.

Provide aggregate gradations that comply with **07-PS0165, latest version** and Contract Documents.

If desired, contact the DME for available information to help determine approximate proportions to produce concrete having the required characteristics on the project.

Take full responsibility for the actual proportions of the concrete mix, even if the Engineer assists in the design of the concrete mix.

Submit all concrete mix designs to the Engineer for review and approval. Submit completed volumetric mix designs on KDOT Form No. 694 (or other forms approved by the DME).

Do not place any concrete on the project until the Engineer approves the concrete mix designs. Once the Engineer approves the concrete mix design, do not make changes without the Engineer's approval.

Design concrete mixes that comply with these requirements:

b. Air-Entrained Concrete for Bridge Decks. Design air-entrained concrete for structures according to **TABLE 1-1**.

TABLE 1-1: AIR ENTRAINED CONCRETE FOR BRIDGE DECKS

Grade of Concrete Type of Aggregate (SECTION 1100)	lb of Cementitious per cu yd of Concrete, min/max	lb of Water per lb of Cementitious*	Designated Air Content Percent by Volume**	Specified 28-day Compressive Strength Range, psi
Grade 3.5 (AE) (LC-HPC)				
MA-4	500 / 540	0.44 – 0.45	8.0 ± 1.0	3500 – 5500

*Limits of lb. of water per lb. of cementitious. Includes free water in aggregates, but excludes water of absorption of the aggregates. With approval of the Engineer, may be decreased to 0.43 on-site.

**Concrete with an air content less than 6.5% or greater than 9.5% shall be rejected. The Engineer will sample concrete for tests at the discharge end of the conveyor, bucket or if pumped, the piping.

c. Portland Cement. Select the type of portland cement specified in the Contract Documents. Mineral admixtures are prohibited for Grade 3.5 (AE) (LC-HPC) concrete.

d. Design Air Content. Use the middle of the specified air content range for the design of air-entrained concrete.

e. Admixtures for Air-Entrainment and Water Reduction. Verify that the admixtures used are compatible and will work as intended without detrimental effects. Use the dosages recommended by the admixture manufacturers to determine the quantity of each admixture for the concrete mix design. Incorporate and mix the admixtures into the concrete mixtures according to the manufacturer's recommendations.

Set retarding or accelerating admixtures are prohibited for use in Grade 3.5 (AE) (LC-HPC) concrete. These include Type B, C, D, E, and G chemical admixtures as defined by ASTM C 494/C 494M – 08. Do not use admixtures containing chloride ion (CL) in excess of 0.1 percent by mass of the admixture in Grade 3.5 (AE) (LC-HPC) concrete.

(1) Air-Entraining Admixture. If specified, use an air-entraining admixture in the concrete mixture. If another admixture is added to an air-entrained concrete mixture, determine if it is necessary to adjust the air-entraining admixture dosage to maintain the specified air content. Use only a vinsol resin or tall oil based air-entraining admixture.

(2) Water-Reducing Admixture. Use a Type A water reducer or a dual rated Type A water reducer – Type F high-range water reducer, when necessary to obtain compliance with the specified fresh and hardened concrete properties.

Include a batching sequence in the concrete mix design. Consider the location of the concrete plant in relation to the job site, and identify the approximate quantity, when and at what location the water-reducing admixture is added to the concrete mixture.

The manufacturer may recommend mixing revolutions beyond the limits specified in **subsection 5.0**. If necessary and with the approval of the Engineer, address the additional mixing revolutions (the Engineer will allow up to 60 additional revolutions) in the concrete mix design.

Slump control may be accomplished in the field only by redosing with a water-reducing admixture. If time and temperature limits are not exceeded, and if at least 30 mixing revolutions remain, the Engineer will allow redosing with up to 50% of the original dose.

(3) Adjust the mix designs during the course of the work when necessary to achieve compliance with the specified fresh and hardened concrete properties. Only permit such modifications after trial batches to demonstrate that the adjusted mix design will result in concrete that complies with the specified concrete properties.

The Engineer will allow adjustments to the dose rate of air entraining and water-reducing chemical admixtures to compensate for environmental changes during placement without a new concrete mix design or qualification batch.

f. Designated Slump. Designate a slump for each concrete mix design within the limits in **TABLE 1-2**.

• TABLE 1-2: DESIGNATED SLUMP*

Type of Work	**• Designated Slump (inches)**
Grade 3.5 (AE) (LC-HPC)	1 ½ - 3

* The Engineer will obtain sample concrete at the discharge end of the conveyor, bucket or if pumped, the piping.

If potential problems are apparent at the discharge of any truck, and the concrete is tested at the truck discharge (according to **subsection 6.0**), the Engineer will reject concrete with a slump greater than 3 ½ inches at the truck discharge, 3 inches if being placed by a bucket.

4.0 REQUIREMENTS FOR COMBINED MATERIALS

a. Measurements for Proportioning Materials.

(1) Cement. Measure cement as packed by the manufacturer. A sack of cement is considered as 0.04 cubic yards weighing 94 pounds net. Measure bulk cement by weight. In either case, the measurement must be accurate to within 0.5% throughout the range of use.

(2) Water. Measure the mixing water by weight or volume. In either case, the measurement must be accurate to within 1% throughout the range of use.

(3) Aggregates. Measure the aggregates by weight. The measurement must be accurate to within 0.5% throughout the range of use.

(4) Admixtures. Measure liquid admixtures by weight or volume. If liquid admixtures are used in small quantities in proportion to the cement as in the case of air-entraining agents, use readily adjustable mechanical dispensing equipment capable of being set to deliver the required quantity and to cut off the flow automatically when this quantity is discharged. The measurement must be accurate to within 3% of the quantity required.

b. Testing of Aggregates. Testing Aggregates at the Batch Site. Provide the Engineer with reasonable facilities at the batch site for obtaining samples of the aggregates. Provide adequate and safe laboratory facilities at the batch site allowing the Engineer to test the aggregates for compliance with the specified requirements.

KDOT will sample and test aggregates from each source to determine their compliance with specifications. Do not batch the concrete mixture until the Engineer has determined that the aggregates comply with the specifications. KDOT will conduct sampling at the batching site, and test samples according to the Sampling and Testing Frequency Chart in Part V. For QC/QA Contracts, establish testing intervals within the specified minimum frequency.

After initial testing is complete and the Engineer has determined that the aggregate process control is satisfactory, use the aggregates concurrently with sampling and testing as long as tests indicate compliance with specifications. When batching, sample the aggregates as near the point of batching as feasible. Sample from the stream as the storage bins or weigh hoppers are loaded. If samples can not be taken from the stream, take them from approved stockpiles, or use a template and sample from the conveyor belt. If test results indicate an aggregate does not comply with specifications, cease concrete production using that aggregate. Unless a tested and approved stockpile for that aggregate is available at the batch plant, do not use any additional aggregate from that source and specified grading until subsequent sampling and testing of that aggregate indicate compliance with specifications. When tests are completed and the Engineer is satisfied that process control is again adequate, production of concrete using aggregates tested concurrently with production may resume.

c. Handling of Materials.

(1) Aggregate Stockpiles. Approved stockpiles are permitted only at the batch plant and only for small concrete placements or for the purpose of maintaining concrete production. Mark the approved stockpile with an "Approved Materials" sign. Provide a suitable stockpile area at the batch plant so that aggregates are stored without detrimental segregation or contamination. At the plant, limit stockpiles of tested and approved coarse aggregate and fine aggregate to 250 tons each, unless approved for more by the Engineer. If mixed aggregate is used, limit the approved stockpile to 500 tons, the size of each being proportional to the amount of each aggregate to be used in the mix.

Load aggregates into the mixer so no material foreign to the concrete or material capable of changing the desired proportions is included. When 2 or more sizes or types of coarse or fine aggregates are used on the same project, only 1 size or type of each aggregate may be used for any one continuous concrete placement.

(2) Segregation. Do not use segregated aggregates. Previously segregated materials may be thoroughly re-mixed and used when representative samples taken anywhere in the stockpile indicated a uniform gradation exists.

(3) Cement. Protect cement in storage or stockpiled on the site from any damage by climatic conditions which would change the characteristics or usability of the material.

(4) Moisture. Provide aggregate with a moisture content of ± 0.5% from the average of that day. If the moisture content in the aggregate varies by more than the above tolerance, take whatever corrective measures are necessary to bring the moisture to a constant and uniform consistency before placing concrete. This may be accomplished by handling or manipulating the stockpiles to reduce the moisture content, or by adding moisture to the stockpiles in a manner producing uniform moisture content through all portions of the stockpile.

For plants equipped with an approved accurate moisture-determining device capable of determining the free moisture in the aggregates, and provisions made for batch to batch correction of the amount of water and the weight of aggregates added, the requirements relative to manipulating the stockpiles for moisture control will be waived. Any procedure used will not relieve the producer of the responsibility for delivery of concrete meeting the specified water-cement ratio and slump requirements.

Do not use aggregate in the form of frozen lumps in the manufacture of concrete.

(5) Separation of Materials in Tested and Approved Stockpiles. Only use KDOT Approved Materials. Provide separate means for storing materials approved by KDOT. If the producer elects to use KDOT Approved Materials for non-KDOT work, during the progress of a project requiring KDOT Approved Materials, inform the Engineer and agree to pay all costs for additional materials testing.

Clean all conveyors, bins and hoppers of unapproved materials before beginning the manufacture of concrete for KDOT work.

5.0 MIXING, DELIVERY, AND PLACEMENT LIMITATIONS

a. Concrete Batching, Mixing, and Delivery. Batch and mix the concrete in a central-mix plant, in a truck mixer, or in a drum mixer at the work site. Provide plant capacity and delivery capacity sufficient to maintain continuous delivery at the rate required. The delivery rate of concrete during concreting operations must provide for the proper handling, placing and finishing of the concrete.

Seek the Engineer's approval of the concrete plant/batch site before any concrete is produced for the project. The Engineer will inspect the equipment, the method of storing and handling of materials, the production procedures, and the transportation and rate of delivery of concrete from the plant to the point of use. The Engineer will grant approval of the concrete plant/batch site based on compliance with the specified requirements. The Engineer may, at any time, rescind permission to use concrete from a previously approved concrete plant/batch site upon failure to comply with the specified requirements.

Clean the mixing drum before it is charged with the concrete mixture. Charge the batch into the mixing drum so that a portion of the water is in the drum before the aggregates and cementitious. Uniformly flow materials into the drum throughout the batching operation. Add all mixing water in the drum by the end of the first 15 seconds of the mixing cycle. Keep the throat of the drum free of accumulations that restrict the flow of materials into the drum.

Do not exceed the rated capacity (cubic yards shown on the manufacturer's plate on the mixer) of the mixer when batching the concrete. The Engineer will allow an overload of up to 10% above the rated capacity for central-mix plants and drum mixers at the work site, provided the concrete test data for strength, segregation and uniform consistency are satisfactory, and no concrete is spilled during the mixing cycle.

Operate the mixing drum at the speed specified by the mixer's manufacturer (shown on the manufacturer's plate on the mixer).

Mixing time is measured from the time all materials, except water, are in the drum. If it is necessary to increase the mixing time to obtain the specified percent of air in air-entrained concrete, the Engineer will determine the mixing time.

If the concrete is mixed in a central-mix plant or a drum mixer at the work site, mix the batch between 1 to 5 minutes at mixing speed. Do not exceed the maximum total 60 mixing revolutions. Mixing time begins after all materials, except water, are in the drum, and ends when the discharge chute opens. Transfer time in multiple drum mixers is included in mixing time. Mix time may be reduced for plants utilizing high performance mixing drums provided thoroughly mixed and uniform concrete is being produced with the proposed mix time. Performance of the plant must comply with Table A1.1, of ASTM C 94, Standard Specification for Ready Mixed Concrete. Five of the six tests listed in Table A1.1 must be within the limits of the specification to indicate that uniform concrete is being produced.

If the concrete is mixed in a truck mixer, mix the batch between 70 and 100 revolutions of the drum or blades at mixing speed. After the mixing is completed, set the truck mixer drum at agitating speed. Unless the mixing unit is equipped with an accurate device indicating and controlling the number of revolutions at mixing speed, perform the mixing at the batch plant and operate the mixing unit at agitating speed while traveling from the plant to the work site. Do not exceed 350 total revolutions (mixing and agitating).

If a truck mixer or truck agitator is used to transport concrete that was completely mixed in a stationary central mixer, agitate the concrete while transporting at the agitating speed specified by the manufacturer of the equipment (shown on the manufacturer's plate on the equipment). Do not exceed 250 total revolutions (additional re-mixing and agitating).

Provide a batch slip including batch weights of every constituent of the concrete and time for each batch of concrete delivered at the work site, issued at the batching plant that bears the time of charging of the mixer drum with cementitious and aggregates. Include quantities, type, product name and manufacturer of all admixtures on the batch ticket.

If non-agitating equipment is used for transportation of concrete, provide approved covers for protection against the weather when required by the Engineer.

Place non-agitated concrete within 30 minutes of adding the cement to the water.

Do not use concrete that has developed its initial set. Regardless of the speed of delivery and placement, the Engineer will suspend the concreting operations until corrective measures are taken if there is evidence that the concrete can not be adequately consolidated.

Adding water to concrete after the initial mixing is prohibited. Add all water at the plant. If needed, adjust slump through the addition of a water reducer according to **subsection 3.0e.(2)**.

b. Placement Limitations.

(1) Concrete Temperature. Unless otherwise authorized by the Engineer, the temperature of the mixed concrete immediately before placement is a minimum of 55°F, and a maximum of 70°F. With approval by the Engineer, the temperature of the concrete may be adjusted 5°F above or below this range.

(2) Qualification Batch. For Grade 3.5 (AE) (LC-HPC) concrete, qualify a field batch (one truckload or at least 6 cubic yards) at least 35 days prior to commencement of placement of the bridge decks. Produce the qualification batch from the same plant that will supply the job concrete. Simulate haul time to the jobsite prior to discharge of the concrete for testing. Prior to placing concrete in the qualification slab and on the job, submit documentation to the Engineer verifying that the qualification batch concrete meets the requirements for air content, slump, temperature of plastic concrete, compressive strength, unit weight and other testing as required by the Engineer.

Before the concrete mixture with plasticizing admixture is used on the project, determine the air content of the qualification batch. Monitor the slump, air content, temperature and workability at initial batching and estimated time of concrete placement. If these properties are not adequate, repeat the qualification batch until it can be demonstrated that the mix is within acceptable limits as specified in this specification.

(3) Placing Concrete at Night. Do not mix, place or finish concrete without sufficient natural light, unless an adequate and artificial lighting system approved by the Engineer is provided.

(4) Placing Concrete in Cold Weather. Unless authorized otherwise by the Engineer, mixing and concreting operations shall not proceed once the descending ambient air temperature reaches 40°F, and may not be initiated until an ascending ambient air temperature reaches 40°F. The ascending ambient air temperature for initiating concreting operations shall increase to 45°F if the maximum ambient air temperature is expected to be between 55°F and 60°F during or within 24 hours of placement and to 50°F if the ambient air temperature is expected to equal or exceed 60°F during or within 24 hours of placement.

If the Engineer permits placing concrete during cold weather, aggregates may be heated by either steam or dry heat before placing them in the mixer. Use an apparatus that heats the weight uniformly and is so arranged as to preclude the possible occurrence of overheated areas which might injure the materials. Do not heat aggregates directly by gas or oil flame or on sheet metal over fire. Aggregates that are heated in bins, by steam-coil or water-coil heating, or by other methods not detrimental to the aggregates may be used. The use of live steam on or through binned aggregates is prohibited. Unless otherwise authorized, maintain the temperature of the mixed concrete between 55°F to 70°F at the time of placing it in the forms. With approval by the Engineer, the temperature of the concrete may be adjusted up to 5°F above or below this range. Do not place concrete when there is a probability of air temperatures being more than 25°F below the temperature of the concrete during the first 24 hours after placement unless insulation is provided for both the deck and the girders. Do not, under any circumstances, continue concrete operations if the ambient air temperature is less than 20°F.

If the ambient air temperature is 40°F or less at the time the concrete is placed, the Engineer may permit the water and the aggregates be heated to at least 70°F, but not more than 120°F.

Do not place concrete on frozen subgrade or use frozen aggregates in the concrete.

(5) Placing Concrete in Hot Weather. When the ambient temperature is above 90ºF, cool the forms, reinforcing steel, steel beam flanges, and other surfaces which will come in contact with the mix to below 90ºF by means of a water spray or other approved methods. For Grade 3.5 (AE) (LC-HPC) concrete, cool the concrete mixture to maintain the temperature immediately before placement between 55°F and 70°F. With approval by the Engineer, the temperature of the concrete may be up to 5°F below or above this range.

Maintain the temperature of the concrete at time of placement within the specified temperature range by any combination of the following:

Shading the materials storage areas or the production equipment.

Cooling the aggregates by sprinkling with potable water.

Cooling the aggregates or water by refrigeration or replacing a portion or all of the mix water with ice that is flaked or crushed to the extent that the ice will completely melt during mixing of the concrete.

- Liquid nitrogen injection.

6.0 INSPECTION AND TESTING

The Engineer will test the first truckload of concrete by obtaining a sample of fresh concrete at truck discharge and by obtaining a sample of fresh concrete at the discharge end of the conveyor, bucket or if pumped, the piping. The Engineer will obtain subsequent sample concrete for tests at the discharge end of the conveyor, bucket or if pumped, the discharge end of the piping. If potential problems are apparent at the discharge of any truck, the Engineer will test the concrete at truck discharge prior to deposit on the bridge deck.

The Engineer will cast, store, and test strength test specimens in sets of 5. See **TABLE 1-3**.

KDOT will conduct the sampling and test the samples according to **SECTION 2500** and **TABLE 1-3**. The Contractor may be directed by the Engineer to assist KDOT in obtaining the fresh concrete samples during the placement operation.

A plan will be finalized prior to the construction date as to how out-of-specification concrete will be handled.

TABLE 1-3: SAMPLING AND TESTING FREQUENCY CHART

Tests Required (Record to)	Test Method	CMS	Verification Samples and Tests	Acceptance Samples and Tests
Slump (0.25 inch)	KT-21	a	Each of first 3 truckloads for any individual placement, then 1 of every 3 truckloads	
Temperature (1°F)	KT-17	a	Every truckload, measured at the truck discharge, and from each sample made for slump determination.	
Mass (0.1 lb)	KT-20	a	One of every 6 truckloads	
Air Content (0.25%)	KT-18 or KT-19	a	Each of first 3 truckloads for any individual placement, then 1 of every 6 truckloads	
Cylinders (1 lbf; 0.1 in; 1 psi)	KT-22 and AASHTO T 22	VER	Make at least 2 groups of 5 cylinders per pour or major mix design change with concrete sampled from at least 2 different truckloads evenly spaced throughout the pour, with a minimum of 1 set for every 100 cu yd. Include in each group 3 test cylinders to be cured according to KT-22 and 2 test cylinders to be field-cured. Store the field-cured cylinders on or adjacent to the bridge. Protect all surfaces of the cylinders from the elements in as near as possible the same way as the deck concrete. Test the field-cured cylinders at the same age as the standard-cured cylinders.	
Density of Fresh Concrete (0.1 lb/cu ft or 0.1% of optimum density)	KT-36	ACI		b,c: 1 per 100 cu yd for thin overlays and bridge deck surfacing.

Note a: "Type Insp" must = "ACC" when the assignment of a pay quantity is being made. "ACI" when recording test values for additional acceptance information.

Note b: Normal operation. Minimum frequency for exceptional conditions may be reduced by the DME on a project basis, written justification shall be made to the Chief of the Bureau of Materials and Research and placed in the project documents. (Multi-Level Frequency Chart (see page 17, Appendix A of Construction Manual, Part V).

Note c: Applicable only when specifications contain those requirements.

The Engineer will reject concrete that does not comply with specified requirements.

The Engineer will permit occasional deviations below the specified cementitious content, if it is due to the air content of the concrete exceeding the designated air content, but only up to the maximum tolerance in the air content. Continuous operation below the specified cement content for any reason is prohibited.

As the work progresses, the Engineer reserves the right to require the Contractor to change the proportions if conditions warrant such changes to produce a satisfactory mix. Any such changes may be made within the limits of the Specifications at no additional compensation to the Contractor.

KANSAS DEPARTMENT OF TRANSPORTATION
SPECIAL PROVISION TO THE
STANDARD SPECIFICATIONS, 2007 EDITION

Add a new SECTION to DIVISION 700:

LOW-CRACKING HIGH-PERFORMANCE CONCRETE – CONSTRUCTION

1.0 DESCRIPTION

Construct the low-cracking high-performance concrete (LC-HPC) structures according to the Contract Documents and this specification.

BID ITEMS	UNITS
Qualification Slab	Cubic Yard
Concrete (*) (AE) (LC-HPC)	Cubic Yard
*Grade of Concrete	

2.0 MATERIALS

Provide materials that comply with the applicable requirements.

LC-HPC ..... **07-PS0166, latest version**
Concrete Curing Materials ..... **DIVISION 1400**

3.0 CONSTRUCTION REQUIREMENTS

a. Qualification Batch and Slab. For each LC-HPC bridge deck, produce a qualification batch of LC-HPC that is to be placed in the deck and complies with **07-PS0166, latest version**, and construct a qualification slab that complies with this specification to demonstrate the ability to handle, place, finish and cure the LC-HPC bridge deck.

After the qualification batch of LC-HPC complies with **07-PS0166, latest version**, construct a qualification slab 15 to 45 days prior to placing LC-HPC in the bridge deck. Construct the qualification slab to comply with the Contract Documents, using the same LC-HPC that is to be placed in the deck and that was approved in the qualification batch. Submit the location of the qualification slab for approval by the Engineer. Place, finish and cure the qualification slab according to the Contract Documents, using the same personnel, methods and equipment (including the concrete pump, if used) that will be used on the bridge deck.

A minimum of 1 day after construction of the qualification slab, core 4 full-depth 4 inch diameter cores, one from each quadrant of the qualification slab, and forward them to the Engineer for visual inspection of degree of consolidation.

Do not commence placement of LC-HPC in the deck until approval is given by the Engineer. Approval to place concrete on the deck will be based on satisfactory placement, consolidation, finishing and curing of the qualification slab and cores, and will be given or denied within 24 hours of receiving the cores from the Contractor. If an additional qualification slab is deemed necessary by the Engineer, it will be paid for at the contract unit price for Qualification Slab.

b. Falsework and Forms. Construct falsework and forms according to **SECTION 708**.

c. Handling and Placing LC-HPC.

(1) Quality Control Plan (QCP). At a project progress meeting prior to placing LC-HPC, discuss with the Engineer the method and equipment used for deck placement. Submit an acceptable QCP according to the Contractor's Concrete Structures Quality Control Plan, Part V. Detail the equipment (for both determining and controlling the evaporation rate and LC-HPC temperature), procedures used to minimize the evaporation rate, plans for maintaining a continuous rate of finishing the deck without delaying the application of curing materials within the time specified in **subsection 3.0f.**, including maintaining a continuous supply of LC-HPC throughout the placement with an adequate quantity of LC-HPC to complete the deck and filling diaphragms and end walls in advance of deck placement, and plans

for placing the curing materials within the time specified in **subsection 3.0f**. In the plan, also include input from the LC-HPC supplier as to how variations in the moisture content of the aggregate will be handled, should they occur during construction.

(2) Use a method and sequence of placing LC-HPC approved by the Engineer. Do not place LC-HPC until the forms and reinforcing steel have been checked and approved. Before placing LC-HPC, clean all forms of debris.

(3) Finishing Machine Setup. On bridges skewed greater than 10º, place LC-HPC on the deck forms across the deck on the same skew as the bridge, unless approved otherwise by State Bridge Office (SBO). Operate the bridge deck finishing machine on the same skew as the bridge, unless approved otherwise by the SBO. Before placing LP-HPC, position the finish machine throughout the proposed placement area to allow the Engineer to verify the reinforcing steel positioning.

(4) Environmental Conditions. Maintain environmental conditions on the entire bridge deck so the evaporation rate is less than 0.2 lb/sq ft/hr. The temperature of the mixed LC-HPC immediately before placement must be a minimum of 55°F and a maximum of 70°F. With approval by the Engineer, the temperature of the LC-HPC may be adjusted 5°F above or below this range. This may require placing the deck at night, in the early morning or on another day. The evaporation rate (as determined in the American Concrete Institute Manual of Concrete Practice 305R, Chapter 2) is a function of air temperature, LC-HPC temperature, wind speed and relative humidity. The effects of any fogging required by the Engineer will not be considered in the estimation of the evaporation rate (**subsection 3.0c.(5)**).

Just prior to and at least once per hour during placement of the LC-HPC, the Engineer will measure and record the air temperature, LC-HPC temperature, wind speed, and relative humidity on the bridge deck. The Engineer will take the air temperature, wind, and relative humidity measurements approximately 12 inches above the surface of the deck. With this information, the Engineer will determine the evaporation rate using KDOT software or **FIGURE 710-1**.

When the evaporation rate is equal to or above 0.2 lb/ft^2/hr, take actions (such as cooling the LC-HPC, installing wind breaks, sun screens etc.) to create and maintain an evaporation rate less than 0.2 lb/ft^2/hr on the entire bridge deck.

(5) Fogging of Deck Placements. Fogging using hand-held equipment may be required by the Engineer during unanticipated delays in the placing, finishing or curing operations. If fogging is required by the Engineer, do not allow water to drip, flow or puddle on the concrete surface during fogging, placement of absorptive material, or at any time before the concrete has achieved final set.

(6) Placement and Equipment. Place LC-HPC by conveyor belt or concrete bucket. Pumping of LC-HPC will be allowed if the Contractor can show proficiency when placing the approved mix during construction of the qualification slab using the same pump as will be used on the job. Placement by pump will also be allowed with prior approval of the Engineer contingent upon successful placement by pump of the approved mix, using the same pump as will be used for the deck placement, at least 15 days prior to placing LC-HPC in the bridge deck. To limit the loss of air, the maximum drop from the end of a conveyor belt or from a concrete bucket is 5 feet and pumps must be fitted with an air cuff/bladder valve. Do not use chutes, troughs or pipes made of aluminum.

Place LC-HPC to avoid segregation of the materials and displacement of the reinforcement. Do not deposit LC-HPC in large quantities at any point in the forms, and then run or work the LC-HPC along the forms.

Fill each part of the form by depositing the LC-HPC as near to the final position as possible.

The Engineer will obtain sample LC-HPC for tests and cylinders at the discharge end of the conveyor, bucket, or if pumped, the piping.

(7) Consolidation.

- Accomplish consolidation of the LC-HPC on all span bridges that require finishing machines by means of a mechanical device on which internal (spud or tube type) concrete vibrators of the same type and size are mounted (**subsection 154.2**).
- Observe special requirements for vibrators in contact with epoxy coated reinforcing steel as specified in **subsection 154.2**.
- Provide stand-by vibrators for emergency use to avoid delays in case of failure.
- Operate the mechanical device so vibrator insertions are made on a maximum spacing of 12 inch centers over the entire deck surface.
- Provide a uniform time per insertion of all vibrators of 3 to 15 seconds, unless otherwise designated by the Engineer.
- Provide positive control of vibrators using a timed light, buzzer, automatic control or other approved method.
- Extract the vibrators from the LC-HPC at a rate to avoid leaving any large voids or holes in the LC-HPC.
- Do not drag the vibrators horizontally through the LC-HPC.

- Use hand held vibrators (**subsection 154.2**) in inaccessible and confined areas such as along bridge rail or curb.
- When required, supplement vibrating by hand spading with suitable tools to provide required consolidation.
- Reconsolidate any voids left by workers.

Continuously place LC-HPC in any floor slab until complete, unless shown otherwise in the Contract Documents.

d. Construction Joints, Expansion Joints and End of Wearing Surface (EWS) Treatment. Locate the construction joints as shown in the Contract Documents. If construction joints are not shown in the Contract Documents, submit proposed locations for approval by the Engineer.

If the work of placing LC-HPC is delayed and the LC-HPC has taken its initial set, stop the placement, saw the nearest construction joint approved by the Engineer, and remove all LC-HPC beyond the construction joint.

Construct keyed joints by embedding water-soaked beveled timbers of a size shown on the Contract Documents, into the soft LC-HPC. Remove the timber when the LC-HPC has set. When resuming work, thoroughly clean the surface of the LC-HPC previously placed, and when required by the Engineer, roughen the key with a steel tool. Before placing LC-HPC against the keyed construction joint, thoroughly wash the surface of the keyed joint with clean water.

e. Finishing. Strike off bridge decks with a vibrating screed or single-drum roller screed, either self-propelled or manually operated by winches and approved by the Engineer. Use a self-oscillating screed on the finish machine, and operate or finish from a position either on the skew or transverse to the bridge roadway centerline. See **subsection 3.0c.(3)**. Do not mount tamping devices or fixtures to drum roller screeds; augers are allowed.

Irregular sections may be finished by other methods approved by the Engineer and detailed in the required QCP. See **subsection 3.0c.(1)**.

Finish the surface by a burlap drag, metal pan or both, mounted to the finishing equipment. Use a float or other approved device behind the burlap drag or metal pan, as necessary, to remove any local irregularities. Do not add water to the surface of LC-HPC. Do not use a finishing aid.

Tining of plastic LC-HPC is prohibited. All LC-HPC surfaces must be reasonably true and even, free from stone pockets, excessive depressions or projections beyond the surface.

Finish all top surfaces, such as the top of retaining walls, curbs, abutments and rails, with a wooden float by tamping and floating, flushing the mortar to the surface and provide a uniform surface, free from pits or porous places. Trowel the surface producing a smooth surface, and brush lightly with a damp brush to remove the glazed surface.

f. Curing and Protection.

(1) General. Cure all newly placed LC-HPC immediately after finishing, and continue uninterrupted for a minimum of 14 days. Cure all pedestrian walkway surfaces in the same manner as the bridge deck. Curing compounds are prohibited during the 14 day curing period.

(2) Cover With Wet Burlap. Soak the burlap a minimum of 12 hours prior to placement on the deck. Rewet the burlap if it has dried more one hour before it is applied to the surface of bridge deck. Apply 1 layer of wet burlap within 10 minutes of LC-HPC strike-off from the screed, followed by a second layer of wet burlap within 5 minutes. Do not allow the surface to dry after the strike-off, or at any time during the cure period. In the required QCP, address the rate of LC-HPC placement and finishing methods that will affect the period between strike-off and burlap placement. See **subsection 3.0c.(1)**. During times of delay expected to exceed 10 minutes, cover all concrete that has been placed, but not finished, with wet burlap.

Maintain the wet burlap in a fully wet condition using misting hoses, self-propelled, machine-mounted fogging equipment with effective fogging area spanning the deck width moving continuously across the entire burlap-covered surface, or other approved devices until the LC-HPC has set sufficiently to allow foot traffic. At that time, place soaker hoses on the burlap, and supply running water continuously to maintain continuous saturation of all burlap material to the entire LC-HPC surface. For bridge decks with superelevation, place a minimum of 1 soaker hose along the high edge of the deck to keep the entire deck wet during the curing period.

(3) Waterproof Cover. Place white polyethylene film on top of the soaker hoses, covering the entire LC-HPC surface after soaker hoses have been placed, a maximum of 12 hours after the placement of the LC-HPC. Use as wide of sheets as practicable, and overlap 2 feet on all edges to form a complete waterproof cover of the entire LC-HPC surface. Secure the polyethylene film so that wind will not displace it. Should any portion of the sheets be broken or

damaged before expiration of the curing period, immediately repair the broken or damaged portions. Replace sections that have lost their waterproof qualities.

If burlap and/or polyethylene film is temporarily removed for any reason during the curing period, use soaker hoses to keep the entire exposed area continuously wet. Replace saturated burlap and polyethylene film, resuming the specified curing conditions, as soon as possible.

Inspect the LC-HPC surface once every 6 hours for the entirety of the 14 day curing period, so that all areas remain wet for the entire curing period and all curing requirements are satisfied.

(4) Documentation. Provide the Engineer with a daily inspection set that includes:

- documentation that identifies any deficiencies found (including location of deficiency);
- documentation of corrective measures taken;
- a statement of certification that the entire bridge deck is wet and all curing material is in place;
- documentation showing the time and date of all inspections and the inspector's signature.
- documentation of any temporary removal of curing materials including location, date and time, length of time curing was removed, and means taken to keep the exposed area continuously wet.

(5) Cold Weather Curing. When LC-HPC is being placed in cold weather, also adhere to **07-PS0166, latest version**.

When LC-HPC is being placed and the ambient air temperature may be expected to drop below 40ºF during the curing period or when the ambient air temperature is expected to drop more than 25°F below the temperature of the LC-HPC during the first 24 hours after placement, provide suitable measures such as straw, additional burlap, or other suitable blanketing materials, and/or housing and artificial heat to maintain the LC-HPC and girder temperatures between 40ºF and 75ºF as measured on the upper and lower surfaces of the LC-HPC. Enclose the area underneath the deck and heat so that the temperature of the surrounding air is as close as possible to the temperature of LC-HPC and between 40ºF and 75ºF. When artificial heating is used to maintain the LC-HPC and girder temperatures, provide adequate ventilation to limit exposure to carbon dioxide if necessary. Maintain wet burlap and polyethylene cover during the entire 14 day curing period. Heating may be stopped after the first 72 hours if the time of curing is lengthened to account for periods when the ambient air temperature is below 40ºF. For every day the ambient air temperature is below 40ºF, an additional day of curing with a minimum ambient air temperature of 50ºF will be required. After completion of the required curing period, remove the curing and protection so that the temperature of the LC-HPC during the first 24 hours does not fall more than 25°F.

(6) Curing Membrane. At the end of the 14-day curing period remove the wet burlap and polyethylene and within 30 minutes, apply 2 coats of an opaque curing membrane to the LC-HPC. Apply the curing membrane when no free water remains on the surface but while the surface is still wet. Apply each coat of curing membrane according to the manufacturer's instructions with a minimum spreading rate per coat of 1 gallon per 80 square yards of LC-HPC surface. If the LC-HPC is dry or becomes dry, thoroughly wet it with water applied as a fog spray by means of approved equipment. Spray the second coat immediately after and at right angles to the first application.

Protect the curing membrane against marring for a minimum of 7 days. Give any marred or disturbed membrane an additional coating. Should the curing membrane be subjected to continuous injury, the Engineer may limit work on the deck until the 7-day period is complete. Because the purpose of the curing membrane is to allow for slow drying of the bridge deck, extension of the initial curing period beyond 14 days, while permitted, shall not be used to reduce the 7-day period during which the curing membrane is applied and protected.

(7) Construction Loads. Adhere to **TABLE 710-2**.

If the Contractor needs to drive on the bridge before the approach slabs can be placed and cured, construct a temporary bridge from the approach over the EWS capable of supporting the anticipated loads. Do not bend the reinforcing steel which will tie the approach slab to the EWS or damage the LC-HPC at the EWS. The method of bridging must be approved by the Engineer.

TABLE 710-2: CONCRETE LOAD LIMITATIONS ON BRIDGE DECKS		
Days after concrete is placed	**Element**	**Allowable Loads**
1*	Subdeck, one-course deck or concrete overlay	Foot traffic only.
3*	One-course deck or concrete overlay	Work to place reinforcing steel or forms for the bridge rail or barrier.
7*	Concrete overlays	Legal Loads; Heavy stationary loads with the Engineer's approval.***
10 (15)**	Subdeck, one-course deck or post-tensioned haunched slab bridges**	Light truck traffic (gross vehicle weight less than 5 tons).****
14 (21)**	Subdeck, one-course deck or post-tensioned haunched slab bridges**	Legal Loads; Heavy stationary loads with the Engineer's approval.***Overlays on new decks.
28	Bridge decks	Overloads, only with the State Bridge Engineer's approval.***

*Maintain a 7 day wet cure at all times (14-day wet cure for decks with LC-HPC).
** Conventional haunched slabs.
*** Submit the load information to the appropriate Engineer. Required information: the weight of the material and the footprint of the load, or the axle (or truck) spacing and the width, the size of each tire (or track length and width) and their weight.
****An overlay may be placed using pumps or conveyors until legal loads are allowed on the bridge.

g. Grinding and Grooving. Correct surface variations exceeding 1/8 inch in 10 feet by use of an approved profiling device, or other methods approved by the Engineer after the curing period. Perform grinding on hardened LC-HPC after the 7 day curing membrane period to achieve a plane surface and grooving of the final wearing surface as shown in the Contract Documents.

Use a self-propelled grinding machine with diamond blades mounted on a multi-blade arbor. Avoid using equipment that causes excessive ravels, aggregate fractures or spalls. Use vacuum equipment or other continuous methods to remove grinding slurry and residue.

After any required grinding is complete, give the surface a suitable texture by transverse grooving. Use diamond blades mounted on a self-propelled machine that is designed for texturing pavement. Transverse grooving of the finished surface may be done with equipment that is not self-propelled providing that the Contractor can show proficiency with the equipment. Use equipment that does not cause strain, excessive raveling, aggregate fracture, spalls, disturbance of the transverse or longitudinal joint, or damage to the existing LC-HPC surface. Make the grooving approximately 3/16 inch in width at 3/4 inch centers and the groove depth approximately 1/8 inch. For bridges with drains, terminate the transverse grooving approximately 2 feet in from the gutter line at the base of the curb. Continuously remove all slurry residues resulting from the texturing operation.

h. Post Construction Conference. At the completion of the deck placement, curing, grinding and grooving for a bridge using LC-HPC, a post-construction conference will be held with all parties that participated in the planning and construction present. The Engineer will record the discussion of all problems and successes for the project.

i. Removal of Forms and Falsework. Do not remove forms and falsework without the Engineer's approval. Remove deck forms approximately 2 weeks (a maximum of 4 weeks) after the end of the curing period (removal of burlap), unless approved by the Engineer. The purpose of 4 week maximum is to limit the moisture gradient between the bottom and the top of the deck.

For additional requirements regarding forms and falsework, see **SECTION 708**.

4.0 MEASUREMENT AND PAYMENT

The Engineer will measure the qualification slab and the various grades of (AE) (LC-HPC) concrete placed in the structure by the cubic yard. No deductions are made for reinforcing steel and pile heads extending into the LP-HPC. The Engineer will not separately measure reinforcing steel in the qualification slab.

Payment for the "Qualification Slab" and the various grades of "(AE) (LC-HPC) Concrete" at the contract unit prices is full compensation for the specified work.

FIGURE 710-1: STANDARD PRACTICE FOR CURING CONCRETE

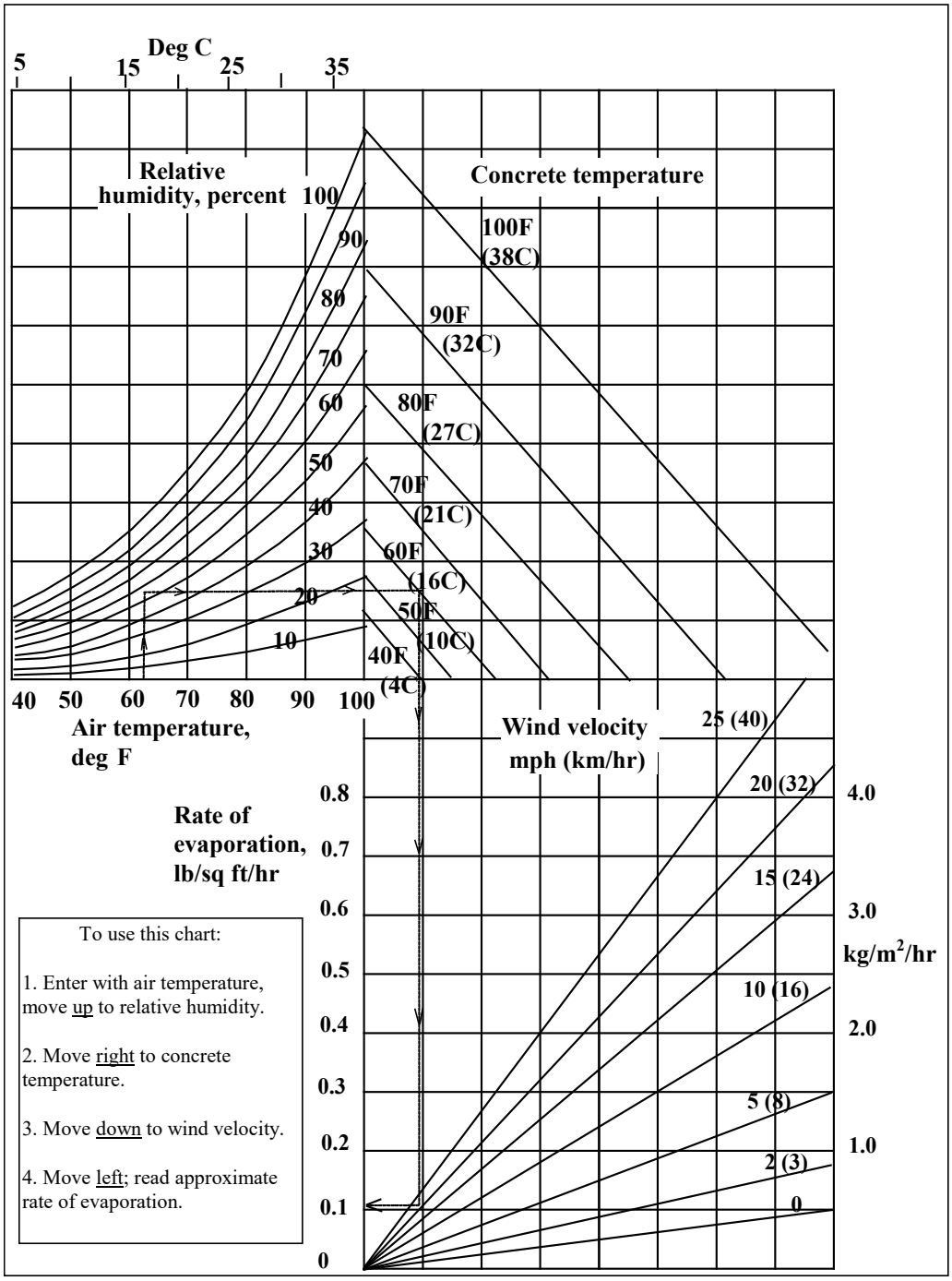

Effect of concrete and air temperatures, relative humidity, and wind velocity on the rate of evaporation of surface moisture from concrete. This chart provides a graphic method of estimating the loss of surface moisture for various weather conditions. To use the chart, follow the four steps outlined above. When the evaporation rate exceeds 0.2 lb/ft^2/hr (1.0 kg/ m^2/hr), measures shall be taken to prevent excessive moisture loss from the surface of unhardened concrete; when the rate is less than 0.2 lb/ft^2/hr (1.0 kg/m^2/hr) such measures may be needed. When excessive moisture loss is not prevented, plastic cracking is likely to occur.

APPENDIX B: LENGTH–CHANGE MEASUREMENTS FOR MIXTURES USED IN CHAPTER 2

TABLE B.1 – LENGTH-CHANGE MEASURENETS FOR CONTROL MIXTURE USED IN CHAPTER 2

Time of Drying day	Time after Cast day	Deformation, microstrain			
		Specimen A	Specimen B	Specimen C	Average
0	0.00		0	0	0
0	0.03		-10	-40	-25
0	0.08		30	0	15
0	0.13		20	-20	0
0	0.16		20	-20	0
0	0.78		30	-30	0
0	2		40	-20	10
0	3		70	50	60
0	4		60	40	50
0	5		50	30	40
0	6		60	40	50
0	7		60	50	55
0	8		60	40	50
0	9		60	40	50
0	10		60	40	50
0	11		60	40	50
0	12		60	40	50
0	13		60	50	55
0	14		60	50	55
1	15		0	-20	-10
2	16		-40	-70	-55
3	17		-60	-120	-90
4	18		-90	-150	-120
5	19		-130	-170	-150
6	20		-140	-190	-165
7	21		-150	-200	-175
8	22		-150	-200	-175
9	23		-200	-240	-220
10	24		-210	-260	-235
11	25		-210	-260	-235
12	26		-220	-270	-245
13	27		-220	-270	-245
14	28		-220	-280	-250
15	29		-250	-300	-275
16	30		-250	-300	-275
17	31		-270	-320	-295
18	32		-270	-320	-295

TABLE B.1 (cont'd) – LENGTH-CHANGE MEASURENETS FOR CONTROL MIXTURE IN CHAPTER 2

Time of Drying day	Time after Cast day	Deformation, microstrain			
		Specimen A	Specimen B	Specimen C	Average
19	33		-270	-320	-295
20	34		-270	-320	-295
21	35		-280	-330	-305
22	36		-280	-330	-305
23	37		-280	-330	-305
24	38		-280	-320	-300
25	39		-280	-320	-300
26	40		-280	-330	-305
27	41		-280	-330	-305
28	42		-280	-340	-310
29	43		-290	-350	-320
30	44		-300	-350	-325
32	46		-310	-360	-335
34	48		-310	-360	-335
36	50		-310	-360	-335
38	52		-320	-370	-345
40	54		-320	-380	-350
42	56		-330	-390	-360
44	58		-330	-390	-360
46	60		-340	-400	-370
48	62		-350	-410	-380
50	64		-340	-400	-370
52	66		-350	-400	-375
54	68		-360	-410	-385
56	70		-360	-410	-385
58	72		-370	-410	-390
60	74		-370	-410	-390
62	76		-370	-410	-390
64	78		-400	-440	-420
66	80		-400	-440	-420
68	82		-400	-440	-420
70	84		-400	-440	-420
72	86		-410	-450	-430
74	88		-410	-450	-430
76	90		-410	-450	-430
78	92		-410	-450	-430
80	94		-410	-450	-430

TABLE B.1 (cont'd) – LENGTH-CHANGE MEASURENETS FOR CONTROL MIXTURE USED IN CHAPTER 2

Time of Drying day	Time after Cast day	Deformation, microstrain			
		Specimen A	Specimen B	Specimen C	Average
82	96		-400	-450	-425
84	98		-400	-450	-425
86	100		-420	-470	-445
88	102		-430	-480	-455
90	104		-450	-490	-470
92	106		-450	-490	-470
94	108		-440	-480	-460
101	115		-430	-480	-455
108	122		-450	-490	-470
115	129		-450	-490	-470
122	136		-440	-490	-465
129	143		-450	-510	-480
136	150		-450	-510	-480
143	157		-450	-520	-485
150	164		-470	-540	-505
157	171		-480	-550	-515
164	178		-470	-530	-500
171	185		-470	-530	-500
178	192		-470	-520	-495
185	199		-470	-540	-505
210	224		-440	-500	-470
238	252		-410	-490	-450
266	280		-430	-500	-465
294	308		-440	-510	-475
322	336		-410	-490	-450
350	364		-400	-480	-440
365	379		-390	-480	-435

TABLE B.2 – LENGTH-CHANGE MEASURENETS FOR MIXTURE SLAG USED IN CHAPTER 2

Time of Drying day	Time after Cast day	Deformation, microstrain			
		Specimen A	Specimen B	Specimen C	Average
0	0.13	0	0	0	0
0	0.57	-40	-30	50	-7
0	1	10	50	90	50
0	2	0	80	130	70
0	3	0	40	130	57
0	4	10	60	120	63
0	5	20	70	120	70
0	6	40	80	110	77
0	7	60	90	110	87
0	8	70	110	100	93
0	9	60	100	110	90
0	10	50	120	120	97
0	11	50	120	130	100
0	12	50	110	130	97
0	13	60	100	120	93
0	14	60	90	120	90
1	15	70	100	130	100
2	16	0	10	50	20
3	17	-40	-20	30	-10
4	18	-40	-20	30	-10
5	19	-60	-30	20	-23
6	20	-80	-50	0	-43
7	21	-90	-60	-10	-53
8	22	-110	-90	-30	-77
9	23	-90	-100	-40	-77
10	24	-130	-120	-50	-100
11	25	-120	-110	-50	-93
12	26	-140	-120	-60	-107
13	27	-150	-130	-70	-117
14	28	-160	-140	-80	-127
15	29	-170	-150	-90	-137
16	30	-180	-160	-100	-147
17	31	-190	-150	-100	-147
18	32	-190	-160	-110	-153
19	33	-200	-170	-120	-163
20	34	-210	-180	-130	-173
21	35	-210	-180	-130	-173

TABLE B.2 (cont'd) – LENGTH-CHANGE MEASURENETS FOR MIXTURE SLAG USED IN CHAPTER 2

Time of Drying day	Time after Cast day	Deformation, microstrain			
		Specimen A	Specimen B	Specimen C	Average
22	36	-210	-180	-130	-173
23	37	-210	-180	-130	-173
24	38	-220	-190	-140	-183
25	39	-220	-200	-140	-187
26	40	-230	-200	-140	-190
27	41	-230	-200	-140	-190
28	42	-240	-200	-140	-193
29	43	-230	-200	-150	-193
30	44	-240	-210	-150	-200
32	46	-230	-200	-140	-190
34	48	-240	-210	-150	-200
36	50	-260	-230	-160	-217
38	52	-250	-230	-160	-213
40	54	-250	-230	-150	-210
42	56	-265	-240	-160	-222
44	58	-280	-250	-170	-233
46	60	-290	-260	-180	-243
48	62	-290	-260	-180	-243
50	64	-290	-260	-180	-243
52	66	-290	-260	-180	-243
54	68	-300	-270	-190	-253
56	70	-300	-270	-190	-253
58	72	-300	-270	-190	-253
60	74	-310	-280	-200	-263
62	76	-310	-285	-210	-268
64	78	-320	-290	-210	-273
66	80	-320	-290	-210	-273
68	82	-320	-290	-210	-273
70	84	-310	-290	-220	-273
72	86	-310	-290	-220	-273
74	88	-310	-290	-220	-273
76	90	-310	-290	-220	-273
78	92	-320	-290	-220	-277
80	94	-330	-310	-240	-293
82	96	-320	-300	-240	-287
84	98	-330	-305	-235	-290
86	100	-340	-310	-230	-293

TABLE B.2 (cont'd) – LENGTH-CHANGE MEASURENETS FOR MIXTURE SLAG USED IN CHAPTER 2

Time of Drying day	Time after Cast day	Deformation, microstrain			
		Specimen A	Specimen B	Specimen C	Average
88	102	-350	-320	-230	-300
90	104	-350	-315	-230	-298
92	106	-350	-315	-230	-298
94	108	-350	-310	-230	-297
101	115	-340	-300	-220	-287
108	122	-350	-310	-230	-297
115	129	-360	-320	-250	-310
122	136	-370	-320	-270	-320
129	143	-370	-320	-280	-323
136	150	-360	-330	-270	-320
143	157	-370	-340	-280	-330
150	164	-370	-330	-280	-327
157	171	-370	-330	-290	-330
164	178	-370	-330	-280	-327
171	185	-370	-330	-280	-327
178	192	-370	-340	-280	-330
180	194	-380	-330	-280	-330
210	224	-390	-340	-290	-340
238	252	-400	-360	-300	-353
266	280	-420	-380	-300	-367
294	308	-410	-370	-300	-360
322	336	-410	-370	-300	-360
350	364	-410	-370	-300	-360
365	379	-410	-370	-300	-360

TABLE B.3 – LENGTH-CHANGE MEASURENETS FOR MIXTURE SCM USED IN CHAPTER 2

Time of Drying day	Time after Cast day	Deformation, microstrain			
		Specimen A	Specimen B	Specimen C	Average
0	0.00		0	0	0
0	0.04		10	-80	-35
0	0.08		0	-140	-70
0	0.13		40	-150	-55
0	0.18		40	-150	-55
0	0.22		60	-120	-30
0	0.75		60	-120	-30
0	2		70	-50	10
0	3		40	-30	5
0	4		60	-50	5
0	5		40	-60	-10
0	6		40	-60	-10
0	7		30	-70	-20
0	8		40	-60	-10
0	9		30	-60	-15
0	10		40	-60	-10
0	11		20	-70	-25
0	12		20	-70	-25
0	13		30	-80	-25
0	14		30	-70	-20
1	15		30	-60	-15
2	16		20	-80	-30
3	17		-10	-100	-55
4	18		-20	-130	-75
5	19		-30	-140	-85
6	20		-50	-150	-100
7	21		-70	-160	-115
8	22		-80	-190	-135
9	23		-90	-210	-150
10	24		-100	-220	-160
11	25		-130	-240	-185
12	26		-130	-240	-185
13	27		-130	-250	-190
14	28		-130	-250	-190
15	29		-140	-260	-200
16	30		-180	-290	-235
17	31		-180	-290	-235

TABLE B.3 (cont'd) – LENGTH-CHANGE MEASURENETS FOR MIXTURE SCM USED IN CHAPTER 2

Time of Drying day	Time after Cast day	Deformation, microstrain			
		Specimen A	Specimen B	Specimen C	Average
18	32		-170	-280	-225
19	33		-180	-290	-235
20	34		-190	-300	-245
21	35		-190	-300	-245
22	36		-210	-320	-265
23	37		-170	-280	-225
24	38		-170	-280	-225
25	39		-170	-290	-230
26	40		-180	-300	-240
27	41		-200	-310	-255
28	42		-210	-310	-260
29	43		-210	-310	-260
30	44		-220	-330	-275
32	46		-210	-330	-270
34	48		-220	-340	-280
36	50		-220	-340	-280
38	52		-220	-340	-280
40	54		-230	-350	-290
42	56		-250	-360	-305
44	58		-240	-360	-300
46	60		-240	-370	-305
48	62		-250	-370	-310
50	64		-250	-370	-310
52	66		-240	-360	-300
54	68		-240	-370	-305
56	70		-250	-380	-315
58	72		-260	-390	-325
60	74		-270	-410	-340
62	76		-270	-410	-340
64	78		-270	-400	-335
66	80		-270	-400	-335
68	82		-280	-410	-345
70	84		-280	-420	-350
72	86		-290	-430	-360
74	88		-280	-420	-350
76	90		-290	-430	-360
78	92		-290	-430	-360

TABLE B.3 (cont'd) – LENGTH-CHANGE MEASURENETS FOR MIXTURE SCM USED IN CHAPTER 2

Time of Drying day	Time after Cast day	Deformation, microstrain			
		Specimen A	Specimen B	Specimen C	Average
80	94		-280	-420	-350
82	96		-290	-430	-360
84	98		-300	-440	-370
86	100		-300	-430	-365
88	102		-280	-420	-350
90	104		-260	-400	-330
92	106		-240	-380	-310
94	108		-250	-400	-325
101	115		-270	-420	-345
108	122		-250	-370	-310
115	129		-260	-390	-325
122	136		-260	-390	-325
129	143		-260	-420	-340
136	150		-270	-420	-345
143	157		-280	-420	-350
150	164		-280	-420	-350
157	171		-310	-430	-370
164	178		-310	-440	-375
171	185		-310	-430	-370
178	192		-300	-420	-360
180	194		-320	-440	-380
210	224		-300	-430	-365
238	252		-300	-420	-360
266	280		-300	-430	-365
294	308		-310	-440	-375
322	336		-320	-440	-380
350	364		-310	-460	-385
365	379		-300	-440	-370

TABLE B.4 – LENGTH-CHANGE MEASURENETS FOR MIXTURE 5.3% IC-SCM USED IN CHAPTER 2

Time of Drying day	Time after Cast day	Deformation, microstrain			
		Specimen A	Specimen B	Specimen C	Average
0	0.00	0	0	0	0
0	0.04	-20	-20	-20	-20
0	0.08	-10	-10	-10	-10
0	0.13	0	-10	-10	-7
0	0.16	-10	0	10	0
0	0.23	0	0	20	7
0	1	10	10	40	20
0	2	0	0	20	7
0	3	-10	0	30	7
0	4	-10	0	30	7
0	5	-10	0	30	7
0	6	-10	0	20	3
0	7	-10	0	20	3
0	8	20	30	60	37
0	9	30	30	60	40
0	10	40	40	60	47
0	11	30	40	60	43
0	12	30	40	60	43
0	13	20	30	70	40
0	14	20	30	70	40
1	15	10	0	20	10
2	16	-30	-30	-10	-23
3	17	-40	-50	-20	-37
4	18	-50	-50	-20	-40
5	19	-60	-60	-30	-50
6	20	-70	-70	-40	-60
7	21	-70	-80	-50	-67
8	22	-80	-90	-60	-77
9	23	-90	-100	-60	-83
10	24	-100	-110	-70	-93
11	25	-100	-120	-70	-97
12	26	-110	-130	-80	-107
13	27	-130	-140	-90	-120
14	28	-140	-150	-100	-130
15	29	-150	-170	-120	-147
16	30	-140	-150	-110	-133
17	31	-120	-150	-110	-127

TABLE B.4 (cont'd) – LENGTH-CHANGE MEASURENETS FOR MIXTURE 5.3% IC-SCM USED IN CHAPTER 2

Time of Drying day	Time after Cast day	Deformation, microstrain			
		Specimen A	Specimen B	Specimen C	Average
18	32	-110	-150	-110	-123
19	33	-90	-150	-110	-117
20	34	-70	-140	-100	-103
21	35	-50	-140	-90	-93
22	36	-100	-140	-90	-110
23	37	-110	-140	-100	-117
24	38	-120	-150	-110	-127
25	39	-150	-160	-120	-143
26	40	-150	-180	-130	-153
27	41	-160	-190	-140	-163
28	42	-160	-200	-150	-170
29	43	-150	-170	-150	-157
30	44	-150	-170	-140	-153
32	46	-160	-170	-140	-157
34	48	-170	-170	-150	-163
36	50	-180	-190	-160	-177
38	52	-160	-190	-150	-167
40	54	-170	-200	-160	-177
42	56	-170	-200	-160	-177
44	58	-160	-170	-170	-167
46	60	-180	-210	-170	-187
48	62	-190	-230	-170	-197
50	64	-200	-240	-190	-210
52	66	-200	-230	-180	-203
54	68	-200	-230	-180	-203
56	70	-210	-230	-180	-207
58	72	-210	-230	-180	-207
60	74	-230	-250	-200	-227
62	76	-230	-250	-200	-227
64	78	-230	-250	-200	-227
66	80	-230	-260	-210	-233
68	82	-230	-260	-210	-233
70	84	-230	-260	-210	-233
72	86	-230	-260	-210	-233
74	88	-240	-270	-210	-240
76	90	-240	-270	-210	-240
78	92	-230	-260	-210	-233

TABLE B.4 (cont'd) – LENGTH-CHANGE MEASURENETS FOR MIXTURE 5.3% IC-SCM USED IN CHAPTER 2

Time of Drying day	Time after Cast day	Deformation, microstrain			
		Specimen A	Specimen B	Specimen C	Average
80	94	-250	-280	-220	-250
82	96	-250	-280	-220	-250
84	98	-250	-280	-220	-250
86	100	-280	-300	-250	-277
88	102	-280	-300	-250	-277
90	104	-270	-300	-260	-277
92	106	-270	-300	-260	-277
94	108	-270	-300	-250	-273
101	115	-270	-290	-240	-267
108	122	-270	-290	-240	-267
115	129	-290	-310	-260	-287
122	136	-290	-320	-270	-293
129	143	-290	-330	-270	-297
136	150	-290	-330	-270	-297
143	157	-280	-320	-270	-290
150	164	-300	-330	-280	-303
157	171	-300	-330	-270	-300
164	178	-290	-320	-270	-293
171	185	-290	-320	-270	-293
178	192	-290	-320	-270	-293
180	194	-300	-320	-290	-303
210	224	-310	-330	-290	-310
238	252	-310	-330	-340	-327
266	280	-310	-330	-330	-323
294	308	-300	-330	-300	-310
322	336	-320	-390	-350	-353
350	364	-310	-390	-280	-327
365	379	-310	-430	-270	-337

TABLE B.5 – LENGTH-CHANGE MEASURENETS FOR MIXTURE 6.5% IC-SCM USED IN CHAPTER 2

Time of Drying day	Time after Cast day	Deformation, microstrain			
		Specimen A	Specimen B	Specimen C	Average
0	0.00	0	0	0	0
0	0.07	50	60	0	37
0	0.12	70	60	-10	40
0	0.18	70	50	20	47
0	0.21	90	80	20	63
0	1	80	60	0	47
0	2	80	70	10	53
0	3	110	100	40	83
0	4	120	110	50	93
0	5	140	120	70	110
0	6	160	140	90	130
0	7	150	130	80	120
0	8	150	130	80	120
0	9	120	110	60	97
0	10	110	100	50	87
0	11	110	100	50	87
0	12	120	110	60	97
0	13	120	120	70	103
0	14	140	120	70	110
1	15	110	90	0	67
2	16	100	60	30	63
3	17	60	60	0	40
4	18	40	50	-20	23
5	19	30	40	-30	13
6	20	20	30	-40	3
7	21	10	10	-40	-7
8	22	0	0	-50	-17
9	23	0	10	-30	-7
10	24	-20	-50	-40	-37
11	25	-10	-50	-60	-40
12	26	-10	-40	-80	-43
13	27	0	-30	-90	-40
14	28	-10	-40	-100	-50
15	29	0	-40	-90	-43
16	30	0	-30	-90	-40
17	31	0	-40	-90	-43
18	32	-10	-40	-90	-47

TABLE B.5 (cont'd) – LENGTH-CHANGE MEASURENETS FOR MIXTURE 6.5% IC-SCM USED IN CHAPTER 2

Time of Drying day	Time after Cast day	Deformation, microstrain			
		Specimen A	Specimen B	Specimen C	Average
19	33	-10	-50	-100	-53
20	34	-20	-50	-100	-57
21	35	-40	-70	-130	-80
22	36	-30	-70	-130	-77
23	37	-40	-70	-140	-83
24	38	-40	-70	-140	-83
25	39	-40	-80	-140	-87
26	40	-50	-90	-150	-97
27	41	-60	-90	-150	-100
28	42	-70	-110	-170	-117
29	43	-80	-110	-180	-123
30	44	-80	-130	-190	-133
32	46	-80	-130	-190	-133
34	48	-90	-140	-190	-140
36	50	-100	-140	-200	-147
38	52	-100	-140	-200	-147
40	54	-110	-150	-200	-153
42	56	-120	-150	-210	-160
44	58	-130	-150	-220	-167
46	60	-130	-150	-220	-167
48	62	-130	-150	-220	-167
50	64	-140	-160	-230	-177
52	66	-150	-170	-240	-187
54	68	-160	-180	-250	-197
56	70	-170	-190	-260	-207
58	72	-180	-200	-270	-217
60	74	-180	-200	-280	-220
62	76	-190	-210	-290	-230
64	78	-190	-210	-280	-227
66	80	-190	-210	-280	-227
68	82	-190	-220	-290	-233
70	84	-190	-230	-290	-237
72	86	-190	-230	-290	-237
74	88	-180	-220	-290	-230
76	90	-170	-210	-270	-217
78	92	-180	-210	-280	-223
80	94	-190	-220	-280	-230

TABLE B.5 (cont'd) – LENGTH-CHANGE MEASURENETS FOR MIXTURE 6.5% IC-SCM USED IN CHAPTER 2

Time of Drying day	Time after Cast day	Deformation, microstrain			
		Specimen A	Specimen B	Specimen C	Average
82	96	-190	-220	-280	-230
84	98	-180	-210	-290	-227
86	100	-210	-240	-310	-253
88	102	-210	-240	-310	-253
90	104	-210	-240	-310	-253
92	106	-220	-260	-330	-270
94	108	-220	-250	-320	-263
101	115	-230	-260	-330	-273
108	122	-220	-250	-320	-263
115	129	-220	-250	-330	-267
122	136	-220	-260	-330	-270
129	143	-220	-260	-330	-270
136	150	-220	-260	-330	-270
143	157	-230	-260	-340	-277
150	164	-230	-260	-340	-277
157	171	-230	-260	-340	-277
164	178	-240	-270	-350	-287
171	185	-230	-270	-360	-287
178	192	-230	-270	-360	-287
180	194	-240	-280	-370	-297
210	224	-270	-310	-400	-327
238	252	-250	-290	-380	-307
266	280	-250	-280	-380	-303
294	308	-260	-290	-400	-317
322	336	-260	-290	-390	-313
350	364	-260	-290	-390	-313
365	379	-260	-290	-390	-313

TABLE B.6 – LENGTH-CHANGE MEASURENETS FOR MIXTURE 9.7% IC-SCM USED IN CHAPTER 2

Time of Drying day	Time after Cast day	Deformation, microstrain			
		Specimen A	Specimen B	Specimen C	Average
0	0.00	0	0	0	0
0	0.08	-10	0	-20	-10
0	0.17	0	30	30	20
0	0.24	-10	20	20	10
0	1	10	50	40	33
0	2	30	70	60	53
0	3	50	90	80	73
0	4	90	120	110	107
0	5	90	90	90	90
0	6	100	120	110	110
0	7	70	110	90	90
0	8	70	100	60	77
0	9	70	100	70	80
0	10	60	90	80	77
0	11	60	90	90	80
0	12	70	120	120	103
0	13	70	130	130	110
0	14	60	150	140	117
1	15	50	50	60	53
2	16	20	50	60	43
3	17	0	50	60	37
4	18	40	50	60	50
5	19	20	50	50	40
6	20	20	60	70	50
7	21	40	70	70	60
8	22	30	60	60	50
9	23	40	20	60	40
10	24	40	20	60	40
11	25	10	20	30	20
12	26	0	0	20	7
13	27	40	0	60	33
14	28	0	10	40	17
15	29	0	20	30	17
16	30	0	20	60	27
17	31	0	20	60	27
18	32	0	20	20	13
19	33	-30	0	0	-10

TABLE B.6 (cont'd) – LENGTH-CHANGE MEASURENETS FOR MIXTURE 9.7% IC-SCM USED IN CHAPTER 2

Time of Drying day	Time after Cast day	Deformation, microstrain			
		Specimen A	Specimen B	Specimen C	Average
20	34	-30	-10	0	-13
21	35	-10	-10	10	-3
22	36	-10	-10	10	-3
23	37	-20	-10	10	-7
24	38	-30	-10	0	-13
25	39	-40	-10	0	-17
26	40	-60	-20	-20	-33
27	41	-60	-30	-20	-37
28	42	-60	-30	-30	-40
29	43	-70	-40	-40	-50
30	44	-80	-40	-40	-53
32	46	-80	-50	-40	-57
34	48	-90	-60	-50	-67
36	50	-90	-60	-40	-63
38	52	-90	-70	-50	-70
40	54	-90	-70	-50	-70
42	56	-100	-80	-60	-80
44	58	-100	-80	-50	-77
46	60	-100	-80	-50	-77
48	62	-100	-80	-60	-80
50	64	-120	-100	-70	-97
52	66	-130	-110	-80	-107
54	68	-140	-110	-90	-113
56	70	-140	-130	-100	-123
58	72	-150	-140	-110	-133
60	74	-150	-140	-120	-137
62	76	-150	-140	-100	-130
64	78	-150	-140	-100	-130
66	80	-150	-140	-110	-133
68	82	-160	-150	-120	-143
70	84	-160	-150	-120	-143
72	86	-160	-150	-120	-143
74	88	-150	-140	-110	-133
76	90	-150	-140	-110	-133
78	92	-160	-140	-110	-137
80	94	-160	-140	-110	-137
82	96	-150	-130	-100	-127

TABLE B.6 (cont'd) – LENGTH-CHANGE MEASURENETS FOR MIXTURE 9.7% IC-SCM USED IN CHAPTER 2

Time of Drying day	Time after Cast day	Deformation, microstrain			
		Specimen A	Specimen B	Specimen C	Average
84	98	-180	-170	-130	-160
86	100	-180	-170	-130	-160
88	102	-190	-180	-140	-170
90	104	-200	-190	-140	-177
92	106	-200	-190	-140	-177
94	108	-220	-200	-160	-193
101	115	-220	-200	-150	-190
108	122	-210	-190	-140	-180
115	129	-210	-190	-140	-180
122	136	-210	-200	-140	-183
129	143	-210	-200	-140	-183
136	150	-220	-200	-150	-190
143	157	-220	-200	-150	-190
150	164	-220	-200	-150	-190
157	171	-220	-210	-160	-197
164	178	-220	-210	-170	-200
171	185	-220	-210	-170	-200
178	192	-230	-210	-180	-207
180	194	-230	-210	-180	-207
210	224	-240	-220	-180	-213
238	252	-240	-230	-190	-220
266	280	-250	-240	-200	-230
294	308	-250	-240	-200	-230
322	336	-250	-230	-190	-223
350	364	-260	-250	-200	-237
365	379	-270	-240	-210	-240

APPENDIX C: DATA COLLECTED FROM FREEZE-THAW AND SCALING SPECIMENS

Table C.1 – SCALING MASS LOSS DATA

Mixture: Control

Specimen	Effective Area	Mass loss at 7 cycles		Mass loss at 21 cycles		Mass loss at 35 cycles		Mass loss at 56 cycles		Total	
	in^2	g	lb/in^2	g	lb/in^2	g	lb/in^2	g	lb/in^2	g	lb/in^2
A	75.98	9.5	2.87E-04	4.3	0.00013	3.9	0.000118	10.1	0.000305	27.800	0.00084
B	76.75	9.8	2.93E-04	3.5	0.000105	1.6	4.79E-05	10.1	0.000302	25.000	0.000748
C	76.28	6.9	2.08E-04	2.4	7.22E-05	2.6	7.83E-05	4.6	0.000138	16.500	0.000497
Average	76.34		2.63E-04		1.02E-04		8.13E-05		0.00		6.95E-04
Cumulative mass loss (lb/ft^2)			3.78E-02		5.25E-02		6.43E-02		1.00E-01		

Mixture: Slag

Specimen	Effective Area	Mass loss at 7 cycles		Mass loss at 21 cycles		Mass loss at 35 cycles		Mass loss at 56 cycles		Total	
	in^2	g	lb/in^2	g	lb/in^2	g	lb/in^2	g	lb/in^2	g	lb/in^2
A	78.29	2.9	8.50E-05	4.5	0.000132	4.5	0.000132	3.9	0.000114	15.800	0.000463
B	75.40	3.5	1.07E-04	3.2	9.74E-05	4.8	0.000146	2.6	7.92E-05	14.100	0.000429
C	75.10	4.3	1.31E-04	5.9	0.00018	4.5	0.000138	4.2	0.000128	18.900	0.000578
Average	76.26		1.08E-04		1.37E-04		1.39E-04		0.00		4.90E-04
Cumulative mass loss (lb/ft^2)			1.55E-02		3.52E-02		5.51E-02		7.06E-02		

Mixture: SCM

Specimen	Effective Area	Mass loss at 7 cycles		Mass loss at 21 cycles		Mass loss at 35 cycles		Mass loss at 56 cycles		Total	
	in^2	g	lb/in^2	g	lb/in^2	g	lb/in^2	g	lb/in^2	g	lb/in^2
A	73.82	5.9	1.83E-04	5.7	0.000177	1.6	4.98E-05	3.1	9.64E-05	16.300	0.000507
B	75.27	6.4	1.95E-04	5	0.000153	2.4	7.32E-05	6.5	0.000198	20.300	0.000619
C	75.10	7.3	2.23E-04	4	0.000122	3.9	0.000119	5.2	0.000159	20.400	0.000624
Average	74.73		2.01E-04		1.51E-04		8.07E-05		0.00		5.83E-04
Cumulative mass loss (lb/ft^2)			2.89E-02		5.06E-02		6.22E-02		8.40E-02		

Mixture: 6.5% IC

Specimen	Effective Area	Mass loss at 7 cycles		Mass loss at 21 cycles		Mass loss at 35 cycles		Mass loss at 56 cycles		Total	
	in^2	g	lb/in^2	g	lb/in^2	g	lb/in^2	g	lb/in^2	g	lb/in^2
A	74.38	3.9	1.20E-04	6.3	0.000194	1.7	5.25E-05	1.1	3.4E-05	13.000	0.000401
B	75.84	2.5	7.57E-05	10.3	0.000312	0.7	2.12E-05	1.3	3.93E-05	14.800	0.000448
C	76.69	1	2.99E-05	4	0.00012	1.6	4.79E-05	2.4	7.18E-05	9.000	0.000269
Average	75.64		7.53E-05		2.09E-04		4.05E-05		0.00		3.73E-04
Cumulative mass loss (lb/ft^2)			1.08E-02		4.09E-02		4.67E-02		5.37E-02		

Mixture: 5.3% IC-SCM

Specimen	Effective Area	Mass loss at 7 cycles		Mass loss at 21 cycles		Mass loss at 35 cycles		Mass loss at 56 cycles		Total	
	in^2	g	lb/in^2	g	lb/in^2	g	lb/in^2	g	lb/in^2	g	lb/in^2
A	74.86	4.3	1.32E-04	16.8	0.000515	35.1	0.001076	41.3	0.001267	97.500	0.00299
B	76.22	2.2	6.63E-05	15.9	0.000479	39.5	0.00119	37	0.001114	94.600	0.002849
C	76.42	4.3	1.29E-04	15.9	0.000478	43.3	0.001301	44.6	0.00134	108.100	0.003247
Average	75.83		1.09E-04		4.91E-04		1.19E-03		0.00		3.03E-03
Cumulative mass loss (lb/ft^2)			1.57E-02		8.64E-02		2.58E-01		4.36E-01		

Table C.1 (cont'd) – SCALING MASS LOSS DATA

Mixture: 6.5% IC-SCM

Specimen	Effective Area	Mass loss at 7 cycles		Mass loss at 21 cycles		Mass loss at 35 cycles		Mass loss at 56 cycles		Total	
	in^2	g	lb/in^2	g	lb/in^2	g	lb/in^2	g	lb/in^2	g	lb/in^2
A	75.95	3.4	1.03E-04	29	0.000877	17	0.000514	7.5	0.000227	56.900	0.00172
B	75.76	3.6	1.09E-04	20.8	0.00063	23.3	0.000706	5.9	0.000179	53.600	0.001624
C	74.69	4.4	1.35E-04	17.4	0.000535	18.2	0.000559	11.7	0.00036	51.700	0.001589
Average	75.47		1.16E-04		6.81E-04		5.93E-04		0.00		1.64E-03
Cumulative mass loss (lb/ft^2)			1.67E-02		1.15E-01		2.00E-01		2.37E-01		

Mixture: 9.7% IC-SCM

Specimen	Effective Area	Mass loss at 7 cycles		Mass loss at 21 cycles		Mass loss at 35 cycles		Mass loss at 56 cycles		Total	
	in^2	g	lb/in^2	g	lb/in^2	g	lb/in^2	g	lb/in^2	g	lb/in^2
A	75.23	4.7	1.43E-04	14	0.000427	20.5	0.000626	40.1	0.001224	79.300	0.00242
B	75.37	2.9	8.83E-05	16.6	0.000506	17.9	0.000545	33.4	0.001017	70.800	0.002156
C	75.89	4.8	1.45E-04	9.9	0.000299	18.3	0.000554	8.7	0.000263	41.700	0.001262
Average	75.49		1.26E-04		4.11E-04		5.75E-04		0.00		1.95E-03
Cumulative mass loss (lb/ft^2)			1.81E-02		7.72E-02		1.60E-01		2.80E-01		

Mixture: 6.5% IC-SCM-SCA 1

Specimen	Effective Area	Mass loss at 7 cycles		Mass loss at 21 cycles		Mass loss at 35 cycles		Mass loss at 56 cycles		Total	
	in^2	g	lb/in^2	g	lb/in^2	g	lb/in^2	g	lb/in^2	g	lb/in^2
A	77.06	46.7	1.39E-03	43.4	0.001293	9	0.000268	40.2	0.001198	139.300	0.00415
B	79.27	42.1	1.22E-03	25.1	0.000727	7.7	0.000223	34.8	0.001008	109.700	0.003177
C	78.40	58	1.70E-03	60	0.001757	12.4	0.000363	60.9	0.001783	191.300	0.005602
Average	78.24		1.44E-03		1.26E-03		2.85E-04		0.00		4.31E-03
Cumulative mass loss (lb/ft^2)			2.07E-01		3.88E-01		4.29E-01		6.21E-01		

Mixture: 6.5% IC-SCM-SCA 2

Specimen	Effective Area	Mass loss at 7 cycles		Mass loss at 21 cycles		Mass loss at 35 cycles		Mass loss at 56 cycles		Total	
	in^2	g	lb/in^2	g	lb/in^2	g	lb/in^2	g	lb/in^2	g	lb/in^2
A	78.60	0.5	1.46E-05	13.1	0.000383	18.3	0.000534	18.9	0.000552	50.800	0.001484
B	79.30	0.3	8.69E-06	13.5	0.000391	18.1	0.000524	19.5	0.000565	51.400	0.001488
C	79.35	11.7	3.38E-04	8.5	0.000246	16.6	0.00048	19.3	0.000558	56.100	0.001623
Average	79.08		1.21E-04		3.40E-04		5.13E-04		0.00		1.53E-03
Cumulative mass loss (lb/ft^2)			1.74E-02		6.63E-02		1.40E-01		2.21E-01		

Mixture: 6.5% IC-SCM-SRA

Specimen	Effective Area	Mass loss at 7 cycles		Mass loss at 21 cycles		Mass loss at 35 cycles		Mass loss at 56 cycles		Total	
	in^2	g	lb/in^2	g	lb/in^2	g	lb/in^2	g	lb/in^2	g	lb/in^2
A	76.52	62.8	1.88E-03	108.8	0.003264	0	0	0	0	171.600	0.005148
B	74.66	55.3	1.70E-03	86.2	0.002651	0	0	0	0	141.500	0.004351
C	77.14	63.2	1.88E-03	98.8	0.00294	0	0	0	0	162.000	0.004821
Average	76.11		1.82E-03		2.95E-03		0.00E+00		0.00		4.77E-03
Cumulative mass loss (lb/ft^2)			2.62E-01		6.87E-01		6.87E-01		6.87E-01		

Table C.1 (cont'd) – SCALING MASS LOSS DATA

Mixture: 6.5% IC-SCM-SRA (2)

Specimen	Effective Area	Mass loss at 7 cycles		Mass loss at 21 cycles		Mass loss at 35 cycles		Mass loss at 56 cycles		Total	
	in^2	g	lb/in^2	g	lb/in^2	g	lb/in^2	g	lb/in^2	g	lb/in^2
A	76.82	19	5.68E-04	12.7	0.00038	101.3	0.003027	0	0	133.000	0.003975
B	75.93	23.1	6.98E-04	15.3	0.000463	113.3	0.003426	0	0	151.700	0.004587
C	78.15	17.6	5.17E-04	8.3	0.000244	99.5	0.002923	0	0	125.400	0.003684
Average	76.96		5.94E-04		3.62E-04		3.13E-03		0.00		4.08E-03
Cumulative mass loss (lb/ft^2)			8.56E-02		1.38E-01		5.88E-01		5.88E-01		

TABLE C.2 – FUNDAMENTAL TRANSVERSE FREQUENCY AND MASS DATA

Mixture: Control

No of Cycles	0			37			67		
	A	B	C	A	B	C	A	B	C
Frequency [Hz]	2201	2191	2218	2214	2213	2240	2206	2205	2234
Mass [g]	7411.9	7452.9	7512.7	7426.1	7464.3	7522.1	7437.5	7462.5	7521.6
Dynamic Modulus	3.89E+10	3.88E+10	4.00E+10	3.94E+10	3.96E+10	4.09E+10	3.92E+10	3.93E+10	4.07E+10
Avg. Dyn. Modulus	3.92E+10			4.00E+10			3.97E+10		

No of Cycles	91			126			158		
	A	B	C	A	B	C	A	B	C
n [Hz]	2249	2231	2264	2199	2196	2225	2203	2200	2229
Mass [g]	7414.2	7451.6	7511.6	7424.2	7462.7	7520.1	7428.1	7465.7	7522.9
Dynamic Modulus	4.06E+10	4.02E+10	4.17E+10	3.89E+10	3.90E+10	4.03E+10	3.91E+10	3.92E+10	4.05E+10
Avg. Dyn. Modulus	4.09E+10			3.94E+10			3.96E+10		

No of Cycles	190			226			270		
	A	B	C	A	B	C	A	B	C
n [Hz]	2202	2196	2231	2206	2195	2233	2212	2202	2239
Mass [g]	7431.8	7466.9	7526.3	7429.7	7465.6	7524.2	7432.9	7469.3	7526.2
Dynamic Modulus	3.90E+10	3.90E+10	4.06E+10	3.92E+10	3.90E+10	4.07E+10	3.94E+10	3.92E+10	4.09E+10
Avg. Dyn. Modulus	3.96E+10			3.96E+10			3.98E+10		

No of Cycles	352			382			412		
	A	B	C	A	B	C	A	B	C
n [Hz]	2198	2185	2225	2200	2190	2230	2203	2200	2235
Mass [g]	7433	7468.4	7524.9	7436.3	7472.7	7529	7435.9	7471.1	7528.3
Dynamic Modulus	3.89E+10	3.86E+10	4.04E+10	3.90E+10	3.88E+10	4.06E+10	3.91E+10	3.92E+10	4.08E+10
Avg. Dyn. Modulus	3.93E+10			3.95E+10			3.97E+10		

No of Cycles	438			468			504		
	A	B	C	A	B	C	A	B	C
n [Hz]	2211	2200	2239	2213	2206	2241	2220	2214	2249
Mass [g]	7436.6	7427.9	7528.7	7439.7	7475.7	7530.3	7437.3	7473.2	7529.4
Dynamic Modulus	3.94E+10	3.90E+10	4.09E+10	3.95E+10	3.94E+10	4.10E+10	3.97E+10	3.97E+10	4.13E+10
Avg. Dyn. Modulus	3.98E+10			4.00E+10			4.02E+10		

No of Cycles	532			571			601		
	A	B	C	A	B	C	A	B	C
n [Hz]	2219	2211	2245	2217	2209	2246	2220	2212	2249
Mass [g]	7437	7473.9	7529	7435.8	7472.9	7528.8	7436.7	7474	7529.4
Dynamic Modulus	3.97E+10	3.96E+10	4.11E+10	3.96E+10	3.95E+10	4.12E+10	3.97E+10	3.96E+10	4.13E+10
Avg. Dyn. Modulus	4.01E+10			4.01E+10			4.02E+10		

No of Cycles	632			660		
	A	B	C	A	B	C
n [Hz]	2218	2210	2250	2228	2219	2255
Mass [g]	7435.6	7472.1	7527.2	7438.1	7474.9	7530.3
Dynamic Modulus	3.96E+10	3.95E+10	4.13E+10	4.00E+10	3.99E+10	4.15E+10
Avg. Dyn. Modulus	4.02E+10			4.05E+10		

TABLE C.2 (cont'd) – FUNDAMENTAL TRANSVERSE FREQUENCY AND MASS DATA

Mixture: Control

No of Cycles	0			37			67		
	A	B	C	A	B	C	A	B	C
Frequency [Hz]	2201	2208	2214	2198	2202	2214	2239	2234	2217
Mass [g]	7406.3	7503.4	7469.9	7411	7508.9	7478	7410.4	7507.4	7475
Dynamic Modulus	3.89E+10	3.96E+10	3.97E+10	3.88E+10	3.95E+10	3.97E+10	4.03E+10	4.06E+10	3.98E+10
Avg. Dyn. Modulus	3.94E+10			3.93E+10			4.02E+10		

No of Cycles	91			126			158		
	A	B	C	A	B	C	A	B	C
Frequency [Hz]	2197	2200	2207	2189	2193	2202	2195	2201	2210
Mass [g]	7403.6	7500.5	7471	7409.5	7509	7476.3	7412.4	7510.1	7479.9
Dynamic Modulus	3.87E+10	3.93E+10	3.94E+10	3.85E+10	3.91E+10	3.93E+10	3.87E+10	3.94E+10	3.96E+10
Avg. Dyn. Modulus	3.92E+10			3.90E+10			3.92E+10		

No of Cycles	190			226			270		
	A	B	C	A	B	C	A	B	C
Frequency [Hz]	2196	2200	2200	2197	2203	2213	2202	2205	2213
Mass [g]	7416.2	7507.9	7480.5	7412.2	7510.1	7480.5	7414.6	7511.7	7481.9
Dynamic Modulus	3.88E+10	3.94E+10	3.92E+10	3.88E+10	3.95E+10	3.97E+10	3.90E+10	3.96E+10	3.97E+10
Avg. Dyn. Modulus	3.91E+10			3.93E+10			3.94E+10		

No of Cycles	352			382			412		
	A	B	C	A	B	C	A	B	C
Frequency [Hz]	2190	2192	2202	2191	2193	2204	2195	2200	2207
Mass [g]	7411.8	7510.2	7479.4	7414.7	7510.9	7480.5	7414.2	7511	7480.8
Dynamic Modulus	3.85E+10	3.91E+10	3.93E+10	3.86E+10	3.91E+10	3.94E+10	3.87E+10	3.94E+10	3.95E+10
Avg. Dyn. Modulus	3.90E+10			3.90E+10			3.92E+10		

No of Cycles	438			468			504		
	A	B	C	A	B	C	A	B	C
Frequency [Hz]	2200	2200	2215	2196	2203	2209	2206	2208	2218
Mass [g]	7415.3	7512.4	7481.9	7414.7	7512.6	7483.5	7416.2	7513.2	7482.6
Dynamic Modulus	3.89E+10	3.94E+10	3.98E+10	3.87E+10	3.95E+10	3.96E+10	3.91E+10	3.97E+10	3.99E+10
Avg. Dyn. Modulus	3.94E+10			3.93E+10			3.96E+10		

No of Cycles	532			571			601		
	A	B	C	A	B	C	A	B	C
Frequency [Hz]	2205	2208	2217	2202	2206	2216	2205	2209	2219
Mass [g]	7416	7513.1	7483.1	7415.7	7512.7	7482.1	7416.1	7513.7	7483.7
Dynamic Modulus	3.91E+10	3.97E+10	3.99E+10	3.90E+10	3.96E+10	3.98E+10	3.91E+10	3.97E+10	3.99E+10
Avg. Dyn. Modulus	3.95E+10			3.95E+10			3.96E+10		

No of Cycles	632			660		
	A	B	C	A	B	C
Frequency [Hz]	2205	2206	2215	2211	2213	2222
Mass [g]	7412.6	7511.4	7481.6	7415.3	7514.2	7483.2
Dynamic Modulus	3.91E+10	3.96E+10	3.98E+10	3.93E+10	3.99E+10	4.00E+10
Avg. Dyn. Modulus	3.95E+10			3.97E+10		

TABLE C.2 (cont'd) – FUNDAMENTAL TRANSVERSE FREQUENCY AND MASS DATA

Mixture: SCM

No of Cycles	0			30			53		
	A	B	C	A	B	C	A	B	C
n [Hz]	2181	2157	2157	2175	2153	2148	2167	2150	2147
Mass [g]	7283.3	7298.8	7292.6	7288.4	7307.3	7297.1	7311.3	7298	7297.8
Dynamic Modulus	3.75E+10	3.68E+10	3.68E+10	3.74E+10	3.67E+10	3.65E+10	3.72E+10	3.66E+10	3.65E+10
Avg. Dyn. Modulus	3.70E+10			3.69E+10			3.67E+10		

No of Cycles	83			115			144		
	A	B	C	A	B	C	A	B	C
n [Hz]	2172	2152	2153	2169	2152	2145	2174	2156	2154
Mass [g]	7292.6	7310.1	7300.7	7293.5	7309.5	7300	7293.3	7309.3	7301.5
Dynamic Modulus	3.73E+10	3.67E+10	3.67E+10	3.72E+10	3.67E+10	3.64E+10	3.74E+10	3.68E+10	3.67E+10
Avg. Dyn. Modulus	3.69E+10			3.68E+10			3.70E+10		

No of Cycles	180			217			246		
	A	B	C	A	B	C	A	B	C
n [Hz]	2172	2151	2148	2168	2149	2145	2170	2150	2147
Mass [g]	7291.3	7308.1	7300.9	7293.3	7310.9	7301.1	7291.8	7307.9	7299.8
Dynamic Modulus	3.73E+10	3.66E+10	3.65E+10	3.71E+10	3.66E+10	3.64E+10	3.72E+10	3.66E+10	3.65E+10
Avg. Dyn. Modulus	3.68E+10			3.67E+10			3.68E+10		

No of Cycles	277			327			357		
	A	B	C	A	B	C	A	B	C
n [Hz]	2178	2158	2153	2171	2151	2151	2176	2156	2155
Mass [g]	7292.2	7309.1	7301	7293.1	7310.6	7301.2	7291.8	7309.2	7301.6
Dynamic Modulus	3.75E+10	3.69E+10	3.67E+10	3.72E+10	3.67E+10	3.66E+10	3.74E+10	3.68E+10	3.67E+10
Avg. Dyn. Modulus	3.70E+10			3.68E+10			3.70E+10		

No of Cycles	409			444			481		
	A	B	C	A	B	C	A	B	C
n [Hz]	2177	2158	2151	2174	2158	2149	2177	2157	2154
Mass [g]	7292.6	7310.4	7301.9	7290.6	7310.8	7303.2	7293.5	7310.4	7302.7
Dynamic Modulus	3.75E+10	3.69E+10	3.66E+10	3.73E+10	3.69E+10	3.65E+10	3.75E+10	3.69E+10	3.67E+10
Avg. Dyn. Modulus	3.70E+10			3.69E+10			3.70E+10		

No of Cycles	511			549			594		
	A	B	C	A	B	C	A	B	C
n [Hz]	2178	2161	2156	2177	2163	2156	2180	2157	2152
Mass [g]	7293.2	7309.1	7300.6	7293.3	7309.4	7301.2	7292.2	7308.3	7301.7
Dynamic Modulus	3.75E+10	3.70E+10	3.68E+10	3.75E+10	3.71E+10	3.68E+10	3.76E+10	3.68E+10	3.66E+10
Avg. Dyn. Modulus	3.71E+10			3.71E+10			3.70E+10		

No of Cycles	630			660		
	A	B	C	A	B	C
n [Hz]	2178	2156	2152	2181	2156	2152
Mass [g]	7291.4	7308.3	7299.3	7292.4	7308.1	7300
Dynamic Modulus	3.75E+10	3.68E+10	3.66E+10	3.76E+10	3.68E+10	3.66E+10
Avg. Dyn. Modulus	3.70E+10			3.70E+10		

TABLE C.2 (cont'd) – FUNDAMENTAL TRANSVERSE FREQUENCY AND MASS DATA

Mixture: 6.5% IC

No of Cycles	0			37			67		
	A	B	C	A	B	C	A	B	C
n [Hz]	2097	2119	2130	2108	2128	2138	2107	2125	2136
Mass [g]	7194	7089.6	7162.4	7209.3	7105.9	7179.1	7208.6	7108.3	7181
Dynamic Modulus	3.43E+10	3.45E+10	3.52E+10	3.47E+10	3.49E+10	3.56E+10	3.47E+10	3.48E+10	3.55E+10
Avg. Dyn. Modulus	3.47E+10			3.50E+10			3.50E+10		

No of Cycles	91			126			158		
	A	B	C	A	B	C	A	B	C
n [Hz]	2148	2182	2189	2098	2118	2126	2105	2128	2135
Mass [g]	7194.4	7191.1	7163.9	7204.1	7100.6	7174	7211	7105.9	7180.8
Dynamic Modulus	3.60E+10	3.71E+10	3.72E+10	3.44E+10	3.45E+10	3.51E+10	3.46E+10	3.49E+10	3.55E+10
Avg. Dyn. Modulus	3.68E+10			3.47E+10			3.50E+10		

No of Cycles	190			226			270		
	A	B	C	A	B	C	A	B	C
n [Hz]	2107	2129	2135	2109	2126	2133	2109	2129	2136
Mass [g]	7209.7	7106.1	7179.4	7211.5	7107.9	7181.6	7211.9	7108.7	7182.2
Dynamic Modulus	3.47E+10	3.49E+10	3.55E+10	3.48E+10	3.48E+10	3.54E+10	3.48E+10	3.49E+10	3.55E+10
Avg. Dyn. Modulus	3.50E+10			3.50E+10			3.51E+10		

No of Cycles	352			382			412		
	A	B	C	A	B	C	A	B	C
n [Hz]	2102	2120	2127	2104	2125	2130	2106	2126	2138
Mass [g]	7206.8	7105.1	7179	7211.9	7108.4	7182.7	7212	7108.5	7182.6
Dynamic Modulus	3.45E+10	3.46E+10	3.52E+10	3.46E+10	3.48E+10	3.53E+10	3.47E+10	3.48E+10	3.56E+10
Avg. Dyn. Modulus	3.48E+10			3.49E+10			3.50E+10		

No of Cycles	438			468			504		
	A	B	C	A	B	C	A	B	C
n [Hz]	2109	2128	2134	2112	2131	2139	2117	2138	2142
Mass [g]	7213.5	7107.8	7185.2	7214.8	7108.7	7184.6	7213.2	7107.4	7184.8
Dynamic Modulus	3.48E+10	3.49E+10	3.55E+10	3.49E+10	3.50E+10	3.56E+10	3.50E+10	3.52E+10	3.57E+10
Avg. Dyn. Modulus	3.50E+10			3.52E+10			3.53E+10		

No of Cycles	532			571			601		
	A	B	C	A	B	C	A	B	C
n [Hz]	2116	2138	2140	2115	2131	2140	2118	2137	2145
Mass [g]	7213.7	7107.2	7184.6	7212.9	7106.8	7182.8	7213.5	7105.5	7184
Dynamic Modulus	3.50E+10	3.52E+10	3.57E+10	3.50E+10	3.50E+10	3.56E+10	3.51E+10	3.52E+10	3.58E+10
Avg. Dyn. Modulus	3.53E+10			3.52E+10			3.53E+10		

No of Cycles	632			660		
	A	B	C	A	B	C
n [Hz]	2115	2136	2141	2120	2141	2145
Mass [g]	7210.4	7101.5	7187.9	7213.6	7104.6	7184.5
Dynamic Modulus	3.50E+10	3.51E+10	3.57E+10	3.51E+10	3.53E+10	3.58E+10
Avg. Dyn. Modulus	3.53E+10			3.54E+10		

TABLE C.2 (cont'd) – FUNDAMENTAL TRANSVERSE FREQUENCY AND MASS DATA

Mixture: 5.3% IC-SCM

No of Cycles	0			37			67		
	A	B	C	A	B	C	A	B	C
n [Hz]	2180	2161	2166	2186	2163	2172	2180	2157	2162
Mass [g]	7300.1	7216.6	7378.1	7308.1	7226.3	7388	7306.1	7225.9	7388.4
Dynamic Modulus	3.76E+10	3.65E+10	3.75E+10	3.78E+10	3.66E+10	3.78E+10	3.76E+10	3.64E+10	3.74E+10
Avg. Dyn. Modulus	3.72E+10			3.74E+10			3.72E+10		

No of Cycles	91			126			158		
	A	B	C	A	B	C	A	B	C
n [Hz]	2183	2173	2180	2174	2150	2158	2177	2153	2160
Mass [g]	7293	7212.3	7374.9	7301.1	7219.8	7382.6	7308.9	7225.5	7388.4
Dynamic Modulus	3.77E+10	3.69E+10	3.80E+10	3.74E+10	3.62E+10	3.73E+10	3.75E+10	3.63E+10	3.74E+10
Avg. Dyn. Modulus	3.75E+10			3.69E+10			3.71E+10		

No of Cycles	246			190			226		
	A	B	C	A	B	C	A	B	C
n [Hz]	2177	2155	2161	2177	2155	2161	2178	2148	2160
Mass [g]	7307.9	7223.1	7386.6	7307.9	7223.1	7386.6	7308.8	7224	7388.8
Dynamic Modulus	3.75E+10	3.63E+10	3.74E+10	3.75E+10	3.63E+10	3.74E+10	3.76E+10	3.61E+10	3.74E+10
Avg. Dyn. Modulus	3.71E+10			3.71E+10			3.70E+10		

No of Cycles	270			352			382		
	A	B	C	A	B	C	A	B	C
n [Hz]	2178	2149	2159	2166	2135	2146	2168	2137	2151
Mass [g]	7309.2	7225.6	7389.2	7304.4	7219.6	7384.2	7310	7223.6	7383
Dynamic Modulus	3.76E+10	3.62E+10	3.73E+10	3.71E+10	3.57E+10	3.69E+10	3.72E+10	3.57E+10	3.70E+10
Avg. Dyn. Modulus	3.70E+10			3.65E+10			3.67E+10		

No of Cycles	412			438			468		
	A	B	C	A	B	C	A	B	C
n [Hz]	2173	2143	2153	2172	2140	2155	2173	2143	2157
Mass [g]	7308.7	7224.7	7383.9	7308	7224	7384	7311.8	7225.8	7387.2
Dynamic Modulus	3.74E+10	3.60E+10	3.71E+10	3.74E+10	3.58E+10	3.72E+10	3.74E+10	3.60E+10	3.72E+10
Avg. Dyn. Modulus	3.68E+10			3.68E+10			3.69E+10		

No of Cycles	504			532			571		
	A	B	C	A	B	C	A	B	C
n [Hz]	2181	2152	2163	2179	2147	2160	2178	2146	2156
Mass [g]	7307.2	7225.3	7383	7305.3	7220.2	7382.5	7305	7219.7	7382.3
Dynamic Modulus	3.77E+10	3.63E+10	3.74E+10	3.76E+10	3.61E+10	3.73E+10	3.76E+10	3.60E+10	3.72E+10
Avg. Dyn. Modulus	3.71E+10			3.70E+10			3.69E+10		

No of Cycles	601			632			660		
	A	B	C	A	B	C	A	B	C
n [Hz]	2177	2146	2155	2178	2145	2158	2184	2155	2162
Mass [g]	7305.7	7220.3	7381.9	7303.8	7216.6	7378.8	7304.1	7217.5	7380.2
Dynamic Modulus	3.75E+10	3.60E+10	3.71E+10	3.75E+10	3.60E+10	3.72E+10	3.78E+10	3.63E+10	3.74E+10
Avg. Dyn. Modulus	3.69E+10			3.69E+10			3.72E+10		

TABLE C.2 (cont'd) – FUNDAMENTAL TRANSVERSE FREQUENCY AND MASS DATA

Mixture: 6.5% IC-SCM

No of Cycles	0			30			53		
	A	B	C	A	B	C	A	B	C
n [Hz]	2129	2101	2091	2134	2103	2092	2133	2102	2098
Mass [g]	7159.5	7065	7033.2	7170	7071.8	7038.4	7173.7	7077.1	7040.2
Dynamic Modulus	3.52E+10	3.38E+10	3.33E+10	3.54E+10	3.39E+10	3.34E+10	3.54E+10	3.39E+10	3.36E+10
Avg. Dyn. Modulus	3.41E+10			3.42E+10			3.43E+10		

No of Cycles	83			115			144		
	A	B	C	A	B	C	A	B	C
n [Hz]	2134	2103	2093	2128	2100	2090	2134	2102	2093
Mass [g]	7175.6	7077.4	7041.8	7175.5	7078.4	7042.7	7174.7	7079.5	7043.1
Dynamic Modulus	3.54E+10	3.39E+10	3.34E+10	3.52E+10	3.38E+10	3.33E+10	3.54E+10	3.39E+10	3.34E+10
Avg. Dyn. Modulus	3.43E+10			3.41E+10			3.42E+10		

No of Cycles	180			217			246		
	A	B	C	A	B	C	A	B	C
n [Hz]	2126	2101	2090	2120	2097	2087	2122	2096	2087
Mass [g]	7174.2	7078.4	7043.3	7176.3	7080.3	7044.1	7175.6	7079.9	7043.1
Dynamic Modulus	3.51E+10	3.39E+10	3.33E+10	3.50E+10	3.37E+10	3.32E+10	3.50E+10	3.37E+10	3.32E+10
Avg. Dyn. Modulus	3.41E+10			3.40E+10			3.40E+10		

No of Cycles	277			327			357		
	A	B	C	A	B	C	A	B	C
n [Hz]	2129	2098	2089	2120	2095	2088	2123	2096	2084
Mass [g]	7175.2	7080.8	7044.4	7177.5	7089.6	7045.9	7176.7	7083.8	7046.3
Dynamic Modulus	3.52E+10	3.38E+10	3.33E+10	3.50E+10	3.37E+10	3.33E+10	3.51E+10	3.37E+10	3.32E+10
Avg. Dyn. Modulus	3.41E+10			3.40E+10			3.40E+10		

No of Cycles	409			444			481		
	A	B	C	A	B	C	A	B	C
n [Hz]	2124	2097	2085	2113	2095	2081	2108	2084	2076
Mass [g]	7177.4	7086.3	7047.6	7178.5	7087.7	7050.9	7181.4	7088.9	7052.4
Dynamic Modulus	3.51E+10	3.38E+10	3.32E+10	3.47E+10	3.37E+10	3.31E+10	3.46E+10	3.34E+10	3.29E+10
Avg. Dyn. Modulus	3.40E+10			3.38E+10			3.36E+10		

No of Cycles	511			549			594		
	A	B	C	A	B	C	A	B	C
n [Hz]	2104	2089	2079	2100	2085	2067	2090	2069	2045
Mass [g]	7182.1	7089.6	7053	7185.7	7092.6	7054.5	7188.2	7096.1	7060.1
Dynamic Modulus	3.45E+10	3.35E+10	3.30E+10	3.43E+10	3.34E+10	3.27E+10	3.40E+10	3.29E+10	3.20E+10
Avg. Dyn. Modulus	3.37E+10			3.35E+10			3.30E+10		

No of Cycles	630			660		
	A	B	C	A	B	C
n [Hz]	2080	2065	2040	2060	2054	2012
Mass [g]	7188.3	7097.5	7058.2	7192	7099.7	7062.4
Dynamic Modulus	3.37E+10	3.28E+10	3.18E+10	3.31E+10	3.25E+10	3.10E+10
Avg. Dyn. Modulus	3.28E+10			3.22E+10		

TABLE C.2 (cont'd) – FUNDAMENTAL TRANSVERSE FREQUENCY AND MASS DATA

Mixture: 9.7% IC-SCM

No of Cycles	0			37			67		
	A	B	C	A	B	C	A	B	C
n [Hz]	2213	2186	2178	2202	2175	2172	2196	2163	2156
Mass [g]	7306.8	7101.9	7168.9	7319.9	7114.2	7180.3	7316.2	7113.7	7191.1
Dynamic Modulus	3.88E+10	3.68E+10	3.69E+10	3.85E+10	3.65E+10	3.67E+10	3.82E+10	3.61E+10	3.62E+10
Avg. Dyn. Modulus	3.75E+10			3.72E+10			3.68E+10		

No of Cycles	91			126			158		
	A	B	C	A	B	C	A	B	C
n [Hz]	2194	2167	2161	2189	2161	2155	2177	2154	2147
Mass [g]	7308.9	7100	7164.6	7316.1	7110.1	7173.1	7325.5	7116.5	7180.7
Dynamic Modulus	3.81E+10	3.61E+10	3.63E+10	3.80E+10	3.60E+10	3.61E+10	3.76E+10	3.58E+10	3.59E+10
Avg. Dyn. Modulus	3.68E+10			3.67E+10			3.64E+10		

No of Cycles	190			226			270		
	A	B	C	A	B	C	A	B	C
n [Hz]	2168	2144	2141	2156	2133	2130	2144	2124	2118
Mass [g]	7328.7	7120.9	7188.9	7331.1	7127.3	7193.5	7341.3	7135.2	7199.8
Dynamic Modulus	3.73E+10	3.55E+10	3.57E+10	3.69E+10	3.51E+10	3.54E+10	3.66E+10	3.49E+10	3.50E+10
Avg. Dyn. Modulus	3.62E+10			3.58E+10			3.55E+10		

No of Cycles	352			382			412		
	A	B	C	A	B	C	A	B	C
n [Hz]	2058	2043	2031	2046	2025	2007	2017	2013	1981
Mass [g]	7343.8	7143	7202.5	7353.9	7150	7210.2	7354.5	7156.9	7218.5
Dynamic Modulus	3.37E+10	3.23E+10	3.22E+10	3.34E+10	3.18E+10	3.15E+10	3.24E+10	3.14E+10	3.07E+10
Avg. Dyn. Modulus	3.27E+10			3.22E+10			3.15E+10		

No of Cycles	438			468			504		
	A	B	C	A	B	C	A	B	C
n [Hz]	2004	1980	1927	1980	1979	1875	1987	1959	1854
Mass [g]	7213.1	7158.1	7351	7439.7	7475.7	7530.3	7361.3	7164.6	7214.9
Dynamic Modulus	3.14E+10	3.04E+10	2.96E+10	3.16E+10	3.17E+10	2.87E+10	3.15E+10	2.98E+10	2.69E+10
Avg. Dyn. Modulus	3.05E+10			3.07E+10			2.94E+10		

No of Cycles	532			571			601		
	A	B	C	A	B	C	A	B	C
n [Hz]	1915	1900	1703	1796	1751	1140	1630	1654	1014
Mass [g]	7361.8	7163.5	7216.2	7365.3	7168.2	7215.5	7367.2	7164.6	7182.2
Dynamic Modulus	2.93E+10	2.80E+10	2.27E+10	2.57E+10	2.38E+10	1.02E+10	2.12E+10	2.12E+10	8.00E+09
Avg. Dyn. Modulus	2.67E+10			1.99E+10			1.68E+10		

TABLE C.2 (cont'd) – FUNDAMENTAL TRANSVERSE FREQUENCY AND MASS DATA

Mixture: 6.5% IC-SCM-SCA 1

No of Cycles	0			30			53		
	A	B	C	A	B	C	A	B	C
n [Hz]	2210	2177	2204	2151	2118	2102	2107	2061	2031
Mass [g]	7425	7472.7	7527.4	7447	7493.2	7550.5	7454.1	7502.5	7562.5
Dynamic Modulus	3.93E+10	3.84E+10	3.96E+10	3.73E+10	3.64E+10	3.62E+10	3.59E+10	3.45E+10	3.38E+10
Avg. Dyn. Modulus	3.91E+10			3.66E+10			3.47E+10		

No of Cycles	83			115			144		
	A	B	C	A	B	C	A	B	C
n [Hz]	2045	2002	1882	1942	1860	1650	1859	1720	1661
Mass [g]	7259.2	7322.8	7323.8	7472.8	7519.7	7580	7476.1	7526.5	7586.1
Dynamic Modulus	3.29E+10	3.18E+10	2.81E+10	3.05E+10	2.82E+10	2.24E+10	2.80E+10	2.41E+10	2.27E+10
Avg. Dyn. Modulus	3.09E+10			2.70E+10			2.49E+10		

No of Cycles	180			217		
	A	B	C	A	B	C
n [Hz]	1560	1380	1670	1259	1010	1643
Mass [g]	7489.7	7532.8	7593.5	7491.1	7538.6	7605.4
Dynamic Modulus	1.98E+10	1.55E+10	2.29E+10	1.29E+10	8.33E+09	2.22E+10
Avg. Dyn. Modulus	1.94E+10			1.45E+10		

TABLE C.2 (cont'd) – FUNDAMENTAL TRANSVERSE FREQUENCY AND MASS DATA

Mixture: 6.5% IC-SCM-SCA 2

No of Cycles	0			37			67		
	A	B	C	A	B	C	A	B	C
n [Hz]	2158	2125	2153	2167	2131	2163	2161	2128	2157
Mass [g]	7246.6	7262.8	7237	7275.6	7291.8	7268	7274.2	7292.2	7271.6
Dynamic Modulus	3.66E+10	3.55E+10	3.64E+10	3.70E+10	3.59E+10	3.68E+10	3.68E+10	3.58E+10	3.67E+10
Avg. Dyn. Modulus	3.62E+10			3.66E+10			3.64E+10		

No of Cycles	91			126			158		
	A	B	C	A	B	C	A	B	C
n [Hz]	2207	2166	2174	2159	2122	2153	2162	2128	2159
Mass [g]	7258.2	7276.6	7255.7	7271.3	7287.6	7265.1	7275.7	7291.1	7272.9
Dynamic Modulus	3.83E+10	3.70E+10	3.72E+10	3.67E+10	3.56E+10	3.65E+10	3.69E+10	3.58E+10	3.67E+10
Avg. Dyn. Modulus	3.75E+10			3.63E+10			3.65E+10		

No of Cycles	190			226			270		
	A	B	C	A	B	C	A	B	C
n [Hz]	2159	2123	2158	2161	2125	2161	2166	2130	2162
Mass [g]	7279.9	7295.8	7274.7	7278.9	7295.4	7274.8	7280.7	7297.2	7277.6
Dynamic Modulus	3.68E+10	3.56E+10	3.67E+10	3.68E+10	3.57E+10	3.68E+10	3.70E+10	3.59E+10	3.69E+10
Avg. Dyn. Modulus	3.64E+10			3.64E+10			3.66E+10		

No of Cycles	352			382			412		
	A	B	C	A	B	C	A	B	C
n [Hz]	2147	2113	2146	2156	2119	2151	2157	2120	2155
Mass [g]	7277.6	7294.5	7272.8	7281.9	7297.8	7277.4	7283.7	7298.9	7278
Dynamic Modulus	3.64E+10	3.53E+10	3.63E+10	3.67E+10	3.55E+10	3.65E+10	3.67E+10	3.55E+10	3.66E+10
Avg. Dyn. Modulus	3.60E+10			3.62E+10			3.63E+10		

No of Cycles	438			468			504		
	A	B	C	A	B	C	A	B	C
n [Hz]	2158	2121	2156	2160	2126	2158	2168	2135	2167
Mass [g]	7283.9	7301.7	7280.9	7287.3	7302.5	7281.2	7285.5	7299.2	7279.5
Dynamic Modulus	3.68E+10	3.56E+10	3.67E+10	3.68E+10	3.58E+10	3.67E+10	3.71E+10	3.61E+10	3.70E+10
Avg. Dyn. Modulus	3.63E+10			3.65E+10			3.67E+10		

No of Cycles	532			571			601		
	A	B	C	A	B	C	A	B	C
n [Hz]	2166	2130	2167	2165	2129	2163	2167	2128	2167
Mass [g]	7286.5	7299.6	7278.6	7283.6	7298.6	7278.1	7285.5	7299.2	7278.7
Dynamic Modulus	3.70E+10	3.59E+10	3.70E+10	3.70E+10	3.58E+10	3.69E+10	3.71E+10	3.58E+10	3.70E+10
Avg. Dyn. Modulus	3.67E+10			3.66E+10			3.66E+10		

No of Cycles	632			660		
	A	B	C	A	B	C
n [Hz]	2168	2130	2167	2169	2135	2169
Mass [g]	7282.8	7299.3	7276.2	7287.3	7301.4	7280.3
Dynamic Modulus	3.71E+10	3.59E+10	3.70E+10	3.72E+10	3.61E+10	3.71E+10
Avg. Dyn. Modulus	3.67E+10			3.68E+10		

TABLE C.2 (cont'd) – FUNDAMENTAL TRANSVERSE FREQUENCY AND MASS DATA

Mixture: 6.5% IC-SCM-SRA

No of Cycles	0			33			65		
	A	B	C	1011A	1011B	1011C	1011A	1011B	1011C
n [Hz]	2214	2197	2161	2052	1988	2006	1836	1758	1785
Mass [g]	7301.2	7380.5	7352.8	7341.8	7423.9	7391.4	7363.7	7444	7414.4
Dynamic Modulus	3.88E+10	3.86E+10	3.72E+10	3.35E+10	3.18E+10	3.22E+10	2.69E+10	2.49E+10	2.56E+10
Avg. Dyn. Modulus	3.82E+10			3.25E+10			2.58E+10		

No of Cycles	91			125		
	1011A	1011B	1011C	1011A	1011B	1011C
n [Hz]	1560	1340	1435	1224	1001	1108
Mass [g]	7369.8	7453.2	7420.7	7374.5	7458.6	7426
Dynamic Modulus	1.94E+10	1.45E+10	1.66E+10	1.20E+10	8.10E+09	9.88E+09
Avg. Dyn. Modulus	1.68E+10			9.98E+09		

Mixture: 6.5% IC-SCM-SRA (2)

No of Cycles	0			37			67		
	A	B	C	A	B	C	A	B	C
n [Hz]	2161	2126	2124	1980	1560	1893	1749	1273	1642
Mass [g]	7400.5	7493.3	7486.8	7441.3	7542.4	7534	7450	7550	7540
Dynamic Modulus	3.74E+10	3.67E+10	3.66E+10	3.16E+10	1.99E+10	2.93E+10	2.47E+10	1.33E+10	2.20E+10
Avg. Dyn. Modulus	3.69E+10			2.69E+10			2.00E+10		

No of Cycles	91			132			208		
	A	B	C	A	B	C	A	B	C
n [Hz]	1720	1240	1626	1304	1001	1240	1005	1001	1001
Mass [g]	7437.9	7535.9	7523.1	7467.6	7568	7554.5	7486.4	7594.4	7594.3
Dynamic Modulus	2.38E+10	1.26E+10	2.16E+10	1.38E+10	8.22E+09	1.26E+10	8.19E+09	8.25E+09	8.25E+09
Avg. Dyn. Modulus	1.93E+10			1.15E+10			8.23E+09		

APPENDIX D: BRIDGE DECK SURVEY SPECIFICATION

1.0 DESCRIPTION.

This specification covers the procedures and requirements to perform bridge deck surveys of reinforced concrete bridge decks.

2.0 SURVEY REQUIREMENTS.

a. Pre-Survey Preparation.

(1) Prior to performing the crack survey, related construction documents need to be gathered to produce a scaled drawing of the bridge deck. The scale must be exactly 1 in. = 10 ft (for use with the scanning software), and the drawing only needs to include the boundaries of the deck surface.

NOTE 1 – In the event that it is not possible to produce a scaled drawing prior to arriving at the bridge deck, a hand-drawn crack map (1 in.= 10 ft) created on engineering paper using measurements taken in the field is acceptable.

(2) The scaled drawing should also include compass and traffic directions in addition to deck stationing. A scaled 5 ft by 5 ft grid is also required to aid in transferring the cracks observed on the bridge deck to the scaled drawing. The grid shall be drawn separately and attached to the underside of the crack map such that the grid can easily be seen through the crack map.

NOTE 2 – Maps created in the field on engineering paper need not include an additional grid.

(3) For curved bridges, the scaled drawing need not be curved, i.e., the curve may be approximated using straight lines.

(4) Coordinate with traffic control so that at least one side (or one lane) of the bridge can be closed during the time that the crack survey is being performed.

b. Preparation of Surface.

(1) After traffic has been closed, station the bridge in the longitudinal direction at ten feet intervals. The stationing shall be done as close to the centerline as possible. For curved bridges, the stationing shall follow the curve.

(2) Prior to beginning the crack survey, mark a 5 ft by 5 ft grid using lumber crayons or chalk on the portion of the bridge closed to traffic corresponding to the grid on the scaled drawing. Measure and document any drains, repaired areas, unusual cracking, or any other items of interest.

(3) Starting with one end of the closed portion of the deck, using a lumber crayon or chalk, begin tracing cracks that can be seen while bending at the waist. After beginning to trace cracks, continue to the end of the crack, even if this includes portions of the crack that were not initially seen while bending at the waist. Cracks not attached to the crack being traced must not be marked unless they can be seen from waist height. Surveyors must return to the location where they started tracing a crack and continue the survey. Areas covered by sand or other debris need not be surveyed. Trace the cracks using a different color crayon than was used to mark the grid and stationing.

(4) At least one person shall recheck the marked portion of the deck for any additional cracks. The goal is not to mark every crack on the deck, only those cracks that can initially be seen while bending at the waist.

NOTE 3 – An adequate supply of lumber crayons or chalk should be on hand for the survey. Crayon or chalk colors should be selected to be readily visible when used to mark the concrete.

c. Weather Limitations.

(1) Surveys are limited to days when the expected temperature during the survey will not be below 60 °F.

(2) Surveys are further limited to days that are forecasted to be at least mostly sunny for a majority of the day.

(3) Regardless of the weather conditions, the bridge deck must be completely dry before the survey can begin.

3.0 BRIDGE SURVEY.

a. Crack Surveys.

Using the grid as a guide, transfer the cracks from the deck to the scaled drawing. Areas that are not surveyed should be marked on the scaled drawing. Spalls, regions of scaling, and other areas of special interest need not be included on the scale drawings but should be noted.

b. Delamination Survey.

At any time during or after the crack survey, bridge decks shall be checked for delamination. Any areas of delamination shall be noted and drawn on a separate drawing of the bridge. This second drawing need not be to scale.

c. Under Deck Survey.

Following the crack and delamination survey, the underside of the deck shall be examined and any unusual or excessive cracking noted.

APPENDIX E: CRACK DENSITIES AT THE TIME OF SURVEY AND CRACK DENSITIES USED FOR ANALYSIS IN CHAPTER 4

Table E.1 – Crack Densities at the Time of Survey and Crack Densities Used for Analysis for Fiber, Control, and SRA Decks

Bridge Deck	Survey A		Survey B		Crack Density Used for Analysis* (m/m^2)
	Deck Age (month)	Crack Density (m/m^2)	Deck Age (month)	Crack Density (m/m^2)	
Fiber-1 p1	33.7	0.112	-	-	0.112
Fiber-1 p2	31.7	0.220	-	-	0.220
Fiber-1 Entire Deck	32.7	0.166	-	-	0.166
Fiber-2 p1	34.0	0.127	-	-	0.127
Fiber-2 p2	32.4	0.456	-	-	0.456
Fiber-2 Entire Deck	33.2	0.291	-	-	0.291
Fiber-3	26.8	0.272	37.8	0.287	0.285
Control-3	36.0	0.233	-	-	0.233
Fiber-4 p1	33.6	0.709	-	-	0.709
Fiber-4 p2	33.4	0.431	-	-	0.431
Fiber-4 Entire Deck	33.5	0.594	-	-	0.594
Control-4 p1	35.8	0.766	-	-	0.766
Control-4 p2	35.6	0.393	-	-	0.393
Control-4 Entire Deck	35.7	0.615	-	-	0.615
Fiber-5	31.1	0.044	44.7	0.091	0.061
Control-5	31.2	0.038	44.8	0.077	0.052
Fiber-6	25.0	0.005	38.6	0.013	0.011
Control-6	25.3	0.002	38.9	0.013	0.011
Fiber-7	24.6	0.000	38.0	0.005	0.004
Control-7	25.8	0.014	38.3	0.037	0.033
VA-SRA-1	19.1	0.455	43.0	0.333	0.369
VA-SRA-2	18.6	0.344	42.5	0.217	0.252
VA-SRA-3	33.9	0.083	-	-	0.083
VA-SRA-4	34.0	0.056	-	-	0.056
VA-Control	31.0	0.222	54.1	0.266	0.232

*: The procedure to establish the crack density used for analysis is described in Section 4.3.

Table E.2 – Crack Densities at the Time of Survey and Crack Densities Used for Analysis for IC and Control Decks in Indiana

Placements	Survey A		Survey B		Crack Density Used for Analysis* (m/m^2)
	Deck Age (month)	Crack Density (m/m^2)	Deck Age (month)	Crack Density (m/m^2)	
IN-Control	71.6	0.507	93	0.67	0.236
IN-IC-1	71.6	0.347	93	0.447	0.181
IN-IC-2 p1	34.7	0	-	-	0.000
IN-IC-2 p2	37.2	0.02	-	-	0.020
IN-IC-3	34.8	0.016	56.8	0.033	0.017
IN-IC-4	21.6	0.003	43.8	0.086	0.057
IN-IC-5 p2	32.8	0.032	-	-	0.032

*: The procedure to establish the crack density used for analysis is described in Section 4.3.

Table E.3 – Crack Densities at the Time of Survey and Crack Densities Used for Analysis for Conventional Decks in Kansas

Placements	Survey A		Survey B		Crack Density Used for Analysis* (m/m^2)
	Deck Age (month)	Crack Density (m/m^2)	Deck Age (month)	Crack Density (m/m^2)	
3-046 East Deck	102	0.402	210	0.418	0.392
3-046 West Deck	102	0.362	210	0.539	0.254
3-046 Ctr. Deck	102	0.153	210	0.334	0.042
75-044 Deck	48	0.179	155	0.304	0.165
75-045 Deck	47	0.468	-	-	0.468
89-204 Deck	34	0.732	82	0.825	0.736
3-045 West Deck	112	0.122	223	0.192	0.074
3-045 East Deck	112	0.196	223	0.368	0.078
3-045 W. Ctr. Deck	112	0.188	223	0.203	0.178
3-045 Ctr. Deck	112	0.215	220	0.273	0.174
3-045 E. Ctr. Deck	112	0.163	220	0.333	0.043
56-142 Pos. Moment	80	0.108	189	0.200	0.071
56-142 Neg. Moment	80	0.093	188	0.163	0.064
56-148 Deck	36	0.259	-	-	0.259
70-095 Deck	106	0.069	212	0.136	0.025
70-103 Right	102	0.395	219	0.647	0.253
70-103 Left	102	0.557	219	0.842	0.396
70-104 Deck	106	0.083	212	0.104	0.069
70-107 Deck	34	0.322	82	0.417	0.326
99-076 p 4	42	0.872	-	-	0.872
99-076 p 5	42	0.861	-	-	0.861
99-076 North (West)	42	0.801	-	-	0.801
99-076 North (East)	42	0.412	-	-	0.412
99-076 p 2	42	1.536	-	-	1.536
99-076 p 3	42	0.739	-	-	0.739
89-208 Deck	36	0.009	-	-	0.009
56-49 Deck	25.8	0.230	47.5	0.265	0.246

*: The procedure to establish the crack density used for analysis is described in Section 4.3.

Table E.4 – Crack densities at the Time of Survey and Crack Densities Used for Analysis for LC-HPC Decks

Placements	Survey A		Survey B		Crack Density Used for Analysis* (m/m^2)
	Deck Age (month)	Crack Density (m/m^2)	Deck Age (month)	Crack Density (m/m^2)	
LC-HPC 1 p1	32.1	0.044	44.1	0.060	0.049
LC-HPC 1 p2	31.5	0.024	-	-	0.024
LC-HPC 2	21.2	0.028	44.5	0.059	0.048
LC-HPC 3	19.2	0.110	54.0	0.173	0.140
LC-HPC 4 p2	32.7	0.094	44.9	0.080	0.090
LC-HPC 5	31.1	0.128	43.0	0.190	0.154
LC-HPC 6	31.4	0.231	43.4	0.336	0.271
LC-HPC 7	34.8	0.012	-	-	0.012
LC-HPC 9	26.5	0.237	38.3	0.362	0.338
LC-HPC 11	23.4	0.060	36.2	0.265	0.262
LC-HPC 15	30.8	0.161	43.0	0.316	0.227
LC-HPC 16	31.2	0.211	43.5	0.311	0.250
LC-HPC 17	32.5	0.274	45.5	0.308	0.283

*: The procedure to establish the crack density used for analysis is described in Section 4.3.

Table E.5 – Crack Densities at the Time of Survey and Crack Densities Used for Analysis for Conventional Decks (Yuan et al. 2011)

Bridge Number	Placement	Survey A		Survey B		Crack Density Used for Analysis* (m/m^2)
		Survey Age (month)	Crack Density (m/m^2)	Survey Age (month)	Crack Density (m/m^2)	
3-046	East Deck	210	0.418	102	0.402	0.392
	West Deck	210	0.539	102	0.362	0.254
	Ctr. Deck	210	.334	102	0.153	0.042
75-044	Deck	155	0.304	48	0.179	0.165
75-045	Deck	154	0.433	47	0.468	0.468
89-204	Deck	82	0.825	34	0.732	0.736
3-045	West Deck	223	0.192	112	0.122	0.074
	East Deck	223	0.368	112	0.196	0.078
	W. Ctr. Deck	223	0.203	112	0.188	0.178
	Ctr. Deck	220	0.273	112	0.215	0.174
	E. Ctr. Deck	220	0.333	112	0.163	0.043
56-142	+ Moment	189	0.2	80	0.108	0.071
	- Moment	188	0.163	80	0.093	0.064
56-148	Deck	36	0.259	-	-	0.259
70-095	Deck	212	0.136	106	0.069	0.025
70-103	Right	219	0.647	102	0.395	0.253
	Left	219	0.842	102	0.557	0.396
70-104	Deck	212	0.104	106	0.083	0.069
70-107	Deck	34	0.322	82	0.417	0.326
99-076	Placement 4	42	0.872	-	-	0.872
	Placement 5	42	0.861	-	-	0.861
	North (West Ln.)	42	0.801	-	-	0.801
	North (East Ln.)	42	0.412	-	-	0.412
	Placement 2	42	1.536	-	-	1.536
	Placement 3	42	0.739	-	-	0.739
89-208	Deck	36	0.009	-	-	0.009
56-49	Deck	25.8	0.230	47.5	0.265	0.246

*: The procedure to establish the crack density used for analysis is described in Section 4.3.